TESIS DOCTORAL

Estudio de dos especies de dinoflagelados marinos productores de Floraciones Algales Nocivas (FANs): *Alexandrium ostenfeldii* y *Protoceratium reticulatum*

Pablo César Salgado Garrido

2017

Universidade Vigo

EIDO
Escola Internacional
de Doutoramento

Universidade Vigo
Escola Internacional de Doutoramento

Pablo César Salgado Garrido

TESIS DOCTORAL

Estudio de dos especies de dinoflagelados marinos productores de Floraciones Algales Nocivas (FANs): *Alexandrium ostenfeldii* y *Protoceratium reticulatum*

Dirigida por:

Dra. Isabel Bravo Portela
Dra. Pilar Riobó Agulla

2017

Universidade Vigo

Escola Internacional de Doutoramento

La Dra. Isabel Bravo Portela, Científico Titular del Instituto Español de Oceanografía (IEO) de Vigo, y la Dra. Pilar Riobó Agulla, Titulado Superior de Actividades Técnicas y Profesionales del Instituto de Investigaciones Marinas (IIM–CSIC) de Vigo,

HACEN CONSTAR que el presente trabajo titulado "**Estudio de dos especies de dinoflagelados marinos productores de Floraciones Algales Nocivas (FANs): *Alexandrium ostenfeldii* y *Protoceratium reticulatum***", presentado por el biólogo marino Pablo César Salgado Garrido para optar al grado de **Doctor por la Universidad de Vigo**, ha sido realizado en el Departamento de Microalgas Nocivas del Centro Oceanográfico de Vigo del IEO bajo nuestra dirección en el Programa de Doctorado en "Ciencias Marinas, Tecnología y Gestión" del Campus de excelencia internacional "Do*Mar", cumpliendo las normas exigidas para su presentación bajo la modalidad de tesis por Compendio de artículos de investigación, la cual autorizamos para que pueda ser juzgada por el tribunal correspondiente.

Vigo, a …. de ……..de 2017

Y para que así conste, a los efectos oportunos, firmamos la presente.

Dra. Isabel Bravo Portela
Directora de la Tesis Doctoral

Dra. Pilar Riobó Agulla
Co-directora de la Tesis Doctoral

Durante el período de desarrollo de esta Tesis Doctoral, Pablo César Salgado Garrido constó con el apoyo financiero del Instituto de Fomento Pesquero (IFOP) de Chile, institución con la cual mantiene un contrato laboral como Investigador desde el año 2006. Los trabajos recogidos en esta Tesis fueron financiados por el proyecto CCVIEO: "*Colección de cultivos de microalgas tóxicas del Centro Oceanográfico de Vigo*", y el proyecto CICAN: "*Estrategias adaptativas de microalgas nocivas: una aproximación innovadora aplicada al estudio de la Ciguatera en Canarias ante el cambio climático*" del Instituto Español de Oceanografía de Vigo.

Esta tesis puede ser citada como:

Salgado, P. 2017. Estudio de dos especies de dinoflagelados marinos productores de Floraciones Algales Nocivas (FANs): *Alexandrium ostenfeldii* y *Protoceratium reticulatum*. Tesis Doctoral. Escola Internacional de Doutoramento, Universidad de Vigo. 179 pág.

A mi familia…

Agradecimientos

Los primeros agradecimientos se los dedico a mis directoras de tesis Isa Bravo y Pilar Riobó, quienes aceptaron guiarme durante estos cuatro años. Sus consejos, excelente disposición y su apoyo incondicional en todo momento fue fundamental para cumplir con los objetivos propuestos en el tiempo estipulado. Agradezco particularmente a Isa, con quien desarrollé la mayor parte de los trabajos, aprendí mucho de su experiencia y de su forma de trabajar, además de ser una excelente investigadora es una gran persona.

A todos los miembros del Tribunal por haber aceptado participar de este proceso desde el primer momento que fueron propuestos. Gracias Ana, Juan, Jesús, Magda y Aitor.

A la Dirección del Centro Oceanográfico de Vigo por permitirme realizar la tesis en el Departamento de Fitoplancton Nocivo. Sin esa posibilidad no hubiese sido posible conocer a grandes personas.

Particularmente agradezco a amigos y colegas, Santi, Fran, Bea, Rosa, Isa Ramilo, Pilar Rial, Pepe, Amelia, Ana, Gerardo, Quique, Paty, Elena, Jorge y Javi. En especial a mi "compi" María, que al final terminó aprendiéndose todas mis palabras "chilenas". Cado uno de ellos colaboró directa o indirectamente en el desarrollo de esta tesis y han hecho que mi estadía en el Centro haya sido muy agradable. Creo que no pude haber estado en un mejor grupo humano y profesional. Gracias por todo!

Agradezco a la Dirección Ejecutiva del Instituto de Fomento Pesquero (IFOP) por haber permitido el financiamiento de mi estancia en Vigo durante estos cuatro años. A Leonardo Guzmán y Gemita Pizarro por apoyarme en todo momento y alentarme a realizar el doctorado.

A los proyectos CCVIEO (Colección de Cultivos de Microalgas Tóxicas del Centro Oceanográfico de Vigo) y CICAN (Estrategias adaptativas de microalgas nocivas: una aproximación innovadora aplicada al estudio de la Ciguatera en Canarias ante el cambio climático) del Instituto Español de Oceanografía de Vigo, los cuales financiaron gran parte de las investigaciones que se llevaron a cabo durante el desarrollo de esta tesis.

Gracias a Olga y Pato por acogernos cuando recién llegamos a Vigo. De ahí en adelante se formó una bonita amistad entre las dos familias y seguirá así cuando regresemos a Chile. También a Fran y Mónica por su amistad y por hacer que el tiempo que pasamos en Vigo haya sido aún más agradable.

A mis padres María y Ovidio y hermano Felipe, quienes desde el otro lado del "charco" estuvieron presentes cada día. Su apoyo fue fundamental para lograr esto. Esta tesis también es suya.

Y por último, pero no por eso menos importante, quiero agradecer de forma muy especial a mis compañeras de vida, mi esposa Marcela y mi hija Antonia, quienes desde el primer minuto se embarcaron en este gran desafío dejando sus atrás sus amigos, trabajos y sueños. Sin su constante apoyo y cariño esto no hubiese sido posible, les estaré a gradecido por siempre.

Acrónimos y abreviaturas

Acrónimos y abreviaturas

AIF	<<All Ion Fragmentation>> = Fragmentación de iones
ASP	<<Amnesic Shellfish Poisoning>> = Intoxicación amnésica por mariscos
AZAs	Azaspirácidos
AZP	<<Azaspiracid Poisoning>> = Intoxicación por azaspirácidos
BI	<<Bayesian Inference method>> = Método de inferencia bayesiana
bp	<<base pairs>> = pares de bases
CACTI	Centro de Apoyo Científico-Tecnológico a la Investigación
CCVIEO	Colección de Cultivos del Centro Oceanográfico de Vigo del Instituto Español de Oceanografía
CFP	<<Ciguatera Fish Poisoning>> = Intoxicación de la Ciguatera por pescado
CIs	<<Cyclic Imines>> = Imínas cíclicas
CI	<<Confidence interval>> = Intervalo de confianza
DA/AD	<<Domoic Acid>> = Ácido Domoico
dcSTX	Decarbamoylsaxitoxina
DNA	<<Deoxi-ribonucleic acid>> = ADN, ácido desoxi-ribonucleico
DSP	<<Diarrhetic Shellfish Poisoning>> = Intoxicación diarreica por mariscos
DTXs	Dinofisistoxinas
FANs	Floraciones Algales Nocivas
G1	Fase G1 (growth = crecimiento) del ciclo celular que precede a la fase S, de síntesis del ADN
G2	Fase G2 (período premitótico) del ciclo celular que precede a la mitosis
GEOHAB	<<Global Ecology and Oceanographic of Harmful Algal Blooms Programme>> = Ecología y Oceanografía Global de las

	Floraciones Algales Nocivas. Programa patrocinado por SCOR y COI
GTR	<<General Time Reversible>> = Tiempo general reversible
GTXs	Gonyautoxinas
GTX-2	Gonyautoxina 2
GTX-3	Gonyautoxina 3
GYMs	Gimnodiminas
GYM-A	Gimnodimina A
GYM-B/-C	Gimnodimina B o C
HAB	<<Harmful Algal Blooms>> = Floraciones Algales Nocivas
HCD	<<High-energy collisional dissociation>> = Energía de colisión
HPLC–FD	<<High-Performance Liquid Cromatography coupled to Fluorimetric Detection>> = Cromatografía líquida de alta eficacia acoplada a detección fluorimétrica
IEO	Instituto Español de Oceanografía
IFOP	Instituto de Fomento Pesquero
IOC/COI	<<Intergovernmental Oceanographic Commission of UNESCO>> = Comisión Oceanográfica Intergubernamental de la UNESCO
ITS	<<Internal transcriber spaces>> = Espacios de transcripción interna, a modo de espaciadores, situados en el gen ribosomal
LC–HRMS	<<Liquid Chromatography coupled to High Resolution Mass Spectrometry>> = Cromatografía líquida acoplada a espectrometría de masas de alta resolución
L:D	<<Light:Dark cycle>> = Ciclo de Luz:Oscuridad, fotoperíodo
LM	<<Light microscopy>> = Microscopía de luz
LSU	<<Large Subribosomal Unit>> = Subunidad ribosomal grande, LSU rDNA, porción mayor del gen que controla la síntesis de ribosomas
M	Fase de Mitosis del ciclo celular
ML	<<Maximum Likelihood method>> = Método de máxima verosimilitud

m/z	Relación masa/carga en el espectrómetro de masas
mu	<<mass units>> = Unidades de masa
NA	No analizado
NCMA	<<Provasoli-Guillar National Center for Marine Algae and Microbiota>> = Centro nacional Provasoli-Guillar de algas marinas y microbiota
NGD	<<No growth detected>> = No se detectó crecimiento celular en cultivos
ND	<<Not Detected>> = No detectado
NS	<<Not Significant>> = No significativo
NRC	<<National Research Council>> = Institución Canadiense dedicada al estudio y ficotoxinas y comercialización de patrones de toxinas
NSP	<<Neurotoxic Shellfish Poisoning>> = Intoxicación neurotóxica por bivalvos
nt	Nucleótido
OA	<<Okadaic Acid>> = Ácido Okadaico
PAR	<<Photosynthetically Active Radiation>> = Radiación fotosintéticamente activa
PBS	**<<**Phosphate Buffer Solution>> = Solución de tampón fosfato
PCR	<<Polymerase Chain Reaction>> = Reacción en cadena de la polimerasa. Permite amplificar (replicar) el contenido de DNA a partir de pequeñas muestras
PSP	<<Paralytic Shellfish Poisoning>> = Intoxicación paralizante por mariscos
PTXs	Pectenotoxinas
RDB	<<Relative Double Bond equivalents>> = Porcentaje relativo de dobles enlaces
RSA	<<Response-Surface Analysis>> = Análisis de superficie de respuesta
S	Fase de síntesis del ADN durante el ciclo celular

SD	<<Standard deviation>> = Desviación estándar
RT	<<Retention Time>> = Tiempo de retención en la columna cromatográfica
SEM	<<Scanning Electron Microscopy>> = Microscopía electrónica de barrido
SPXs	Espirólidos
SPX-C	Espirólido C
STXs	Saxitoxinas
SUBPESCA	Subsecretaría de Pesca y Acuicultura
YTXs	Yesotoxinas

Índice de contenido

Índice de contenido

Introducción

Introducción

1. Floraciones algales nocivas

1.1. Definición e impactos

El término fitoplancton puede ser definido como un grupo polifilético de organismos principalmente fototróficos unicelulares que derivan con las corrientes en aguas marinas y dulces (Falkowski & Raven, 1997). Junto a estos, por su similitud aunque viviendo en diferente hábitat, también se debe mencionar el microfitobentos que vive adherido a sustratos inertes, algas o entre arena. Aunque representan menos del 1% de la biomasa fotosintética de la tierra, estos organismos microscópicos pigmentados son responsables de más del 45% de la producción primaria neta anual del planeta, siendo éste, el mayor flujo de materia orgánica a los niveles tróficos más altos (Falkowski & Raven, 1997; Field et al., 1998). Como productores primarios altamente eficientes, estos organismos son imprescindibles para mantener la biodiversidad y sustentar, directa o indirectamente, la vida marina en todos los océanos. Sin embargo, a pesar de cumplir un rol beneficioso, los eventos conocidos comúnmente como *mareas rojas*—y que técnicamente han sido denominados como Floraciones Algales Nocivas (FANs, en inglés HABs = *Harmful Algal Blooms*) por la Comisión Oceanográfica Intergubernamental (COI) de la UNESCO—en ocasiones amenazan seriamente la salud pública y causan, frecuentemente, enormes pérdidas económicas para las pesquerías y diversos sectores productivos en diversas áreas del planeta.

Las FANs han sido definidas técnicamente como "*proliferaciones, en ambientes acuáticos, de algas microscópicas que pueden causar la muerte masiva de peces y una gran variedad de otros organismos, contaminar los mariscos con toxinas, y alterar los ecosistemas de manera que los seres humanos las perciban como dañinas o nocivas*" (GEOHAB, 2001). Esta definición se refiere tanto a

eventos donde ocurre una rápida proliferación y/o alta acumulación de biomasa de microalgas principalmente tóxicas o nocivas (Fig. 1), o en otras ocasiones a que un bajo número de células de alguna especie tóxica pueda causar serios problemas en concentraciones reducidas. Paradójicamente, muchas floraciones tóxicas no provocan una coloración del agua sino que su nocividad es producida porque sus toxinas son acumuladas en otros organismos de niveles superiores en la cadena trófica. La capacidad de una especie para producir toxinas no se traduce directamente en su capacidad para proliferar. Aunque la mayoría de las especies tóxicas actualmente conocidas sí lo hacen, también hay muchas especies no tóxicas que pueden formar floraciones, provocar coloración del agua y causar problemas debido a las elevadas concentraciones que alcanzan. Los ecosistemas se ven perturbados en general por estos fenómenos que pueden alterar la cadena trófica y producir mortandad de organismos por la falta de oxígeno.

Fig. 1. Coloración del agua de mar producida por una floración del dinoflagelado ictiotóxico *Cochlodinium polykrikoides* en el sur de Corea. Extraído de Anderson et al. (2014).

El conocimiento sobre las FANs ha avanzado significativamente durante la última década, sin embargo, los factores que dan origen a estos eventos aún necesitan mayor comprensión debido a su complejidad y diversidad. Se ha mencionado que estos factores incluyen aspectos biológicos, bioquímicos, hidrográficos, meteorológicos y geográficos que requieren de un estudio multidisciplinar que abarque áreas tan diversas como la molecular, la ecología y biología de las especies, modelado numérico, taxonomía, física, química y bioquímica, hasta estudios de campo con series de tiempo de gran escala (Anderson et al., 2012a).

Una problemática en el estudio y manejo de las FANs ha sido la alta diversidad de especies, los complejos ciclos de vida que presentan, y los distintos tipos de ecosistemas donde estas microalgas se desarrollan. El fitoplancton clasificado como potencialmente nocivo no pertenece a un único grupo evolutivamente distinto, sino más bien abarca la mayoría de los clados taxonómicos algales, incluyendo eucariotas (dinoflagelados, rafidofitas, diatomeas, euglenofitas, criptofitas, haptofitas, y clorofitas) y procariotas microbianos (cianobacterias fijadoras de nitrógeno que se presentan en sistemas marinos y de agua dulce) (Anderson et al., 2014). Entre las miles de especies que conforman el fitoplancton marino actual, solo unas 300 (~6%) son conocidas por alcanzar elevadas concentraciones (Hallegraeff, 1993), y cerca de 60–80 (~2%) tienen la capacidad de ser nocivas al producir biotoxinas, provocar daño físico y/o muerte a mamíferos marinos, aves y peces, y de generar anoxia (Smayda, 1997; Glibert et al., 2005). Entre este reducido número de microalgas nocivas, algunas especies, principalmente del grupo de las diatomeas, pueden ser letales para peces e invertebrados al dañar u obstruir sus branquias cuando alcanzan altas concentraciones (Anderson et al., 2014). Otras no son tóxicas ni tienen morfologías particulares que provoquen daño físico (i.e., largas espinas como en *Chaetoceros convolutus* o frústulos muy silificados en *Leptocylindrus* spp.), pero al dominar la comunidad planctónica y al encontrarse en altas concentraciones, agotan el oxígeno y los nutrientes provocando la muerte de otros organismos presentes en la

zona (Smayda, 1997). En tercer lugar están las especies tóxicas, que generalmente no se encuentran en concentraciones elevadas por lo cual no producen cambios en el color del agua, pero a través de la cadena trófica sus toxinas pueden acumularse en mariscos y peces dando lugar a intoxicaciones en humanos.

A nivel global, hay evidencia que los eventos FAN en aguas costeras han incrementado en décadas recientes en relación a la frecuencia, intensidad y cobertura geográfica (GEOHAB, 2001; Anderson et al., 2012a). Se han propuesto varias hipótesis para explicar este aumento:

1) El aumento del conocimiento como resultado de los avances metodológicos en detección de eventos FAN y determinación de toxinas, y el incremento de la acuicultura en zonas costeras (Anderson, 1989; Landsberg et al., 2002).
2) La alteración de la proporción de nutrientes en las zonas costeras producto de la intensificación de la carga de nutrientes antropogénicos lo cual, en determinadas circunstancias ha podido favorecer a especies toxicas o nocivas o incrementando la intensificación de las proliferaciones en general (Tilman, 1977; Smayda, 1990, 1997).
3) El transporte de especies y sus quistes de resistencia en aguas de lastre y en mariscos trasplantados desde un área a otra, cuya eliminación desde embarcaciones de cabotaje y desde los moluscos, puede favorecer la dispersión de especies nocivas a zonas que previamente estaban libres de estos taxa (Hallegraeff, 1993; GEOHAB, 2001),
4) El transporte de células vegetativas y/o de los quistes mediante mecanismos físicos naturales como corrientes y la advección de plumas costeras ha expandido la distribución geográfica de especies nocivas permitiendo que haya floraciones donde antes no las había (Franks & Anderson, 1992; Anderson et al., 2012a).
5) El cambio climático global—expresado como alteraciones en la temperatura, la estratificación, la luz, la acidificación de los océanos, y el desacoplamiento en los niveles tróficos, entre otros factores—que explicaría

el incremento de aquellas floraciones que no se pueden atribuir a un proceso de eutrofización antrópica de las aguas costeras (Hallegraeff, 1993; Anderson et al. 2012a).

1.2. Toxinas de microalgas

Algunas microalgas producen metabolitos que pueden dar lugar a intoxicaciones de diversa gravedad en humanos. En función de los síntomas observados se han descrito clínicamente seis síndromes (Anderson et al., 2014) (Tabla 1). Tanto las toxinas como las microalgas se pueden clasificar según el síndrome, es decir, el tipo de intoxicación o envenenamiento que producen en los siguientes grupos: Intoxicación Paralizante por Mariscos (VPM, en inglés PSP = *Paralytic shellfish Poisoning*), Intoxicación Diarreica por Mariscos (VDM, en inglés DSP = *Diarrhetic shellfish Poisoning*), Intoxicación Amnésica por Mariscos (VAM, en inglés ASP = *Amnesic Shellfish Poisoning*), Intoxicación Neurotóxica por Mariscos (VNM, en inglés NSP = *Neurotoxic Shellfish Poisoning*), Intoxicación de la Ciguatera por Pescado (VCP en inglés CFP = *Ciguatera Fish Poisoning*) y la Intoxicación por Azaspiracidos (AZP).

Las microalgas también pueden producir metabolitos biológicamente activos pero que no se han asociado con casos de intoxicación en humanos. Es el caso de las Imínas Cíclicas (ICs) (Richard et al., 2001), familia de biotoxinas marinas presentes en mariscos donde se incluyen espirólidos (SPXs), gimnodiminas (GYMs), pinnatoxinas (PnTXs), pteriatoxinas (PtTXs) y prorocentrólidos (PcTXs) (Tabla 1). Todas ellas presentan una estructura molecular similar caracterizada por un anillo bicíclico con un grupo imina (Molgó et al., 2014) y resultan altamente tóxicas en el bioensayo de ratón via intraperitoneal (AOAC, 1990), provocando la muerte fulminante de los ratones (Marrouchi et al., 2010; Otero et al., 2011), de ahí que se las denomine toxinas de acción rápida "Fast acting toxins" (Cembella & Krock, 2008). Se trata de compuestos neurotóxicos que actúan inhibiendo los

receptores muscarínicos y nicotínicos de la acetilcolina a nivel del Sistema Nervioso Central y Periférico (Munday et al., 2008). El síndrome más peligroso para el ser humano, debido a su letalidad cuando las toxinas alcanzan una elevada concentración en mariscos, es el PSP. Las toxinas que incluye este síndrome son la saxitoxina (STX) y al menos 21 derivados que pueden ser producidos en varias combinaciones y concentraciones (Starr et al., 2017). Algunos de estos compuestos son altamente neurotóxicos, actuando como agentes bloqueadores de canales de sodio que restringen la transmisión de señales entre neuronas, particularmente en mamíferos, aves y peces (Anderson et al., 2012b). Puede llevar a producir debilidad muscular, parálisis respiratoria, coma, y eventualmente la muerte en casos extremadamente severos (Anderson et al., 2014; Visciano et a., 2016).

Cada uno de los grupos de toxinas mencionados es causado por diferentes especies y/o cepas de microalgas (Tabla 1). El síndrome amnésico (ASP) es el único producido por diatomeas, mientras que el resto son producidos por dinoflagelados. El grupo de los dinoflagelados, curiosamente, es el que representa la mayoría (~75%) de las especies vinculadas a eventos FAN a nivel global (Smayda, 1997; Moestrup et al., 2009). En el síndrome PSP, además de los dinoflagelados (Tabla 1), también pueden estar implicadas cianobacterias de agua dulce (Aráoz et al., 2010).

Se desconoce por qué sólo algunas especies fitoplanctónicas producen toxinas o por qué algunas cepas de una misma especie pueden ser toxicas y otras no. Más aún, por qué diferentes cepas de una misma especie pueden producir toxinas distintas. De lo que sí se tiene conocimiento es de los factores químicos, físicos, y bióticos como los nutrientes, temperatura, salinidad, irradiancia y predación que tienen influencia en la producción de toxinas (Granéli & Flynn, 2006; Senft-Batoh, et al., 2015a,b). Las biotoxinas marinas son metabolitos secundarios que varían en estructura, composición atómica y actividad funcional. Por lo tanto, no es raro que los factores que estimulan la producción de las mismas en una especie/grupo de microalgas puedan tener un impacto diferente en otra (Granéli & Flynn, 2006). Se

ha planteado que las toxinas pueden desempeñar funciones disuasorias ante potenciales predadores (Selander et al., 2006; Wohlrab et al., 2010; Senft-Batoh et al., 2015b), inmovilizar a presas (Sheng et al., 2010), o competir por espacio vital (Gerssen et al., 2010), pero aún es escasa la información sobre el rol ecológico de las toxinas para las microalgas.

Tabla 1. Clasificación de las toxinas marinas, síndrome toxicológico, organismos fuente primaria, y sintomatología en humanos. Modificado de Anderson et al. (2014).

Toxina	**Síndrome**	**Fuente**	**Sintomatología**
Saxitoxina (STX) y sus derivados	PSP	*Alexandrium* spp. *Gymnodinium catenatum* *Pyrodinium bahamense*	Parestesia en casos leves, parálisis respiratoria y muerte en casos muy severos
Ácido Domoico (DA)	ASP	*Pseudo-nitzschia* spp. *Nitzschia* spp.	Síntomas gastrointestinales y/o signos neurológicos, coma o muerte en casos extremos
Acido Okadaico (OA) y dinofisistoxinas (DTXs)	DSP	*Dinophysis* spp. *Prorocentrum lima*	Efectos gastrointestinales, diarrea, vómitos, recuperación en 3 días
Pectenotoxinas (PTXs) Yesotoxinas (YTXs)		*Dinophysis* spp. *Protoceratium reticulatum** *Lingulodinium polyedra* *Gonyaulax spinifera* *Gonyaulax taylori*	No determinada Sin observación en humanos
Azaspiracidos (AZAs)	AZP	*Azadinium spinosum* *Amphidoma languida*	Síntomas gastrointestinales, nauseas, vómitos, diarrea
Brevetoxinas (BTXs)	NSP	*Karenia brevis*	Síntomas gastrointestinales y neurológicos, problemas respiratorios
Ciguatoxina (CTXs)	CFP	*Gambierdiscus* spp.	Efectos gastrointestinales, cardiovasculares y neurológicos
Espirólidos (SPXs), Gimnodiminas (GYMs), Pinnatoxinas (PnTXs), Pteriatoxinas (PtTXs) Prorocentrolidos (PcTXs)		*Alexandrium ostenfeldii** *Karenia* spp. *Alexandrium ostenfeldii** *Vulcanodinium rugosum* Producto de biotransformación de PnTXs en mariscos *Prorocentrum* spp.	Sin síntomas en humanos
Palitoxinas (PlTXs)		*Ostreopsis* sp. *Palythoa* spp.	Efectos gastrointestinales, problemas musculares y cutáneos

PSP: Paralytic Shellfish Poisoning = Intoxicación Paralizante por Mariscos (VPM); ASP: Amnesic Shellfish Poisoning = Intoxicación Amnésica por Mariscos (VAM); DSP: Diarrhetic Shellfish Poisoning = Intoxicación Diarreica por Mariscos (VDM); AZP: Azaspiracids Poisoning = Intoxicación por Azaspirácidos (AZA); NSP: Neurotoxic Shellfish Poisoning = Intoxicación Neurotóxica por Mariscos; CFP: Ciguatera Fish Poisoning = Veneno de la Ciguatera por Pescado (VCP). * especies estudiadas en esta tesis.

Los mariscos bivalvos (e.g. mejillones, almejas, ostiones, ostras, entre muchos otros) son el grupo de organismos marinos más propensos a acumular estas biotoxinas debido a su modo de alimentación, basada fundamentalmente en la filtración de microalgas planctónicas (Doucette et al., 2006). Un importante problema en la detección de estos mariscos contaminados radica en que estas toxinas no alteran las características organolépticas (color, olor o sabor) de los bivalvos, haciendo que sea muy fácil para los humanos ingerirlas sin percatarse de su presencia, causando trastornos gastrointestinales y neurológicos. Además, en el metabolismo de los bivalvos se producen transformaciones de las toxinas que en ocasiones incrementan su potencia tóxica (Paz et al., 2008). Estas toxinas se transfieren a través de la cadena trófica debido a la depredación que ejercen otros organismos sobre los moluscos bivalvos o sobre las propias microalgas (Fig. 2)—como es el caso de los gasterópodos y del zooplancton o peces planctívoros, respectivamente—generando bioacumulación y un potencial riesgo para consumidores mayores. Adicionalmente, numerosas microalgas tóxicas tienen quistes bentónicos como parte de su ciclo de vida. Éstos también pueden hacer que las comunidades bentónicas se vuelvan tóxicas (Dale & Yentsch, 1978). Además, células tóxicas y toxinas adsorbidas pueden hundirse y sedimentar y ser consumidas por organismos bentónicos, siendo recicladas dentro de la cadena trófica.

2. Los dinoflagelados

2.1. Características generales

Los dinoflagelados son organismos unicelulares eucariotas de tamaño microscópico que se caracterizan por poseer un tipo de núcleo especializado denominado dinocarion (Rizzo, 1991). Estos microorganismos habitan una amplia diversidad de ambientes acuáticos, tanto en agua dulce como marina (incluidas aguas salobres), y en todas las latitudes, desde el Ecuador hasta los polos (Hackett

et al., 2004; Le Bescot et al., 2016). Poseen diferentes formas de alimentación (autotrofía, heterotrofía, y mixotrofía) y morfologías (Hackett et al., 2004; Jeong et al., 2005). Se caracterizan por presentar una extraordinaria diversidad fisiológica y adaptaciones a nichos específicos, lo cual se cree son las principales razones de su éxito ecológico y evolutivo (Sournia, 1995; Smayda & Reynolds, 2003; de Vernal & Marret, 2007; Dyhrman, 2008; Price et al., 2016); por ejemplo, muchos dinoflagelados son capaces de utilizar fuentes de carbono orgánico y alimentarse mixotróficamente (Glibert et al., 2008, Stoecker 1999; Jeong et al., 2005); actuar como simbiontes o parásitos, utilizar hábitats planctónicos o bénticos (Hoppenrath et al., 2014); y producir compuestos químicos complejos que influyen en las interacciones con los competidores y los depredadores (Selander et al., 2006; Tillmann et al., 2008; Senft-Batoh et al., 2015b) (Fig. 2). Muchas especies producen importantes impactos ecológicos y económicos, incluyendo la formación de floraciones tóxicas y un papel biogeoquímico y trófico clave en los ambientes oceánicos y costeros pelágicos (Murray et al., 2016). Ellos son reconocidos como los más prolíficos productores de dimetilsufoniopropionato (DMSP) (Caruana & Malin, 2014), principal precursor biogénico del dimetilsulfuro (DMS), compuesto que una vez en la atmósfera influye en la producción y el albedo de las nubes, lo que posteriormente afecta a la regulación climática (Charlson et al., 1987).

Los dinoflagelados de vida libre son uno de los grupos planctónicos que presentan mayor movilidad en la columna de agua. Durante su fase vegetativa poseen dos flagelos, uno alrededor del cíngulo (transversal) y otro longitudinalmente paralelo al sulco (Fig. 3). El flagelo transversal es ondulado y con forma de cinta, mientras que el longitudinal es cilíndrico o aplanado y es el que le da propulsión a la célula (Fensome et al., 1993). La mayoría de las especies son de ambientes marinos y sólo unos pocos cientos de aguas continentales. Usualmente son abundantes en ambientes neríticos, incluyendo estuarios, mares interiores y plataformas continentales. Esta diversidad de ambientes se debe a que muchas especies presentan una alta tolerancia a variaciones de salinidad, temperatura, y de nutrientes (de Vernal & Marret, 2007). En general están

particularmente bien adaptados para vivir en condiciones relativamente calmas y estratificadas (Margalef, 1978). El eficiente movimiento flagelar acoplado con la capacidad fototáctica les da una gran capacidad para mantenerse en la zona eufótica y migrar verticalmente para poder recolectar partículas orgánicas y/o nutrientes inorgánicos en profundidad si éstos se agotan en las aguas superficiales (Margalef, 1978; Cullen & MacIntyre, 1998). Los dinoflagelados que producen floraciones y que reiteradamente se presentan en áreas específicas son especies que se han adaptado con el tiempo o aclimatado a los regímenes ambientales (e.g. temperatura del agua, salinidad, luz, patrones de circulación del agua, y nutrientes) de cada lugar (Levandowsky & Kaneta, 1987). Los productores de eventos FAN son en su mayoría especies fototróficas y alcanzan generalmente los mayores niveles de crecimiento poblacional (10^7–10^8 células L^{-1}) en aguas calmas o a lo largo de bordes de frentes formados en la unión de aguas estratificadas de océano abierto y de zonas costeras.

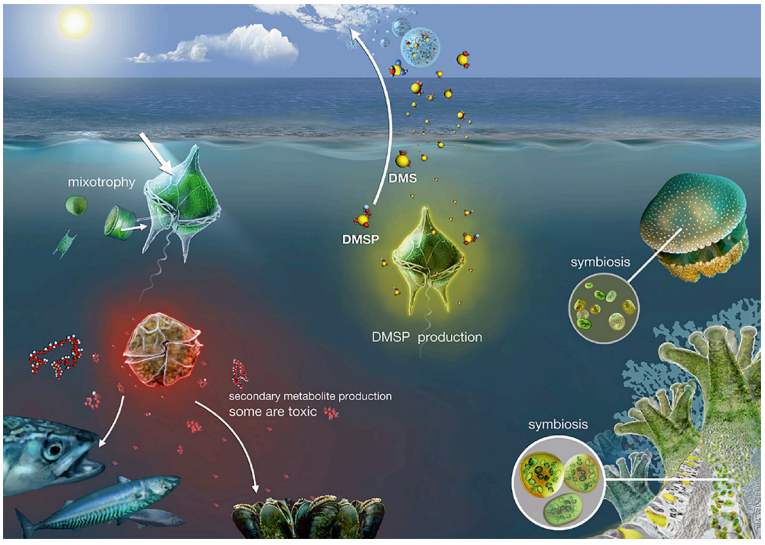

Fig. 2. Algunos de los principales rasgos ecológicos de los dinoflagelados: células planctónicas libres y simbiosis en corales y otros invertebrados, producción de DMSP, mixotrofia y producción de metabolitos tóxicos / no tóxicos con impactos en otras especies marinas. Extraído de Murray et al. (2016).

2.2. Taxonomía

La correcta caracterización taxonómica de una especie productora de floraciones tóxicas es fundamental para poder replicar todos los conocimientos sobre sus toxinas, fisiología y ecología. Los diferentes rasgos morfológicos de estas especies muchas veces son concordantes con diferencias genéticas, aunque en otras ocasiones esto no es así. Es por esto que se ha argumentado que los rasgos morfológicos conservativos son fundamentales en la clasificación tradicional de las especies (Anderson et al., 2012a). En muchos casos, sin embargo, sobre todo en las especies crípticas y en dinoflagelados desnudos, la clasificación tradicional de los dinoflagelados basada en el concepto morfológico de especie, no es suficiente. Es por ello que, con la expansión de las técnicas moleculares de secuenciación de ácidos nucleicos, en las últimas décadas se combina cada vez más la clasificación morfológica con la filogenética. Aún así, el uso de los rasgos morfológicos, sobre todo en dinoflagelados tecados como los tratados en esta tesis, siguen siendo ampliamente utilizados en la actualidad.

En taxonomía general de dinoflagelados se ha determinado que el polo de la célula que va en dirección de la natación se considera anterior o apical, y el polo opuesto posterior o antapical (Fensome et al., 1993). Los flagelos que producen el movimiento de la célula pueden estar insertos ventralmente (condición dinoconte), o más raramente, anteriormente (condición desmoconte). Ejemplos típicos de estas dos condiciones son los géneros *Alexandrium* y *Prorocentrum*, respectivamente. Las tres especies abordadas en esta memoria presentan la condición dinoconte, es decir, el aparato flagelar se posiciona ventralmente. En dinoflagelados de este último grupo, como la base de los flagelos está en el área ventral, el lado opuesto de la célula se denomina dorsal, y los lados izquierdo y derecho son consecuentemente determinados por convención biológica como en humanos (Fensome et al., 1993).

Una característica de particular importancia taxonómica en dinoflagelados es la composición y estructura de su pared celular, la cual ha sido denominada anfiesma

(Loeblich, 1970). El anfiesma presenta vesículas aplanadas que pueden estar rellenas o no de celulosa u otros polisacáridos dando a las células una pared más rígida (Hackett et al., 2004). Las primeras clasificaciones en este grupo fueron hechas de acuerdo con su presencia (llamados tecados) o ausencia (atecados o desnudos). Sin embargo, también hay dinoflagelados que presentan vesículas con un contenido intermedio de celulosa ubicados filogenéticamente entre el grupo de los tecados y el de los atecados y que han sido llamados Suessiales (Price & Bhattacharya, 2017). En esta tesis solo se tratarán dinoflagelados tecados.

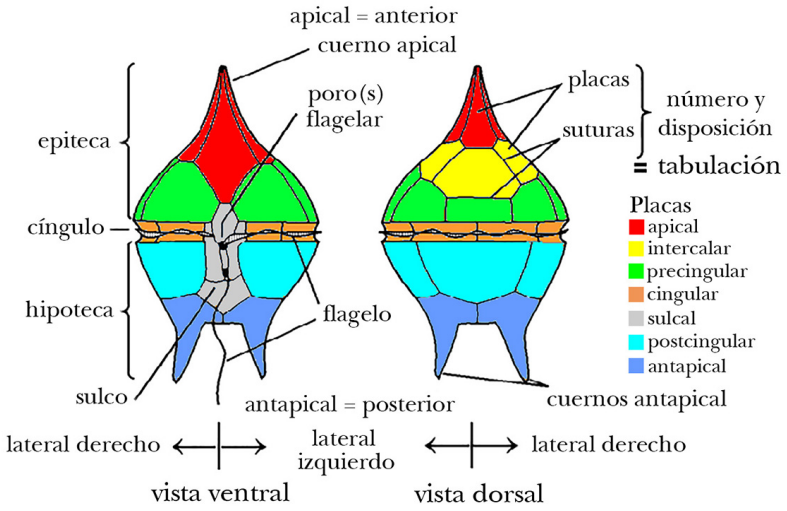

Fig. 3 Morfología externa y terminología de un dinoflagelado tecado. Modificado de Evitt (1985).

Las placas de celulosa son fundamentales en taxonomía de dinoflagelados debido a que características como su forma, número y disposición es propia de cada especie (Fig. 4). Esto hace que sea uno de los criterios más importantes junto a la genética en la identificación de nuevas especies. La disposición de las placas de celulosa ha sido referida dentro de la taxonomía con el término "tabulación"

(Hackett et al., 2004). Estas placas se caracterizan porque se apoyan una sobre otra a lo largo de líneas de sutura y, en general, se distribuyen de manera uniforme en cada especie (Fensome et al., 1993). Las placas pueden estar perforadas por poros de distinto tamaños y presentar ornamentaciones adicionales, tales como espinas, cuernos, estrías o reticulación (Fig. 4). Estas características varían en su desarrollo durante el ciclo de maduración de la célula. Un ejemplo claro ocurre en una de las especies estudiadas en esta tesis, el gonyaulacal *Protoceratium reticulatum*, donde las placas de células recién divididas, o de células germinadas recientemente de quistes de resistencia (planomeiocitos), presentan una superficie tecal fina y sin reticulación la cual se va haciendo cada vez más gruesa y reticulada con el paso de las horas. El crecimiento de la célula, y por consiguiente el crecimiento de sus placas, produce bandas de crecimiento—denominadas también bandas intercalares—que suelen ser estriadas y se disponen en ángulo recto a las suturas (Fensome et al., 1993).

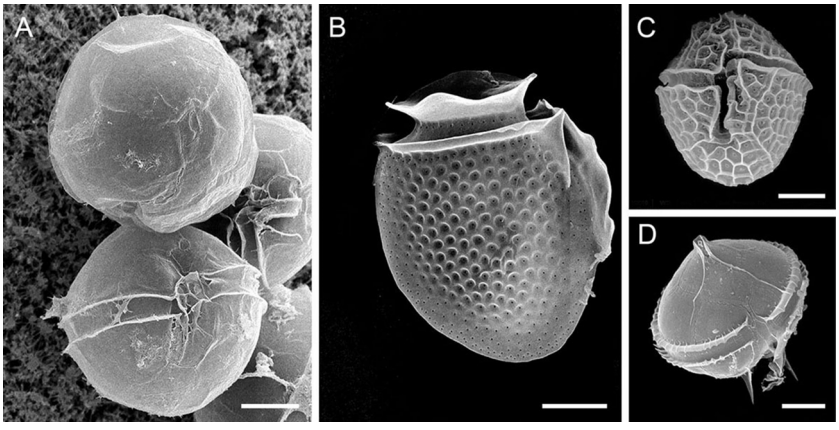

Fig. 4. Imágenes de microscopía electrónica de barrido de dinoflagelados del sur de Chile con diferentes tipos de superficie tecal. (A) *Alexandrium ostenfeldii*. (B) *Dinophysis acuminata*. (C) *Protoceratium reticulatum*. (D) *Protoperidinium* sp. Barras de escala 10µm.

Las tabulaciones de dinoflagelados pueden agruparse dentro de seis tipos: gymnodinioide, suessioide, gonyaulacoide, peridinioide, nanoceratopsioide, dinofisioide, y prorocentroide (Fensome et al., 1993). Dado que en esta memoria se estudian especies pertenecientes al grupo de los gonyaulacales, sólo este tipo de tabulación será mencionada en detalle. Las placas tecales están dispuestas en 5 o 6 series latitudinales (apical, intercalar, precingular, cingular, postcingular y antapical) y una longitudinal, la serie de placas sulcal (Fig. 3). El sistema de tabulación más utilizado fue desarrollado por Kofoid (1907a,b, 1909, 1911) donde se describe la serie de placas precingular, las cuales están inmediatamente anterior al cíngulo; la serie de placas postcingular que se posicionan inmediatamente posterior al cíngulo; las placas que contactan el complejo del poro apical (CPA) llamada serie de placas apical; las placas intercalar anterior que ocurren entre las series apical y precingular (epiteca) y no tienen contacto con el CPA, denominándose como intercalar posterior si ocurren en la hipoteca (Fensome et al., 1993). Las placas presentes en el cíngulo se denominan como cingulares y las del sulco como sulcales. En el sistema de Kofoid (Fensome et al., 1993), las placas de cada serie (excepto las sulcales) se enumeran en orden correlativo, iniciando la numeración de acuerdo a la cercanía a la posición medioventral (i.e., a la izquierda del sulco) manteniendo sentido antihorario en vista apical. Además, el sistema de Kofoid utilizó una notación de superíndice para designar las placas de cada serie: placas apicales ('), placas intercalares anteriores (a), placas precingulares (''), placas cingulares (c), placas postcingulares ('''), placas intercalares posteriores (p), placas antapicales (''''') y placas sulcales (s). De acuerdo a Balech (1995) la denominación de las placas sulcales es la siguiente: sulcal anterior (Sa), sulcal posterior (Sp), placa sulcal anterior izquierda (Ssa), placa sulcal posterior izquierda (Ssp), placa sulcal anterior derecha (Sda), placa lateral posterior derecha (Sdp), placa sulcal media anterior (Sma), placa sulcal media posterior (Smp), placa sulcal accesoria anterior (Saca), placa sulcal accesoria posterior (Sacp). Aunque existen distintas terminologías utilizadas para mencionar todas estas placas, en esta memoria se ha utilizado como referencia las mencionadas anteriormente.

2.3. Reproducción y estrategias de supervivencia

La dinámica de las FANs varía de un sitio a otro dependiendo no sólo de las condiciones hidrográficas y topográficas específicas, sino también de las características ecológicas y biológicas de los organismos causantes (Garcés et al., 2001). Los organismos productores de eventos FAN, como también muchos otros, han sobrevivido durante siglos debido a la adaptabilidad que han desarrollado a distintas condiciones ambientales. Esta adaptación se ha dado gracias a la capacidad de producir formas distintas, principalmente a través de la reproducción sexual y a la herencia de rasgos genéticos que han ayudado a mantener las poblaciones, tal como ha ocurrido con microalgas nocivas evolutivamente antiguas y exitosas en el tiempo (Steidinger & Garcés, 2006). Para entender la dinámica de las floraciones de dinoflagelados es esencial conocer la diversidad de estados del ciclo de vida y los mecanismos que los regulan dentro del ciclo de cada especie (Kremp, 2013). La alternancia de estos estados es una característica general en el ciclo de vida de las algas, mostrando diferente nivel de ploidía y ocupando diferentes nichos en el tiempo y espacio. Los organismos asexuales, a diferencia, reducen la diversidad genética y tienen menos éxito en la adaptación a un entorno cambiante (Holsinger, 2000). En dinoflagelados, los ciclos de vida pueden variar de simples a complejos, y su versatilidad y complejidad contribuye a la diversidad y estructura de los sistemas acuáticos. En aguas productivas boreales y templadas, donde los organismos están expuestos a cambios ambientales periódicos, los ciclos de vida son comúnmente heteromórficos y tienen como particular característica ampliar la gama de condiciones ambientales donde la especie puede sobrevivir (Dale, 1983; Kremp, 2013). Un ciclo de vida heteromórfico representa una ventajosa estrategia para la especie debido a que permite distribuir la biomasa en estados de diferentes rangos de tamaño, morfologías, y capacidades de supervivencia y defensa. La capacidad de formar estados morfológicamente diferenciados está generalizada en dinoflagelados, pero no parece estar presente en la mayoría de las especie (Von Dassow & Montresor, 2011).

2.3.1. Ciclo de vida

En el ciclo de vida de una especie, la fase vegetativa es la etapa donde ocurre el crecimiento poblacional mediante reproducción asexual, es decir, por mitosis. Si el crecimiento sólo se expresa mediante células haploides (1N) el ciclo de vida es haplonte. Si sólo las células diploides (2N) experimentan crecimiento, el ciclo de vida es considerado diplonte. Mientras que si ambas células, 1N y 2N, experimentan crecimiento (mitótico), el ciclo de vida es haplodiplonte (Von Dassow & Montresor, 2011). Se considera que los dinoflagelados presentan un ciclo de vida haplonte (Fig. 5) durante el cual la fase vegetativa es haploide y es ésta la que se reproduce asexualmente por mitosis y sufre un aumento concomitante en la biomasa (Elbrächter, 2003). El ritmo de crecimiento puede variar dependiendo de la capacidad de crecimiento específico de la especie, el cual puede estar regulado por factores ambientales. Dentro del ciclo haplonte, por determinadas condiciones que se desconocen en dinoflagelados, las células vegetativas forman gametos que se fusionan y forman un planocigoto diploide que puede dividirse por meiosis o enquistar (Kremp, 2013) (Fig. 5).

Hasta la década de los 90 se consideró que en dinoflagelados el ciclo sexual era raro y limitado a condiciones ambientales desfavorables y que mayoritariamente desembocaba inequívocamente en la producción de quistes de resistencia (von Stosch 1973; Anderson and Wall, 1978). Sin embargo, la sexualidad en estos microorganismos ha sido reconocida como un paso independiente al enquistamiento ya que se ha demostrado experimentalmente que los cigotos móviles se dividen en muchas especies (Uchida et al., 1996; Figueroa et al., 2006a,b,c; Figueroa et al., 2007; Figueroa et al., 2008a; Figueroa et al., 2009; Gribble et al., 2009; Tillman & Hoppenrath, 2013). Más aún, recientemente ha sido sugerido mediante estudios de campo que la formación y las tasas de inducción sexual son mucho más altas de lo que previamente se ha reportado en cultivos (Brosnahan et al., 2014). Adicionalmente, en un estudio del dinoflagelado formador de floraciones tóxicas *Alexandrium minutum* en cultivo, se ha

demostrado que los planocigotos se comportan como una población con un ciclo de división independiente del enquistamiento, y que siguen un ritmo diario y dependiente de la luz similar al del ciclo mitótico haploide (Figueroa et al., 2015). Todos estos conocimientos sobre las transiciones entre las formas planctónicas y bentónicas y entre las etapas asexuales y sexuales han revelado las complejas historias de vida de los dinoflagelados (Fig. 5) y que la sexualidad es más frecuente de lo que se pensaba anteriormente.

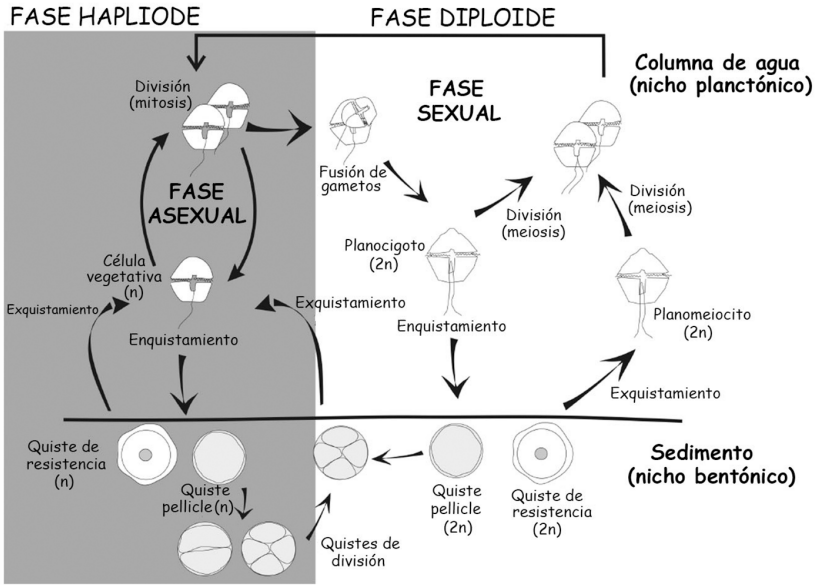

Fig. 5. Ciclo de vida de un dinoflagelado donde se incluyen todas las posibles transiciones. Modificado de Bravo & Figueroa (2014).

Cabe mencionar que la generalización del carácter haplonte del ciclo de vida de los dinoflagelados se ha basado en la observación de la división meiótica en los cigotos de algunas especies, e indicaría, por lo tanto, que los cigotos son las únicas células diploides en estos microorganismos. Esta definición se ha basado en la observación de la ciclosis nuclear—movimiento giratorio del contenido nuclear

que ha sido descrito como signo de meioisis (Pouchet 1883)—en los cigotos de dinoflagelados (von Stosch, 1972; Elbrächter, 2003; Parrow & Burkholder, 2004). Sin embargo, esto se ha puesto en cuestión para algunas especies. La primera y muy ampliamente citada como excepción a esa generalización fue la especie *Noctiluca scintillans* que fue previamente descrita como diplonte por Zingmark (1970) aunque refutado posteriormente por Schnepf & Drebes (1993). También recientemente se ha descrito mitosis y meiosis en el planocigoto del dinoflagelado pseudocolonial *Polykrikos kofoidii* que indicaría que su ciclo es haplodiplonte (Tillmann & Hoppenrath, 2013). Estos autores observaron que la ciclosis nuclear ocurrió posteriormente a la división mitótica de los planocigotos. Además, en el ciclo de división sexual de *A. minutum*, su parecido al ciclo celular mitótico de las células vegetativas haploides sugiere que la división del planocigoto podría ser por división mitótica (Figueroa et al., 2015). Es importante señalar que la meiosis en dinoflagelados ha sido poco estudiada y pobremente caracterizada (Bhaud et al 1988; Soyer-Gobillard et al., 2002; Parrow & Burholder, 2004), y si bien es cierto que se ha descrito ciclosis nuclear en cigotos de algunas especies, queda mucho por dilucidar para poder generalizar ese patrón para todos los dinoflagelados. Realmente, hoy por hoy no hay pruebas que demuestren que la división de los cigotos en dinoflagelados sea únicamente meiótica.

2.3.2. Tipos de compatibilidad sexual

En el ciclo de vida de dinoflagelados los sistemas de apareamiento son un importante aspecto a considerar. Las especies han sido tradicionalmente clasificadas como homotálicas y heterotálicas dependiendo de la capacidad de un clon de producir quistes de resistencia (homotalismo) o de la necesidad de requerir de dos cepas clonales compatibles (heterotalismo) para producir estos estados sexuales (Blackburn, et al., 2001). De acuerdo a estas definiciones, el dinoflagelado tóxico *Alexandrium catenella* ha sido tradicionalmente clasificado como heterotálico (Yoshimatsu, 1981), y *Alexandrium taylorii* como homotálico (Giacobbe & Yang, 1999). Sin embargo, se ha demostrado que el sistema de

apareamiento puede ser variable y complejo, ocurriendo homotalismo y heterotalismo en una misma especie y los patrones de compatibilidad cambiando en el tiempo (Montresor et al., 2003; Kremp, 2013) como se ha reportado en las especies *Scrippsiella trochoidea* (Montresor et al., 2003) y *Gymnodinium catenatum* (Figueroa et al., 2008b). Además, actualmente se sabe que en dinoflagelados la sexualidad se expresa no sólo a través de la formación de quistes, por lo que la definición del tipo de compatibilidad sexual basada en formación de quistes de resistencia, aunque hoy en día todavía en uso, es limitada; más apropiado sería incluir otros niveles de sexualidad como formación y división del cigoto (Blackburn et al., 2001).

2.3.3. Formas bentónicas

Dentro de la fase sexual del ciclo de vida (Fig. 5), los quistes de dinoflagelados han sido ampliamente estudiados. Se sabe que al menos 10% de todos los dinoflagelados, y en áreas templadas hasta el 28% de ellos, tienen quistes de resistencia durante sus ciclo de vida (Dale, 1983; Persson et al., 2000, 2008). El rol ecológico que se le ha atribuido a los quistes de resistencia ha sido muy variado, entre ellos el de producir dispersión de la especie (Hallegraeff, 1993), sustentar el desarrollo y recurrencia de las floraciones (Anderson, 1998; Ishikawa & Taniguchi, 1996), proporcionar supervivencia bajo condiciones adversas (Dale, 1983), y producir recombinación genética mediante la fusión de gametos (Anderson, 1998). Adicionalmente, los quistes son muy importantes en estudios de fitoplancton nocivo debido a que pueden dar alerta temprana ante la presencia de especies tóxicas, revelar especies no observadas comúnmente en el plancton, especies de vida corta, frágiles, o difícil de identificar (Hesse et al., 1996), esto último debido a que en ciertos géneros (e.g. *Scrippsiella*) las diferencias morfológicas entre especies son más obvias a nivel de quiste que en estados vegetativos (Lewis, 1991).

Los quistes pellicle, o también denominados quistes temporales o ecdísicos, se definieron primeramente cómo estados no móviles de pared fina formados cuando

células vegetativas móviles eran expuestas a condiciones desfavorables, tales como choques mecánicos o cambios súbitos de temperatura (Anderson & Wall, 1978; Garcés et al., 2002). Hoy en día se sabe que estos quistes también pueden ser de origen sexual (Fig. 5) y que algunas especies los forman como estrategia para el mantenimiento de sus poblaciones en ambientes cuyas condiciones cambian en periodos cortos de tiempo (Bravo & Figueroa, 2014). Por ejemplo, *A. taylorii* y *A. minutum* forman este tipo de quistes en circunstancias que han sido asociadas a evitar la dispersión por el viento. Estas transformaciones rápidas de células móviles a quistes minimizan las pérdidas por advección y facilitan el desarrollo de sus floraciones. Esta estrategia a corto plazo se complementa con la estrategia de largo plazo que esas especies llevan a cabo a través de sus quistes de resistencia (Garcés et al., 2002; Bravo et al., 2010).

3. Especies y aspectos estudiados

En esta tesis se abordan de manera experimental los siguientes estudios de los dinoflagelados productores de FANs *Alexandrium ostenfeldii* y *Protoceratium reticulatum*:

Alexandrium ostenfeldii es una especie de gran interés por su amplia distribución geográfica y por la producción de toxinas. En el **Artículo I** se aborda el estudio genético, morfológico, y de perfiles de toxinas de cepas de *A. ostenfeldii* procedentes del Mar Mediterráneo, Mar Báltico, y sur de Chile. Y en el **Artículo II** se describe la cinética y el efecto de la temperatura y salinidad en el crecimiento y la producción de toxinas (toxinas PSP y GYMs) de la cepa del Mar Báltico mediante un diseño factorial.

En relación a *Protoceratium reticulatum*, primeramente se abordó el estudio filogenético de las diferentes cepas de la Colección de Cultivos del Centro Oceanográfico de Vigo (CCVIEO). Al observarse que había cepas clasificadas

como *P. reticulatum* pero que morfológica y genéticamente constituían una nueva especie, se realizó su descripción como *Ceratocorys mariaovidii* (**Artículo III**). Estas cepas habían sido identificadas erróneamente como *P. reticulatum* debido a su similitud morfológica. Se realizó también la descripción de un tipo de células con forma de vida bentónica de esas dos especies (**Artículo IV**) que sugieren estrategias adaptativas peculiares. Por otra parte, debido a la escasa literatura que había sobre el ciclo de vida de *P. reticulatum*, se realizó el estudio en detalle de los diferentes estados celulares (asexuales/sexuales, plantónicos/bentónicos) a través de los cuales se sugieren diferentes estrategias de vida que caracterizan a la especie (**Artículo V**).

A continuación se hace una introducción de los aspectos más sobresalientes de estas dos especies de dinoflagelados:

3.1. *Alexandrium ostenfeldii*

Dentro de los dinoflagelados tóxicos a nivel mundial, el género *Alexandrium* es el que incluye el mayor número de especies productoras de eventos FANs asociadas a brotes de intoxicación por toxinas PSP (Anderson et al., 2012b). Además de estas toxinas, otros grupos tales como SPXs y GYMs han sido detectados en el género (Cembella et al., 2000; Van Wagoner et al., 2011; Artículo I de esta tesis). Estos tres tipos de toxinas pueden presentarse en variadas combinaciones en una especie o cepa (Tomas et al., 2012; Martens et al., 2017). De las ~30 especies definidas morfológicamente en *Alexandrium*, alrededor de la mitad de ellas son conocidas por producir toxinas (Anderson et al., 2012b), y su área de distribución se ha extendido en las últimas décadas en diversas partes del mundo (Cho et al., 2008). El éxito de colonización y persistencia de este género en diversos ambientes ha sido atribuido a adaptaciones ecofisiológicas (e.g. quistes de resistencia, alta capacidad de migración vertical) que muchos de sus miembros poseen (Anderson et al., 2012b). *Alexandrium* además de presentar el mayor número de especies

tóxicas entre los dinoflagelados (Anderson et al., 2012b) es el mayor productor de saxitoxina (STX) y sus análogos asociados a síndromes PSP en zonas subárticas, templadas y tropicales (Taylor et al., 1995). Dentro de las especies tóxicas de este género una de las menos estudiadas es *A. ostenfeldii* (Fig. 6), y el interés en esta microalga durante la última década ha aumentado debido a sus cada vez más frecuentes y densas floraciones (Van de Waal., 2015; Martens et al., 2017).

A mediados de la década del 90, Balech (1995) clasificó el género *Alexandrium* en distintos grupos de acuerdo a criterios morfológicos. Uno de esos fue el denominado "Grupo *Alexandrium ostenfeldii*" que incluía las especies *Alexandrium peruvianum* (Balech & Mendiola, 1977), *A. ostenfeldii* (Balech & Tangen 1985) y *Gonyaulax dimorpha* (Biecheler, 1952). La agrupación de aquellas especies se basó en que todas tienen una forma globular, una fina pared tecal, y una angosta y alargada primera placa apical (1') con un gran poro ventral ubicado en el lado anterior derecho la principal característica de este grupo. Entre las tres, *G. dimorpha* nunca ha sido transferida al género *Alexandrium* debido a que su identidad no ha sido aceptada por algunos autores y porque no se ha verificado el material tipo. Las otras dos, sin embargo, fueron separadas sólo por muy sutiles diferencias morfológicas en placas definitorias, tales como la 1', sexta precingular (6''), y sulcal anterior (Sa). Uno de los rasgos más mencionados en la literatura para diferenciar ambas especies, por ejemplo, era la forma de la Sa, la cual en *A. ostenfeldii* era más ancha que larga con un borde anterior horizontal, mientras que en *A. peruvianum* era triangular o en forma de "A" (Bravo et al., 2006; Tomas et al., 2012). Recientemente, sin embargo, se ha establecido mediante estudios filogenéticos y morfológicos de cepas de *A. ostenfeldii* y *A. peruvianum* de distintas zonas geográficas, que ambas especies corresponden a una misma especie y que *A. peruvianum* debe ser considerado como sinónimo de *A. ostenfeldii*, y por lo tanto, descartado como taxón distinto (Kremp et al., 2014).

Las células de *A. ostenfeldii* se caracterizan por tener una forma globular en vistas ventral y dorsal, y redonda en vistas apical o antapical (Figs. 3A y 6A–D).

La epiteca es ligeramente variable en forma con un contorno que va desde sigmoideo a forma de domo o redondo. La hipoteca generalmente es redonda. El cíngulo es ligeramente escavado y desplazado menos de un ancho del cíngulo hacia la izquierda de la célula (Fig. 6B). El sulco es muy poco profundo. Su teca es fina y puede presentar pequeños poros casi imperceptibles en microscopía de luz. El patrón de placas es Po, 4', 6", 6c, 9–10s, 5"', 2"" (Balech & Tangen, 1985). Los tamaños celulares pueden ser muy variables, desde 26.6 a 53.4 µm de largo y de 30.6 a 40.5 µm de ancho. Los cloroplastos orientados radialmente y el núcleo en forma de U ubicado ecuatorialmente (Fig. 6D) se ajustan a los de otras especies de *Alexandrium*. Su quiste de resistencia tiene una forma esférica con una doble pared y una gran cantidad de compuestos de reserva en su interior (Fig. 6E).

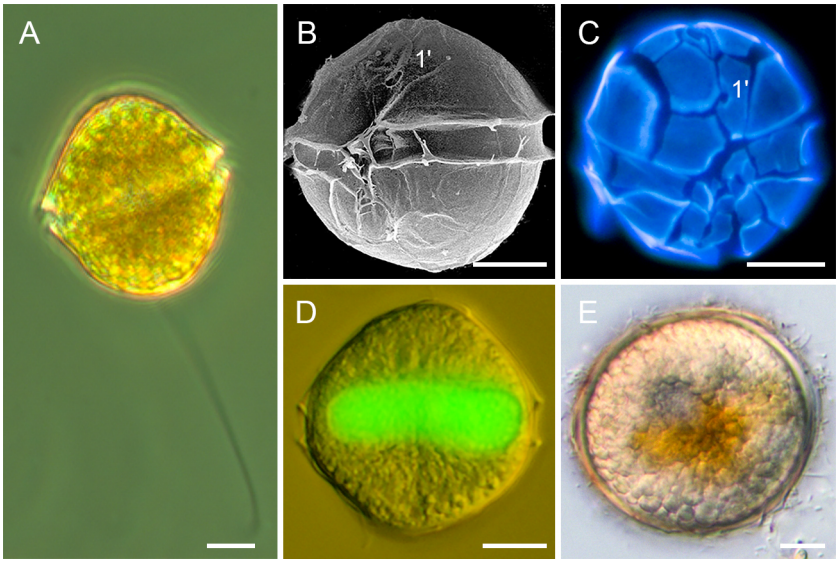

Fig. 6. Imágenes de microscopía de luz (A, C–E) y microscopia electrónica de barrido (B) de *Alexandrium ostenfeldii*. (A) Célula vegetativa. (B) Célula en vista ventral. (C) Célula teñida con Calcofluo en vista ventral. (D) Núcleo teñido con Sybr Green. (E) Quiste de resistencia. Barras de escala 10 µm. 1': primera placa apical.

3.1.1. Distribución geográfica

Alexandrium ostenfeldii es una especie cosmopolita. La mayoría de sus registros son de aguas frías y ha sido considerado tener una distribución ártico-boreal (Okolodkov, 2005). Sin embargo, también ha sido identificado en zonas cálidas y tropicales. Sus células móviles y/o quistes bentónicos han sido ampliamente observados en zonas templadas de Europa (Balech & Tangen, 1985, Kremp et al., 2014), Norte América (Cembella et al., 2000, Tomas et al., 2012), Ártico Ruso (Okolodkov & Dodge, 1996), y Patagonia chilena y argentina (Guzmán et al., 2011; Almandoz et al., 2014). También ha sido reportado en aguas y/o sedimentos de la península ibérica (Fraga & Sánchez, 1985, Bravo et al., 2006), Nueva Zelanda (Mackenzie et al., 1996), Perú (Sánchez et al., 2004), y Japón (Nagai et al., 2010). Aunque *A. ostenfeldii* fue inicialmente descrito en las costas de Perú—como *A. peruvianum* por Balech & de Mendiola, 1977—muy poco se conoce aún acerca de su distribución y sus toxinas en Sudamérica. En el Pacífico chileno su presencia ha sido citada tanto en el norte, centro, y sur del país (Guzmán et al., 2011; Salgado et al., 2012, 2013), aunque con presencia notoriamente más habitual en todo el sistema de fiordos y canales de la Patagonia (~41.5–55ºS; Guzmán et al., 2011; Guzmán et al., 2015). Su distribución más austral (~55º S) corresponde actualmente al Canal Beagle (Almandoz et al., 2014), que es compartido por Chile y Argentina. *Alexandrium ostenfeldii* ha sido considerado presentarse comúnmente en bajas concentraciones junto a otros dinoflagelados formadores de floraciones. Sin embargo, durante la última década sus floraciones masivas y cada vez mas frecuentes han sido reportadas en distintas áreas costeras, tales como sistemas estuarinos de Holanda (Van de Waal et al., 2015), Mar Báltico (Kremp et al., 2009) y costa este de Estados Unidos (Tomas et al., 2012).

3.1.2. Toxinas

Alexandrium ostenfeldii es el único miembro del género *Alexandrium* capaz de producir toxinas PSP, SPXs, y GYMs (Cembella et al., 2000; Van Wagoner et al., 2011; Artículo I de esta tesis). La producción de estas toxinas puede variar de acuerdo a la cepa y a su distribución geográfica. Inicialmente, las toxinas PSP en *A. ostenfeldii* fueron detectadas en cepas aisladas desde un fiordo Danés (Hansen et al., 1992), un descubrimiento que luego fue confirmado en cepas provenientes desde lugares tan distantes como el Mar Báltico (Kremp et al., 2014) y los fiordos chilenos (Pizarro et al., 2012; Artículo I de esta tesis). Sin embargo, la especie se vincula cada vez con mayor frecuencia a la producción de SPXs y GYMs. Los SPXs fueron descubiertos inicialmente en glándulas digestivas de mariscos (Hu et al., 1995) y luego en cepas de *A. ostenfeldii* del Atlántico canadiense (Cembella et al., 2000). Aunque los primeros estudios identificaron los espirólidos A, B, C y D, además de los isómeros C y D y algunos derivados (13-desMetil-SPX C y D), estudios posteriores indicaron que la diversidad de este grupo de compuestos producidos por *A. ostenfeldii* era mucho mayor (Ciminiello et al., 2006, 2007; Tillmann et al., 2014). Dentro del grupo de toxinas producidas por *A. ostenfeldii* los SPXs han sido los más documentados, sin embargo, en los últimos años la detección de GYMs se ha hecho cada vez más frecuente (Van Wagoner et al., 2011; Martens et al., 2017, Artículo I de esta tesis). Antes del primer descubrimiento de GYMs en *A. ostenfeldii* de la costa Este de Estados Unidos (Van Wagoner et al., 2011) estas toxinas solo habían sido encontradas en el filogenéticamente distante género *Karenia* (Haywood et al., 2004). Posteriormente se identificaron en cepas de *A. ostenfeldii* provenientes de los Países Bajos (Van de Waal et a., 2015), y en el Artículo I y II de esta tesis se describe y se cuantifica, respectivamente, en una cepa del Mar Báltico. La diversidad de compuestos perteneciente al grupo de las GYMs que han sido identificado en *A. ostenfeldii* en los últimos años (Harju et al., 2016; Martens et al., 2017) indicaría que la producción de estas toxinas puede ser un rasgo más común de lo que se pensaba.

3.2. *Protoceratium reticulatum*

Protoceratium reticulatum fue descrito inicialmente como *Peridinium reticulatum* por Claparède y Lachmann (1858–1859) y posteriormente traspasado al género *Protoceratium* por Bütschli (1885). Cuando Reinecke (1967) describió *Gonyaulax grindleyi* desde Bahía Elands en Sudáfrica como una nueva especie—probablemente desconociendo el trabajo realizado anteriormente por Bütschli (1885)—creó una confusión de nombres ya que correspondía exactamente a *P. reticulatum*. Actualmente, ambas especies son consideradas como sinónimos pero el nombre de esta última tuvo prioridad por antigüedad.

Protoceratium reticulatum (Fig. 7) es considerado un importante dinoflagelado dentro del fitoplancton marino debido a su amplia distribución geográfica y a la producción de yesotoxinas (YTXs) (Paz et al., 2004, 2007). Sus células vegetativas tienen una forma subesferoidal cuando se observan en vista ventral y dorsal (Fig. 7A–C), y casi redondas en vista apical y antapical. El tamaño de esta especie puede variar entre 24 y 52 µm de largo y entre 20 y 43 µm de ancho. Su morfología destaca frente a otros dinoflagelados debido a que presenta una teca fuertemente ornamentada con retículos (Figs. 3C y 7C). Su epiteca es más corta que la hipoteca y no presenta cuernos ni espinas (Reinecke, 1967). Se ha mencionado que la fuerte reticulación puede ocultar las suturas que demarcan los bordes de las placas haciendo que sea difícil realizar estudios taxonómicos detallados sin una tinción adecuada (e.g. Calcofluor). La placa 1' se caracteriza por ser un poco más larga que ancha, por presentar un poro ventral en su borde anterior derecho y por contactar claramente la placa sulcal anterior (Sa) (Fig. 7C). La tabulación de sus placas es Po, 4', 0a, 6'', 6c, ~7s, 5''', 0p, 2'''', aunque también se ha mencionado que en lugar de cuatro placas apicales—como se documenta en esta tesis—tiene tres apicales y una intercalar (Reinecke, 1967). La diferente interpretación está basada en que algunas cepas presentan células en que la primera placa intercalar (1a según sistema de Kofoid) no toca la placa del poro apical (Po), mientras que en otras sí lo hace, por lo cual debiera ser considerada como parte de las placas apicales y no de

las intercalares. Debido a que en una misma cepa una placa no puede ser nombrada de distinta forma, se ha adoptado una versión relajada del sistema de nomenclatura de Kofoid denominándola como tercera apical (3') debido a que ésta es probablemente la placa homóloga de la intercalar 1a (Fensome et al., 1993). La variabilidad de contacto de esta placa con la Po ha sido mencionada en otros estudios de *P. reticulatum* (ver Woloszynka, 1928; von Stosch, 1969; Hansen et al., 1996/97; Sala-Pérez et al., 2016; Artículo V de esta tesis) y en la descripción de la nueva especie del género *Ceratocorys*, *C. mariaovidii*, presentada en el Artículo III de esta tesis.

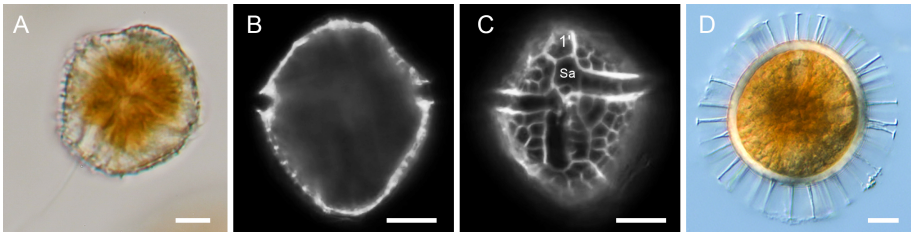

Fig. 7. Imágenes de microscopía de luz de *Protoceratium reticulatum*. (A) Célula vegetativa. (B) Célula teñida con Calcofluor. (C) Célula teñida con Calcofluo en vista ventral. (D) Quiste de resistencia. Barras de escala 10 µm. 1': primera placa apical; Sa: placa sulcal anterior.

Protoceratium reticulatum es una especie fototrófica que contiene cloroplastos que irradian desde el centro de la célula (Hansen et al. 1996/97). Una de sus peculiaridades es la producción de bioluminiscencia (Poupin et al., 1999) al igual que *Lingulodinium polyedrum*, otro dinoflagelado productor de yesotoxinas (Paz et al., 2004). Los estudios que tratan sobre la biología de *P. reticulatum* son muy escasos. Gran parte de los trabajos realizados sobre esta especie se centran en las toxinas (Aasen et al., 2005; Guerrini et al., 2007; Paz et al., 2004), la distribución espacio-temporal de sus quistes de resistencia (Marret & Zonneveld, 2003) y el potencial de estos últimos como proxy ambiental (Mertens et al., 2011; Jansson et

al., 2014; Sildever et al., 2015). Este dinoflagelado posee un ciclo de vida heteromórfico (Artículo V). En el ciclo se produce un estado no móvil (quiste de resistencia, Fig. 7D) cuya pared está formada de sustancias orgánicas con un alto potencial de preservación. Braarud (1945) fue el primer autor quien describió los quistes de *P. reticulatum*, los cuales se caracterizan por presentar una forma esférica con una gruesa pared de la cual emergen numerosos procesos delgados con extremos planos (Marret & Zonneveld, 2003). Se ha determinado que el número y la longitud de estos procesos, como también los de *L. polyedrum*, está asociada principalmente a la salinidad del mar en el momento de su formación (Mertens et al., 2011; Sildever et al., 2015).

3.2.1. Distribución geográfica

Protoceratium reticulatum es una especie que se encuentra ampliamente distribuida en áreas costeras de todo mundo. Su forma móvil y bentónica se encuentra en zonas frías y templadas del Atlántico, tales como Groenlandia, Mar del Norte, Mar Báltico, Patagonia argentina, Mar Mediterráneo y África occidental (e.g. Hansen et al., 1996/97; Marret & Zonneveld 2003; Mertens et al., 2011; Akselman et al., 2015; Sala-Pérez et al., 2016); y también en el áreas del Pacífico oriental y occidental, tales como Chile, Japón, Australia y la costa oeste de Estados Unidos (Deflandre & Cookson, 1955; Seguel et al., 2010; Álvarez et al., 2011; Alves-de-Souza et al., 2014; Guzmán et al., 2015). Se ha identificado también en zonas más cálidas como el Golfo de México, Pacífico Mexicano, y Belice (Scorzetti et al., 2009; Hernández-Becerril et al., 2010; EOL, 2017); aunque es más frecuente en zonas templadas. En Chile se encuentra en las costas norte y sur (Seguel et al., 2010; Álvarez et al., 2011), aunque su presencia es notablemente mayor en aguas de las regiones australes. En el sur de Chile ha sido registrada en las Regiones de Los Lagos, Aysén y Magallanes (~41.5–53º S), mientras que por el norte, solo en la región de Antofagasta (~23º S). Se ha mencionado su presencia en Los Lagos principalmente en los meses de verano (diciembre a febrero) y una floración fue correlacionada positivamente con alta concentración de YTXs en

bivalvos y en muestras de plancton (Alves-de-Souza et al. 2014). En la Región de Aysén—ubicada al sur de Los Lagos—la fase móvil es escasa en agosto (invierno austral) y noviembre (primavera austral) pero sus quistes en este período están distribuidos en los sedimentos de toda el área (Seguel et al. 2010). En el norte del país (Bahía Mejillones en la Región de Antofagasta) *P. reticulatum* también produce floraciones que han sido asociadas a procesos físico–biológicos. Álvarez et al. (2011) reportó una floración en verano de 2007, la cual se habría iniciado en alta mar por células móviles y quistes durante un pulso de surgencia, y habría sido empujada hacia la costa por efecto de la relajación de la surgencia. En aquel estudio se confirmó la capacidad de *P. reticulatum* del norte de Chile de producir YTXs. Otras floraciones también han sido documentadas en distintas zonas templadas del planeta como Flødevigen en Noruega (Aasen et al., 2005) y en el norte de Japón (Koike et al., 2006). Todos estos eventos han hecho que *P. reticulatum* sea habitualmente incluido en estudios de especies nocivas.

3.2.2. Toxinas

La yesotoxina (YTX) y los análogos 45-hidroxiyesotoxina (45–OHYTX) y 45,46,47–trinoryesotoxina (norYTX) fueron aislados por primera vez desde glándulas digestivas del ostión *Patinopecten yessoensis* en Bahía Mutsu, Japón a raíz de un episodio de intoxicación alimentaria con toxinas diarreicas (toxinas DSP) (Murata et al., 1987). Posteriormente las YTXs fueron identificadas en diferentes bivalvos (e.g. *Mytilus edulis*, *M. galloprovincialis, M. chilensis*, *Perna canaliculus*) en Noruega (Lee et al., 1988), Rusia, Chile, Nueva Zelanda (Yasumoto and Takizawa, 1997) e Italia (Ciminiello et al., 1997). Más tarde la producción de estas toxinas fue confirmada en el dinoflagelado *P. reticulatum* (Satake et al., 1997a, 1999; Boni et al., 2001).

Las YTXs son un grupo de toxinas poliéter disulfatadas cuyo peso molecular varía entre 955 y 1551 (mu). Su estructura química se caracteriza por contener 11 anillos éter adyacentes y se asemeja a la de otras ficotoxinas como las brevetoxinas y ciguatoxinas (Rodríguez et al., 2015). Teóricamente se han descrito alrededor de

100 análogos de YTXs, pero la estructura de la mayoría todavía no ha sido elucidada. Varios análogos también han sido reportados desde los dinoflagelados *L. polyedra*, *Gonyaulax spinifera* y *Gonyaulax taylorii* (Satake et al., 1997b; Rhodes et al., 2006; Álvarez et al., 2016) aunque *P. reticulatum* es responsable de la mayor parte de análogos encontrados posiblemente debido a que al ser el mayor productor de YTXs es la especie más estudiada (Paz et al., 2007). Algunas YTXs son producidas directamente por las microalgas, mientras que otros compuestos se producen por transformaciones enzimáticas ocurridas en los mariscos. Por ejemplo, la YTX y homoYTX son producidas por dinoflagelados, mientras que la 45–hidroxyYTX o la carboxyYTX han sido aisladas sólo a partir de bivalvos (Alfonso et al., 2016). En los moluscos, las YTXs sufren un extenso metabolismo con una vida media de 20–24 días (Aasen et al., 2005). Extracelularmente también se ha registrado la presencia de YTXs, lo cual indica que *P. reticulatum* libera las toxinas (exotoxina) al medio acuoso circundante (Hess & Aasen, 2007).

La inclusión de las YTXs en la lista de toxinas marinas se debe a que estos compuestos son tóxicos para ratones de laboratorio cuando se les inyecta intraperitonealmente, aunque su toxicidad oral es baja y no hay registros de intoxicaciones en humanos (Munday et al., 2008). Inicialmente las YTXs se incluían dentro del complejo DSP pues los dos grupos de toxinas son lipofílicas, por lo cual se extraían conjuntamente. La clasificación actual tiene en cuenta los efectos biológicos y por tanto se han excluido del complejo DSP puesto que no inhiben las proteínas fosfatasas y por tanto no tienen efecto diarreogénico (Ogino et al., 1997). El 31 de Diciembre de 2014, en la UE se reemplaza el bioensayo de ratón (AOAC, 1990) por métodos analíticos basados en cromatografía líquida acoplada a espectrometría de masas (LC-MS/MS) siguiendo el procedimiento oficial de análisis de la EFSA (EFSA Panel, 2010). Por otro lado, se ha descubierto que las YTXs son potentes citotoxinas (Pérez-Gómez et al., 2006) lo cual ha llevado a Autoridades Europeas establecer un nivel máximo permitido en mariscos para la suma de YTXs de 1 mg de YTX equivalentes/Kg.

Objetivos y contenido de la tesis

Objetivos y contenido de la tesis

Las FANs producidas por dinoflagelados son recurrentes en aguas costeras de todo el planeta y pueden ser eventos locales o afectar grandes áreas. En cualquier caso, pueden perjudicar la salud humana, los ecosistemas marinos y los recursos como el turismo, la pesca y la acuicultura. Aunque las medidas para contrarrestar las FANs son aún escasas, es claro que el control de estos eventos requiere de un conocimiento detallado de sus características básicas, como por ejemplo las estrategias adaptativas de las especies responsables, los factores ambientales que regulan a estas especies, y la taxonomía, genética y toxinas de las especies involucradas. Este tipo de estudios son necesarios debido a que el impacto de las FANs depende de las características intrínsecas de cada especie, de la dinámica de la floración y de las condiciones del ambiente.

Entre la gran mayoría de las microalgas productoras de eventos FANs, los dinoflagelados destacan por su nocividad. Este grupo tiene como característica general presentar organismos con complejos ciclos de vida que incluyen estados celulares con marcadas diferencias morfológicas y fisiológicas. Las transiciones entre las fases asexual y sexual y/o entre los diferentes estados en ciclos de vida heteromórficos requieren estudios detallados para comprender la dinámica de sus floraciones. Además, es importante conocer los factores ambientales que regulan su crecimiento y sus estrategias de supervivencia.

El trabajo de investigación de esta tesis tiene como objetivo principal profundizar en el conocimiento de las estrategias de supervivencia y producción de toxinas de dos dinoflagelados marinos productores de eventos FANs: *Alexandrium ostenfeldii* y *Protoceratium reticulatum*, especies que actualmente presentan lagunas de conocimiento respecto a sus características básicas tanto en poblaciones del sur de Chile como en muchas otras zonas geográficas. En las dos especies se necesitó la realización de estudios genéticos y morfológicos para la definición

detallada de las mismas. En concreto, los objetivos específicos se centraron en el estudio de:

1) Genética, morfología, y condiciones óptimas de crecimiento y producción de toxinas de *A. ostenfeldii* del Mar Mediterráneo, Mar Báltico, y sur de Chile bajo diferentes condiciones de salinidad y temperatura (**Artículos I** y **II**).

2) Genética, morfología y toxinas de las cepas de *P. reticulatum* de la Colección de Cultivos del Centro Oceanográfico de Vigo (CCVIEO) (**Artículos III** y **IV**). Aquí se describe la nueva especie de dinoflagelado marino *Ceratocorys mariaovidii* (**Artículo III)** y un estado desconocido del ciclo de vida de *P. reticulatum* y de *C. mariaovidii* (**Artículo IV**).

3) Ciclo de vida de *P. reticulatum* (**Artículo V**). Se determinan los patrones de división asexual y la fase sexual de la especie; se caracterizan las diferentes fases del ciclo de vida; y se estudian los procesos de enquistamiento y germinación.

Con el fin de cumplir el objetivo principal, se realizaron los siguientes trabajos de investigación incluidos en esta memoria:

I **Salgado, P**., Riobó, P., Rodríguez, F., Franco, J.M. & I. Bravo. 2015. Differences in the toxin profiles of *Alexandrium ostenfeldii* (Dinophyceae) strains isolated from different geographic origins: Evidence of paralytic toxin, spirolide, and gymnodimine. *Toxicon* 103:85–98.

II **Salgado, P**., Vázquez, J.A., Riobó, P., Franco, J.M., Figueroa, R.I., Kremp, A. & I. Bravo. 2015. A kinetic and factorial approach to study the effects of temperature and salinity on growth and toxin production by the dinoflagellate *Alexandrium ostenfeldii* from the Baltic Sea. *PLoS ONE*:10, e0143021

III **Salgado, P**., Fraga, S., Rodríguez, F., Riobó, P. & I. Bravo. *Ceratocorys mariaovidii* sp. nov. (Gonyaulacales), a new dinoflagellate species previously reported as *Protoceratium reticulatum*. *Journal of Phycology* XX:XX–XX (Aceptado).

IV **Salgado, P**., Fraga, S., Rodríguez, F. & I. Bravo. Benthic flattened cells of the phylogenetically related marine dinoflagellates *Protoceratium reticulatum* and *Ceratocorys mariaovidii*: a new type of cyst? *Journal of Phycology* XX:XX–XX (Aceptado).

V **Salgado, P**., Figueroa, R.I., Ramilo, I. & I. Bravo. 2017. The life history of the marine dinoflagellate *Protoceratium reticulatum* (Dinophyceae) in culture. *Harmful Algae* 68:67–81.

Anexos

I **Salgado P**, Riobó P, Rodríguez F and Bravo I (2016). Life cycle, toxinological features, and genetic characterization of the Harmful Algal Bloom producer dinoflagellate *Protoceratium reticulatum* from the austral coast of Chile (~44º–53º S). Front. Mar. Sci. *Conference Abstract: XIX Iberian Symposium on Marine Biology Studies, Porto, Portugal, 5 Sep - 9 Sep*.

Discusión de los resultados

Discusión de los resultados

1. Estudio de *Alexandrium ostenfeldii*

1.1. Distribución geográfica y diferenciación de perfiles de toxinas

En los últimos años se ha demostrado que *A. ostenfeldii* es capaz de producir una amplia variedad de toxinas por lo que su estudio resulta de gran interés, más aún si es el único dinoflagelado que presenta esta particular característica. En el Artículo I se estudiaron cepas de *A. ostenfeldii* provenientes de distintas áreas geográficas: Mar Mediterráneo, Mar Báltico, y sur de Chile. El propósito fue obtener poblaciones provenientes de condiciones ambientales diferentes y ver diferencias en los perfiles de toxinas cuando eran expuestas a diversas condiciones de salinidad y temperatura. Los resultados mostraron que la cepa del Mediterráneo produjo sólo SPXs, la del Báltico toxinas PSP y GYMs, y la del sur de Chile sólo toxinas PSP. Entre estas cepas se observó una diferenciación a nivel de perfiles de toxinas, morfología, y genética, aunque los perfiles de las cepas de cada área geográfica fueron siempre constantes bajo las distintas condiciones experimentales, no así el contenido de toxina que se sabe es modulado por factores ambientales (Maclean et al., 2003; Tatters et al., 2012). En el artículo se corrobora mediante morfología y genética que *A. ostenfeldii* y *A. peruvianum* corresponden a la misma especie y que *A. peruvianum* debe ser considerado actualmente como un sinónimo de *A. ostenfeldii* por su antigüedad taxonómica (e.g. Kremp et al., 2014, Tillmann et al., 2014).

Además en el Artículo I se incluye una tabla con gran parte de la información bibliográfica que hay hasta la fecha sobre tipos de toxinas producidas por *A. ostenfeldii* (considerando lo citado previamente como *A. peruvianum*) de muy diversos orígenes geográficos. Esta tabla ordena toda la información que estaba muy dispersa, por lo que facilita su comparación y pone de manifiesto una alta

diversidad de compuestos producidos por la especie. Como resumen se puede apuntar que: 1) el tipo de toxina más frecuentemente identificada en *A. ostenfeldii* son los espirólidos (SPXs); 2) se observan variadas combinaciones de toxinas dependiendo de las cepas y del origen geográfico (toxinas PSP/SPXs, toxinas PSP/GYMs y SPXs/GYMs); y 3) la producción de las tres toxinas distintas sólo fue documentada en muy pocos casos, siendo uno de ellos *A. ostenfeldii* de la costa este de USA (Borkman et al., 2012). Además, el estudio comparativo arrojó que los perfiles se encuentran mayormente distribuidos por áreas: 1) Los SPXs y las toxinas PSP aparecen de forma bastante consistente en el Atlántico norte, Mar Mediterráneo y Mar Báltico. 2) Las cepas del Atlántico norte y Mar mediterráneo fueron mayormente caracterizados por producir SPXs. 3) Las cepas del Mar Báltico se caracterizaron por producir principalmente toxinas PSP. Sin embargo, para sacar conclusiones definitivas sobre estas regiones, como sobre otras menos estudiadas como el sur de Chile, se requieren todavía más estudios.

1.2. Crecimiento y producción de toxinas

La capacidad de *A. ostenfeldii* del Mar Báltico de producir dos tipos de toxinas distintas (toxinas PSP y GYMs) generó el interés de estudiar en detalle el efecto conjunto de la salinidad y la temperatura sobre el crecimiento y la producción de toxinas mediante un análisis de diseño factorial. Los resultados presentados en el Artículo II describen las cinéticas de crecimiento así como las cinéticas de producción de un análogo de GYM-A y de toxinas PSP las cuales ocurrieron, en la mayoría de los casos, concomitantemente a la cinética de crecimiento (fases exponencial y estacionaria). Este comportamiento ha sido reportado también para otras especies de *Alexandrium* de diversos orígenes geográficos (Hwang et al., 2000; Grzebyk et al., 2003; Wang & Hsieh, 2005), como también para el productor de yesotoxinas *Protoceratium reticulatum* (Paz et al., 2006). Sin embargo, a diferencia de lo ocurrido con la mayoría de las condiciones experimentales

utilizadas, en condiciones con baja temperatura (12.5ºC y 14ºC) la producción de toxinas no fue consistente con el crecimiento. Este resultado podría estar relacionado con la inducción de sexualidad, la cual fue demostrada por la observación de planocigotos y de un mayor número de quistes de resistencia en bajas temperaturas.

El uso del enfoque cinético y factorial es una herramienta de gran utilidad que permitió estudiar la ventana ambiental de crecimiento de *A. ostenfeldii* del Mar Báltico. Información de este tipo es esencial para especies que cuentan con una amplia distribución geográfica y para las cuales se carece de información ecológica, tal como ocurre con *A. ostenfeldii*. La ventana de crecimiento de la cepa estudiada fue amplia (5–21 y 12.5–25.5ºC, respectivamente), alcanzando un crecimiento óptimo a una salinidad de 11.2 y a una temperatura de al menos 25.5ºC, lo cual particularmente para la salinidad concuerda con estudios llevados a cabo con cepas de la especie provenientes de la misma área geográfica (Kremp et al., 2009). Los resultados principalmente de temperatura de la cepa báltica apoyan las preocupaciones expresadas por otros investigadores con respecto al potencial aumento de las floraciones de esta especie como una posible respuesta al cambio climático (Kremp et al., 2012). Análisis de este tipo son adecuados para estudiar tanto la variabilidad intraespecífica dentro de una región geográfica, como con poblaciones de otras regiones para conocer y ampliar el conocimiento de la autoecología de la especie.

2. Estudio de *Protoceratium reticulatum*

El estudio de *P. reticulatum* se realizó inicialmente mediante el análisis genético, toxinológico, y morfológico de las cepas incluidas en la Colección de Cultivos del centro Oceanográfico de Vigo (CCVIEO). Los resultados obtenidos permitieron identificar que dentro del grupo de cepas identificadas como *P. reticulatum*, dos de ellas presentaban una notoria variabilidad genética, las cepas CCMP404 y

CCMP1720, ambas provenientes de Estados Unidos. La variabilidad señalada había sido ya mencionada en estudios preliminares (Akselman et al., 2015; Sala-Pérez et al., 2016) los cuales habían dado luces de una posible nueva especie. En los análisis de toxinas realizados con ambas cepas no se detectaron yesotoxinas (YXTs), lo cual coincidió con los resultados de Paz et al. (2007). Sin embargo, fueron los estudios morfológicos junto con los genéticos los que mostraron definitoriamente que las cepas CCMP404 y CCMP1720 constituían una nueva especie del género *Ceratocorys*, la cual fue descrita en el Artículo III como *Ceratocorys mariaovidii*. Hasta el momento, esta nueva especie es la más distinta del género *Ceratocorys* y la más parecida al género *Protoceratium*.

2.1. Descripción de *Ceratocorys mariaovidii* sp. nov.

En el Artículo III de esta tesis se describe *Ceratocorys mariaovidii*. Morfológicamente se diferenció de *P. reticulatum* principalmente por: 1) la ausencia de una de sus placas epitecales—la cuarta precingular (4")— y 2) la presencia de cinco placas precingulares. Este último rasgo ha sido documentado para el género *Ceratocorys* (Fensome et al., 1993; Carbonell-Moore, 1996), mientras que las seis precingulares que presenta *P. reticulatum* es común dentro de orden Gonyaulacales (Balech 1988), del cual *Ceratocorys* también forma parte (Graham, 1942). Estas diferencias morfológicas claves fueron pasadas por alto durante varias décadas probablemente debido a que, al igual como ocurre con *P. reticulatum*, *C. mariaovidii* presenta una superficie tecal fuertemente reticulada que impide distinguir con claridad la tabulación y orientación de las placas (Hargraves & Maranda, 2002). En el Artículo III, entre otros caracteres morfológicos de esta nueva especie, se resalta la forma del poro apical de la placa Po, un carácter específico de géneros de dinoflagelados (Karen A. Steidinger, comunicación personal). Las interrogantes que se presentan en el trabajo en torno a este tema deben ser resueltas en estudios que incluyan cepas obtenidas desde las

localidades tipo de cada una de las especies de los dos géneros con la finalidad de realizar análisis morfométricos, estudios de placas—particularmente la Po—y de sus secuencias genéticas, validando de esta manera la tabulación de placas de cada especie y su identidad.

Los análisis filogenéticos apoyaron la clasificación de *C. mariaovidii* como una nueva especie del género *Ceratocorys*. Aunque debido a la falta de secuencias adicionales de especies de *Ceratocorys*—existe sólo la de *C. horrida*—el clado monofilético de *Ceratocorys* presentado en el Artículo III no fue bien definido. Basados sobre criterios taxonómicos actuales y a la falta de secuencias que entregaran más información, se consideró que la integración de *C. mariaovidii* en el género *Ceratocorys* era la acción más adecuada en este momento. Esta integración además es apoyada por la estrecha relación filogenética entre el género *Ceratocorys* y *Protoceratium* (Saldarriaga et al., 2004; Gómez et al., 2011).

La distribución de *C. mariaovidii* indica que es una especie de aguas cálidas. La especie ha sido aislada desde el mar de Salton—un lago hipersalino que presenta temperaturas anuales entre 12ºC y 40ºC (Reifel et al., 2002)—ubicado al sureste de California, y desde aguas del sur de Florida (NCMA, 2017). Además se puede deducir su presencia desde información proveniente de la costa de Belice (Faust et a., 2005; EOL, 2017). Un hecho interesante es la presencia de *P. reticulatum* en estas últimas dos zonas (Scorzetti et al., 2009; EOL, 2017). Adicionalmente se sospecha fuertemente de la presencia de *C. mariaovidii* en aguas de Kuwait (María Saborova (María Saborova, comunicación personal) pero aún requiere estudios definitorios. La correcta identificación y clarificación de qué especie o especies están presentes en una zona determinada es esencial dada la toxicidad de *P. reticulatum* pero no de *C. mariaovidii*.

2.2. Células planas de *P. reticulatum* y *C. mariaovidii*

Durante los diversos estudios de *C. mariaovidii* y *P. reticulatum*, en los cultivos de las dos especies se observaron células con una morfología diferente a la característica de cada especie, pero que sin embargo seguían conservando la tabulación de las placas tecales. La morfología de estas células, así como su tabulación y cinética de formación, se describen en el Artículo IV, donde también se discute si pueden constituir un tipo de quiste. De hecho, algunas características mostradas en diferentes grados en las células planas sugieren que son quistes, como por ejemplo su comportamiento bentónico y mayormente inmóvil, la forma irradiada de los cloroplastos que se concentran en el centro de las células, los gránulos de reserva, el citoplasma reducido, la ecdisis, y la formación y división de nuevas células vegetativas después de ser transferidas a medio repleto de nutrientes. Sin embargo, el hecho de tener flagelos hace que sean distintas a cualquier tipo de célula que haya sido denominada como quiste (Garcés et al., 2001; Von Dassow & Montresor, 2011). En cualquier caso, su existencia sugiere para las dos especies una elevada plasticidad en relación a su adaptabilidad desde plancton al bentos y viceversa, como ya se ha sugerido para dinoflagelados u otros grupos de organismos planctónicos (Boero et al., 1996; Marcus & Boero 1998). Dada la complejidad de formas bentónicas en morfología y función descritas en las últimas décadas en dinoflagelados (Kremp 2013; Bravo & Figueroa 2014), las cuales han demostrando un acoplamiento del plancton al bentos mucho más continuo de lo que se pensaba, en la discusión del Artículo IV se incluye un debate sobre los diversos tipos de quistes en dinoflagelados y cuál de ellos podría asimilarse mejor a las células planas descritas.

2.3. Ciclo de vida de *P. reticulatum*

En el Artículo V se describe por primera vez el ciclo de vida de *P. reticulatum* en cultivo. En esta publicación no se incluye la célula plana (descrita en Artículo IV),

sin embargo se debe destacar que este estado también forma parte del ciclo de vida de *P. reticulatum*. La célula plana junto con el ya descrito anteriormente quiste de resistencia (Braarud, 1945; Wall & Dale, 1968) pone de manifiesto la gran plasticidad ecológica que poseería esta especie a la hora de adaptarse a diferentes ambientes, lo cual podría estar relacionado con su amplia distribución geográfica (Marret & Zonneveld, 2003; de Vernal & Marret, 2007). El largo periodo de latencia (~4 meses) descrito en el Artículo V para el quiste de resistencia, en oposición a la rápida reversibilidad de las células planas (Artículo IV), revela una función diferente para cada una de estas formas bentónicas y por lo tanto más versatilidad ecológica para la especie.

Además de las características de la división vegetativa (estudio morfológico y del ciclo celular por citometría), en el Artículo V se ponen de manifiesto peculiaridades importantes de su ciclo sexual: 1) su cualidad de heterotálico complejo en relación a la formación de quistes de resistencia, pero homotálico en relación a la formación de planocigotos; 2) la elevada diferenciación de formas nucleares de los estados sexuales demuestran una destacada división sexual tanto en número y formas diferenciadas; y 3) una de las células hijas resultante de la primera división de los planocigotos y planomeiocitos (éste último referido en el artículo como *germling*) es biflagelada. Estos resultados sugieren la posibilidad de que las diferentes formas de división de los planocigotos y planomeiocitos detectados a través de las distintas configuraciones nucleares pudieran corresponder a mitosis y meiosis y no sólo a esta última cómo correspondería en relación al ciclo haplóntico descrito para dinoflagelados. Este punto es de gran interés en dinoflagelados ya que muy recientemente se han publicado trabajos que sugieren la ocurrencia de división mitótica en *P. kofoidii* (Tillmann & Hoppenrrath, 2013) y *A. minutum* (Figueroa et al 2015).

Conclusiones

Conclusiones

1. *Alexandrium ostenfeldii* puede producir toxinas paralizantes (toxinas PSP), espirólidos (SPXs), y gimnodiminas (GYMs), por ello los estudios toxinológicos de la especie deben considerar estos tres grupos de compuestos. En esta tesis se observaron diferentes perfiles de toxinas los cuales dependieron de la distribución geográfica de las cepas. Mientras que la cepa del Mar Mediterráneo produjo SPXs, el perfil de la cepa del Mar Báltico estuvo definido por toxinas PSP y GYMs, y la del sur de Chile sólo por toxinas PSP.

2. Las cepas de *A. ostenfeldii* procedentes del Báltico y del sur de Chile estudiadas en esta tesis presentaron el mismo perfil de toxinas paralizantes: GTX–3, GTX–2, y STX. Este perfil como los otros se mantuvieron invariables frente a distintas condiciones ambientales de salinidad y temperatura pero se modificó el contenido de toxina por célula.

3. El diseño factorial resultó ser una herramienta estadística adecuada para estudiar con un número reducido de experimentos la ventana ambiental y los óptimos de crecimiento y producción de toxinas de *A. ostenfeldii* Báltico a diferentes condiciones de temperatura y salinidad. El aumento de temperatura estimuló el crecimiento y la producción de toxinas (toxinas PSP y un análogo de GYM-A) y salinidades por encima de 21 limitaron el crecimiento de la cepa. El crecimiento óptimo se consiguió a una temperatura de 25.5ºC y a una salinidad de 11.2. Los óptimos de temperatura y salinidad para la producción del análogo de GYM-A fueron 20.9ºC y salinidad 17, y para las toxinas PSP a >19ºC y salinidad 15.

4. La caracterización morfológica y genética de dos cepas de la colección de cultivos CCVIEO, originariamente identificadas como *Protoceratium reticulatum*, permitió la diferenciación y descripción de una nueva especies del género *Ceratocorys*, *Ceratocorys mariaovidii*. Esta especie no produce toxinas y se diferencia de *P. reticulatum* principalmente por la presencia de cinco placas precingulares en vez de seis. Para una correcta caracterización ecológica y biogeográfica de estas dos especies se hace necesario el uso de técnicas morfológicas y/o genéticas que las discriminen. Lo que se sabe hasta ahora sobre la distribución de *C. mariaovidii* indicaría que esta especie es de aguas cálidas.

5. *Protoceratium reticulatum* presentó un ciclo de vida heteromórfico caracterizado por células vegetativas haploides móviles, planocigotos, quistes de resistencia sexuales, y formas bentónicas aplanadas y flageladas. Como conclusiones se destacan: 1) heterotalismo complejo en relación a la formación de quistes de resistencia pero homotalismo en relación a la formación de planocigotos; 2) abundancia de división de planocigotos y abundante presencia de quistes sexuales; 3) el tiempo de latencia del quiste de resistencia fue de ~4 meses.

6. El proceso de aplanamiento de las células en cultivos de *P. reticulatum* y *C. mariaovidii* y la pérdida de sus placas reticuladas por otras más finas y lisas, pero exactamente con la misma tabulación de cada especie, es un proceso por el momento de función desconocida pero que merece ser estudiado para entender la ecología de la especie. Estas células sugieren una adaptación adicional a ecosistemas con un fuerte acoplamiento plancto-bentónico, y probablemente contribuye a la supervivencia de la especie a diferentes condiciones ambientales.

Referencias

Referencias

Aasen, J., Samdal, I.A., Miles, C.O., Dahl, E., Briggs, L.R. & Aune, T. 2005. Yessotoxins in Norwegian blue mussels (*Mytilus edulis*): Uptake from *Protoceratium reticulatum*, metabolism and depuration. Toxicon 45: 265–272.

Akselman, R., Krock, B., Alpermann, T., Tillmann, U., Borel, M., Almandoz, G. & Ferrario, M. 2015. *Protoceratium reticulatum* (Dinophyceae) in the austral Southwestern Atlantic and the first report on YTX-production in shelf waters of Argentina. Harmful Algae 45: 40–52.

Alfonso, A., Vieytes, M.R. & Botana, L.M. .2016. Yessotoxin, a Promising Therapeutic Tool. Mar. Drugs 14(2): doi:10.3390/md14020030

Almandoz, G., Montoya, N., Hernando, M., Benavides, H., Carignan, M. & Ferrario, M. 2014. Toxic strains of the *Alexandrium ostenfeldii* complex in southern South America (Beagle Channel, Argentina). Harmful Algae 37: 100–109.

Álvarez, G., Uribe, E., Díaz, R., Braun, M., Mariño, C. & Blanco, J. 2011. Bloom of the yessotoxin producing dinoflagellate *Protoceratium reticulatum* (Dinophyceae) in Northern Chile. J. Sea Res. 65: 427–434.

Álvarez, G., Uribe, E., Regueiro, J., Blanco, J. & Fraga, S. 2016. *Gonyaulax taylorii*, a new yessotoxins-producer dinoflagellate species from Chilean waters. Harmful Algae 58: 8–15.

Alves-de-Souza, K., Varela, D., Contreras, C., de La Iglesia, P., Fernández, P., Hipp, B., Hernández, C., Riobó, P., Reguera, B., Franco, J.M., Diogène, J., García, C. & Lagos, N. 2014. Deep-Sea Res. Part II. Top. Stud. Oceanogr. 101: 152–162.

Anderson, D. M. & Wall, D. 1978. Potential importance of the benthic cysts of *Gonyaulax tamarensis* and *G. excavata* in initiating toxic dinoflagellate blooms. J. Phycol. 14: 224–234.

Anderson, D.M. 1989. Toxic algal blooms and red tides: A global perspective. In Okaichi, T., Anderson, D.M. & Nemoto, T. (eds.). Red Tides: Biology, Environmental Science and Toxicology. Elsevier Science, pp. 11–16.

Anderson, D.M. 1998. Physiology and bloom dynamics of toxic *Alexandrium*

species, with emphasis on life cycle transitions. In: Anderson, D.M., Cembella, A.D. & Hallegraeff, G.M. (eds.). Physiological ecology of harmful algal blooms, NATO ASI Series, Vol 41, Springer-Verlag Berlin Heidelberg, pp 29–48.

Anderson, D.M., Cembella, A.D. & Hallegraeff, G.M. 2012a. Progress in understanding harmful algal blooms: Paradigm shifts and new technologies for research, monitoring, and management. Annu. Rev. Mar. Sci. 4: 143–176.

Anderson, D.M., Alpermann, T.J., Cembella, A.D., Collos, Y., Masseret, E. & Montresor, M. 2012b. The globally distributed genus *Alexandrium*: multifaceted roles in marine ecosystems and impacts on human health. Harmful Algae 14: 10–35.

Anderson, C.R., Moore, S.K., Tomlinson, M.C., Silke, J. & Cusack, C.K. 2014. Living with harmful algal blooms in a changing world: strategies for modeling and mitigating their effects in coastal marine ecosystems. In: Ellis, J.T. & Sherman, D.J. (Eds.) Coastal and Marine Hazards, Risks, and Disasters. Elsevier B.V., Amsterdam, pp. 495–561.

AOAC. 1990. Paralytic shellfish poison, biological method, final action. In Official Methods of Analysis. AOAC (ed) 15th Ed, Method no 959.08. Arlington, VA.

Aráoz, R., Molgó, J., Tandeau de Marsac, N. 2010. Neurotoxic cyanobacterial toxins. Toxicon 56: 813–828

Balech, E. 1995. The genus *Alexandrium* Halim (Dinoflagellata). Sherkin Island Marine Station, Sherkin Island Co., Cork, Ireland. pp. 151.

Balech, E. & de Mendiola, B.R. 1977. Un nuevo *Gonyaulax* productor de hemotalasia en Perú. Neotropica 23: 49–54.

Balech, E. & Tangen, K. 1985. Morphology and taxonomy of toxic species in the tamarensis group (Dinophyceae): *Alexandrium excavatum* (Braarud) comb. nov. and *Alexandrium ostenfeldii* (Paulsen) comb. nov. Sarsia 70: 333–343.

Balech, E. 1988. Los dinoflagelados del Atlántico Sudoccidental. Publicación Especial del Instituto Español de Oceanografía, Nº 1, Madrid, 310 pp.

Bhaud, Y., Soyer-Gobillard, M.O. & Salmon, J.M. 1988. Transmission of gametic nuclei through a fertilization tube during mating in a primitive dinoflagellate *Prorocentrum micans* Ehr. J. Cell Sci. 89: 197–206.

Biecheler, B. 1952. Recherches sur les Peridinens. Bull. Biol. France Belgique

Suppl. 36: 1–149.

Blackburn, S.I., Bloch, C.J.S., Haskard, K.A. & Hallegraeff, G.M. 2001. Reproductive compatibility among four global populations of the toxic dinoflagellate *Gymnodinium catenatum* (Dinophyceae). Phycologia 40: 78–87.

Boero F., Belmonte, G., Fanelli, G., Piraino, S. & Rubino, F. 1996 The continuity of living matter and the discontinuities of its constituents: do plankton and benthos really exist? Trends Ecol. Evol. 11(4): 177–180.

Boni, L., Ceredi, A., Guerrini, F., Milandri, A., Pistocchi, R., Poletti, R. & Pompei, M. 2001. Toxic *Protoceratium reticulatum* (Peridiniales, Dinophyta) in the north-western Adriatic sea (Italy). In: Hallegraef, G.M., Blackburn, S.I., Bold, C.I. & Lewis, R.I. (Eds.). Harmful Algal Blooms 2000, Intergovernmental Oceanographic Commission of UNESCO, pp. 137–140.

Borkman, D., Smayda, T., Tomas, C., York, R., Strangman, S. & Wright, J. 2012. Toxic *Alexandrium peruvianum* (Balech and de Mendiola) Balech and Tangen in Narragansett Bay, Rhode Island (USA). Harmful Algae 19: 92–100.

Braarud, T. 1945. Morphological observations on marine dinoflagellate cultures (*Porella perforata*, *Goniaulax tamarensis*, *Protoceratium reticulatum*). Avh. Norske Videnskakad. Oslo Mat.-nat. Kl. 11(11): 1–18.

Bravo, I., Garcés, E., Diogène, J., Fraga, S., Sampedro, N. & Figueroa, R. 2006. Resting cysts of the toxigenic dinoflagellate genus *Alexandrium* in recent sediments from the Western Mediterranean coast, including the first description of cysts of *A. kutnerae* and *A. peruvianum*. Eur. J. Phycol. 41: 293–302.

Bravo, I., Figueroa, R.I., Garcés, E., Fraga, S. & Massanet, A. 2010. The intricacies of dinoflagellate pellicle cysts: The example of *Alexandrium minutum* cysts from a bloom-recurrent area (Bay of Baiona, NW Spain). Deep-Sea Res. Part II Top. Stud. Oceanogr. 57: 166–174.

Bravo, I. & Figueroa, R.I. 2014. Towards an ecological understanding of dinoflagellate cyst functions. Microorganisms 2: 11–32.

Brosnahan, M.L., Farzan, S., Keafer, B., Sosik, H.M., Olson, R.J. & Anderson, D.M. 2014. Complexities of bloom dynamics in the toxic dinoflagellate *Alexandrium fundyense* revealed through DNA measurements by imaging flow cytometry coupled with species-specific rRNA probes. Deep-Sea Res. Part II Top. Stud. Oceanogr. 103: 185–198.

Bütschli, O. 1885. Dinoflagellata, in Protozoa (1880–89) in Bronn. Klass u. Ordn. Des Tierreichs 1: 906–1029.

Carbonell-Moore, M. C. 1996. *Ceratocorys anacantha*, sp. nov., a new member of the family Ceratocoryaceae Lindemann (Dinophyceae). Bot. Mar. 39: 1–10.

Caruana, A.M. & Malin, G. 2014. The variability in DMSP content and DMSP lyase activity in marine dinoflagellates. Prog. Oceanogr. 120: 410–424.

Cembella, A., Lewis, N. & Quilliam, M. 2000. The marine dinoflagellate *Alexandrium ostenfeldii* (Dinophyceae) as a causative organism of spirolide shellfish toxins. Phycologia 39: 67–74.

Cembella, A. & Krock, B. 2008. Cyclic imine toxins: chemistry, biogeography, biosynthesis and pharmacology. In: Botana, L.M. (ed.). Seafood and Freshwater toxins: Pharmacology, Physiology and Detection. 2nd edition. CRC Press (Taylor and Francys Group), Boca Raton, FL, pp. 561–580.

Charlson, R.J., Lovelock, J.E., Andreae, M.O. & Warren, S.G. 1987. Oceanic phytoplankton, atmospheric sulphur, cloud albedo and climate. Nature 326: 655–661.

Cho, Y., Hiramatsu, K., Ogawa, M., Omura, T., Ishimaru, T. & Oshima, Y. 2008. Non-toxic and toxic subclones obtained from a toxic clonal culture of *Alexandrium tamarense* (Dinophyceae). Toxicity and molecular biological feature. Harmful Algae 7: 740–751.

Ciminiello, P., Fattorusso, E., Forino, M., Magno, S., Poletti, R., Satake, M., Viviani, R. & Yasumoto, M. 1997. Yessotoxin in mussels of the northern Adriatic Sea. Toxicon 35: 177–183.

Ciminiello, P., Dell'Aversano, C., Fattorusso, E., Magno, S., Tartaglione, L., Cangini, M., Pompei, M., Guerrini, F., Boni, L. & Pistocchi, R. 2006. Toxin profile of *Alexandrium ostenfeldii* (Dinophyceae) from the Northern Adriatic Sea revealed by liquid chromatography mass spectrometry. Toxicon 47: 597–604.

Ciminiello, P., Dell'Aversano, C., Fattorusso, E., Forino, M., Grauso, L., Tartaglione, L., Guerrini, F. & Pistocchi, R. 2007. Spirolide toxin profile of adriatic *Alexandrium ostenfeldii* cultures and structure elucidation of 27-Hydroxy-13,19-didesmethyl Spirolide C. J. Nat. Prod. 70: 1878–1883.

Claparède, E. & Lachmann, J. 1858–1959. Etude sur les infusoires et les rhizopodes. Mém. Inst. Genevois 5–6, 489 pp.

Cullen, J.J. & MacIntyre, J.G. 1998. Behavior, physiology, and the niche of depth-

regulating phytoplankton. In Physiological ecology of harmful algal blooms. Edited by Anderson, D.M., Cembella, A.D. & Hallegraeff, G.M. NATO ASI Series. Vol. G41. Springer-Verlag, Berlin, Heidelberg. pp. 559–579.

Dale, B. 1983. Dinoflagellate resting cysts: "benthic plankton". In: Fryxell, G. A. (Ed.) Survival Strategies of the Algae. Cambridge University Press, New York, pp. 69–136.

Dale, B. & Yentsch, C.M. 1978. Red tide and paralytic shellfish poisoning. Oceanus 21: 41–49.

Deflandre, G. & Cookson, I.C. 1955. Fossil microplankton from australian late mesozoic and tertiary sediments. Aust. J. Mar. Freshw. Res. 6: 242–313.

Doucette, G., Maneiro, I., Riveiro, I. & Svensen, C. 2006. Phycotoxin pathways in aquatic food webs: transfer, accumulation and degradation. In: Granéli, E. & Turner, J.T. (eds). Ecology of harmful algae. Berlin: Springer Verlag, pp. 283–295.

Dyhrman, S.T. 2008. Molecular approaches to diagnosing nutritional physiology in harmful algae: Implications for studying the effects of eutrophication. Harmful Algae 8: 167–174.

de Vernal, A. & Marret, F. 2007. Organic-walled dinoflagellate cysts: tracers of sea-surface conditions. In: Proxies in Late Cenozoic Paleoceanography, edited by: Hillaire-Marcel, C. & de Vernal, A., Elsevier, Amsterdam, 371–408.

EFSA Panel on Contaminants in the Food Chain (CONTAM). 2010. Scientific opinión on marine biotoxins in shellfish e cyclic imines (spirolides, gymnodimines, pinnatoxins and pteriatoxins) [39 pp.] EFSA J. 8(6): 1628.

Elbrächter, M. 2003. Dinophyte reproduction: progress and conflicts. J. Phycol. 39: 629–632.

EOL. 2017. *Protoceratium reticulatum*. Accessed through: EOL Encyclopedia of Life at http://content.eol.org/pages/899397/hierarchy_entries/51383713/media on 2017-04-20.

Evitt, W.R. 1985. Sporopollenin dinoflagellate cysts: Their morphology and interpretation. American Association Stratigraphic Palynologists Foundation, Monograph Series, no. I, 333 pp.

Falkowski, P.G. & Raven, J.A. 1997. Aquatic photosynthesis. 1a Edition, Blackwell Science, Oxford, p. 375.

Faust, M.A., Litaker, R.W., Vandersea, M.W., Kibler, S.R. & Tester, P.A. 2005. Dinoflagellate diversity and abundance in two Belizean coral-reef mangrove lagoons: a test of Margalef's Mandala. Atoll. Research Bulletin 534: 103–132.

Fensome, R.A., Taylor, F.J., Norris, G., Sarjeant, W.A., Wharton, D.I. & Williams, D. L. 1993. A classification of living and fossil dinoflagellates. American Museum of Natural History, Micropaleontology Special Publishing 7

Field, C., Behrenfeld, M., Randerson, J. & P. Falkowski. 1998. Primary production of the biosphere. Integrating terrestrial and oceanic components. Science 281: 237–240.

Figueroa, R.I., Bravo, I. & Garcés, E. 2006a. Multiple routes of sexuality in *Alexandrium taylorii* (Dinophyceae) in culture. J. Phycol. 42: 1028–1039.

Figueroa, R.I, Bravo, I., Garcés, E. & Ramilo, I. 2006b. Nuclear features and effect of nutrients on *Gymnodinium catenatum* (Dinophyceae) sexual stages. J. Phycol. 42: 67–77.

Figueroa, R.I, Rengefors, K. & Bravo, I. 2006c. Effects of parental factors and meiosis on sexual offspring of *Gymnodinium nolleri* (Dinophyceae). J. Phycol. 42: 350–362.

Figueroa, R.I., Garcés, E. &. Bravo, I. 2007. Comparative study of the life cycles of *Alexandrium tamutum* and *Alexandrium minutum* (Gonyaulacales, Dinophyceae) in culture. J. Phycol. 43: 1039–1053.

Figueroa, R.I., Bravo, I. & Garcés, E. 2008a. The significance of sexual versus asexual cyst formation in the life cycle of the noxious dinoflagellate *Alexandrium peruvianum*. Harmful Algae 7: 653–663.

Figueroa, R.I., Bravo, I., Ramilo, I., Pazos, Y. & Moroño, A. 2008b. New life-cycle stages of *Gymnodinium catenatum* (Dinophyceae): laboratory and field observation. Aquat. Microb. Ecol. 52: 13–23.

Figueroa, R.I., Bravo, I. Fraga, S., Garcés, E. & Llaveria, G. 2009. The life history and cell cycle of *Kryptoperidinium foliaceum*, a dinoflagellate with two eukaryotic nuclei, Protist 160: 285–300.

Figueroa, R.I., Dapena, C., Bravo, I. & Cuadrado, A. 2015. The hidden sexuality of *Alexandrium minutum*: An example of overlooked sex in dinoflagellates. PLoS ONE 10(11): e0142667.

Fraga, S. & Sánchez, F.J. 1985. Toxic and potentially toxic dinoflagellates found in Galician Rias (NW Spain). In: Anderson, D.M., White, A.W. & Baden,

D.G. (eds.), Toxic Dinoflagellates. Elsevier, North Holland, New York, pp. 51–54.

Franks, P.J.S. & Anderson, D.M. 1992. Toxic phytoplankton blooms in the southwestern Gulf of Maine: testing hypotheses of physical control using historical data. Mar. Biol. 112: 165–174.

Garcés, E., Zingone, A., Montresor, M., Reguera, B. & Dale, B (eds). 2001. LIFEHAB (Life histories of microalgal species causing harmful Blooms). European Commission Directorate General, Science, Research and Development. Calvià, Majorca, Spain 214 pp.

Garcés, E., Masó, M. & Camp, J. 2002. Role of temporary cysts in the population dynamics of *Alexandrium taylorii* (Dinophyceae). J. Plankton Res. 24: 681–686.

GEOHAB (Global Ecology and Oceanography of Harmful Algal Blooms Programme). 2001. In: Glibert, P. & Pitcher, G. Science Plan. SCOR and IOC, Baltimore and Paris, 86 pp.

Gerssen, A., Pol-Hofstad, I.E., Poelman, M., Mulder, P.P.J., van den Top, H.J., & de Boer, J. 2010. Marine toxins: chemistry, toxicity, occurrence and detection, with special reference to the Dutch situation. Toxins 2(4): 878–904.

Giacobbe, M.G. & Yang, X. 1999. The life history of *Alexandrium taylori* (Dinophyceae). J. Phycol. 35: 331–338.

Glibert, P., Anderson, D.M., Gentien, P., Granéli, E. & Sellner, K. 2005. The global, complex phenomena of Harmful Algal Blooms. Oceanography 18(2): 136–147.

Glibert, P.M., Mayorga, E. & Seitzinger, S. 2008. *Prorocentrum minimum* tracks anthropogenic nitrogen and phosphorus inputs on a global basis: application of spatially explicit nutrient export models. Harmful Algae 8: 33–38.

Gómez, F., Moreira, D. & López-García, P. 2011. Avances en el estudio de los dinoflagelados (Dinophyceae) con la filogenia molecular. Hidrobiológica 21: 343–364.

Graham, H. W. 1942. Studies in the morphology, taxonomy, and ecology of the Peridiniales. Sci. Results Cruise VII Carnegie Biol. Ser. 3: 1–129.

Granéli, E. & Flynn, K. 2006. Chemical and physical factors influencing toxin content. In: Granéli, E. & Turner, J.T. (eds). Ecology of harmful algae. Ecological studies, Vol 189. Springer-Verlag, Berlin, pp. 229−242.

Gribble, K.E., Anderson, D.M. & Coast, W. 2009. Sexual and asexual processes in *Protoperidinium steidingerae* Balech (Dinophyceae), with observations on life-history stages of *Protoperidinium depressum* (Bailey) Balech (Dinophyceae). J. Eukaryot. Microbiol. 56: 88–103.

Grzebyk, D., Béchemin, C., Ward, C.J., Vérité, C., Codd, G.A. & Maestrini, S.Y. 2003. Effects of salinity and two coastal waters on the growth and toxin content of the dinoflagellate *Alexandrium minutum*. J. Plankton Res. 25(10): 1185–1199.

Guerrini, F., Ciminiello, P., Dell'Aversano, C., Tartaglione, L., Fattorusso, E., Boni, L. & Pistocchi, R., 2007. Influence of temperature, salinity and nutrient limitation on yessotoxin production and release by the dinoflagellate *Protoceratium reticulatum* in batch-cultures. Harmful Algae 6: 707–717.

Guzmán, L., Vidal, G., Pizarro, G., Vivanco, X., Iriarte, L., Alarcón, C., Arenas, V., Mercado, S., Pacheco, H., Mejías, P., Salgado, P., Palma, M., Espinoza, C., Fernández-Niño, E., Monsalve, J., Zamora, C. & Hinojosa, P. 2011. Manejo y monitoreo de las mareas rojas, en las regiones de Los Lagos, Aysén y Magallanes. IV Etapa, 2009–2010. Convenio Asesoría integral para la pesca y la acuicultura (ASIPA). Subsecretaría de Economía y empresas de menor tamaño (EMT)—Instituto de Fomento Pesquero, 16 pp + Figuras + Tablas + Anexos.

Guzmán, L., Vidal, G., Pizarro, G., Espinoza, O., Vivanco, X., Iriarte, L., Mercado, S., Pacheco, H., Alarcón, C., Labra, G., López, L., Calderón, M., Tardón, H., Muñoz, V., Mellado, C., Cornejo, M.F., Toro, C., Palma, M., Monsalve, J., Fernández-Niño, E. & Espinoza, C. 2015. Programa de manejo y monitoreo de las mareas rojas en las regiones de Los Lagos, Aysén y Magallanes, Etapa VIII 2014-15. Tomo I y II, Convenio Desempeño 2014. Subsecretaría de Economía y empresas de menor tamaño (EMT)—Instituto de Fomento Pesquero, 187 pp + Figuras + Tablas + Anexos.

Hackett, J.D., Anderson, D.M., Erdner, D.L. & Bhattacharya, D. 2004. Dinoflagellates: a remarkable evolutionary experiment. Am. J. Bot. 91: 1523–1534.

Hallegraeff, G.M. 1993. Review of harmful algal blooms and their apparent global increase. Phycologia 32: 79–99.

Hansen, P.J., Cembella, A.D. & Moestrup, Ø. 1992. The marine dinoflagellate *Alexandrium ostenfeldii*: Paralytic shellfish toxin concentration, composition, and toxicity to a tintinnid ciliate. J. Phycol. 28: 597–603.

Hansen, G., Moestrup, Ø. & Roberts, K.R. 1996/97. Light and electron microscopical observations on *Protoceratium reticulatum* (Dinophyceae). Arch. Protistenkd. 147: 381–391.

Hargraves, P. E. & Maranda, L. 2002. Potentially toxic or harmful microalgae from the northeast coast. Northeast. Nat. 9: 81–120.

Harju, K., Koskela, H., Kremp, A., Suikkanen, S., de la Iglesia, P., Miles, C.O., Krock, B. & Vanninen, P. 2016. Identification of gymnodimine D and presence of gymnodimine variants in the dinoflagellate *Alexandrium ostenfeldii* from the Baltic Sea. Toxicon 112: 68–76.

Haywood, A., Steidinger, K., Truby, E., Bergquist, P., Bergquist, P., Adamson, J. & Mackenzie, L. 2004. Comparative morphology and molecular phylogenetic analysis of three new species of the genus *Karenia* (Dinophyceae) from New Zealand. J. Phycol. 40: 165–179.

Hernández-Becerril, D.U., Rodríguez-Palacio, M.C. & Lozano-Ramírez, C. 2010. Morphology of two bloom-forming or potentially toxic marine dinoflagellates from the Mexican Pacific, *Heterocapsa pygmaea* and *Protoceratium reticulatum* (Dinophyceae). Cryptogamie, Algol. 31(2): 245–254.

Hess, P. & Aasen, J. 2007. Chemistry, origins and distribution of yessotoxin and its analogues. In: Botana, L.M. (ed.). Phycotoxins, Chemistry and Biochemistry. Blackwell Publishing: Ames, IA, USA; pp. 187–202.

Hesse, K., Tillmann, U., Nehring, S. & Brockmann, U. 1996. Factors controlling phytoplankton distribution in coastal waters of the German Bight (North Sea). In: A. Eleftheriou, A.D. Ansell and C.J. Smith (eds.), Biology and ecology of shallow coastal waters. Olsen & Olsen, Fredensborg. pp. 11–22.

Holsinger, K.E. .2000. Reproductive systems and evolution in vascular plants. PNAS 97: 7037–7042.

Hoppenrath, M., Murray, S.A., Chomérat, N. & Horiguchi, T. 2014. Marine benthic dinoflagellates – unveiling their worldwide biodiversity. Kleine Senckenberg Reihe 54: 1–276.

Hu, T., Curtis, J.M., Oshima, Y., Quilliam, M.A., Walter, J.A., Watson-Wright, W.M. & Wright, J.L.C. 1995. Spirolides B and D, two novel macrocycles isolated from the digestive glands of shellfish. J. Chem. Soc. Chem. Commun. 0: 2159–2161.

Hwang, D. & Lu, Y. 2000. Infuence of environmental and nutritional factors on

growth, toxicity, and toxin profile of dinoflagellate *Alexandrium minutum*. Toxicon. 38: 1491–1503.

Ishikawa, A. & Taniguchi, A. 1996. Contribution of benthic cysts to the population dynamics of *Scrippsiella* spp. (Dinophyceae) in Onagawa Bay, northeast Japan. Mar. Ecol. Prog. Ser. 140: 169–178.

Jansson, I.-M., Mertens, K.N. & Head, M.J. 2014. Statistically assessing the correlation between salinity and morphology in cysts produced by the dinoflagellate *Protoceratium reticulatum* from surface sediments of the North Atlantic Ocean, Mediterranean–Marmara–Black Sea region, and Baltic–Kattegat–Skagerrak estuarine system. Palaeogeogr. Palaeoclimatol. Palaeoecol. 399: 202–213.

Jeong, H.J., Park, J.Y., Nho, J.H., Park, M.O., Ha, J.H., Seong, K.A., Jeng, C., Seong, C.N., Lee, K.Y. & Yih, W.H. 2005. Feeding by red-tide dinoflagellates on the cyanobacterium *Synechococcus*. Aquat Microb Ecol. 41: 131–143.

Kofoid, C.A. 1907a. The plates of *Ceratium* with a note on the unity of the genus. Zoologischer Anzeiger 31: 291–293.

Kofoid, C.A. 1907b. Dinoflagellata of the San Diego región. III. Descriptions of the new species. University of California Publications in Zoology 3(13): 299–340.

Kofoid, C.A. 1909. On *Peridinium steini* Jörgensen, with a note on the nomenclature of the skeleton of the Peridinidae. Archiv für Protistenkunde 16: 25–47.

Kofoid, C.A. 1911. Dinoflagellata of the San Diego región, IV. The genus *Gonyaulax*, with notes on its skeletal morphology and a discussion of its generic and specific characters. University of California Publications in Zoology 8(4): 187–286.

Koike, K., Horie, Y., Suzuki, T., Kobiyama, A., Kurihara, K., Takagi, K., Kaga, S-N. & Oshima, O. 2006. *Protoceratium reticulatum* in northern Japan: environmental factors associated with seasonal occurrence and related contamination of yessotoxin in scallops. J. Plankton Res. 28: 103–112.

Kremp, A., Lindholm, T., Dreßler, N., Erler, K., Gerdts, G., Eirtovaara, S. & Leskinen, E. 2009. Bloom forming *Alexandrium ostenfeldii* (Dinophyceae) in shallow waters of the Åland Archipelago, Northern Baltic Sea. Harmful Algae 8: 318–328.

Kremp, A., Godhe, A., Egardt, J., Dupont, S., Suikkanen, S., Casabianca, S. &

Penna, A. 2012. Intraspecific variability in the response of bloom-forming marine microalgae to changed climate conditions. Ecol. Evol. 2(6): 1195–1207

Kremp, A. 2013. Diversity of dinoflagellate life cycles: facets and implications of complex strategies. In: Lewis, J. M., Marret, F. & Bradlay, L. (eds.) Biological and Geological Perspectives of Dinoflagellates. The Micropalaeontological Society, Special Publications, Geological Society, London, pp. 189–98.

Kremp, A., Tahvanainen, P., Litaker, W., Krock, B., Suikkanen, S., Leaw, C.P., Tomas, C. & Clerck, O. 2014. Phylogenetic relationships, morphological variation, and toxin patterns in the *Alexandrium ostenfeldii* (Dinophyceae) complex: Implications for species boundaries and identities. J. Phycol. 50: 81–101.

Landsberg, J.H. 2002. The effects of harmful algal blooms on aquatic organisms. Rev. Fish. Sci. 10: 113–390.

Le Bescot, N., Mahé, F., Audic, S., Dimier, C., Garet, M.J., Poulain, J., Wincker, P., de Vargas, C. & Siano, R. 2016. Global patterns of pelagic dinoflagellate diversity across protist size clases unveiled by metabarcoding. Environ. Microbiol. 18: 609–626.

Lee, J.-S., Tangen, K., Dahl, E., Hovgaard, P. & Yasumoto, T. 1988. Diarrhetic shellfish toxins in Norwegian mussels. Nippon Suisan Gakkaishi/Bull. Jap. Soc. Sci. Fish 54: 1953–1957.

Levandowsky, M. & Kaneta, P. 1987. Behaviour in dinoflagellates. In: Taylor, F.J.R. (ed.). The biology of dinoflagellates, Oxford: Blackwell Scientific, pp. 330–397

Lewis, J. 1991. Cyst-theca relationship in *Scrippsiella* (Dinophyceae) and related Orthoperidinioids genera. Bot. Mar. 34: 91–106.

Loeblich, A.R. 1970. The amphiesma or dinoflagellate cell covering. In: North American Paleontological. Convention, Chicago, September, 1969, Proceedings, Part G, p. 867–929.

Mackenzie, L., White, D., Oshima, Y., Kapa, J. 1996. The resting cysts and toxicity of *Alexandrium ostenfeldii* (Dinophyceae) in New Zealand. Phycologia 35: 148–155.

Maclean, C., Cembella, A.D., & Quilliam, M.A. 2003. Effects of light, salinity and inorganic nitrogen on cell growth and spirolide production in the marine

dinoflagellate *Alexandrium ostenfeldii* (Paulsen) Balech et Tangen. Bot. Mar. 46: 466–476.

Marcus, N.H. & Boero, F. 1998. Minireview: The importance of benthic-pelagic coupling and the forgotten role of life cycles in coastal aquatic systems. Limnol Oceanogr 43(5): 763–768.

Margalef, R. 1978. Life-forms of phytoplankton as survival alternatives in an unstable environment. Oceanol. Acta 1: 493–509.

Marret, F. & Zonneveld, K.A.F. 2003. Atlas of modern organic-walled dinofagellate cyst distribution. Rev. Palaeobot. Palynol. 125: 1–200.

Marrouchi, R., Benoit, E., Kharrat, R. & Molgó, J. 2010. Gymnodimines: a family of phycotoxins contaminating shellfish. In: Berbier, J., Benoit, E., Marchot, P., Mattei, C., Servent, D. (eds.). Advances and New Technologies in Toxinology. SFET Editions: Meetings on Toxinology, pp. 79–83.

Martens, H., Tillmann, U., Harju, K., Dell'Aversano, C, Tartaglione, L., & Krock, B. 2017. Toxin variability estimations of 68 *Alexandrium ostenfeldii* (Dinophyceae) strains from The Netherlands reveal a novel abundant gymnodimine. Microorganisms 5(29): doi:10.3390/microorganisms5020029

Mertens, K. N., Dale, B., Ellegaard, M., Jansson, I. M., Godhe, A., Kremp, A. & Louwye, S. 2011. Process length variation in cysts of the dinoflagellate *Protoceratium reticulatum*, from surface sediments of the Baltic–Kattegat–Skagerrak estuarine system: a regional salinity proxy. Boreas 40: 242–455.

Moestrup, Ø., Akselmann, R., Fraga, S., Hoppenrath, M., Iwataki, M., Komárek, J., Larsen, J., Lundholm, N., Zingone, A. (eds). 2009. IOC-UNESCO Taxonomic Reference List of Harmful Micro Algae. Accessed at http://www.marinespecies.org/hab on 2017-09-19

Molgó, J., Aráoz, R., Benoit, E. & Iorga, B. 2014. Cyclic imine toxins: chemistry, origin, metabolism, pharmacology, toxicology, and detection. In: Botana, L. M. (ed.) Seafood and Freshwater Toxins. 3rd edition, CRC Press, Boca Raton, pp. 951–989.

Montresor, M., Sgrosso, S., Procaccini, G. & Kooistra, W.H.C.F. 2003. Intraspecific diversity in *Scrippsiella trochoidea* (Dinopbyceae): evidence for cryptic species. Phycologia 42: 56–70.

Munday, R., Aune, T. & Rossini, J.P. 2008. Toxicology of the yessotoxins. In: Seafood and Freshwater Toxins, 2nd ed.; Botana, L.M. (ed.). CRC Press, Taylor and Francis Group: London, UK, pp. 371–380.

Murata, M., Kumakai, M., Soo Lee, J. & Yasumoto, T. 1987. Isolation and structure of yessotoxin, a novel polyether compound implicated in diarrhetic shellfish poisoning. Tetrahedron Lett. 28: 5869–5872.

Murray, S.A., Suggett, D.J., Doblin, M.A., Kohli, G.S., Seymour, J.R., Fabris, M. & Ralph, P.J. 2016. Unravelling the functional genetics of dinoflagellates: a review of approaches and opportunities. Perspect. Phycol. 3(1): 37–52.

Nagai, S., Baba, B., Miyazono, A., Tahvanainen, P., Kremp, A., Godhe, A., Mackenzie, L. & Anderson, D.M. 2010. Polymorphisms of the nuclear ribosomal RNA genes found in the different geographic origins in the toxic dinoflagellate *Alexandrium ostenfeldii* and the species detection from a single cell by LAMP. DNA Polymorph 18: 122–126.

NCMA. 2017. *Accessed through: Bigelow, National Center for Marine Algae and Microbiota at https://ncma.bigelow.org/search?q=protoceratium+reticulatum on 2014-04-20.*

Ogino, H., Kumagai, M. & Yasumoto, T. 1997. Toxicologic evaluation of yessotoxin. Nat. Toxins 5: 255–259.

Okolodkov, Y.B. & Dodge, J.D. 1996. Biodiversity and biogeography of planktonic dinoflagellates in the Arctic Ocean. J. Exp. Mar. Biol. Ecol. 202: 19–27.

Okolodkov, Y.B. 2005. The global distributional pattern of toxic, bloom dinoflagellate recorded from the Eurasian Artic. Harmful Algae 4: 351–369.

Otero, A., Chapela, M.J., Atanassova, M., Vieites, J.M. & Cabado, A.G. 2011. Cyclic imines: chemistry and mechanism of action: a review. Chem. Res. Toxicol. 24: 1817–1829.

Parrow, M. & Burkholder, J. 2004. The sexual life cycles of *Pfiesteria piscicida* and cryptoperidiniopsoids (Dinophyceae). J. Phycol. 40: 664–673.

Paz, B., Riobó , P., Fernández, M.L., Fraga, S., Franco, J.M., 2004. Production and release of yessotoxins by the dinoflagellates *Protoceratium reticulatum* and *Lingulodinium polyedrum* in culture. Toxicon 44: 251–258.

Paz, B., Vázques, J.A., Riobó, P. & Franco, J.M. 2006. Study of the effect of temperature, irradiance and salinity on growth and yessotoxin production by the dinoflagellate *Protoceratium reticulatum* in culture by using a kinetic and factorial approach. Mar. Environ. Res. 62: 286–300.

Paz, B., Riobó, P., Ramilo, I., & Franco, J.M. 2007. Yessotoxins profile in strains

of *Protoceratium reticulatum* from Spain and USA. Toxicon 50: 1–17.

Paz, P., Daranas, A.H., Norte, M., Riobó, P., Franco, J.M. & Fernández, J.J. 2008. Yessotoxins, a group of marine polyether toxins: an overview. Mar. Drugs 6: 73–102.

Pérez-Gómez, A., Novelli, A., Ferrero-Gutiérrez, A., Franco, J.M., Paz, B. & Fernández-Sánchez, M.T. 2006. Potent neurotoxic action of the shellfish biotoxin yessotoxin on cultured cerebellar neurons. Toxicol. Sci. 90: 168–177.

Persson, A., Godhe, A. & Karlson, B. 2000. Dinoflagellate cysts in recent sediments from the west coast of Sweden. Bot. Marina 43: 69–79.

Persson, A., Smith, B.C., Wikfors, G.H. & Alix, J.H. 2008. Dinoflagellate gamete formation and environmental cues: Observations, theory, and synthesis. Harmful Algae 7: 798–801.

Pizarro, G., Pesse, N., Salgado, P., Alarcón, C., Garrido, C. & Guzmán, L. 2012. Determinación de capacidad de adherencia, mecanismos de propagación y métodos de destrucción de *Alexandrium catenella* (célula vegetativa y quiste). Informe Final. Subsecretaría de Pesca y Acuicultura, p. 278.

Pouchet, G. 1883. Contribution á l´histoire des Cilioflagelles. J. Anat. Physiol. Norm. Pathol. Homme Amin. 19: 399–455.

Poupin, J., Cussatlegras, A.-S. & Geistdoerfer, P. 1999. Plancton Marine Bioluminescent. Inventaire documentè des espèces et bilan des formes les plus communes de la mer d'Iroise, Rapport Scientifique du Loen, Laboratoire d'Océanographie de l'École Navale, LOEN Lanvéoc-Poulmic, 29 240 Brest Naval, France, pp. 1–83.

Price, D.C. & Bhattacharya, D. 2017. Robust dinoflagellata phylogeny inferred from public transcriptome databases. J. Phycol. 53(3): 725–729.

Price, D.C., Farinholt, N., Gates, C., Shumaker, A., Wagner, N.E., Bienfang, P. & Bhattacharya, D. 2016. Analysis of *Gambierdiscus* transcriptome data supports ancient origins of mixotrophic pathways in dinoflagellates. Environ. Microbiol. 18:4501–4510. doi:10.1111/1462-2920.13478

Reifel, K. M., McCoy, M. P., Rocke, T. E., Tiffany, M. A., Hurlbert, S. H. & Faulkner, D. J. 2002. Possible importance of algal toxins in the Salton Sea, California. Hidrobiologia 473: 275–292.

Reinecke, P. 1967. *Gonyaulax grindleyi* sp. nov.: a dinoflagellate causing a red tide at Elands Bay, Cape Province, in December 1966. S. Afr. J. Bot. 33: 157–

160.

Rhodes, L., McNabb, P., de Salas, M., Briggs, L., Beuzenberg, V. & Gladstone, M. 2006. Yessotoxin production by *Gonyaulax spinifera*. Harmful Algae 5: 148–155.

Richard, D., Arsenault, E., Cembella, A. & Quilliam, M. 2001. Investigations into the toxicology and pharmacology of spirolides, a novel group of shellfish toxins. In: Hallegraeff, G.M., Blackburn, S.I., Bolch, C.J. & Lewis, R.J. (Eds.), Harmful Algal Blooms 2000. Intergovernmental Oceanographic Commission of UNESCO, pp. 383–386.

Rizzo, P.J. 1991. The enigma of the dinoflagellate chromosome. J. Protozool 38: 246–252.

Rodríguez, I., Genta-Jouve, G., Alfonso, C., Calabro, K., Alonso, E., Sánchez, J.A., Alfonso, A., Thomas, O.P. & Botana, L.M. 2015. Gambierone, a ladder-shaped polyether from the dinoflagellate *Gambierdiscus belizeanus*. Org. Lett. 17: 2392–2395.

Sala-Pérez, M., Alpermann, T.J., Krock, B. & Tillmann, U. 2016. Growth and bioactive secondary metabolites of arctic *Protoceratium reticulatum* (Dinophyceae). Harmful Algae 55: 85–96.

Saldarriaga, J. F., Taylor, F. J. R., Cavalier-Smith, T., Menden-Deuer, S. & Keeling, P. J. 2004. Molecular data and the evolutionary history of dinoflagellates. Eur. J. Protistol. 40: 85–111.

Salgado, P., Díaz, L., Pesse, N. & Vivanco, X. 2012. Monitoreo de *Alexandrium catenella* en zona no declarada de la región de Atacama y Coquimbo. Informe Final. 16p. + Figuras + Tablas + Anexos. Ministerio de Economía, Fomento y Reconstrucción- Subsecretaría de Pesca y Acuicultura.

Salgado, P., Guzmán, L., Labra, G. & Garrido, C. 2013. Monitoreo de especies nocivas en la región del Biobío. Informe Final. 48p. + Figuras + Tablas + Anexos. Ministerio de Economía, Fomento y Reconstrucción- Subsecretaría de Pesca y Acuicultura.

Sánchez, S., Villanueva, P. & Carbajo, L. 2004. Distribution and concentration of *Alexandrium peruvianum* (Balech and de Mendiola) in the Peruvian coast (03º24'–18º20' LS) between 1982–2004. In: Abstracts, XI International Conference on Harmful Algal Blooms, Cape Town, South Africa, November 15–19, p. 227.

Satake, M., Mackenzie, L. & Yasumoto, T. 1997a. Identification of *Protoceratium*

reticulatum as the biogenetic origin of yessotoxin. Nat. Toxins 5(4): 164–167.

Satake, M., Tubaro, A., Lee, J.S. & Yasumoto, T. 1997b. Two new analogs of yessotoxin, homoyessotoxin and 45-hydroxyhomoyessotoxin, isolated from mussels of the Adriatic Sea. Nat. Toxins 5: 107–110.

Satake, M., Ichimura, T., Sekiguchi, K., Yoshimatsu, S. & Oshima, Y. 1999. Confirmation of yessotoxin and 45,46,47-trinoryessotoxin production by *Protoceratium reticulatum* collected in Japan. Nat. Toxins 7: 147–150.

Scorzetti, G., Brand, L.E., Hitchcock, G.L., Rein, K.S., Sinigalliano, C.D. & Fell, J.W. 2009. Multiple simultaneous detection of Harmful Algal Blooms (HABs) through a high throughput bead array technology, with potential use in phytoplankton community analysis. Harmful Algae 8: 196–211.

Schnepf, E. & Drebes, G. 1993. Anisogamy in the dinoflagellate *Noctiluca*? Helgoländer Meeresunters 47: 265–273.

Seguel, M., Sfeir, A., Alvornoz, V., Gangas, M., Molinet, C. & Díaz, P. 2010. Distribución de los quistes de *Alexandrium catenella* y *Protoceratium reticulatum* (Dinophyceae) en la región Sur-Austral de Chile. Cienc. Tecnol. Mar. 33:59–70.

Selander, E., Thor, P., Toth, G. & Pavia, H. 2006. Copepods induce paralytic shellfish toxin production in marine dinoflagellates. Proc. R. Soc. Lond., Ser. B: Biol. Sci. 273: 1673–1680.

Senft-Batoh, C.D., Dam, H.G., Shumway, S.E., Wikfors, G.H. 2015a. A multi-phylum study of grazer-induced paralytic shellfish toxin production in the dinoflagellate *Alexandrium fundyense*: A new perspective on control of algal toxicity. Harmful Algae 44: 20–31.

Senft-Batoh, C.D., Dam, H.G., Shumway, S.E., Wikfors, G.H. & Schlichting, C.D. 2015b. Influence of predator–prey evolutionary history, chemical alarm-cues, and feeding selection on induction of toxin production in a marine dinoflagellate. Limnol Oceanogr. 00:1–21.

Sheng, J., Malkiel, E., Katz, J., Adolf, J.E. & Place, A.R. 2010. A dinoflagellate exploits toxins to immobilize prey prior to ingestion. Proc. Natl. Acad. Sci. 107: 2082–2087.

Sildever, S., Andersen, T.J., Ribeiro, S. & Ellegaard, M. 2015. Influence of surface salinity gradient on dinoflagellate cyst community structure, abundance and morphology in the Baltic Sea, Kattegat and Skagerrak. Estuar. Coast. Shelf

Sci. 155: 1–7.

Smayda, T.J. 1990. Novel and nuisance phytoplankton blooms in the sea: Evidence for a global epidemic. In: Granéli, E., Sundström, B., Edler, L. & Anderson, D.M. (eds.), Toxic Marine Phytoplankton. Elsevier Science Publishing, New York, pp. 29–40.

Smayda, T. 1997. Harmful Algal Blooms: Their Ecophysiology and General Relevance to Phytoplankton Blooms in the Sea. Limnol. Oceanogr. 42(5, part 2): 1137–1153.

Smayda, T. J. & C. Reynolds. 2003. Strategies of marine dinoflagellate survival and some rules of assembly. J. Sea Res. 49(2): 95–106.

Soyer-Gobillard, M.O., Bhaud, Y. & Saint Hilaire, D. 2002. New data on mating in an autotrophic dinoflagellate, *Prorocentrum micans* Ehrenberg. Vie Milieu 52: 167–175.

Sournia, A. 1995. Red tide and toxic marine phytoplankton of the world ocean: an inquiry into biodiversity. In: Lassus, P., Arzul, G., Erard-Le-Denn, E., Gentien, P. & Marcaillou-Le-Baut, C. (eds.). Harmful Marine Algal Blooms, Paris, Lavoisier, 103–112.

Starr, M., Lair, S., Michaud S., Scarratt, M., Quilliam, M., Lefaivre, D., Robert, M., Wotherspoon, A., Michaud, R., Ménard, N., Sauvé, G., Lessard, S., Béland, P. & Measures, L. 2017. Multispecies mass mortality of marine fauna linked to a toxic dinoflagellate bloom. PLoS ONE 12(5): e0176299.

Steidinger, K. & Garcés, E. 2006. Importance of Life Cycles in the Ecology of Harmful Microalgae. In: Granéli, E. and Turner, J.T. (eds.). Ecology of Harmful Algae. Vol. 189. pp 37–49.

Stoecker, D.K. 1999. Mixotrophy among dinoflagellates. J. Eukaryot. Microbiol. 46: 397–401.

Tatters, A.O., van Wagoner, R.M., Wright, J.L. & Tomas, C.R. 2012. Regulation of spiroimine neurotoxins and hemolytic activity in laboratory cultures of the dinoflagellate *Alexandrium peruvianum* (Balech & Mendiola) Balech & Tangen. Harmful Algae 19: 160–168.

Taylor, F.J., Fukuyo, Y. & Larsen, J. 1995. Taxonomy of harmful dinoflagellates. In: Hallegraeff, G.M., Anderson, D.M. & Cembella, A.D. (eds.). Manual on Harmful Marine Microalgae: 283–309, IOC Manuals and Guides No. 33. Intergovernmental Oceanographic Commission of UNESCO, Paris.

Tilman, D. 1977. Resource competition between planktonic algae: An

experimental and theoretical approach. Ecology 58: 338–348.

Tillmann, U., Alpermann, T., John, U. & Cembella, A. 2008. Allelochemical interactions and short-term effects of the dinoflagellate *Alexandrium* on selected photoautotrophic and heterotrophicprotists. Harmful Algae 7: 52–64.

Tillmann, U. & Hoppenrath, M. 2013. Life Cycle of the pseudo colonial dinoflagellate *Polykrikos kofoidii* (Gymnodiniales, Dinoflagellata). J. Phycol. 49(2): 298–317.

Tillmann, U., Kremp, A., Tahvanainen, P., & Krock, B. 2014. Characterization of spirolide producing *Alexandrium ostenfeldii* (Dinophyceae) from the western Arctic. Harmful Algae 39: 259–270.

Tomas, C.R., van Wagoner, R., Tatters, A.O., Hall, S., White, K. & Wright, J.L.C. 2012. *Alexandrium peruvianum* (Balech and Mendiola) Balech and Tangen a new toxic species for coastal North Carolina. Harmful Algae 17: 54–63.

Uchida, T., Matsuyama, Y., Yamaguchi, M. & Honjo, T. 1996. The life cycle of *Gyrodinium instriatum* (Dinophyceae) in culture. Phycological Res. 44(3): 119–123.

Van de Waal, D. B., Tillmann, U., Martens, H., Krock, B., van Scheppingen, Y. & John, U. 2015. Characterization of multiple isolates from an *Alexandrium ostenfeldii* bloom in The Netherlands. Harmful Algae 49: 94–104.

Van Wagoner, R., Misner, I., Tomas, C. & Wright, J. 2011. Occurrence of 12-methylgymnodimine in a spirolide-producing dinoflagellate *Alexandrium peruvianum* and the biogenetic implications. Tetrahedron Lett. 52: 4243–4246.

Visciano, P., Schirone, M., Berti, M., Milandri, M., Tofalo, R. & Suzzi G. 2016. Marine biotoxins: occurrence, toxicity, regulatory limits and reference methods. Front. Microbiol. 7: 1051. doi: 10.3389/fmicb.2016.01051

Von Dassow, P. & Montresor, M. 2011. Unveiling the mysteries of phytoplankton life cycles: patterns and opportunities behind complexity. J. Plankton Res. 33: 3–12.

von Stosch, H.A. 1969. Dinoflagellaten aus der Nordsee I. Über *Cachonina niei* Loeblich (1968), *Gonyaulax grindleyi* Reinecke (1967) und eine Methode zur Darstellung von Peridineenpanzern. Helgol. Wiss. Meeresunters. 19: 558–568.

von Stosch, H.A. 1972. La signification cytologique de la "cyclose nucléaire" dans le cycle de vie des Dinoglagellés. Mem. Soc. Bot. Fr. (1949–1973): 201–212.

von Stosch, H.A. 1973. Observations on vegetative reproduction and sexual life cycles of two freshwater dinoflagellates, *Gymondinium pseudopalustre* Schiller and *Woloszynskia apiculata* sp. nov. Br. phycol. J. 8: 105–134.

Wall, D. & Dale, B. 1968. Modern Dinoflagellate Cysts and Evolution of the Peridiniales. Micropaleontology 14: 265–304.

Wang, D. & Hsieh, D. .2005. Growth and toxin production in batch cultures of a marine dinoflagellate *Alexandrium tamarense* HK9301 isolated from the South China Sea. Harmful Algae 4: 401–410.

Wohlrab, S., Iversen, M.H. & John, U. 2010. A molecular and coevolutionary context for grazer induced toxin production in *Alexandrium tamarense*. PLoS ONE 5: e15039.

Woloszynska, H.J. 1928. Dinoflagellatae der polnischen Ostsee sowie der Piasnica gelegenen Sümpfe. Archwm. Hydrobiol. Ryb. 3: 155–278.

Yasumoto, T. & Takizawa, A. 1997. Fluorometric measurement of yessotoxin in shellfish by high-pressure liquid chromatography. Biosci. Biotech. Biochem. 61: 1775–1777.

Yoshimatsu, S. 1981. Sexual reproduction of *Protogonyaulax catenella* in culture. Bull. Plankton Soc. Jpn. 28: 131–139.

Zingmark, R.G. 1970. Sexual reproduction in the dinoflagellate *Noctiluca miliaris* Suriray. J. Phycol. 6(2): 122–126.

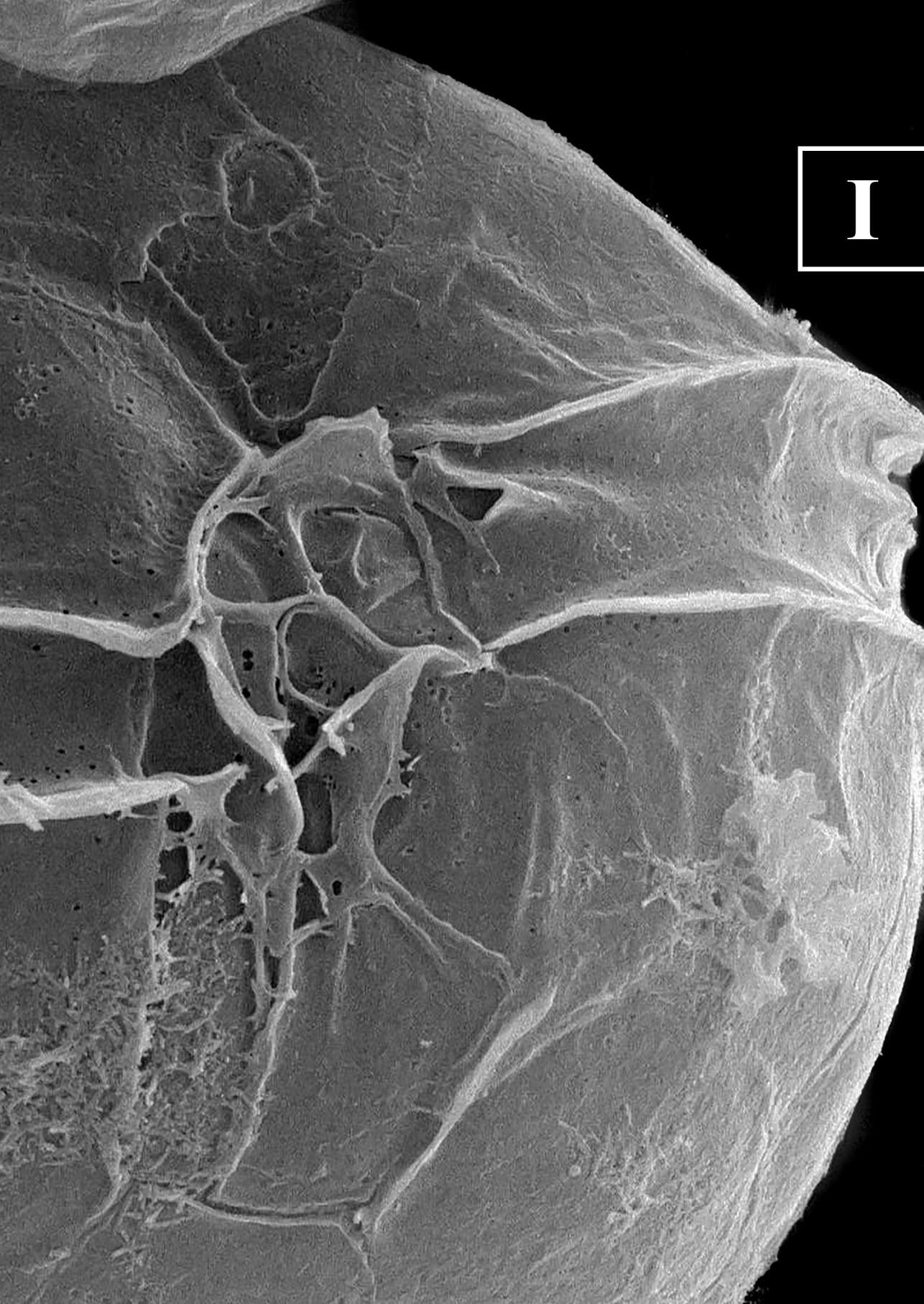

I

Toxicon 103 (2015) 85–98

Contents lists available at ScienceDirect

Toxicon

journal homepage: www.elsevier.com/locate/toxicon

Differences in the toxin profiles of *Alexandrium ostenfeldii* (Dinophyceae) strains isolated from different geographic origins: Evidence of paralytic toxin, spirolide, and gymnodimine

Pablo Salgado [a, 1], Pilar Riobó [b], Francisco Rodríguez [c], José M. Franco [b], Isabel Bravo [c, *]

[a] Instituto de Fomento Pesquero (IFOP), Enrique Abello 0552, Casilla 101, Punta Arenas, Chile
[b] Instituto de Investigaciones Marinas (IIM-CSIC), Eduardo Cabello 6, 36208, Vigo, Spain
[c] Instituto Español de Oceanografía (IEO), Centro Oceanográfico de Vigo, Subida a Radio Faro 50, 36390, Vigo, Spain

ARTICLE INFO

Article history:
Received 10 March 2015
Received in revised form
5 June 2015
Accepted 16 June 2015
Available online 18 June 2015

Keywords:
Alexandrium ostenfeldii
Toxin profile
Paralytic toxin
Spirolide
Gymnodimine

ABSTRACT

Among toxin-producing dinoflagellates of the genus *Alexandrium*, *Alexandrium ostenfeldii* is the only species able to produce paralytic shellfish poisoning (PSP) toxins, spirolides (SPXs) and gymnodimines (GYMs). In this study we characterized and compared three *A. ostenfeldii* strains isolated from the Baltic, Mediterranean, and southern Chile Seas with respect to their toxin profiles, morphology, and phylogeny. Toxin analyses by HPLC–FD and LC–HRMS revealed differences in the toxin profiles of the three strains. The PSP toxin profiles of the southern Chile and Baltic strains were largely the same and included gonyautoxin (GTX)-3, GTX-2, and saxitoxin (STX), although the total PSP toxin content of the Chilean strain (105.83 ± 72.15 pg cell^{-1}) was much higher than that of the Baltic strain (4.04 ± 1.93 pg cell^{-1}). However, the Baltic strain was the only strain that expressed detectable amounts of analogues of GYM-A and GYM-B/-C (48.27 ± 26.12 pg GYM-A equivalents cell^{-1}). The only toxin expressed by the Mediterranean strain was 13-desmethyl SPX-C (13dMeC; 2.85 ± 4.76 pg cell^{-1}). Phylogenetic analysis based on the LSU rRNA showed that the studied strains belonged to distinct molecular clades. The toxin profiles determined in this study provide further evidence of the taxonomic complexity of this species.

1. Introduction

The frequency of harmful algal blooms (HABs) produced by marine dinoflagellates has increased worldwide over the last several decades, with serious negative impacts on public health and on the economies of the affected areas (Hallegraeff, 2010). The genus *Alexandrium* is one of the most important genera among HAB species because of its toxicity and cosmopolitan distribution in the coastal environments of sub-arctic, temperate, and tropical zones (Anderson et al., 2012). Unlike other species of *Alexandrium*, and most toxin-producing microalgae, which produce only a single type of toxin, *Alexandrium ostenfeldii* produces toxins of two different groups: paralytic or saxitoxins (STXs) and cyclic imines of the spirolide (SPX) and gymnodimine (GYM) type (Hansen et al., 1992; Cembella et al., 2000; Van Wagoner et al., 2011). Of these, STXs and their analogues are the most significant because they are responsible for outbreaks of paralytic shellfish poisoning (PSP), which pose a serious risk for environmental and human health (Hallegraeff, 1993). Although SPXs and GYMs have yet to be linked directly to human intoxications (Richard et al., 2001), these fast-acting toxins induce the rapid death (within minutes) in laboratory mice injected intraperitoneally with toxic methanolic extracts from shellfish contaminated with those lipophilic toxins (Marrouchi et al., 2010; Otero et al., 2011). SPXs, and GYMs are commonly co-extracted with other lipophilic toxins, such as the diarrheic toxins okadaic acid and its analogues, which are produced by several *Dinophysis* and *Prorocentrum* species. Thus, in HAB monitoring programs, the presence of SPXs and GYMs in shellfish samples can produce false-positives in mouse bioassay tests for the detection of diarrheic shellfish poisoning toxins (Biré et al., 2002).

SPXs were first isolated and characterized from shellfish collected along the southeastern coast of Nova Scotia, Canada (Hu et al., 1995). Subsequently, *A. ostenfeldii* was identified as the producer of these toxins (Cembella et al., 2000). However, some strains

* Corresponding author.
E-mail address: isabel.bravo@vi.ieo.es (I. Bravo).
[1] *Present address*: Instituto Español de Oceanografía (IEO), Centro Oceanográfico de Vigo, Subida a Radio Faro 50, 36390, Vigo, Spain.

http://dx.doi.org/10.1016/j.toxicon.2015.06.015
0041-0101/

of *A. ostenfeldii*, from diverse geographic regions, also produce PSP toxins (Hansen et al., 1992; MacKenzie et al., 1996; Lim et al., 2005; Kremp et al., 2009; Borkman et al., 2012; Gu et al., 2013) (see Table 1 for additional references). Moreover, this species was recently confirmed to produce GYMs, which block acetylcholine receptors (Kharrat et al., 2008) and are associated with neurotoxic shellfish poisoning. The only other producer of GYMs identified to date is the phylogenetically distant dinoflagellate *Karenia selliformis* (Haywood et al., 2004). GYM-A was initially isolated and characterized in the early 1990s from New Zealand oysters (MacKenzie,

Table 1
Toxin profiles of *A. ostenfeldii* strains from different geographic origins worldwide.

Species	Geographical location	Region	Type of toxins			Reference
			PSP[a]	SPXs[b]	GYMs[c]	
A. ostenfeldii	Åland, Finland	(1)	2	ND	NA	Kremp et al. (2009); Suikkanen et al. (2013)
A. ostenfeldii	Åland, Finland	(1)	4	ND	A, B/C anals.	Riobó et al. (2013)
A. ostenfeldii	Gotland, Sweden	(1)	2	ND	NA	Suikkanen et al. (2013); Kremp et al. (2014)
A. ostenfeldii	Hel, Poland	(1)	2	ND	NA	Kremp et al. (2014)
A. ostenfeldii	Öresund, Denmark	(1)	2	ND	NA	Kremp et al. (2014)
A. ostenfeldii	Baltic Sea	(1)	NI	NI	unkn. comps.; A, B/C anals.	Harju et al. (2014)
A. ostenfeldii	Åland, Finland	(1)	3	ND	A, B/C anals.	This study
A. ostenfeldii	Limfjord, Denmark	(2)	6	NA	NA	Hansen et al. (1992)
A. ostenfeldii	Limfjord, Denmark	(2)	12	NA	NA	Ravn et al. (1995)
A. ostenfeldii	Limfjord, Denmark	(2)	NA	G; 13dMeC; 13,19ddMeC	NA	MacKinnon et al. (2006)
A. ostenfeldii	Kattegat Sea, Denmark	(2)	8	13dMeC; 13,19ddMeC	NA	Otero et al. (2010)
A. ostenfeldii	Sognefjord, Norway	(3)	NA	G; 20MeG	NA	Aasen et al. (2005)
A. ostenfeldii	Ouwerkerkse Kreek, The Netherland	(3)	2	13dMeC	NA	Burson et al. (2014)
A. ostenfeldii	Arcachón, French	(3)	NA	A; 13dMeC	ND	Amzil et al. (2007)
A. ostenfeldii	Bantry Bay, Ireland	(3)	ND	C; D	NA	Touzet et al. (2008)
A. peruvianum	Lough Swilly, Ireland	(3)	ND	13dMeC; 13dMeD	NA	Touzet et al. (2008)
A. ostenfeldii	East coast, Scotland	(3)	1	20MeG	NA	Brown et al. (2010)
A. ostenfeldii	Cork Harbour, Ireland	(3)	NA	13dMeC; 20MeG	NA	Touzet et al. (2011)
A. ostenfeldii	Coast, Norway	(3)	NA	G; isoC; 13dMeC; 13, 19ddMeC; 20MeG	NA	Rundberget et al. (2011)
A. ostenfeldii	Skagerrak, North Sea	(3)	ND	20MeG; 13dMeC	NA	Suikkanen et al. (2013)
A. ostenfeldii	East coast, Scotland	(3)	ND	20MeG; 13dMeC	NA	Suikkanen et al. (2013)
A. peruvianum	Lough Swilly, Ireland	(3)	ND	13dMeC	NA	Suikkanen et al. (2013); Kremp et al. (2014)
A. ostenfeldii	Fal River, UK	(3)	ND	13dMeC	NA	Kremp et al. (2014)
A. ostenfeldii	Breidafjord, Iceland	(3)	ND	C; G; 13dMeC; 20MeG	NA	Kremp et al. (2014)
A. ostenfeldii	Oslofjord, Norway	(3)	ND	A; 13,19ddMeC	NA	Kremp et al. (2014)
A. ostenfeldii	North Sea, Norway	(3)	ND	20MeG	NA	Kremp et al. (2014)
A. ostenfeldii	North Sea, Scotland	(3)	ND	20MeG	NA	Kremp et al. (2014)
A. ostenfeldii	North Sea, Scotland	(3)	ND	A; 13dMeC; 20MeG	NA	Kremp et al., (2014)
A. ostenfeldii	West and South coasts, Greenland	(3)	ND	C; H; 13dMeC; 20MeG; 8 unknown SPXs	NA	Tillmann et al. (2014)
A. peruvianum	Palamós, Spain	(4)	ND	B; C; D; 13dMeC; 13dMeD	NA	Franco et al. (2006)
A. ostenfeldii	Northern Adriatic Sea, Italy	(4)	NA	13dMeC; 13,19ddMeC; 27OH13,19ddMeC	NA	Ciminiello et al. (2007)
A. ostenfeldii	Thermaikos Gulf, Greek	(4)	NA	A; 13dMeC	ND	Katikou et al. (2010)
A. ostenfeldii	Northern Adriatic Sea, Italy	(4)	NA	27OH13dMeC; 27oxo13, 19ddMeC	NA	Ciminiello et al. (2010)
A. peruvianum	Palamós, Spain	(4)	ND	13dMeC	NA	Riobó et al. (2013); Kremp et al. (2014); This study
A. ostenfeldii	Nova Scotia, Canada	(5)	NA	A; B; C; D; D2; 13dMeC	NA	Cembella et al. (2001)
A. ostenfeldii	Nova Scotia, Canada	(5)	NA	C; C3; 13dMeC; 13dMeD	NA	Maclean et al. (2003)
A. ostenfeldii	Nova Scotia, Canada	(5)	NA	H; I	NA	Roach et al. (2009)
A. ostenfeldii	Gulf of Maine, USA	(5)	ND	A; B; C; C2; D, D2; 13dMeC	NA	Gribble et al. (2005)
A. peruvianum	New River, NC, USA	(5)	NA	D; 13dMeC	12Me	Van Wagoner et al. (2011)
A. peruvianum	Narragansett, RI, USA	(5)	7	13dMeC	12Me	Borkman et al. (2012)
A. peruvianum	New River, NC, USA	(5)	7	D; 13dMeC	NA	Tomas et al. (2012)
A. ostenfeldii	Saanich, Canada	(5)	NI	NI	A	Harju et al. (2014)
A. ostenfeldii	Big Glory Bay, New Zealand (NZ)	(6)	+	D; 13dMeC; 13dMeD	NA	Jester et al. (2009); Beuzenberg et al. (2012)
A. ostenfeldii	Kaitaia and Tahaora; Timaru, NZ	(6)	2; 9	NA	NA	MacKenzie et al. (1996)
A. peruvianum	Samariang River, Malaysia	(7)	11; 5	NA	NA	Lim et al. (2005); Lim and Ogata (2005)
A. ostenfeldii	Toni Bay, Japan	(7)	10	NA	NA	Kaga et al. (2006)
A. ostenfeldii	Bohai Sea, China	(7)	1	ND	NA	Gu et al. (2013)
A. ostenfeldii	Beagle Channel, Argentina	(8)	ND	13dMeC; 20MeG	NA	Almandoz et al. (2014)
A. peruvianum	Callao, Peru	(8)	2	ND	NA	Kremp et al. (2014)
A. ostenfeldii	Vergara Island, Aysén, Chile	(8)	3	ND	ND	This study

[a] **1**: STX, neoSTX; **2**: GTX-2/3, STX; **3**: GTX-2/3, STX, dcSTX; **4**: GTX-2/3, STX, dcSTX, neoSTX; **5**: GTX-1/4/6, dcSTX, neoSTX; **6**: GTX-2/3/6, C1/2; **7**: GTX-2/3/5, STX, C1/2; **8**: GTX-1–5, C1/2; **9**: GTX-2/3/5, STX, dcSTX, neoSTX, C2/3; **10**: GTX-1–6, STX, neoSTX; **11**: GTX-1/2/4/5/6, STX, dcSTX, neoSTX; **12**: GTX-2–6, STX, neoSTX, C2–4.

[b] **A**: SPX-A; **B**: SPX-B; **C**: SPX-C; **C2**: SPX-C2; **C3**: SPX-C3; **isoC**: SPX-isoC; **D**: SPX-D; **D2**: SPX-D2; **G**: SPX-G; **H**: SPX-H, **I**: SPX-I; **13dMeC**: 13-desmethyl SPX-C; **13dMeG**: 13-desmethyl SPX-G; **20MeG**: 20-methyl SPX-G; **13,19ddMeC**: 13,19-didesmethyl SPX-C; **27OH13,19ddMeC**: 27-hydroxy-13,19-didesmethyl SPX-C; **27OH13dMeC**: 27-hydroxy-13-desmethyl SPX-C; **27oxo13,19ddMeC**: 27-oxo-13,19-didesmethyl SPX-C.

[c] **A**: GYM-A; **B/C**: GYM-B/-C; **12Me**: 12-methyl GYM. **ND**: Not detected; **NI**: Not information; **NA**: Not analyzed; +: Positive to PSP toxins; **(1)**: Baltic Sea; **(2)**: Kattegat Sea (Limfjord); **(3)**: Northeastern Atlantic Ocean; **(4)**: Mediterranean Sea, **(5)**: Northwest Atlantic Ocean, **(6)**: New Zealand, **(7)**: Western Pacific Ocean, **(8)**: South America.

1994; Seki et al., 1995). Later, two additional isomeric analogues (GYM-B and GYM-C) were isolated from cultures of *K. selliformis* (Miles et al., 2000, 2003). GYMs were detected for the first time in a dinoflagellate genus other than *K. selliformis* in an isolate of *Alexandrium peruvianum* from North Carolina (USA), in which a novel GYM congener (12-methylgymnodimine, 12MeGYM) was identified (Van Wagoner et al., 2011). This was followed by a report of acyl ester derivatives of GYMs in Tunisian clams (De la Iglesia et al., 2012).

The difficulties in distinguishing the geographic boundaries of *A. ostenfeldii* and the morphologically very similar and also toxic *A. peruvianum* have complicated attempts to define the toxin profiles of these species. According to Balech (1995) *A. ostenfeldii* differs from *A. peruvianum* mainly in the shape of the first apical (1′), and the anterior (s.a.), and posterior (s.p.) sulcal plates. However, plate morphology is highly variable within populations from the same geographic area and even within strains (Lim et al., 2005; Kremp et al., 2009, 2014), resulting in a great deal of confusion in assigning specimens to one species or the other (Kremp et al., 2009). In fact, recent phylogenetic analysis from cultures characterized as *A. ostenfeldii* or *A. peruvianum* based on morphological characters identified six distinct but closely related groups, although these characters were highly variable and not consistently distributed among the groups (Kremp et al., 2014). This demonstrated the invalid initial separation of the two species and led those authors to propose the discontinuation of *A. peruvianum* as a species and its consideration as synonymous with *A. ostenfeldii*, at least until additional data become available.

In this study, we used toxin profiles and morphological and molecular taxonomy to characterize three *A. ostenfeldii* strains isolated from three different geographic origins, the Baltic, Mediterranean, and Chilean Southern Seas. To facilitate comparisons of these strains with those from other regions, the literature information on *A. ostenfeldii* toxin profiles worldwide is summarized in Table 1.

2. Material and methods

2.1. Strains and culture conditions

Cultures were established from three non-clonal strains of *A. ostenfeldii* (or its synonymous *A. peruvianum*) maintained in the culture collection of toxic microalgae of the Spanish Institute of Oceanography in Vigo (CCVIEO: http://www.vgohab.es/). The three strains, from three distantly separated geographic origins, were (Table 2): 1) the Baltic Sea strain AOTV-B4A (Åland, Finland), 2) the Mediterranean Sea strain VGO956 (Palamós, Spain), and 3) the southern Chilean strain AOA32-2 (Vergara Island, Aysén, Chile). These three strains can be considered as geographically representative of each region based on literature data and on our own preliminary study. Specifically, the Baltic and Mediterranean Sea strains were described in Kremp et al. (2009) and Franco et al. (2006), respectively, showing the consistency of their toxin profiles with those of other strains from the respective region. For the Chilean strain, our preliminary analyses carried out with three strains (AOIVAY, AOA32-1, and AOA32-2) from Aysén showed that their toxin profiles were identical, although with different total PSP toxin contents (estimations in early stationary phase of 21.1, 33.5, and 16.2 pg cell^{-1}, respectively) in the same experimental conditions (salinity of 32, 15 °C). The strain AOA32-2 was chosen because it presented the best physiological state, reaching in early stationary phase higher cell concentrations than the other two strains.

The strains (starting density 500–800 cell mL^{-1}) were cultured in 100-mL Erlenmeyer flasks filled with 75 mL of L1 medium without silica (Guillard and Hargraves, 1993) and incubated with a photon flux density of 80–100 μmol m^{-2} s^{-1} and a photoperiod of 12:12 h light:dark. Different temperatures and salinities were settled for each strain (Table 2). The medium was prepared using seawater collected from the Galician continental shelf at a depth of 5 m and adjusted to the salinities listed in Table 2 by the addition of sterile MQ water (Milli-Q; Millipore, USA). The cultures were acclimated gradually to the different salinities (max. 3–4 salinity units at a time) and temperatures for at least three transfers after reaching the early stationary phase. A 66-mL sample was taken from each of the 27 cultures during the exponential growth phase and used as follows: 60 mL were processed for toxin analyses (PSP toxin and cyclic imines), 3 mL were fixed with Lugol for cell measurements and counts, and 3 mL were fixed with formaldehyde for morphological studies. Additionally, a 1.5-mL sample was processed from three cultures (one culture of each strain, chosen randomly) for molecular analysis, thereby obtaining a total sample volume of 67.5 mL from these cultures.

2.2. Morphological characterization

Morphological studies, including examination of the plates of the cultured cells by Calcofluor white staining (Flourescent Brightner 28, Sigma) (Fritz and Triemer, 1985), were performed using a Leica DMLA microscope (Leica Microsystems, Wetzlar, Germany) equipped with UV epifluorescence and an AxioCam HRc camera (Zeiss, Göttingen, Germany). Species identification and morphological comparisons among the three studied strains were based on the original descriptions and on more recent ones (Balech and de Mendiola, 1977; Balech and Tangen, 1985; Balech, 1995).

The lengths and widths of 30 randomly selected cells were measured at 630× magnification using an Axiocam HRC digital camera (Zeiss, Germany) connected to a Leica DMLA light microscope. Mean cell biovolume (v) was calculated by assuming that the cells were prolate spheroids (Sun and Liu, 2003) and using the following equation:

$$v = \frac{\pi}{6} \cdot b^2 \cdot \alpha$$

where α is the cell length and b is the cell width. The statistical analyses were performed using SPSS v.21 software. One-way ANOVA followed by Tukey's post-hoc test was used to identify significant differences in morphometric measurements between strains and treatments.

2.3. Toxin extraction

Toxin analyses were performed on exponentially growing

Table 2
Strains and treatments used in this study. The original name of the species, the strain code, geographic origin, culture origin, group that isolated the strain, salinity and temperature conditions, and number of treatments of each strain are shown.

Species orig. name	Strain	Location	Culture origin	Isolator	Salinities/Temperatures	Treatments (n)
A. ostenfeldii	AOTV-B4A	Åland, Finland	Vegetative cell	A. Kremp	10, 18, 25/15, 19, 26	9
A. peruvianum	VGO956	Palamós, Spain	Resting cyst	I. Bravo	14, 25, 37/15, 19, 26	9
A. ostenfeldii	AOA32-2	Vergara I., Chile	Resting cyst	P. Salgado	25, 32, 37/10, 15, 19	9

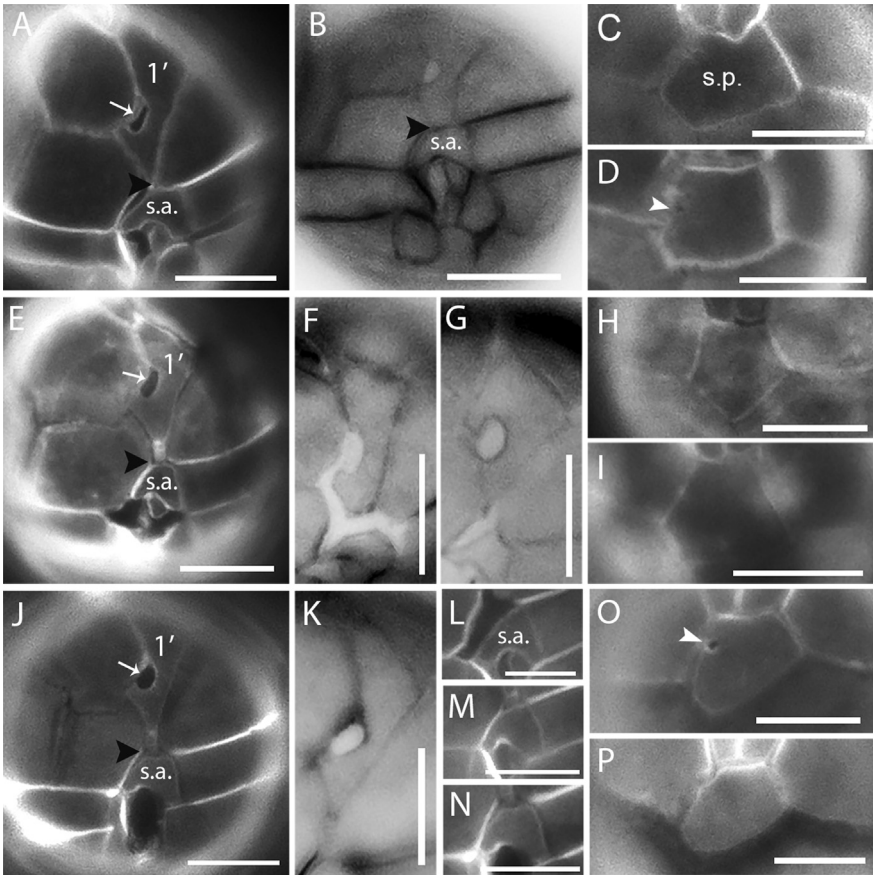

Fig. 1. Light micrographs of calcofluor-stained *A. ostenfeldii* cells from cultures of strains AOTV-B4A (A–D), VGO956 (E–I), and AOA32-2 (J–P). The 1′ plate including a prominent right-sided ventral pore (arrow) and terminated with a pointed (A) or flat (B, E, J, K) margin (black arrowhead indicates different types of margin that made contact with s.a. plate). Different s.a. plates are shown for each strain (A, E, J). Cells from strains VGO956 and AOA32-2 showing different shapes of 1′ (F, G, K) and s.a. (L–N) plates; are also shown, as is the diversity of the s.p. plates (C, D, H, I, O, P) of the three strains (white arrowhead indicates posterior connection pore). Scale bar = 10 μm.

cultures. A Lugol-fixed aliquot was collected from each flask to determine cell density by light microscopy using a Sedgewick–R-after chamber. Two 30-mL culture subsamples were filtered through GF/F glass-fiber filters (25 mm diameter) (Whatman, Maidstone, England) and kept at −20 °C. Once removed from the freezer, followed by sonication (1 min, 50 Watts) and two rounds of centrifugation (14,000 rpm, 10 min, 5 °C), one of the filters was extracted twice with 0.05 M acetic acid for PSP toxin analysis and the other with 100% methanol for SPX and GYM toxin analyses. The extracts (1.5 mL) were kept at −20 °C until used in the respective analyses, at which time acetic extracts were thawed and methanolic extracts were tempered to be subsequently filtered through 0.45-μm syringe filters.

2.4. Analysis of PSP toxins

PSP toxins were analyzed by high-performance liquid chromatography (HPLC) with post-column oxidation and fluorescence detection (FD) according to the method of Rourke et al. (2008) with slight modifications using a Zorbax Bonus RP column (4.6 × 150 mm, 3.5 μm). The analyses were carried out using a Waters Acquity ultra performance liquid chromatography (UPLC) system (Waters, USA). Mobile phase A was composed of 11 mM heptane sulfonate in a 5.5 mM phosphoric acid aqueous solution adjusted to pH 7.1 with ammonium hydroxide. Mobile phase B consisted of 88.5% 11 mM heptane sulfonate in a 16.5 mM phosphoric acid aqueous solution adjusted to pH 7.1 with ammonium hydroxide and 11.5% acetonitrile. The mobiles phases were filtered through a 0.2-μm membrane before use. A gradient was run at a flow rate of 0.8 mL min^{-1} starting at 100% A and held for 8 min. Mobile phase B was then increased linearly to 100% in 8 min. The gradient was kept at 100% B for 9 min and then returned in 0.1 min–100% A. An equilibration time of 5 min was allowed prior to the next injection. The total duration of the run was 30 min. The eluate from the column was mixed continuously with 7 mM periodic acid in 50 mM potassium phosphate buffer (pH 9.0) at a rate of 0.4 mL min^{-1} and was heated at 65 °C by passage through a coil of Teflon tubing (0.25 mm i.d., 8 m long). It was then mixed with 0.5 M acetic acid at 0.4 mL min^{-1} and pumped by a two-pump Waters Reagent Manager into the fluorescence detector, which was operated at an excitation wavelength of 330 nm. Emission at 390 nm was recorded. Data acquisition and data processing were performed using the Empower data system (Waters). Toxin concentrations were calculated from calibration curves obtained for the peak area and amount of each toxin. Injection volumes of 20 μL were used for each extract. Standards for the PSP toxins gonyautoxin (GTX)-4, GTX-1, dcGTX-3, dcGTX-2, GTX-3, GTX-2, neoSTX, dcSTX, and STX were acquired from the NRC Certified Reference Materials program (Halifax, NS, Canada). To verify the presence of, GTX-6 and GTX-5, the samples were boiled with an equal volume of 0.4 M HCl for 15 min to hydrolyze the sulfonic group of the N-sulfocarbamoyl, yielding the corresponding carbamoyl toxins (Franco and Fernandez Vila, 1993).

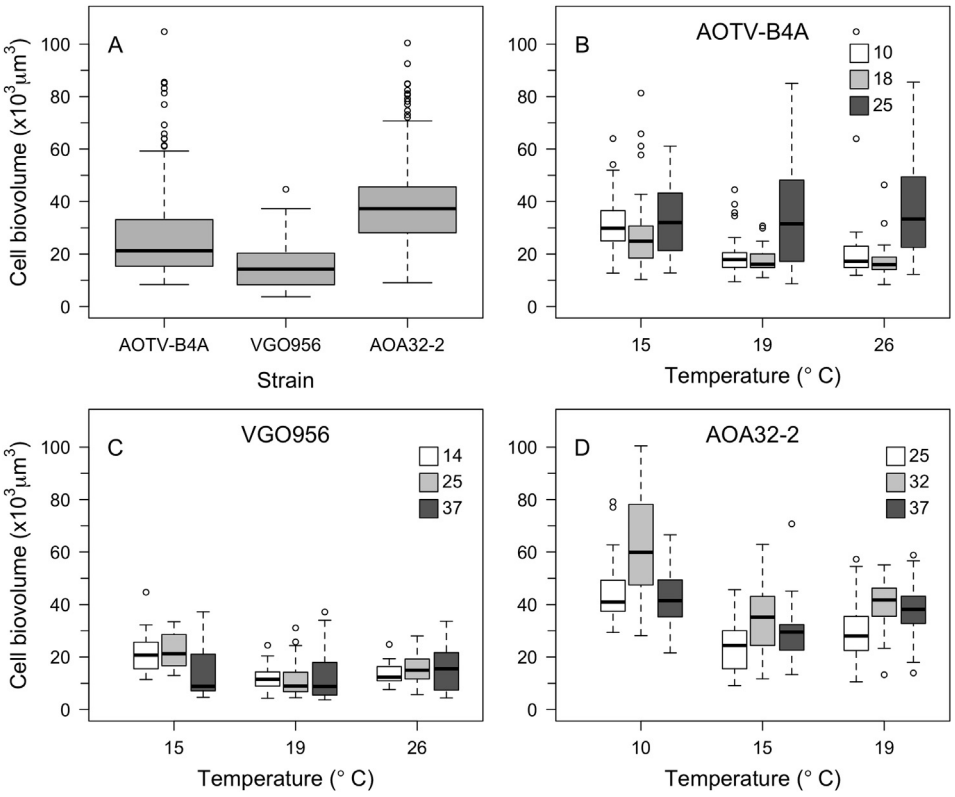

Fig. 2. Box-plots of the total cell biovolume ($n = 270$) of the three *A. ostenfeldii* strains (A) and the cell biovolume of strains AOTV-B4A (B), VGO956 (C), and AOA32-2 (D) exposed to different salinity and temperature conditions ($n = 30$). Salinity values are shown by colored boxes in the chart.

2.5. Analyses of lipophilic toxins (SPXs and GYMs)

SPX and GYM toxins were identified by liquid chromatography coupled to high-resolution mass spectrometry (LC–HRMS). Samples in methanol were analyzed on a Dionex Ultimate 3000 LC system (Thermo Fisher Scientific, San Jose, California) coupled to an Exactive mass spectrometer (Thermo Fisher Scientific, Bremen, Germany) equipped with an Orbitrap mass analyzer and a heated electrospray source (H–ESI II). Nitrogen (purity > 99.999%) was used as the sheath gas, auxiliary gas, and collision gas. The instrument was calibrated daily in positive and negative ion modes. Mass acquisition was performed in positive ion mode without and with all ion fragmentation (AIF) with a high-energy collisional dissociation (HCD) of 45 eV. The mass range was *m/z* 100–1000 in both full-scan and AIF modes.

SPXs and GYMs were separated and quantified according to the Standardized Operating Procedure (SOP) validated by the European Union Reference Laboratory for Marine Biotoxins (EURLMB, 2011). The X-Bridge C18 column (100 × 2.1 mm, 2.5 µm) was maintained at 25 °C; the injection volume was 20 µL and the flow rate 400 µL min^{-1}. Mobile phase A consisted of water, and mobile phase B of acetonitrile/water (95:5 v/v), both containing 2 mM ammonium formate and 50 mM formic acid. Linear gradient elution started at 10% B, increasing to 80% B in 4 min, where it was held for 2 min before the initial conditions of 10% B were restored in 0.5 min; the latter condition was maintained for 2.5 min to allow column equilibration. The total duration of the run was 9 min. Cyclic imines were identified by comparing their retention times with those of the available standards. The peaks in the chromatogram were identified by the exact masses of the diagnostic, fragment, and isotope ions. Cyclic imine standards for 13-desmethyl SPX-C (13dMeC; CRM-SPX-1 7.06 ± 0.4 µg mL^{-1}) and GYM-A (CRM-GYM-A 5 ± 0.2 µg mL^{-1}) were acquired from the NRC Certified Reference Materials program (Halifax, NS, Canada). In case another SPX or GYM different from the standards was identified in samples, they were quantified as 13dMeC or GYM-A equivalents, based on the respective calibrations available and assuming equal responses.

2.6. DNA extraction, PCR amplification, and sequencing

Exponentially growing vegetative cells from strains AOTV-B4A, VGO956, and AOA32-2 were harvested from the respective 1.5-mL subsamples by centrifugation (13,000 rpm for 2 min) in 1.5-mL Eppendorf tubes. The cells were washed with sterile MQ water, centrifuged as described above, and the resulting pellet was stored overnight at −80 °C. The next day, the samples were thawed, treated with 100 µL of 10% Chelex 100 beads (BioRad, Hercules, CA, USA), placed in a 95 °C Eppendorf Mastercycler EP5345 thermocycler (Eppendorf, New York, USA) for 10 min, and then vortexed. The boiling and vortex steps were repeated, after which the samples were centrifuged (13,000 rpm for 1 min) and the supernatants subsequently transferred to clean 200-µL tubes, avoiding carryover of the Chelex beads. The samples were kept at −20 °C until needed.

Polymerase chain reaction (PCR) amplification of the D1/D2 domains of the large subunit (LSU) rRNA gene was performed using the primer pair D1R/D2C (5′-ACCCGCTGAATTTAAGCATA-3′/5′-ACGAACGATTTGCACGTCAG-3′) (Lenaers et al., 1989). The 25-µL amplification reaction mixtures contained 2.5 µL of reaction buffer, 2 mM $MgCl_2$, 0.25 pmol of each primer, 2 mM of dNTPs, 0.65 units of Taq DNA polymerase (Qiagen, CA, USA), and 1 µL of the Chelex extracts. The DNA was amplified in an Eppendorf Mastercycler EP5345 under the following conditions: initial denaturation at 95 °C for 1 min, followed by 40 cycles of denaturation at 54 °C for

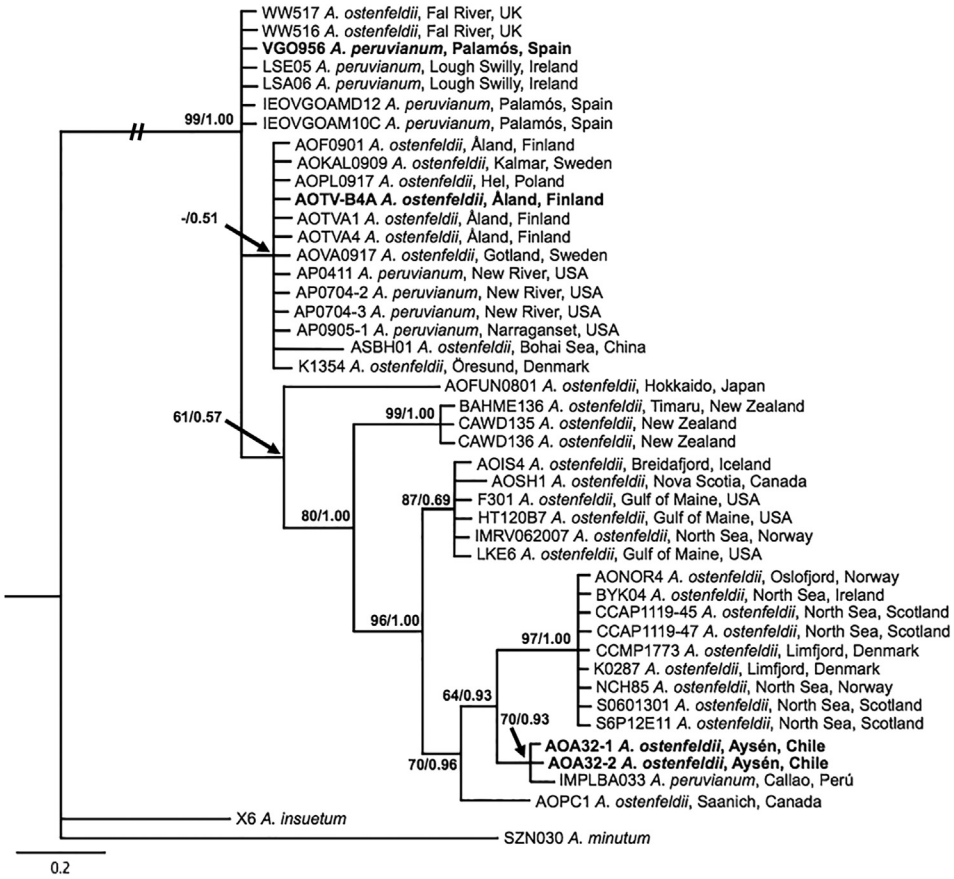

Fig. 3. Phylogenetic relationships among *A. ostenfeldii* strains based on the D1-D2 LSU rDNA sequences obtained in this study and from GenBank. *A. insuetum* and *A. minutum* sequences were used as outgroups. The phylogenetic tree was constructed using the maximum-likelihood method. Numbers at the branches indicate the percentage of bootstrap support ($n = 1000$) and posterior probabilities based on Bayesian inference as a search criterion. Bootstrap values <50% and probabilities <0.5 are denoted by hyphens. Names in bold represent isolates sequenced for this study.

1 min, annealing at 72 °C for 3 min, extension at 72 °C for 3 min, and a final extension at 72 °C for 10 min. A 10-μL aliquot of each PCR was checked by agarose gel electrophoresis (1% TAE, 50 V) and SYBR Safe DNA gel staining (Invitrogen, CA, USA).

The PCR products were purified with ExoSAP–IT (USB, Cleveland, OH, USA). The purified DNA was sequenced using the Big Dye Terminator v3.1 reaction cycle sequencing kit (Applied Biosystems, Foster City, CA, USA) and separated on an AB 3130 sequencer (Applied Biosystems) at the CACTI sequencing facilities (Universidade de Vigo, Spain). The LSU sequences obtained in this study for strains AOTV-B4A and VGO956 were deposited in the GenBank database (Acc. Nos. KP782039 and KP782040, respectively). The LSU sequence for Chilean strain AOA32-2 (Acc. No. KF479200) was deposited in Genbank during a Chilean study carried out in parallel to this one (G. Pizarro, IFOP, personal comm.). The sequences of the studied strains were compared with 40 sequences of other *A. ostenfeldii*/*peruvianum* strains obtained from Genbank. *Alexandrium insuetum* and *Alexandrium minutum* sequences were used as outgroups to root the tree.

The LSU sequences were aligned using BioEdit v.7.2.5. The final alignment for the LSU phylogeny consisted of 543 positions. The phylogenetic model was selected using MEGA 6 software. A Tamura's 3-parameter model (Tamura, 1992) with a gamma-shaped parameter ($\gamma = 0.213$) was selected. The phylogenetic relationships were determined using the maximum likelihood (ML) method of MEGA 6 and the Bayesian inference method (BI) with a general time reversible model from Mr.Bayes v3.1 (Huelsenbeck and Ronquist, 2001). The reconstructed topologies were very similar with the two methods. The phylogenetic tree was represented using the ML results, with bootstrap values from the ML method ($n = 1000$ replicates) and posterior probabilities from the BI method.

3. Results

3.1. Morphology of the organisms

Microscopic examination of the plate morphologies of cultured cells from the Baltic Sea (AOTV-B4A) and the Chilean Southern Sea (AOA32-2) generally agreed well with the original description of *A. ostenfeldii* by Balech and Tangen (1985), and those of the Mediterranean Sea strain (VGO956) with the original description of *A. peruvianum* by Balech and de Mendiola (1977). A detailed analysis of the thecal plates showed that most of the specimens of the three strains had a narrow and elongated 1′ plate with a prominent ventral pore located on its anterior right side. These plates terminated with a pointed or flat margin that made contact with the s.a. plate (Fig. 1A, B, E, J). However, other 1′ plate features were also observed, mainly in strains VGO956 and AOA32-2. In VGO956, two other types of 1′ plates were seen: one with a less elongated shape and a widely opened ventral pore (Fig. 1F) and another with a rhomboid shape and large enclosed ventral pore (Fig. 1G). Strain AOA32-2 (southern Chile) also exhibited another different elongated 1′ plate (Fig. 1K) with straight margins and an elliptical ventral pore.

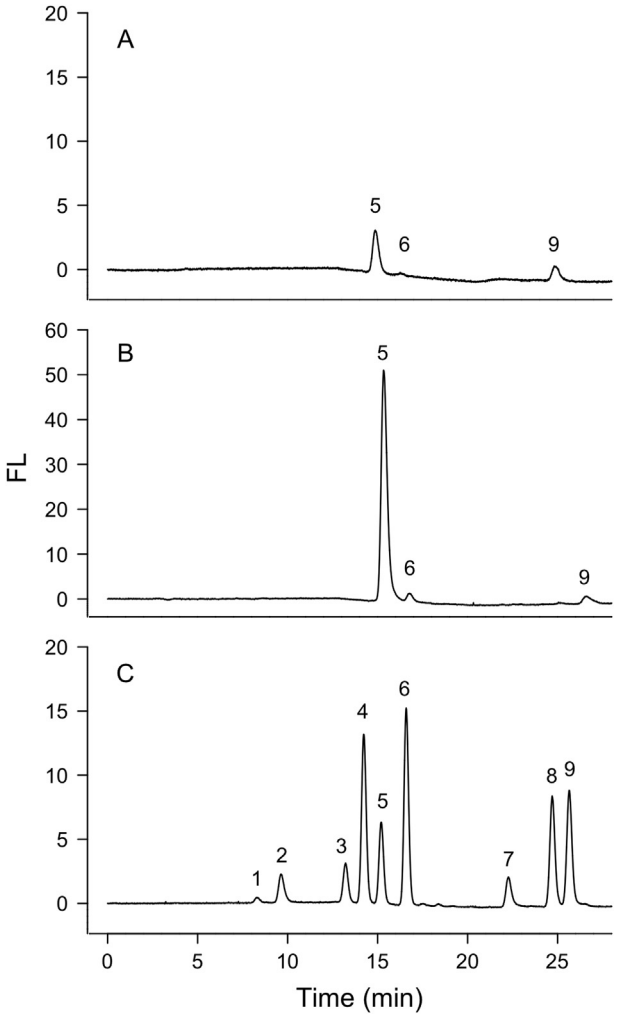

Fig. 4. Liquid chromatography PSP toxin profiles of *A. ostenfeldii* cultivated at a salinity of 25 and a temperature 19 °C. Strains AOTV-B4A (A) and AOA32-2 (B) produce GTX-3 (5), GTX-2 (6), and STX (9). Chromatogram of the standard PSP mixture (C) of GTX-4 (1), GTX-1 (2), dcGTX-3 (3), dcGTX-2 (4), GTX-3 (5), GTX-2 (6), neoSTX (7), dcSTX (8), and STX (9).

The s.a. plate in strain VGO956 was almost always triangular (Fig. 1E), but door-latch-shaped plates were also seen. Both shapes were also characteristic of the s.a. plates of strains AOTV-B4A and AOA32-2 but door-latch-shaped plates were more common (Fig. 1B, J, N). In the Chilean strain (AOA32-2), an additional s.a. plate type, with a shape intermediated between the door-latch and triangular shapes, was also detected (Fig. 1M). Finally, the s.p. plates of all strains were highly variable in shape and not all of them had a connection pore (Fig. 1C, D, H, I, O, P).

The cells occurred as solitary individuals in most cultures, but chains of two cells were observed occasionally. In general, the cells were round to ellipsoidal in shape, with a cell biovolume ranging from 3,691 μm^3 (equivalent to 20.63 μm long and 18.49 μm wide) to 104,746 μm^3 (61.03 μm long and 57.26 μm wide) (Fig. 2A). The largest cells were generally more ellipsoidal in shape than the smaller cells, which were round. The sizes of the cells differed significantly among the three strains (ANOVA: $P < 0.05$; $n = 270$), with cells of strain AOA32-2 being significantly ($P < 0.001$) the largest and those of strain VGO956 the smallest (Fig. 2A). The 95% mean confidence intervals (95% CIs) for the cell lengths and widths of the three strains were: 38.40 ± 0.89 μm and 34.97 ± 0.72 μm for strain AOTV-B4A; 31.53 ± 0.68 μm and 29.07 ± 0.62 μm for strain VGO956, and 43.22 ± 0.80 μm and 40.05 ± 0.64 μm for strain AOA32-2. Although cultures of all three strains consisted of both large and small cells, the largest size ranges occurred in strains AOTV-B4A and AOA32-2 (Fig. 2B–D). The size range also varied depending on the temperature and salinity, besides the intrinsic characteristics of the strains. For example, as shown in Fig. 2B, when strain AOTV-B4A was incubated at 19 °C, the cell size ranges observed at salinities of 18 and 25 differed significantly (cell length: mean ± SD of 33.88 ± 3.25 μm and 42.89 ± 9.98 μm, respectively; $P < 0.05$; $n = 30$). Growth at the lowest temperatures resulted in significantly ($P < 0.05$; $n = 90$) larger cells for all three strains (Fig. 2B–D), with those of strain AOA32-2 incubated at a salinity of 32 (Fig. 2D) having the highest mean cell biovolume (95% CIs for a mean length and width: 51.94 ± 2.32 μm and 46.96 ± 1.82 μm).

3.2. Phylogeny

The three selected strains from the three distant geographic regions grouped in different clades (Fig. 3). In the LSU rDNA phylogeny, Baltic strain AOTV-B4A grouped together with other *A. ostenfeldii* strains from the Baltic Sea (Finland, Sweden, Poland, and Denmark), New River and Narragansett (USA), and Bohai Sea (China). These sequences constituted a clade with low support (BI 0.51). Strain VGO956 grouped with its sister strains (IEOVGOAMD12 and IEOVGOAM10C) from the Spanish Mediterranean Sea, near Palamós, but also with North Sea strains from Fal River (UK) and Lough Swilly (Ireland) in a well-supported monophyletic clade (ML 99%, BI 1.0). Strain AOA32-2, from southern Chile, emerged in a separate branch (ML 70%, BI 0.93) together with a strain (IMPLBA033) from Callao (Peru).

3.3. PSP toxins

LC analyses showed detectable amounts of PSP toxins in all of the cultures of Baltic and Chilean strains (AOTV-B4A and AOA32-2, respectively), but not in the Mediterranean strain (VGO956). The toxin profiles of the two PSP-toxin-producing strains were the same (Fig. 4), although the toxin content of the Chilean strain (mean ± SD of 105.83 ± 72.15 pg $cell^{-1}$) was much higher than that of the Baltic strain (mean ± SD of 4.04 ± 1.93 pg $cell^{-1}$), which is according to the observed differences in their cell sizes (biovolume in Table 3, Figs. 2 and 5A). Toxin contents and cellular biovolume values for both strains in all of culture conditions are specified in Table 3. Differences in toxin content in relation to temperatures and salinities as well as cell sizes were assessed in Chilean strain AOA32-2; the small amounts of toxin content in AOTV-B4A did not allow that estimation. A significant correlation between toxin content and biovolume was observed for Chilean strain ($R = 0.96$, $P < 0.01$). Toxin values were highest when the strain was cultured at lower temperatures (10 °C) (mean ± SD of 174.47 ± 91.62 pg $cell^{-1}$) coinciding with the highest values of biovolume (Table 3). Lowest toxin contents (around 40–50 pg $cell^{-1}$) also agreed with the smallest cells and were detected in several temperatures and salinities.

The principal compounds produced by strains AOTV-B4A and AOA32-2 under all experimental conditions were GTX-3, GTX-2, and STX (Fig. 4). However, the toxin profiles of both strains also included trace amounts of dcSTX toxins in all treatments, except two, in which the levels of the latter toxin were undetectable: strain AOTV-B4A at 26 °C and a salinity of 25 and strain AOA32-2 at 10 °C and a salinity of 32. In the latter case, this was the condition in which cell biovolume and PSP toxin content were highest (Fig. 5A and Table 3). The toxin profile of strain AOTV-B4A was dominated by GTX-3 (81.9%), followed by STX (14.7%), GTX-2 (3%), and trace amounts (<0.5%) of dcSTX. The toxin profile of strain AOA32-2 was very similar to that of strain AOTV-B4A: GTX-3 (88.2%), STX (7.6%),

Table 3
Toxins (pg cell^{-1}) and mean of cell biovolume of the *A. ostenfeldii* strains under different salinity and temperature conditions. (ND: Not detected).

Strain	Salinity	Temperature °C	Biovolume (μm^3)	PSP toxins	SPXs	GYMs
AOTV-B4A	10	15	31,227	4.926	ND	32.748
AOTV-B4A	18	15	28,729	6.975	ND	54.673
AOTV-B4A	25	15	32,838	4.953	ND	47.341
AOTV-B4A	10	19	19,689	6.140	ND	27.893
AOTV-B4A	18	19	17,873	2.314	ND	27.774
AOTV-B4A	25	19	36,040	1.001	ND	39.663
AOTV-B4A	10	26	22,769	4.111	ND	46.676
AOTV-B4A	18	26	17,249	2.476	ND	44.243
AOTV-B4A	25	26	37,286	3.442	ND	113.435
VGO956	14	15	21,383	ND	0.004	ND
VGO956	25	15	22,298	ND	0.167	ND
VGO956	37	15	13,943	ND	0.577	ND
VGO956	14	19	11,922	ND	0.054	ND
VGO956	25	19	11,399	ND	0.370	ND
VGO956	37	19	12,503	ND	0.022	ND
VGO956	14	26	13,310	ND	2.309	ND
VGO956	25	26	15,637	ND	10.033	ND
VGO956	37	26	15,273	ND	12.158	ND
AOA32-2	25	10	45,077	130.686	ND	ND
AOA32-2	32	10	61,979	279.771	ND	ND
AOA32-2	37	10	42,645	112.958	ND	ND
AOA32-2	25	15	24,368	55.616	ND	ND
AOA32-2	32	15	34,137	73.030	ND	ND
AOA32-2	37	15	29,645	49.047	ND	ND
AOA32-2	25	19	29,837	43.772	ND	ND
AOA32-2	32	19	40,116	99.240	ND	ND
AOA32-2	37	19	37,955	108.307	ND	ND

GTX-2 (3.8%), and dcSTX (<0.5%). These proportions were mostly unchanged when the strains were cultured at different temperatures and salinities.

3.4. Cyclic imine toxins

LC–HRMS analyses of the organic extracts from the cultures showed that only strain VGO956 produced SPXs. Extracts of this Mediterranean strain contained 13dMeC at a retention time (RT) = 8.832 min 13dMeC yielded a protonated molecule at *m/z* 692.4522 $[M+H]^+$. The fragment ions generated in the HCD cell from the peak of 13dMeC were: the loss of a water molecule at *m/z* 674.4415 $[C_{42}H_{60}NO_6]^+$, *m/z* 444.3108 $[C_{27}H_{42}NO_4]^+$, *m/z* 342.2796 $[C_{23}H_{36}NO]^+$, *m/z* 230.1904 $[C_{16}H_{24}N]^+$, *m/z* 220.2062 $[C_{15}H_{26}N]^+$, *m/z* 206.1906 $[C_{14}H_{24}N]^+$, *m/z* 204.1749 $[C_{14}H_{22}N]^+$, *m/z* 177.1513 $[C_{12}H_{19}N]^+$, and *m/z* 164.1435 $[C_{11}H_{18}N]^+$. The fragment ion at *m/z* 164.1435 was the most intense and characteristic. In addition to 13dMeC, others SPXs were screened [20MeG, A, B, C, and D, desmethyl SPX-D, and the unknown SPXs listed in Sleno et al. (2004)], but they were not detected in any of the samples.

On a per cell basis, content of 13dMeC increased with increasing salinity and temperature. The highest contents were recorded at 26 °C (Fig. 5B and Table 3). At temperatures of 15 °C and 19 °C, the toxin content ranged from 0.004 pg cell^{-1} to 0.58 pg cell^{-1}, with the lowest content measured in cells grown at 15 °C and a salinity of 14 (Fig. 5B and Table 3). No correlation between SPX content and cell size was observed.

GYM content by the three strains was also analyzed using LC–HRMS. GYM compounds were observed only in Baltic strain AOTV-B4A, GYM-B/-C analogues (Fig. 6A, B) and an analogue of GYM-A (Fig. 6C, D). The latter compound was probably a positional isomer based on its mass and fragmentation spectrum (Table 4). The RT of this unknown GYM-A analogue was 4.27 min, which differed by 0.71 min from the RT of the GYM-A standard 3.56 min (Fig. 6E, F). To verify that the difference in the RT was not due to the sample matrix, one sample extract of AOTV-B4A was spiked with GYM-A standard. The RT of GYM-A was not altered by a matrix effect. Their mass spectra were qualitatively the same, including HCD fragment ions, but the percentages of the fragments differed (Fig. 6B, D). Thus, in the mass spectrum of the GYM-A standard (Fig. 6F) the abundance of the fragment $[M + H-H_2O]^+$ at *m/z* 490.3312 was more intense than that by the protonated molecule at *m/z* 508.3418 $[M+H]^+$, while the opposite was true for the GYM-A analogue (Fig. 6D). Characteristic HCD fragment ions of GYM-A were also detected in the GYM-A analogue (Table 4). In our search for GYM-B/-C toxins, a chromatogram for the mass range *m/z* 524–525 was acquired for the extract prepared from strain AOTV-B4A. It showed one peak at a RT of 4.01 min (Fig. 6A), which differed by +0.45 min from the RT of GYM-A (Fig. 6E, F). GYM-B/-C standards were not available to confirm the identity of these analogues in our samples but based on their more polar chemical structure, characterized by an additional exocyclic methylene at C17 and a hydroxyl group at C-18 (Miles et al., 2000, 2003), a shorter retention than that of GYM-A (RT 3.56 min) (Fig. 6E, F) in a reverse phase column (Marrouchi et al., 2010) was expected. The compound eluted at RT 4.01 min and produced by strain AOTV-B4 is probably a more lipophilic analogue of GYM-B/-C.

As there are, as yet, no standards for GYM-B and GYM-C and detailed descriptions of their fragmentation patterns have been published, we confirmed these compounds as follows. The accurate mass for the $[M+H]^+$ ion *m/z* 524.3365 $[C_{32}H_{46}NO_5]^+$ with 10.5 relative double bond (RDB) equivalents and −1.049 Δ ppm was observed. The mass spectral characterization from the AIF experiment for this GYM-B/-C analogue is shown in Table 5. It was compared with the HCD mass spectrum of GYM-B/-C detailed by De la Iglesia et al. (2012). Three characteristic water losses from the protonated molecule, at *m/z* 506.3257, *m/z* 488.3147, and *m/z* 470.3039, were observed. Moreover, a series of common ions with GYM-A as the parent compound were generated in the HCD cell (Table 5).

All samples were also screened for the presence of 12MeGYM but this compound was not detected under any conditions. The highest content of GYMs (113.44 pg GYM-A equivalents cell^{-1}) was measured in cells cultured at the highest temperature and salinity

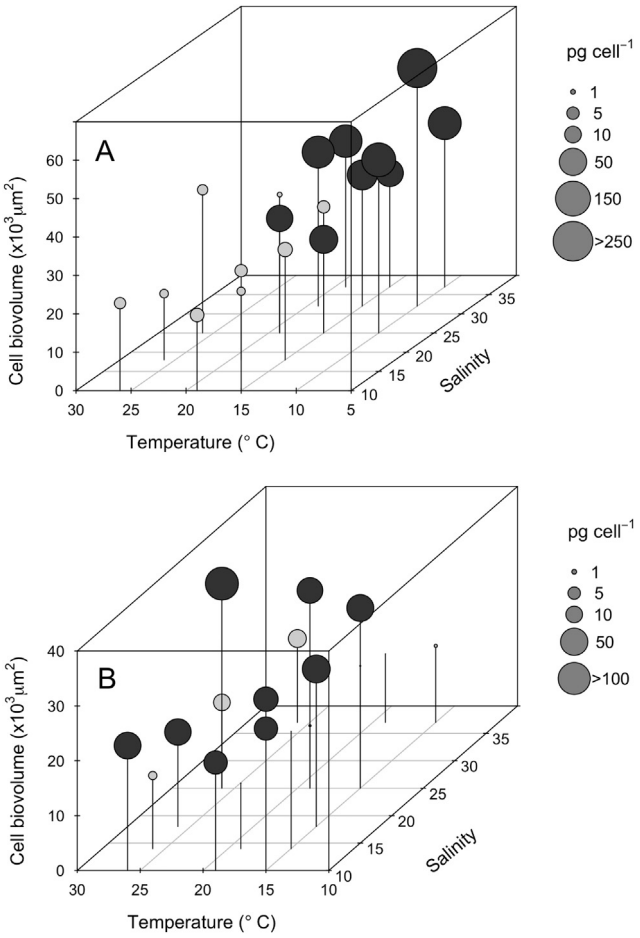

Fig. 5. Cell biovolume and toxin content of *A. ostenfeldii* cultures exposed to different salinity and temperature conditions. Total PSP toxin content (A) in cultures of strains AOTV-B4A (gray circle) and AOA32-2 (black circle). Total content of SPXs in cultures of strains VGO956 (gray circle) and GYMs in cultures of strains AOTV-B4A (black circle) (B). Note that the temperature axis is inverted.

(26 °C, salinity of 25). These were also the largest cells (biovolume in Fig. 5B). However, the lowest content of GYMs (around 30–40 pg GYM-A equivalents cell^{-1}) were in cells cultured under several intermediate experimental conditions (19 °C, salinity of 18).

4. Discussion

4.1. The detected toxins and their relevance

Toxins from the STX group, SPXs, and GYMs were found in *A. ostenfeldii* (Syn. *A. peruvianum*) in the present study, although their distributions differed in the three studied strains from different geographic locations. Mediterranean strain (VGO956) produced SPXs but not PSP toxins, in agreement with the findings in the literature for *A. ostenfeldii* and *A. peruvianum* strains of the same region (Ciminiello et al., 2006, 2007, 2010; Franco et al., 2006; Riobó et al., 2013; Kremp et al., 2014). The Baltic Sea strain (AOTV-B4A) produced PSP toxins but not SPXs, consistent with the results from other strains from that region (Hakanen et al., 2012; Suikkanen et al., 2013; Kremp et al., 2014). Finally, Chilean strain (AOA32-2) produced only PSP toxins. While this finding is in agreement with that of Pizarro et al. (2012), it contradicts those reported by Almandoz et al. (2014) for *A. ostenfeldii* strains isolated from the Argentinean part of the Beagle Channel (1,000 km south of the area where our Chilean strain was isolated), which produced only SPXs (13dMeC and 20MeG).

Among all the toxins detected in *A. ostenfeldii*, those of the STX group are the most dangerous because they may result in the severe and occasionally fatal illness known as PSP syndrome. The threat of PSP syndrome is not only a major cause of concern for public health but is also detrimental to the economy (Anderson et al., 2012). Outbreaks of PSP toxins often result in the death of marine life and livestock and the closure of contaminated fisheries. Together with the continual expenditures required for the maintenance and running of monitoring programs, the economic burden of PSP syndrome is of worldwide significance. Regarding these toxins, it is worth highlight the high PSP toxin content (max. 279.77 pg cell^{-1}) measured in *A. ostenfeldii* cultures from Aysén suggested that this species may be more toxic than previously thought. This conclusion is supported by the environmental conditions in the fjords and channels of Patagonia, where the temperature and salinity (10 °C and 32, respectively; see Molinet et al., 2003; Almandoz et al., 2014) can be easily the same as those that resulted in the highest cell biovolume and toxin content for this strain in our study (Table 3).

The other two (SPXs and GYMs), belonging to the cyclic imines group have not been directly linked to human intoxications (Richard et al., 2001; Molgó et al., 2014). Currently, there is still a lack of information on the chronic toxicity of cyclic imines or their possible synergy with other toxins that may be present in the same samples. Thus, no regulatory controls have been established for these toxins. The toxicological relevance of this group of toxins and its implication for the safety of shellfish production are not yet completely clear. The European Food Safety Authority has therefore requested more exposure data to properly assess the risk posed by cyclic imines to shellfish consumers.

4.2. GYM compounds in A. ostenfeldii

The detection of GYM compounds in the *A. ostenfeldii* strain from the Baltic Sea, analyzed in this work, provides further insights into both the toxin profile of this specie and scientific knowledge about the GYM complex. As we noted in the Results section, peaks distinct from those of the GYM-A standard appeared in the chromatogram with the same spectrum as GYM-A, although with RTs indicative of their more lipophilic nature. A similar profile was observed by Naila et al. (2012) in clams from the Gulf of Gabes (Tunisia), related to blooms of *K. selliformis*. The authors hypothesized that it was a new isomer of GYM-A or a derivative or weakly bonded aggregate that releases free GYM-A in the ion source. Later, De la Iglesia et al. (2012) confirmed the presence in those samples of gymnodimine fatty acid ester metabolites produced by shellfish. Our search for these compounds in the Baltic strain was, as expected, negative. Harju et al. (2014) found related analogues of GYM-A, B, and C in some Baltic strains. The analogue of GYM-A detected in that study was more lipophilic than the GYM-A standard, as was the derivative present in the Baltic strain from the present work. Therefore, we suspect that these GYM-A analogues are the same compound although we do not have the detailed mass spectrum of their compound to compare with ours. Regarding the GYM-B/-C analogue detected in the present work, it was more lipophilic than GYM-A and therefore also more lipophilic than GYM-B/-C. However, this analogue seems to be different from the two related GYM-B/-C compounds discovered by Harju et al. (2014), since both are less lipophilic than the GYM-B/-C standard, according to the information on their RTs provided by the authors.

4.3. Differences on the toxin profiles of A. ostenfeldii

The information summarized in Table 1 shows the great

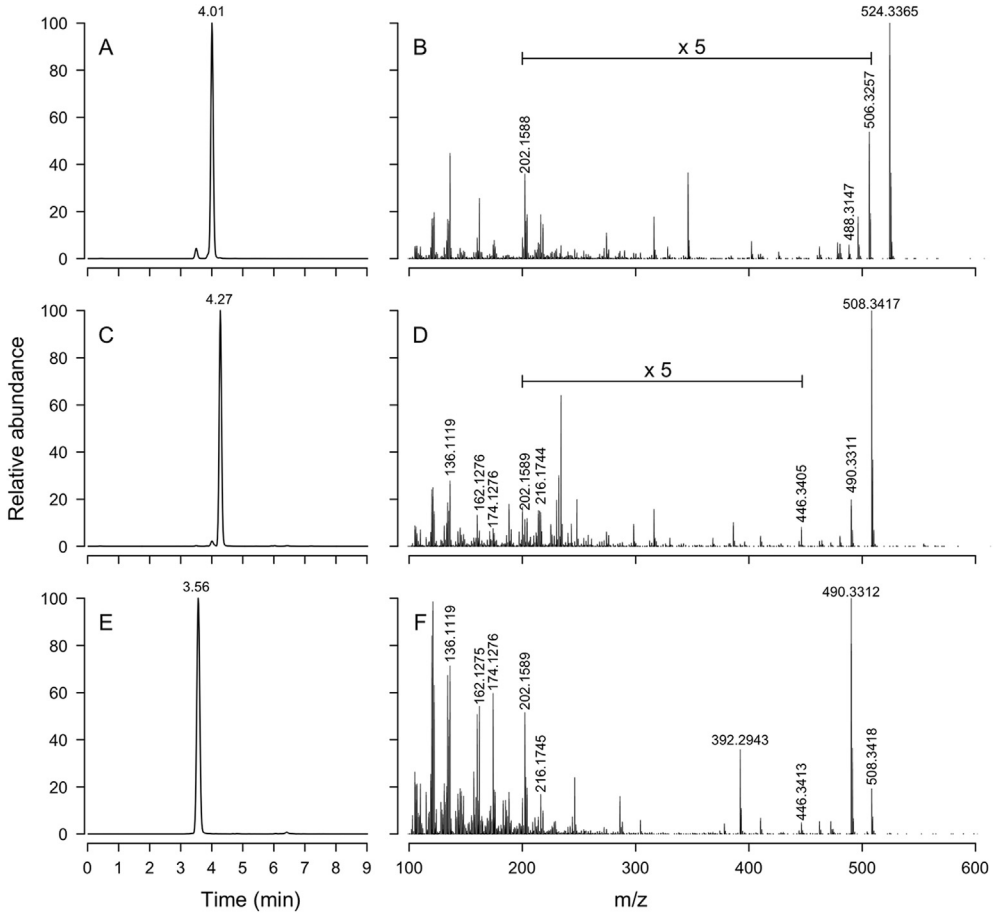

Fig. 6. Selected liquid chromatography coupled to high-resolution mass spectrometry chromatograms (left) and mass spectra (right) from positive ionization mode for *A. ostenfeldii* strain AOTV-B4A (A–D) and the GYM-A standard (E, F). *m/z* 524.3365 [M+H]+ for GYM-B/-C analogue (A, B); *m/z* 508.3417 [M+H]+ for GYM-A analogue (C, D).

variation in the toxin profiles of *A. ostenfeldii* (Syn. *A. peruvianum*) strains from all of the geographic regions where this species and its toxins have been reported. Comparisons of the toxin profiles of these strains are difficult because many of the respective studies do not report all of the toxin groups (PSP toxins and the cyclic imines SPXs and GYMs). In addition, for most of the regions information is still scarce. Nonetheless, valuable information is obtained by preliminary comparisons of the differences in the PSP toxins and/or SPX from different geographic zones. Thus, in the case of the North Atlantic, Baltic Sea, and Mediterranean Sea strains, the PSP/SPX profiles are highly consistent (Fig. 7, see references in Table 1): 1) North Atlantic and Mediterranean Sea strains are mostly characterized by SPX; 2) the Baltic Sea strain is defined by PSP toxin; and 3) the Kattegat Sea strain produces SPX toxins. The latter region can be viewed as a transitional one between the Baltic Sea and the North Sea (Hansen et al., 1992). For the Chilean strains, our data showed an invariable toxin profile characterized only by PSP toxins, although more data are required from Aysén and other nearby areas to confirm the distribution and variability of *A. ostenfeldii*'s toxin profiles in the region.

An important question is whether toxin profiles change in response to changing environmental conditions. In the present study, the strains steadily produced the same types of toxins (PSP toxins, SPXs, and GYMs) independent of the experimental temperature and salinity conditions. Rather, these variables affected only cell growth and the quantity of the PSP toxins, although the order of dominance (GTX-3, STX, and GTX-2) was preserved. The same has been reported in other studies showing that the production of either SPXs or PSP toxins was not induced by changes in salinity, temperature, or CO_2 supply, which instead affected the relative content of the different PSP toxins and SPX analogues (Otero et al., 2010; Kremp et al., 2012; Suikkanen et al., 2013). Similar effects have been reported for nutrients and growth phase in *A. ostenfeldii* cultures (Anderson et al., 1990; Hwang and Lu, 2000; Granéli and Flynn, 2006; Hu et al., 2006). In the case of GYMs, the scarce data prevent any conclusions on the consistency of the appearance of these toxins and the variations related to the physicochemical conditions of the cultures. We found much higher content of GYMs (maximum of 113.44 pg GYM-A equivalents cell^{-1} vs. a minimum of 27.77 pg GYM-A equivalents cell^{-1}) under the highest temperature and salinity (26 °C, salinity of 25) than under other conditions.

4.4. Phylogeny and morphology related to strains and their toxin profiles

The results of the phylogenetic analysis showed that the three strains of *A. ostenfeldii* grouped with other strains of different geographic origin and their phylogenetic classification was coincident with previous studies (Kremp et al., 2014; Tillmann et al., 2014). Moreover, the toxin profiles of those groups have common features that merit discussion. According to our LSU analysis, Mediterranean strain (VGO956), with a toxin profile composed solely of 13dMeC, was grouped with strains sharing the same toxin profile as those from Fal River (UK), Lough Swilly (Ireland), and Palamós (Mediterranean Spain) (Table 1). Such clade corresponds

Table 4
HRMS data obtained from the AIF spectra acquired in the mass range *m/z* 100–1000. List of the measured accurate masses (*m/z*) for $[M+H]^+$ and the product ions of GYM-A as recorded by De la Iglesia et al. (2012) (left), the GYM-A standard from this study (middle), and the GYM-A analogue detected in the Baltic strain from this work (right). Retention times, exact mass and assigned formulae with relative double bonds (RDB) equivalents, and mass accuracy measurements (Δ in ppm) are detailed. ND (not detected).

	Mass spectrum GYM-A (De la Iglesia et al., 2012)	Mass spectrum GYM-A (standard) RT 3.56 min	Mass spectrum GYM-A analogue (AOTV-B4A) RT 4.27 min
m/z	508.3414	508.3418	508.3417
FORMULA	$C_{32}H_{46}NO_4^+$	$C_{32}H_{46}NO_4^+$	$C_{32}H_{46}NO_4^+$
RDB, Δ ppm	NI, −1.4	10.5, −0.66	10.5, −0.856
m/z	490.3305	490.3312	490.3311
FORMULA	$C_{32}H_{44}NO_3^+$	$C_{32}H_{44}NO_3^+$	$C_{32}H_{44}NO_3^+$
RDB, Δ ppm	NI, −2.2	11.5, −0.756	11.5, −0.960
m/z	446.3408	446.3413	446.3405
FORMULA	$C_{31}H_{44}NO_2^+$	$C_{31}H_{44}NO_2^+$	$C_{31}H_{44}NO_2^+$
RDB, Δ ppm	NI, −2.2	10.5, −0.989	10.5, −2.782
m/z	410.3045	410.3048	410.305
FORMULA	$C_{27}H_{40}NO_2^+$	$C_{27}H_{40}NO_2^+$	$C_{27}H_{40}NO_2^+$
RDB, Δ ppm	NI, −2.1	8.5, −1.355	8.5, −0.868
m/z	392.2939	392.2943	3922941
FORMULA	$C_{27}H_{38}NO^+$	$C_{27}H_{38}NO^+$	$C_{27}H_{38}NO^+$
RDB, Δ ppm	NI, −2.2	9.5, −1.252	9.5, −1.762
m/z	368.294	ND	368.2583
FORMULA	$C_{24}H_{37}NO^+$	$C_{24}H_{34}NO_2^+$	$C_{24}H_{34}NO_2^+$
RDB, Δ ppm	NI, −2.2	8.5, −4.089	8.5, −0.287
m/z	304.2266	304.2267	304.2254
FORMULA	$C_{19}H_{30}NO_2^+$	$C_{19}H_{30}NO_2^+$	$C_{19}H_{30}NO_2^+$
RDB, Δ ppm	NI, −1.8	5.5, −1.334	5.5, −5.607
m/z	286.2159	286.2163	286.2163
FORMULA	$C_{19}H_{28}NO^+$	$C_{19}H_{28}NO^+$	$C_{19}H_{28}NO^+$
RDB, Δ ppm	NI, −2.4	6.5, −0.842	6.5, −0.842
m/z	246.1847	246.185	246.1848
FORMULA	$C_{16}H_{24}NO^+$	$C_{16}H_{24}NO^+$	$C_{16}H_{24}NO^+$
RDB, Δ ppm	NI, −2.1	5.5, −0.979	5.51, −1.791
m/z	216.1742	216.1745	216.1744
FORMULA	$C_{15}H_{22}N^+$	$C_{15}H_{22}N^+$	$C_{15}H_{22}N^+$
RDB, Δ ppm	NI, −2.1	5.5, −0.815	5.5, −1.278
m/z	202.1586	202.1589	202.1589
FORMULA	$C_{14}H_{20}N^+$	$C_{14}H_{20}N^+$	$C_{14}H_{20}N^+$
RDB, Δ ppm	NI, −2.0	5.5, −1.119	−0.624
m/z	174.1274	174.1276	174.1276
FORMULA	$C_{12}H_{16}N^+$	$C_{12}H_{16}N^+$	$C_{12}H_{16}N^+$
RDB, Δ ppm	NI, −2.0	5.5, −0.724	5.5, −0.724
m/z	162.1274	162.1275	162.1276
FORMULA	$C_{11}H_{26}N^+$	$C_{11}H_{26}N^+$	$C_{11}H_{26}N^+$
RDB, Δ ppm	NI, −2.0	4.5, −1.394	4.5, −0.778
m/z	136.1118	136.1119	136.1119
FORMULA	$C_9H_{14}N^+$	$C_9H_{14}N^+$	$C_9H_{14}N^+$
RDB, Δ ppm	NI, −1.9	3.5, −1.293	3.5, −1.293

to the Group 2 of other phylogenetic studies (Kremp et al., 2014; Tillmann et al., 2014). The Chilean strains analyzed in the present study grouped within a phylogenetic clade, a subgroup of Group 6 of Kremp et al. (2014), that includes a Peruvian strain (IMPLBA033), with which they shared the characteristic of producing only PSP toxins (Kremp et al., 2014, Table 1). The only difference in the toxin profiles was that in some cases trace amounts of dcSTX were detected in the Chilean strains (Table 1). Finally, the Baltic Sea strain (AOTV-B4A) formed a monophyletic group with other strains from the same area, as reported by Tahvanainen et al. (2012). The clade also includes strains from the Atlantic coast of the USA (Borkman et al., 2012; Tomas et al., 2012), one Chinese strain (ASBH01) (Gu et al., 2013), and another from eastern Denmark (K1354) (Kremp et al., 2014). All Baltic strains of this monophyletic clade, which correspond to Group 1 of Kremp et al. (2014), are known to produce PSP toxins. The toxin profile of Baltic *A. ostenfeldii* was shown by Kremp et al. (2014) and Suikkanen et al. (2013) to include GTX-3, STX, and GTX-2, which agrees with the results of our study. However, unlike the other strains in the clade, the Chinese strain produces only STX and neoSTX (Gu et al., 2013) and not GTXs. However, all of these Group 1 strains are STX producers (Kremp et al., 2014).

With respect to the morphological features of the strains, the Baltic Sea (AOTV-B4A) and Chilean Southern Sea (AOA32-2) strains more closely match the *A. ostenfeldii* description of Balech and Tangen (1985), and the Mediterranean Sea strain (VGO956) the *A. peruvianum* description of Balech and de Mendiola (1977). However, coinciding with Kremp et al. (2014), the morphological study carried out in this work showed a tabulation of the thecal plates too variable to be of use in defining and separating the above mentioned genetically determined groups.

5. Conclusions

The morphology, phylogeny, and toxin profiles of the three geographically differentiated strains of *A. ostenfeldii* investigated in this study corroborate both the dissimilarities in toxin production and the taxonomic complexities reported in the literature for this species complex. While the Mediterranean Sea strain was characterized by its SPX content, the Chilean strain was defined by PSP toxins and the Baltic Sea strain by PSP toxins and GYM analogues. The PSP toxin profiles of the southern Chile and Baltic strains were coincident in their inclusion of GTX-3, GTX-2, and STX. However, the Chilean strain was much more toxic than the Baltic strain. The latter was the only strain with detectable amounts of GYM compounds: analogues of GYM-A and GYM-B/-C. The toxin contents (PSP toxins and/or SPX) of the three strains coincide with those of

Table 5
HRMS data obtained from AIF spectra acquired in the mass range *m/z* 100–1000. List of measured accurate masses (*m/z*) for $[M+H]^+$ and product ions of GYM-B/-C as recorded by De la Iglesia et al. (2012) (left) and the GYM-B/-C analogue detected in the Baltic strain from this work (right). Retention times, exact mass and assigned formulae with relative double bonds (RDB) equivalents, and mass accuracy measurements (Δ in ppm) are detailed. NI (no information).

	Mass spectrum GYM-B/-C (De la Iglesia et al., 2012)	Mass spectrum GYM-B/-C analogue (AOTV-B4A) RT 4.01 min
m/z	524.3365	524.3375
FORMULA	$C_{32}H_{46}NO_5^+$	$C_{32}H_{46}NO_5^+$
RDB, Δ ppm	NI, −1.1	10.5, 1.240
m/z	506.4	506.3257
FORMULA	$C_{32}H_{44}NO_4^+$	$C_{32}H_{44}NO_4^+$
RDB, Δ ppm	NI, NI	11.5, −1.551
m/z	488.4	488.3147
FORMULA	$C_{32}H_{42}NO_3^+$	$C_{32}H_{42}NO_3^+$
RDB, Δ ppm	NI, NI	12.5, −2.5
m/z	NI	470.3039
FORMULA	NI	$C_{32}H_{40}NO_2^+$
RDB, Δ ppm	NI, NI	13.5, −3.096
m/z	462	462.3358
FORMULA	$C_{31}H_{44}NO_2^+$	$C_{31}H_{44}NO_2^+$
RDB, Δ ppm	NI, NI	10.5, −1.852
Product ion spectrum common with GYM-A		
m/z	368.294	368.2569
FORMULA	$C_{24}H_{37}NO^+$	$C_{24}H_{34}NO_2^+$
RDB, Δ ppm	NI, −2.2	8.5, −4.089
m/z	304.2266	304.2266
FORMULA	$C_{19}H_{30}NO_2^+$	$C_{19}H_{30}NO_2^+$
RDB, Δ ppm	NI, −1.8	5.5, −1.662
m/z	286.2159	286.2159
FORMULA	$C_{19}H_{28}NO^+$	$C_{19}H_{28}NO^+$
RDB, Δ ppm	NI, −2.4	6.5, −2.240
m/z	246.1847	246.1848
FORMULA	$C_{16}H_{24}NO^+$	$C_{16}H_{24}NO^+$
RDB, Δ ppm	NI, −2.1	5.5, −1.791
m/z	216.1742	216.1744
FORMULA	$C_{15}H_{22}N^+$	$C_{15}H_{22}N^+$
RDB, Δ ppm	NI, −2.1	5.5, −1.278
m/z	202.1586	202.1588
FORMULA	$C_{14}H_{20}N^+$	$C_{14}H_{20}N^+$
RDB, Δ ppm	NI, −2.0	5.5, −1.119
m/z	174.1274	174.1276
FORMULA	$C_{12}H_{16}N^+$	$C_{12}H_{16}N^+$
RDB, Δ ppm	NI, −2.0	5.5, −0.724
m/z	162.1274	162.1275
FORMULA	$C_{11}H_{26}N^+$	$C_{11}H_{26}N^+$
RDB, Δ ppm	NI, −2.0	4.5, −1.394
m/z	136.1118	136.1119
FORMULA	$C_9H_{14}N^+$	$C_9H_{14}N^+$
RDB, Δ ppm	NI, −1.9	3.5, −1.293

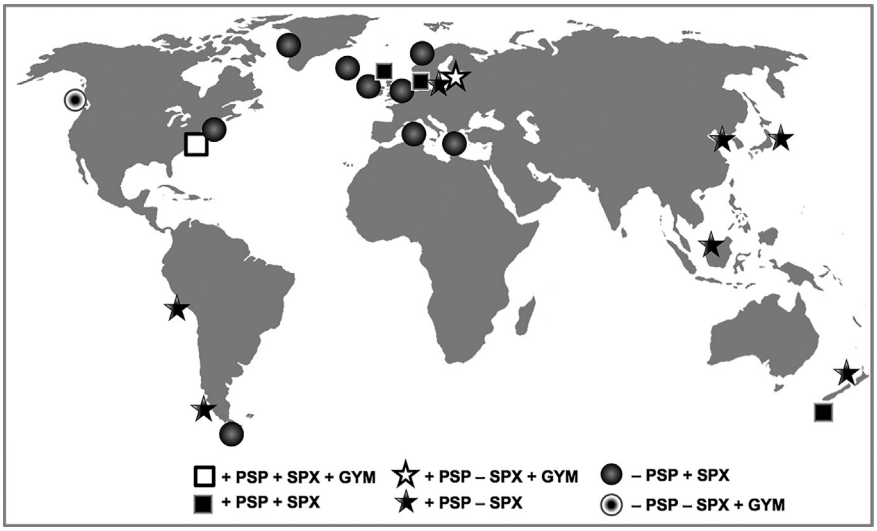

Fig. 7. Global distribution of PSP toxins, SPXs, and GYMs of *A. ostenfeldii* strains reported in the literature. The figure is based on the studies listed in Table 1, which include analyses of PSP toxins and SPXs performed for the same strains as well as literature data on GYMs.

other strains already reported from the same geographic origin and belonging to the same phylogenetic group. This provides support for the recognition of PSP toxins and/or SPX production as a characteristic phenotypic trait of the genetically isolated populations, as already suggested in the literature. However, in the case of GYM compounds, further studies are needed before any related, definitive conclusions can be reached.

Ethical Statement

The authors of manuscript "Differences in the toxin profiles of *Alexandrium ostenfeldii* (Dinophyceae) strains isolated from different geographic origins: Evidence of paralytic toxin, spirolide, and gymnodimine" submitted to Toxicon confirm that the experiments are in accordance with current European Union laws.

They state that no animals were used during experimental work and that the methodology used has no ethical implications or biosecurity related.

Acknowledgments

We thank P.A. Díaz for help with R plotting, M. García for support in the phylogeny, A. Fernández-Villamarín for technical assistance in processing the toxin samples, and I. Ramilo and P. Rial for technical assistance with the cultures. This work is a contribution of Unidad Asociada "Microalgas Nocivas" (CSIC-IEO) and was carried out at the Instituto Español de Oceanografía (IEO) in Vigo and was financially supported by the CCVIEO project and CICAN-2013-40671-R (Ministry of Economy and Competitiveness). P. Salgado is a researcher at the IFOP, which provides financial support for his doctoral staying.

Transparency document

Transparency document related to this article can be found online at http://dx.doi.org/10.1016/j.toxicon.2015.06.015.

References

Aasen, J., MacKinnon, S., LeBlanc, P., Walter, J., Hovgaard, P., Aune, T., Quilliam, M., 2005. Detection and identification of spirolides in Norwegian shellfish and plankton. Chem. Res. Toxicol. 18, 509–515.

Almandoz, G., Montoya, N., Hernando, M., Benavides, H., Carignan, M., Ferrario, M., 2014. Toxic strains of the *Alexandrium ostenfeldii* complex in southern South America (Beagle Channel, Argentina). Harmful Algae 37, 100–109.

Amzil, Z., Sibat, M., Royer, R., Masson, N., Abadie, E., 2007. Report on the first detection of Pectenotoxin-2, spirolide-a and their derivatives in French shellfish. Mar. Drugs 5, 168–179.

Anderson, D.M., Alpermann, T., Cembella, A., Collos, Y., Masseret, E., Montresor, M., 2012. The globally distributed genus *Alexandrium*: multifaceted roles in marine ecosystems and impacts on human health. Harmful Algae 14, 10–35.

Anderson, D.M., Kulis, D.M., Sullivan, J.J., Hall, S., 1990. Toxin composition variations in one isolate of the dinoflagellate *Alexandrium fundyense*. Toxicon 28, 885–893.

Balech, E., 1995. The Genus *Alexandrium* Halim (Dinoflagellata). Sherkin Island Marine Station, Sherkin Island Co., Cork, Ireland.

Balech, E., de Mendiola, B.R., 1977. Un nuevo *Gonyaulax* productor de hemotalasia en Perú. Neotropica 23, 49–54.

Balech, E., Tangen, K., 1985. Morphology and taxonomy of toxic species in the tamaresis group (Dinophyceae): *Alexandrium excavatum* (Braarud) comb. nov. and *Alexandrium ostenfeldii* (Paulsen) comb. nov. Sarsia 70, 333–343.

Beuzenberg, V., Mountfort, D., Holland, P., Shi, F., MacKenzie, L., 2012. Optimization of growth and production of toxins by three dinoflagellates in photobioreactor cultures. J. Appl. Phycol. 24, 1023–1033.

Biré, R., Krys, S., Frémy, J.M., Dragacci, S., Stirling, D., Kharrat, R., 2002. First evidence on occurrence of gymnodimine in clams from Tunisia. J. Nat. Toxins 11, 269–275.

Borkman, D., Smayda, T., Tomas, C., York, R., Strangman, S., Wright, J., 2012. Toxic *Alexandrium peruvianum* (Balech and de Mendiola) Balech and Tangen in Narragansett Bay, Rhode Island (USA). Harmful Algae 19, 92–100.

Brown, L., Bresnan, E., Graham, J., Lacaze, J.P., Turrell, E., Collins, C., 2010. Distribution, diversity and toxin composition of the genus *Alexandrium* (Dinophyceae) in Scottish waters. Eur. J. Phycol. 45, 375–393.

Burson, A., Matthijs, H., de Bruijne, W., Talens, R., Hoogenboom, R., Gerssen, A., Visser, P., Stomp, M., Steur, K., van Scheppingen, Y., Huisman, J., 2014. Termination of a toxic *Alexandrium* bloom with hydrogen peroxide. Harmful Algae 31, 125–135.

Cembella, A., Bauder, A., Lewis, N., Quilliam, M., 2001. Association of the gonyaulacoid dinoflagellate *Alexandrium ostenfeldii* with spirolide toxins in size-fractionated plankton. J. Plankton Res. 23, 1413–1419.

Cembella, A., Lewis, N., Quilliam, M., 2000. The marine dinoflagellate *Alexandrium ostenfeldii* (Dinophyceae) as the causative organism of spirolide shellfish toxins. Phycologia 39, 67–74.

Ciminiello, P., Dell'Aversano, C., Dello Iacovo, E., Fattorusso, E., Forino, M., Grauso, L., Tartaglione, L., Guerrini, F., Pezzolesi, L., Pistocchi, R., 2010. Characterization of 27-hydroxy-13-desmethyl spirolide C and 27-oxo-13,19-didesmethyl spirolide C. Further insights into the complex Adriatic *Alexandrium ostenfeldii* toxin profile. Toxicon 56, 1327–1333.

Ciminiello, P., Dell'Aversano, C., Fattorusso, E., Forino, M., Grauso, L., Tartaglione, L., Guerrini, F., Pistocchi, R., 2007. Spirolide Toxin Profile of Adriatic *Alexandrium ostenfeldii* Cultures and Structure Elucidation of 27-Hydroxy-13,19-didesmethyl Spirolide C. J. Nat. Prod. 70, 1878–1883.

Ciminiello, P., Dell'Aversano, C., Fattorusso, E., Magno, S., Tartaglione, L., Cangini, M., Pompei, M., Guerrini, F., Boni, L., Pistocchi, R., 2006. Toxin profile of *Alexandrium ostenfeldii* (Dinophyceae) from the Northern Adriatic Sea revealed by liquid chromatography–mass spectrometry. Toxicon 47, 597–604.

De la Iglesia, P., McCarron, P., Diogène, J., Quilliam, M.A., 2012. Discovery of gymnodimine fatty acid ester metabolites in shellfish using liquid chromatography/mass spectrometry. Rapid Commun. Mass Spectrom. 27, 643–653.

EURLMB, 2011. EU-Harmonised Standard Operating Procedure for Determination of Lipophilic Marine Biotoxins in Molluscs by LC–MS/MS. European Union Reference Laboratory for Marine Biotoxins. http://aesan.msps.es/en/CRLMB/web/home.shtml.

Franco, J.M., Fernandez Vila, P., 1993. Separation of paralytic shellfish toxins by reversed phase high performance liquid chromatography with postcolumn reaction and fluorimetric detection. Cromatographia 35, 613–620.

Franco, J.M., Paz, B., Riobó, P., Pizarro, G., Figueroa, R., Fraga, S., Bravo, I., 2006. First report of the production of spirolids by *Alexandrium peruvianum* (Dinophyceae) from the Mediterranean Sea. In: 12th International Conference on Harmful Algae, Copenhagen, Denmark, 4–8 September.

Fritz, L., Triemer, R.E., 1985. A rapid simple technique utilizing Calcoflour White M2R for the visualization of dinoflagellate thecal plates. J. Phycol. 21, 662–664.

Granéli, E., Flynn, K., 2006. Chemical and physical factors influencing toxin content. In: Granéli, E., Turner, J. (Eds.), Ecology of Harmful Algae, Ecological Studies Series, 189. Springer-Verlag, Berlin Heidelberg.

Gribble, K., Keafer, B., Quilliam, M., Cembella, A., Kulis, D., Manahan, A., Anderson, D.M., 2005. Distribution and toxicity of *Alexandrium ostenfeldii* (Dinophyceae) in the Gulf of Maine, USA. Deep-Sea Res. Pt. II 52, 2745–2763.

Gu, H., Zeng, N., Liu, T., Yang, W., Müller, A., Krock, B., 2013. Morphology, toxicity, and phylogeny of *Alexandrium* (Dinophyceae) species along the coast of China. Harmful Algae 27, 68–81.

Guillard, R.R.L., Hargraves, P.E., 1993. Stichochrysis immobilis is a diatom, not achrysophyte. Phycologia 32, 234–236.

Hakanen, P., Suikkanen, S., Franzén, J., Franze, H., Kankaanpää, H., Kremp, A., 2012. Bloom and toxin dynamics of *Alexandrium ostenfeldii* in a shallow embayment at the SW coast of Finland, northern Baltic Sea. Harmful Algae 15, 91–99.

Hallegraeff, G.M., 1993. A review of harmful algal blooms and their apparent global increase. Phycologia 32, 79–99.

Hallegraeff, G.M., 2010. Ocean climate change, phytoplankton community responses, and harmful algal blooms: a formidable predictive challenge. J. Phycol. 46, 220–235.

Hansen, P., Cembella, A., Moestrup, Ø., 1992. The marine dinoflagellate *Alexandrium ostenfeldii*: paralytic shellfish toxin concentration, composition, and toxicity to a tintinnid ciliate. J. Phycol. 28, 597–603.

Harju, K., Kremp, A., Suikkanen, S., Kankaanpää, H., Vanninen, P., 2014. Mass spectrometric screening of novel gymnodimine-like compounds in isolates of *Alexandrium ostenfeldii*. In: 16th Internation Conference on Harmful Algae, Wellington, New Zealand.

Haywood, A., Steidinger, K., Truby, E., Bergquist, P., Bergquist, P., Adamson, J., MacKenzie, L., 2004. Comparative morphology and molecular phylogenetic analysis of three new species of the genus *Karenia* (Dinophyceae) from New Zealand. J. Phycol. 40, 165–179.

Hu, T., Chen, W., Shi, Y., Cong, W., 2006. Nitrate and phosphate supplementation to increase toxin production by the marine dinoflagellate *Alexandrium tamarense*. Mar. Pollut. Bull. 52, 756–760.

Hu, T., Curtis, J., Oshima, Y., Quilliam, M., Walter, J., Watson-Wright, W., Wright, J., 1995. Spirolides B and D, two novel macrocycles isolated from the digestive glands of shellfish. J. Chem. Soc. Chem. Commun. 2159–2161.

Huelsenbeck, J.P., Ronquist, F., 2001. MrBAYES: Bayesian inference of phylogenetic trees. Bioinformatics 17, 754–755.

Hwang, D., Lu, Y., 2000. Influence of environmental and nutritional factors on growth, toxicity, and toxin profile of dinoflagellate *Alexandrium minutum*. Toxicon 38, 1491–1503.

Jester, R., Rhodes, L., Beuzenberg, V., 2009. Uptake of paralytic shellfish poisoning and spirolide toxins by paddle crabs (*Ovalipes catharus*) via a bivalve vector. Harmful Algae 8, 369–376.

Kaga, S., Sekiguchi, K., Yoshida, M., Ogata, T., 2006. Occurrence and toxin production *Alexandrium* spp. (Dinophyceae) in coastal waters of Iwate Prefecture, Japan. Nippon Suisan Gakk 72, 1068–1076.

Katikou, P., Aligizaki, K., Zacharaki, T., Iossifidis, D., Nikolaidis, G., 2010. First report of spirolides in Greek shellfish associated with causative *Alexandrium* species. In: 14th International Conference on Harmful Algae, Crete, Greek, 1–5 November.

Kharrat, R., Servent, D., Girard, E., Ouanounou, G., Amar, M., Marrouchi, R., Benoit, E., Molgó, J., 2008. The marine phycotoxin gymnodimine targets muscular and neuronal nicotinic acetylcholine receptor subtypes with high affinity. J. Neurochem. 107, 952–963.

Kremp, A., Godhe, A., Egardt, J., Dupont, S., Suikkanen, S., Casabianca, S., Penna, A., 2012. Intraspecific variability in the response of bloom-forming marine microalgae to changed climate conditions. Ecol. Evol. 2, 1195–1207.

Kremp, A., Lindholm, T., Dreßler, N., Erler, K., Gerdts, G., Eirtovaara, S., Leskinen, E., 2009. Bloom forming *Alexandrium ostenfeldii* (Dinophyceae) in shallow waters of the Åland Archipelago, Northern Baltic Sea. Harmful Algae 318–328.

Kremp, A., Tahvanainen, P., Litaker, W., Krock, B., Suikkanen, S., Leaw, C.P., Tomas, C., 2014. Phylogenetic relationships, morphological variation, and toxin patterns in the *Alexandrium ostenfeldii* (Dinophyceae) complex: implications for species boundaries and identities. J. Phycol. 50, 81–100.

Lenaers, G., Maroteaux, L., Michot, B., Herzog, M., 1989. Dinoflagellates in evolution. A molecular phylogenetic analysis of large subunit ribosomal RNA. J. Mol. Evol. 29, 40–51.

Lim, P.T., Ogata, T., 2005. Salinity effect on growth and toxin production of four tropical *Alexandrium* species (Dinophyceae). Harmful Algae 45, 699–710.

Lim, P.T., Usup, G., Leaw, C.P., Ogata, T., 2005. First report of *Alexandrium taylori* and *Alexandrium peruvianum* (Dinophyceae) in Malaysia waters. Harmful Algae 4, 391–400.

MacKenzie, L., 1994. More blooming problems: toxic algae and shellfish biotoxins in the South Island (January–May 1994). Seaf. N. Z. 2, 47–52.

MacKenzie, L., White, D., Oshima, Y., Kapa, J., 1996. The resting cyst and toxicity of *Alexandium ostenfeldii* (Dinophyceae) in New Zealand. Phycologia 35, 148–155.

MacKinnon, S., Walter, J., Quilliam, M., Cembella, A., LeBlanc, P., Burton, I., Hardstaff, W., Lewis, N., 2006. Spirolides Isolated from Danish Strains of the Toxigenic Dinoflagellate *Alexandrium ostenfeldii*. J. Nat. Prod. 69, 983–987.

Maclean, C., Cembella, A., Quilliam, M., 2003. Effects of Light, Salinity and Inorganic Nitrogen on Cell Growth and Spirolide Production in the Marine Dinoflagellate *Alexandrium ostenfeldii* (Paulsen) Balech et Tangen. Bot. Mar. 46, 466–476.

Marrouchi, R., Benoit, E., Kharrat, R., Molgo, J., 2010. Gymnodimines: a family of phycotoxins contaminating shellfish. In: Berbier, J., Benoit, E., Marchot, P., Mattei, C., Servent, D. (Eds.), Advances and New Technologies in Toxinology. SFET Editions: Meetings on Toxinology, pp. 79–83. E-book RT18.

Miles, C., Wilkins, A., Stirling, D., MacKenzie, L., 2000. New Analogue of Gymnodimine from a *Gymnodinium* Species. J. Agric. Food Chem. 48, 1373–1376.

Miles, C., Wilkins, A., Stirling, D., MacKenzie, L., 2003. Gymnodimine C, an Isomer of Gymnodimine B, from *Karenia selliformis*. J. Agric. Food Chem. 51, 4838–4840.

Molgó, J., Aráoz, R., Benoit, E., Iorga, B., 2014. Cyclic imine toxins: chemistry, origin, metabolism, pharmacology, toxicology, and detection. In: Botana, L.M. (Ed.), Seafood and Freshwater Toxins, third ed. CRC Press, Boca Raton, pp. 951–989.

Molinet, C., Lafon, A., Lembeye, G., Moreno, C., 2003. Patrones de distribución espacial y temporal de floraciones de *Alexandrium catenella* (Whedon & Kofoid) Balech 1985, en aguas interiores de la Patagonia noroccidental de Chile. Rev. Chil. Hist. Nat. 76, 681–698.

Naila, I.B., Hamza, A., Gdoura, R., Diogène, J., de la Iglesia, P., 2012. Prevalence and persistence of gymnodimines in clams from the Gulf of Gabes (Tunisia) studied by mouse bioassay and LC–MS/MS. Harmful Algae 18, 56–64.

Otero, A., Alfonso, A., Vieytes, M.R., Cabado, A.G., Vieites, J.M., Botana, L.M., 2010. Effects of environmental regimens on the toxin profile of *Alexandrium ostenfeldii*. Environ. Toxicol. Chem. 29, 301–310.

Otero, A., Chapela, M.J., Atanassova, M., Vieites, J.M., Cabado, A.G., 2011. Cyclic imines: chemistry and mechanism of action: a review. Chem. Res. Toxicol. 24, 1817–1829.

Pizarro, G., Pesse, N., Salgado, P., Alarcón, C., Garrido, C., Guzmán, L., 2012. Determinación de capacidad de adherencia, mecanismos de propagación y métodos de destrucción de *Alexandrium catenella* (célula vegetativa y quiste). Informe Final. Subsecretaría de Pesca y Acuicultura, p. 278.

Ravn, H., Schmidt, C., Sten, H., Anthoni, U., Christophersen, C., Nielsen, P., 1995. Elicitation of *Alexandrium ostenfeldii* (Dinophyceae) affects the toxin profile. Comp. Biochem. Physiol. 111C, 405–412.

Richard, D., Arsenault, E., Cembella, A., Quilliam, M., 2001. Investigations into the toxicology and pharmacology of spirolides, a novel group of shellfish toxins. In: Hallegraeff, G.M., Blackburn, S.I., Bolch, C.J., Lewis, R.J. (Eds.), Harmful Algal Blooms 2000. Intergovernmental Oceanographic Commission of UNESCO, pp. 383–386.

Riobó, P., Rodriguez, F., Garrido, J.L., Franco, J.M., 2013. Toxin profiles of *A. ostenfeldii* and *A. peruvianum*. Comparison of two clonal strains with different light tolerance, Marine and Freshwater Toxins Analysis. In: Fourth Joint Symposium and AOAC Task Force Meeting, Baiona-Pontevedra, Spain, 5–9 May.

Roach, J., LeBlanc, P., Lewis, N., Munday, R., Quilliam, M., MacKinnon, S., 2009. Characterization of a Dispiroketal Spirolide Subclass from *Alexandrium ostenfeldii*. J. Nat. Prod. 72, 1237–1240.

Rourke, W.A., Murphy, C.J., Pitcher, G., Van de Riet, J.M., Garth Burns, B., Thomas, K.M., Quilliam, M.A., 2008. Rapid postcolumn methodology for determination of paralytic shellfish toxins in shellfish tissue. J. AOAC Int. 91, 589–597.

Rundberget, T., Bunæs, J., Selwood, A., Miles, C., 2011. Pinnatoxins and spirolides in Norwegian blue mussels and seawater. Toxicon 58, 700–711.

Seki, T., Satake, K., Mackenzie, L., Kaspar, H., Yasumoto, T., 1995. Gymnodimine, a new marine toxin of unprecedented structure isolated from New Zealand Oysters and the dinoflagellate, *Gymnodinium* sp. Tetrahedron Lett. 36, 7093–7096.

Sleno, L., Chalmers, M., Volmer, D., 2004. Structural study of spirolide marine toxins by mass spectrometry. Part II. Mass Spectrometric characterization of unknown spirolides and related compounds in a cultured phytoplankton extract. Anal. Bioanal. Chem. 378, 977–986.

Suikkanen, S., Kremp, A., Hautala, H., Krock, B., 2013. Paralytic shellfish toxins or spirolides? The role of environmental and genetic factors in toxin production of the *Alexandrium ostenfeldii* complex. Harmful Algae 26, 52–59.

Sun, J., Liu, D., 2003. Geometric models for calculating cell biovolume and surface area for phytoplankton. J. Plankton Res. 25, 1331–1346.

Tahvanainen, P., Alpermann, T., Figueroa, R., John, U., Hakanen, P., Nagai, S., Blomster, J., Kremp, A., 2012. Patterns of post-glacial genetic differentiation in marginal populations of a marine microalga. PLoS ONE 7, e53602.

Tamura, K., 1992. Estimation of the number of nucleotide substitutions when there are strong transition-transversion and G + C-content biases. Mol. Biol. Evol. 9, 678–687.

Tillmann, U., Kremp, A., Tahvanainen, P., Krock, B., 2014. Characterization of spirolide producing *Alexandrium ostenfeldii* (Dinophyceae) from the western Arctic. Harmful Algae 39, 259–270.

Tomas, C., Van Wagoner, R., Tatters, R., White, K., Hall, S., Wright, J., 2012. *Alexandrium peruvianum* (Balech and Mendiola) Balech and Tangen a new toxic species for coastal North Carolina. Harmful Algae 17, 54–63.

Touzet, N., Franco, J.M., Raine, R., 2008. Morphogenetic diversity and biotoxin composition of *Alexandrium* (dinophyceae) in Irish coastal waters. Harmful Algae 7, 782–797.

Touzet, N., Lacaze, J., Maher, M., Turrell, E., Raine, R., 2011. Summer dynamics of *Alexandrium ostenfeldii* (Dinophyceae) and spirolide toxins in Cork Harbour, Ireland. Mar. Ecol. Prog. 425, 21–33.

Van Wagoner, R., Misner, I., Tomas, C., Wright, J., 2011. Occurrence of 12-methylgymnodimine in a spirolide-producing dinoflagellate *Alexandrium peruvianum* and the biogenetic implications. Tetrahedron Lett. 52, 4243–4246.

II

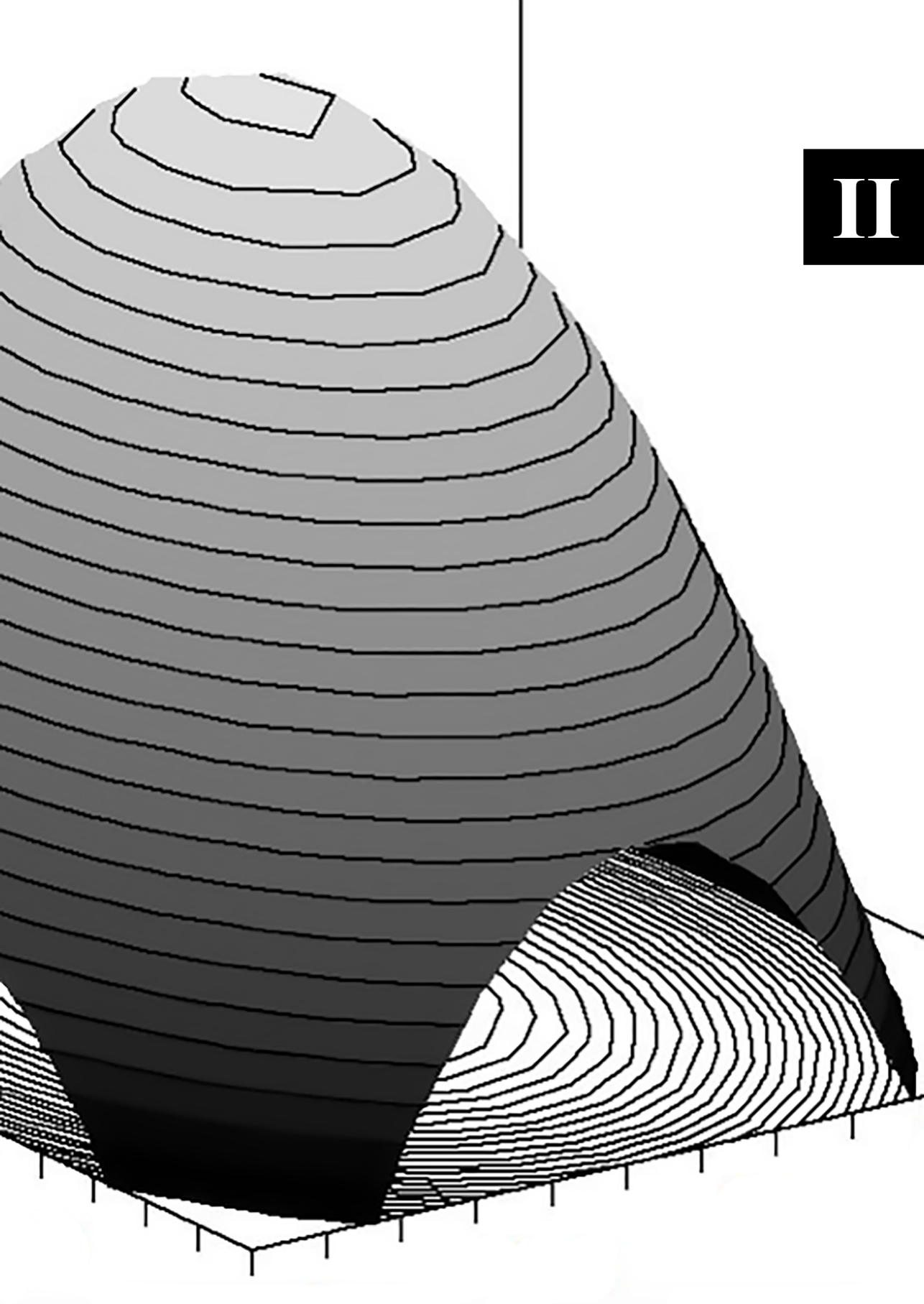

PLOS ONE

RESEARCH ARTICLE

A Kinetic and Factorial Approach to Study the Effects of Temperature and Salinity on Growth and Toxin Production by the Dinoflagellate *Alexandrium ostenfeldii* from the Baltic Sea

Pablo Salgado[1,4]*, José A. Vázquez[2], Pilar Riobó[3], José M. Franco[3], Rosa I. Figueroa[4], Anke Kremp[5], Isabel Bravo[4]

1 Departamento de Medio Ambiente, División de Investigación en Acuicultura, Instituto de Fomento Pesquero (IFOP), Punta Arenas, Chile, **2** Grupo de Reciclado y Valorización de Materiales Residuales (REVAL), Instituto de Investigaciones Marinas (IIM-CSIC), Vigo, Spain, **3** Instituto de Investigaciones Marinas (IIM-CSIC), Vigo, Spain, **4** Centro Oceanográfico de Vigo, Instituto Español de Oceanografía (IEO), Vigo, Spain, **5** Marine Research Centre, Finnish Environment Institute (SYKE), Helsinki, Finland

* pablo.salgado@ifop.cl

OPEN ACCESS

Citation: Salgado P, Vázquez JA, Riobó P, Franco JM, Figueroa RI, Kremp A, et al. (2015) A Kinetic and Factorial Approach to Study the Effects of Temperature and Salinity on Growth and Toxin Production by the Dinoflagellate *Alexandrium ostenfeldii* from the Baltic Sea. PLoS ONE 10(12): e0143021. doi:10.1371/journal.pone.0143021

Editor: Hans G. Dam, University of Connecticut, UNITED STATES

Received: May 6, 2015

Accepted: October 29, 2015

Published: December 4, 2015

Data Availability Statement: All relevant data are within the paper.

Funding: This work is a contribution of the Unidad Asociada "Microalgas Nocivas" (CSIC-IEO) and was financially supported by the CCVIEO project and CICAN-2013-40671-R (Ministry of Economy and Competitiveness). P. Salgado is a researcher at IFOP, which has provided financial support for his doctoral stay.

Abstract

Alexandrium ostenfeldii is present in a wide variety of environments in coastal areas worldwide and is the only dinoflagellate known species that produces paralytic shellfish poisoning (PSP) toxins and two types of cyclic imines, spirolides (SPXs) and gymnodimines (GYMs). The increasing frequency of *A*. *ostenfeldii* blooms in the Baltic Sea has been attributed to the warming water in this region. To learn more about the optimal environmental conditions favoring the proliferation of *A*. *ostenfeldii* and its complex toxicity, the effects of temperature and salinity on the kinetics of both the growth and the net toxin production of this species were examined using a factorial design and a response-surface analysis (RSA). The results showed that the growth of Baltic *A*. *ostenfeldii* occurs over a wide range of temperatures and salinities (12.5–25.5°C and 5–21, respectively), with optimal growth conditions achieved at a temperature of 25.5°C and a salinity of 11.2. Together with the finding that a salinity > 21 was the only growth-limiting factor detected for this strain, this study provides important insights into the autecology and population distribution of this species in the Baltic Sea. The presence of PSP toxins, including gonyautoxin (GTX)-3, GTX-2, and saxitoxin (STX), and GYMs (GYM-A and GYM-B/-C analogues) was detected under all temperature and salinity conditions tested and in the majority of the cases was concomitant with both the exponential growth and stationary phases of the dinoflagellate's growth cycle. Toxin concentrations were maximal at temperatures and salinities of 20.9°C and 17 for the GYM-A analogue and > 19°C and 15 for PSP toxins, respectively. The ecological implications of the optimal conditions for growth and toxin production of *A*. *ostenfeldii* in the Baltic Sea are discussed.

Competing Interests: The authors have declared that no competing interests exist.

Introduction

In recent decades, dinoflagellate species that are causative agents of harmful algal blooms (HABs) have been studied intensively, due to their global proliferation and their adverse effects on public health, recreation and tourism, fisheries, aquaculture and the ecosystems in which they are found. Although measures to counter HABs are still lacking, it is clear that the control of bloom events requires detailed knowledge of their basic features, including the adaptive strategies of the responsible dinoflagellate species and the environmental factors that regulate them [1]. Among toxin-producing dinoflagellates, members of the genus *Alexandrium* are the causative agents of the most widespread seafood poisoning syndrome caused by HABs, paralytic shellfish poisoning (PSP) syndrome. Toxigenic *Alexandrium* species are mainly distributed within coastal and temperate waters, although toxic populations are also found in subtropical, tropical, and perhaps even Arctic waters [2]. Currently, this genus includes 31 morphologically defined species, of which 12 produce PSP toxins [3, 4]. Among these well-known species, *Alexandrium ostenfeldii* (or synonym *Alexandrium peruvianum*) is the only member of the genus *Alexandrium* able to produce toxins of the cyclic imine type, including spirolide (SPX) and gymnodimine (GYM) [5–8]. Cyclic imine toxins are a family of structurally related marine neurotoxins of dinoflagellate origin that contaminate shellfish. Their basic structure consists of an imine moiety as a part of a bicyclic ring system [9]. These toxins display fast-acting toxicity when injected intraperitoneally in laboratory mice, although there have been no reported cases of poisoning in humans [10, 11]. The toxin profiles of *A. ostenfeldii* are complex. *A. ostenfeldii* was identified as the source of SPX toxins in Nova Scotia, Canada [5], even though it had been previously reported as a source of PSP-associated neurotoxin, which also causes a toxic syndrome [12]. In recent studies [6–8], GYM was shown to be produced by *A. ostenfeldii* strains of different geographic origin.

A recent study on phylogenetic, morphological, and toxin profiles of *A. ostenfeldii* and *A. peruvianum* strains from diverse geographic origins showed that *A. peruvianum* should be considered synonymous with *A. ostenfeldii*, and therefore discontinued as a distinct taxon [13]. Thus, the two species are considered synonymous herein. The first record of *A. ostenfeldii* was from the northern coast of Iceland [14], but the species has since been reported in most cold water environments, from the high latitudes of the Atlantic Ocean and northern Europe [12, 15–18] to the southern Pacific Ocean off the coast of austral Chile and Argentina [19–22]. However, *A. ostenfeldii* also occurs in warm waters, including off the coasts of Peru [23, 24], Malaysia [25], Spain [26], Italy [27], and Greece [28]. *A. ostenfeldii* also tolerates a wide range of salinities, based on its presence in the low-salinity environments of the Baltic Sea [29] and Chilean fiords and channels [22, 30] but also along the Mediterranean coast, where the salinities are higher [27, 31].

The toxin profiles of strains from those diverse environments also vary, with the production of SPX or PSP toxin by some strains depending upon the region of origin [6, 29]. For example, strains of *A. ostenfeldii* from the Baltic Sea mainly produce PSP toxins but not SPXs; those of the North Sea and Mediterranean Sea produce SPXs [6, 13]; and those of the Kattegat Sea (located between the Baltic Sea and the North Sea) produce both. The production of GYM toxins by Baltic Sea strains was recognized only recently [6, 8] and, thus far, only Narragansett and New River (USA) strains of *A. ostenfeldii* contain PSP toxins and the two cyclic imines (SPX and GYM) [7, 32, 33].

The relationship between environmental factors and toxin production by dinoflagellates is complex. Experimental studies have shown that the production of either SPXs or PSP toxins by *A. ostenfeldii* is influenced by salinity, temperature, and nutrients (see [29, 34, 35]). Whether this is also the case for the recently discovered GYM toxins in *A. ostenfeldii* strains is unclear.

Thus, in the present work, we used a kinetic and factorial approach to study the effects of salinity and temperature on growth and toxin production by a strain of *A. ostenfeldii* isolated from the Baltic Sea.

Material and Methods

Culture conditions

Alexandrium ostenfeldii strain AOTV-B4A was isolated from the Baltic Sea (Åland, Finland) in summer 2004 and is maintained as part of our culture collection of toxic microalgae at the Spanish Institute of Oceanography in Vigo (CCVIEO: http://www.vgohab.es/). The cultures were acclimated gradually to different salinities (max. 3–4 salinity units at a time) and temperatures for at least during three transfers after reaching the stationary phase, according to the experimental conditions selected to develop the factorial design (Table 1). Pyrex glass bottles (1 L) containing 500 mL of L1 medium without silicate [36] were inoculated with exponentially growing cells (2,000–4,000 cells mL^{-1}) to a final concentration of 900 cells mL^{-1}. The medium was prepared using seawater collected from the Galician shelf at a depth of 5 m and adjusted to the salinities listed in Table 1 by the addition of sterile MQ water (Milli-Q; Millipore, USA). A photoperiod of 12 h of light (photon flux approximately 100 μmol m^{-2} s^{-1}) and 12 h of darkness was used. Growth was monitored as cell yield (cells mL^{-1}) throughout the growth cycle of *A. ostenfeldii*. Eight or nine samples (6–28 mL) were collected in total from each of the cultures during the experimental period and used in the toxin analyses (PSP toxins and cyclic imines: SPX and GYM) and cell counts. Sampling resulted in the removal of no more than 27% of the total volume of each culture. Samples used to determine cell counts were fixed with Lugol solution. Cell density was determined by light microscopy using a Sedgwick–Rafter chamber.

Harmful effects due to a high pH and the pH changes resulting from the different cell concentrations in the treatments were controlled through a pH-measurement experiment performed throughout the entire growth cycle of the *A. ostenfeldii* strain using two replicates at *S*5/*T*19 and *S*9.7/*T*23.6. The pH kinetics were very similar in the two cultures, which yielded high (*S*9.7/*T*23.6 maximum of 22,266 cells mL^{-1}) and low (*S*5/*T*19 maximum of 8,485 cells mL^{-1}) rates of growth. The pH varied during growth progression by 1 and 1.5 units,

Table 1. Experimental domain and codification of the independent variables in the factorial rotatable design.

Coded values	Natural values	
	S	***T* (°C)**
-1.41	5.0	12.5
-1	9.7	14.4
0	21.0	19.0
+1	32.3	23.6
+1.41	37.0	25.5

Codification: $V_c = (V_n - V_0)/\Delta V_n$.

Decodification: $V_n = V_0 + (\Delta V_n \times V_c)$.

Vn = natural value of the variable to be codified.

Vc = codified value of the variable.

V_0 = natural value in the center of the domain.

ΔV_n = increment of V_n for unit of V_c.

doi:10.1371/journal.pone.0143021.t001

respectively, and never exceeded 9.10. The results showed that CO_2 was not a limiting factor for cell growth in the cultures.

Extraction and analysis of toxins

The content and relative proportions of PSP toxin and cyclic imines (SPXs and GYMs) in samples from cultures exposed to different experimental conditions were determined as follows: Two culture subsamples were filtered through GF/F glass-fiber filters (25 mm diameter; Whatman, Maidstone, England) and maintained in a freezer at –20°C. After two freeze/thaw cycles, the samples were sonicated (1 min, 50 Watts) and then centrifuged (14,000 rpm, 10 min, 5°C). One of the filters was extracted twice with 0.05 M acetic acid for PSP toxin analysis and the other twice with 100% methanol for SPX and GYM toxin analyses. The extracts (1.5 mL each) were kept at –20°C until used in the respective analysis, at which time they were left at ambient temperature and then filtered through 0.45-μm syringes filter.

PSP toxins were analyzed by high-performance liquid chromatography (HPLC) with post-column oxidation and fluorescence detection (FD) according to the method of Rourke et al. [37], with slight modifications, and by using a Zorbax Bonus RP (4.6 × 150 mm, 3.5 μm) column. SPX and GYM toxins were identified by liquid chromatography coupled to high-resolution mass spectrometry (LC–HRMS). The methanolic extracts were analyzed on a Dionex Ultimate 3000 LC system (Thermo Fisher Scientific, San Jose, California) coupled to an Exactive mass spectrometer (Thermo Fisher Scientific, Bremen, Germany) equipped with an Orbitrap mass analyzer and a heated electrospray source (H–ESI II). Nitrogen (purity > 99.999%) was used as the sheath gas, auxiliary gas, and collision gas. The instrument was calibrated daily in positive and negative ion modes. Mass acquisition was performed in positive ion mode without and with all ion fragmentation (AIF) higher-energy collisional dissociation (HCD) of 45 eV. The mass range was *m/z* 100–1000 in both full-scan and AIF modes. SPXs and GYMs were separated and quantified according to the Standardized Operating Procedure validated by the European Union Reference Laboratory for Marine Biotoxins [38]. In case another SPX or GYM different from the standards was identified in samples, it was quantified as 13-desmethyl SPX-C or as GYM-A equivalents, based on the respective calibrations available and assuming equal responses. The X-Bridge C18 (100 × 2.1 mm, 2.5 μm) column was maintained at 25°C; the injection volume was 20 μL and the flow rate 400 μL min^{-1} (for details, see [6]).

Mathematical modeling of *A. ostenfeldii* growth and toxin production

The sigmoid kinetics of *A. ostenfeldii* growing under different experimental conditions were fitted to the logistic equation [39, 40]:

$$G = \frac{G_m}{1 + \exp\left[2 + \frac{4v_m}{G_m}(\lambda - t)\right]} \quad (1)$$

This equation can be easily reformulated to obtain parameters that describe and characterize the different phases represented in the sigmoid growth curves [41]:

$$G = \frac{G_m}{1 + \exp[\,\mu_m(\tau - t)]} \quad \text{and} \quad t_m = \tau + \frac{G_m}{2v_m} \quad (2)$$

where G is the dinoflagellate growth concentration (cells mL^{-1}); t, the culture time in days (d); G_m, the maximum cell concentration (cells mL^{-1}); μ_m, the maximum specific growth rate (d^{-1}); τ, the time required to achieve the semi-maximum cell concentration or $Gm/2$ (d); v_m, the

maximum growth rate (cells mL^{-1} d^{-1}); λ, the lag phase (d); and t_m, is the time required to achieve the beginning of G_m or plateau phase (d).

Net toxin production followed first-order kinetics [39], described by:

$$T_x = T_0 \exp(rt) \quad (3)$$

where T_x is the net production of the PSP (pg $cell^{-1}$) or the GYM-A analogue (pg GYM-A eq. $cell^{-1}$) toxins; t, the culture time (d); T_0, the initial toxin content (pg $cell^{-1}$); and r, the specific net toxin production rate (d^{-1}).

Numerical methods for growth and toxin production curve modeling

Dinoflagellate growth and net toxin production were modeled by minimizing the sum of the quadratic differences between the observed and predicted values, using the non-linear least-squares (quasi-Newton) method provided by the macro "Solver" of the Microsoft Excel spreadsheet. Confidence intervals from the parametric estimates (Student's *t* test) and the consistency of the mathematical models (Fisher's *F* test) and residual analysis (Durbin-Watson test) were evaluated by "SolverAid" macro (Levie's Excellaneous website: http://www.bowdoin.edu/~rdelevie/excellaneous).

Experimental design and statistical analysis

The effects of the independent variables salinity (S), in the range 5–37, and temperature (T), in the range 12.5–25.5°C, on the kinetic parameters that characterize the growth (G, in cells mL^{-1}) and net toxin production (T_x, in pg $cell^{-1}$) of *A. ostenfeldii* were studied using a rotatable second-order design, with five replicates in the center of the experimental domain [42]. Table 1 summarizes the encoding of the independent variables and the experimental conditions employed.

Orthogonal least-squares calculation of the factorial design data were used to obtain [42] empirical equations describing the combined effects of the environmental factors (S and T) on the kinetic parameters obtained from Eqs (1–3). The general form of the polynomial equations is:

$$R = b_0 + \sum_{i=1}^{n} b_i X_i + \sum_{\substack{i=1 \\ j>i}}^{n-1} \sum_{j=2}^{n} b_{ij} X_i X_j + \sum_{i=1}^{n} b_{ii} X_i^2 \quad (4)$$

where R represents the response (dependent variable) to be modeled (growth and net toxin production parameters); b_0 is the constant coefficient; b_i, the coefficient of the linear effect; b_{ij}, the coefficient of the interaction effect; b_{ii}, the coefficients of the squared effect; n, the number of variables; and X_i and X_j, the independent variables (S and T). The statistical significance of the coefficients was verified using Student t-test ($\alpha = 0.05$). Goodness-of-fit was established as the adjusted determination coefficient (R^2_{adj}), and the model's consistency by Fisher's F test ($\alpha = 0.05$) using the following mean squares ratios:

	The model is acceptable when
F1 = Model / Total error	$F1 \geq F_{den}^{num}$
F2 = (Model + Lack of fit) / Model	$F2 \leq F_{den}^{num}$
F3 = Total error / Experimental error	$F3 \leq F_{den}^{num}$
F4 = Lack of fit / Experimental error	$F4 \leq F_{den}^{num}$

where F_{den}^{num} are the theoretical values for $\alpha = 0.05$, with the corresponding degrees of freedom for numerator (num) and denominator (den). The model is acceptable when *F1* and *F2* are validated. *F3* and *F4* were additionally calculated to improve the degree of robustness and the

consistency of the empirical equations obtained. All fitting procedures, coefficient estimates, and statistical calculations were performed on a Microsoft Excel spreadsheet.

Results

Toxin characterization

The LC analyses showed detectable amounts of PSP toxins in all of the culture extracts of *A. ostenfeldii* strain AOTV-B4A. The toxin profile was dominated by gonyautoxin (GTX)-3, followed by saxitoxin (STX), and GTX-2 in proportions of 62.7%, 35.5%, and 1.8%, respectively. The proportions were similar in all cultures. In LC–HRMS analyses of the culture methanolic extracts, GYM-A and GYM-B/-C analogues but not SPXs were detected. Since only the standard for GYM-A is available, an equimolar response for the GYM-A analogue detected was assumed and the analogue was quantified as GYM-A equivalents (pg GYM-A eq. $cell^{-1}$). In addition, although all culture samples were also screened for the presence of 12-methyl GYM, it was not detected under any conditions.

Growth and toxin production kinetics

Both the analysis of the growth of *A. ostenfeldii* under the conditions defined by the factorial design (Table 1) and the kinetic profiles fitted to the experimental data according to Eq (1) are shown in Fig 1. Table 2 lists the values of the kinetic parameters and provides the data used in the statistical analyses of the numerical fittings. The predictive ability of Eq (1) in modeling the experimental data was high, as shown by determination coefficients (R^2) $\geq$ 0.965. All of the parameters for *A. ostenfeldii* growth, except the numerical values of the lag phases (λ), were statistically significant (α = 0.05). Autocorrelation was not observed in the residuals distribution (data not shown). In three of the experimental conditions (salinities $\geq$ 32), there was no significant growth of *A. ostenfeldii*, as determined by the kinetic analysis; the cell yields were not higher than the inoculum (900 cells mL^{-1}) (Fig 1). In those cases, the values of the parameters used as dependent variables (responses) in the subsequent response-surface analysis (RSA) and calculation were set at zero.

Fig 2 shows the kinetics of the net production of the PSP toxins (sum of GTX-3, GTX-2, and STX) and the GYM-A analogue under the conditions defined by the factorial design (Table 1) and fitted to the first-order kinetic model (3). In general, the experimental kinetics of the net production of those biotoxins over time were acceptably modeled by Eq (3). The coefficients of determination of the fittings were in the range of 0.246–0.957 for PSP toxins and 0.101–0.981 for GYM-A analogue. The kinetics of both groups of toxins were consistent with a mixed-growth-associated model, since content toxin increased during the exponential phase of growth and continued to increase during stationary phase (Figs 1 and 2). No change in toxin content was detected under the experimental conditions in which there was no significant growth (salinities $\geq$ 32) (Fig 2).

Combined effect of temperature and salinity on growth parameters by RSA

The simultaneous effects of the environmental factors *S* and *T* on the kinetic parameters of *A. ostenfeldii* obtained from the logistic model (Table 2) were studied using a RSA. For the cases in which no growth detected (NGD in Table 2), the experimental response was considered to be zero. The design and numerical responses of the 2-factor rotatable design are summarized in Table 2. Parameter data describing the growth of *A. ostenfeldii* were converted into second-order polynomial equations as a function of *S* and *T*. The polynomial model describing the

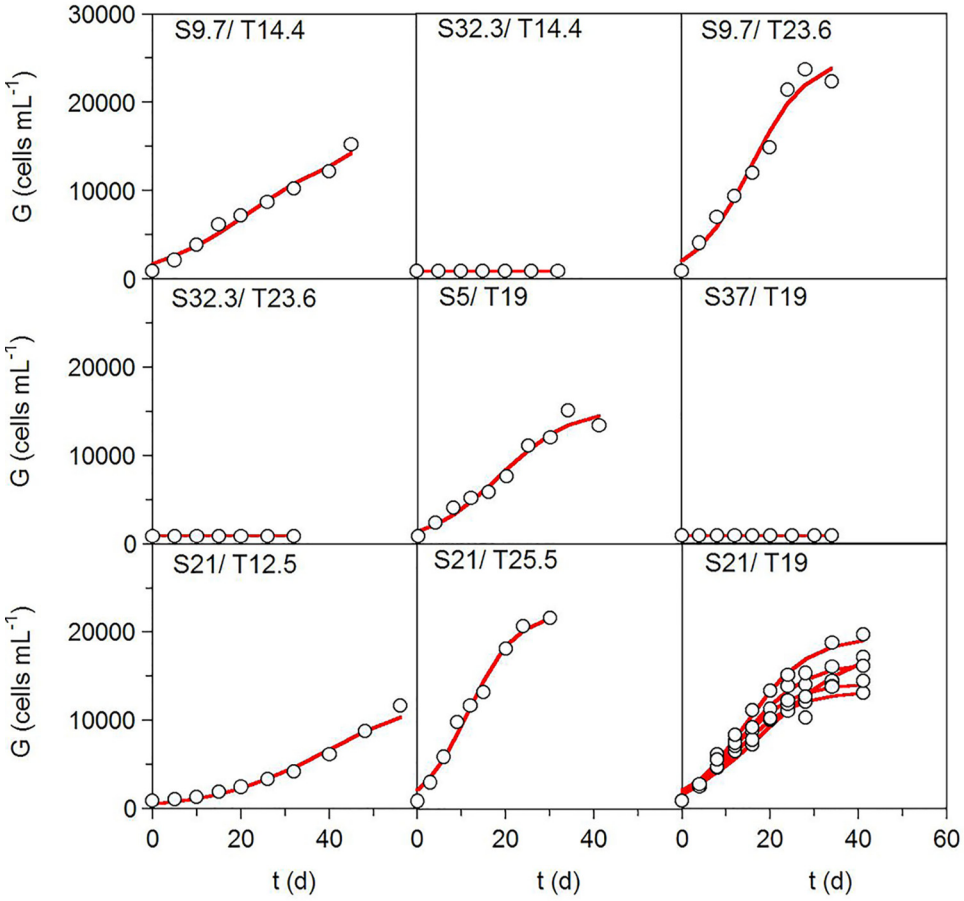

Fig 1. Growth kinetic profiles. Growth kinetics of *Alexandrium ostenfeldii* strain AOTV-B4A cultivated under the environmental conditions defined by the factorial design summarized in Table 1. Experimental data (symbols) were fitted to Eq (1) (lines).

doi:10.1371/journal.pone.0143021.g001

correlation between the responses and the variables therefore followed the general form described by Eq (4) (Table 3).

A high proportion of variability (83% for G_m and 84% for v_m) was successfully explained by the second-order equations. The agreement between the experimental and predicted data was always > 69% (Table 3). The robustness of the equations was perfect in all cases except the *F4* (Fisher F test) of τ, which was not significant. Thus, the empirical equations shown in Table 3 were very good predictors of the growth of *A. ostenfeldii* in the *S* and *T* ranges evaluated in this study.

Fig 3 shows the theoretical surfaces for each parameter as the response of a dependent variable. The results of the multivariate analysis showed that, for all growth parameters, the effect of *T* was only linear whereas *S* always had significant quadratic negative terms ($P < 0.05$). The coefficient of interaction between the variables ($S \times T$) was only significant for the v_m response. The statistical significance of the coefficient of S^2 and its negative value were graphically translated as a convex dome with a clear maximum point within the experimental domain of the salinity (Fig 3). The salinity concentrations that maximize *A. ostenfeldii* growth were determined by mathematical optimization using the numerical or manual derivation of the equations in Table 3 [43]. The natural values of those optima and the maximum value of the responses in each case (Y_{max}) are summarized in Table 4. Thus, the conditions yielding the maximum growth of the dinoflagellate (average of the G_m, v_m and μ_m results) were a salinity of 11.2 and a temperature of at least 25.5°C.

Table 2. Summary of the parameter values (dependent variables) obtained from fitting the data on *A. ostenfeldii* growth to Eqs (1) and (2). X_1: salinity and X_2: temperature (°C). The natural values of the experimental conditions are shown in brackets.

Independent variables		Growth parameters							
X_1: S	X_2: T	G_m (cells mL^{-1})	v_m (cells mL^{-1} d^{-1})	λ (d)	μ_m (d^{-1})	τ (d)	t_m (d)	R^2	p-value
-1 (9.7)	-1 (14.4)	17,912 ± 6,775	351.2 ± 88.6	1.0 (NS)	0.082 ± 0.043	25.5 ± 12.3	50.0 ± 24.6	0.976	<0.001
1 (32.3)	-1 (14.4)	NGD	NGD	NGD	NGD	NGD	NGD	NGD	NGD
-1 (9.7)	1 (23.6)	25,239 ± 6,775	983.1 ± 314.4	2.8 (NS)	0.156 ± 0.071	15.7 ± 4.2	28.5 ± 9.2	0.973	<0.001
1 (32.3)	1 (23.6)	NGD	NGD	NGD	NGD	NGD	NGD	NGD	NGD
-1.41 (5)	0 (19)	15,372 ± 3,132	479.3 ± 141.4	2.3 (NS)	0.125 ± 0.054	18.3 ± 4.9	34.4 ± 11.0	0.97	<0.001
1.41 (37)	0 (19)	NGD	NGD	NGD	NGD	NGD	NGD	NGD	NGD
0 (21)	-1.41 (12.5)	13,110 ± 2,389	261.1 ± 52.0	14.1 ± 5.0	0.080 ± 0.024	39.2 ± 6.7	64.3 ± 13.4	0.982	<0.001
0 (21)	1.41 (25.5)	22,237 ± 2,772	1,053.5 ± 257.8	1.1 (NS)	0.190 ± 0.060	11.7 ± 2.2	22.3 ± 5.0	0.987	<0.001
0 (21)	0 (19)	18,361 ± 3,542	476.8 ± 94.9	0.4 (NS)	0.104 ± 0.034	19.6 ± 5.0	38.9 ± 10.7	0.983	<0.001
0 (21)	0 (19)	16,523 ± 1,506	608.5 ± 125.3	0.5 (NS)	0.147 ± 0.038	14.0 ± 2.1	27.6 ± 5.0	0.988	<0.001
0 (21)	0 (19)	13,222 ± 1,838	512.7 ± 184.2	-0.4 (NS)	0.155 ± 0.068	12.5 ± 3.3	25.4 ± 7.8	0.965	<0.001
0 (21)	0 (19)	14,234 ± 1,435	538.4 ± 141.5	-1.2 (NS)	0.151 ± 0.049	12.0 ± 2.4	25.2 ± 5.8	0.981	<0.001
0 (21)	0 (19)	19,459 ± 2,062	710.2 ± 161.8	-1.1 (NS)	0.146 ± 0.042	14.8 ± 2.5	28.4 ± 5.7	0.986	<0.001

Codification: $V_c = (V_n - V_0)/\Delta V_n$; Decodification: $V_n = V_0 + (\Delta V_n \times V_c)$

V_n = natural value in the center of the variable to be codified; ΔV_n = increment of V_n per unit of V_c. V_c = codified value of the variable; V_0 = natural value in the center of the domain

NS: not significant; NGD: no growth detected. Error values associated with the parameter determinations are the confidence intervals (CI) for α = 0.05.

doi:10.1371/journal.pone.0143021.t002

Combined effect of temperature and salinity on toxin production by RSA

Based on Eq (3), the specific net production rates (r) of the PSP toxins and the GYM-A analogue were selected as the response to be studied with respect to T and S. The effects of temperature and salinity on the toxin concentrations obtained at the end of their production by *A. ostenfeldii* cells were also evaluated. Fig 4 depicts the surfaces predicted by the second-order equations shown in Table 5. In all cases, the coefficient of the salinity effect (linear and quadratic) was negative, with a parabolic pattern (dome surface), and was in complete concordance with the results obtained for dinoflagellate cell growth. The influence of T was also quadratic except for the r-response of PSP toxin, in which only a linear term was significant as previously described for the growth of *A. ostenfeldii* (Fig 3).

The optimal S and T values needed to maximize toxin concentrations and the theoretical maximum values of the variables (Y_{max}) calculated from these optima are summarized in Table 6. These levels were different depending on the toxin; thus, the S_{opt} values for PSP toxin and GYM-A analogue were 15 and 17, respectively (calculated in each case as the average of the two responses selected). The T_{opt} for the GYM-A analogue was 20.9°C whereas that for PSP toxin was 19°C.

Discussion

Growth and toxin production kinetics and the combined effects of temperature and salinity

The results of the present work clearly demonstrated the effects of temperature and salinity on the growth of one strain of *A. ostenfeldii* from the Baltic Sea. The values of the six kinetic parameters used (G_m, v_m, λ, μ_m, τ, and t_m) during each experimental condition were accurately

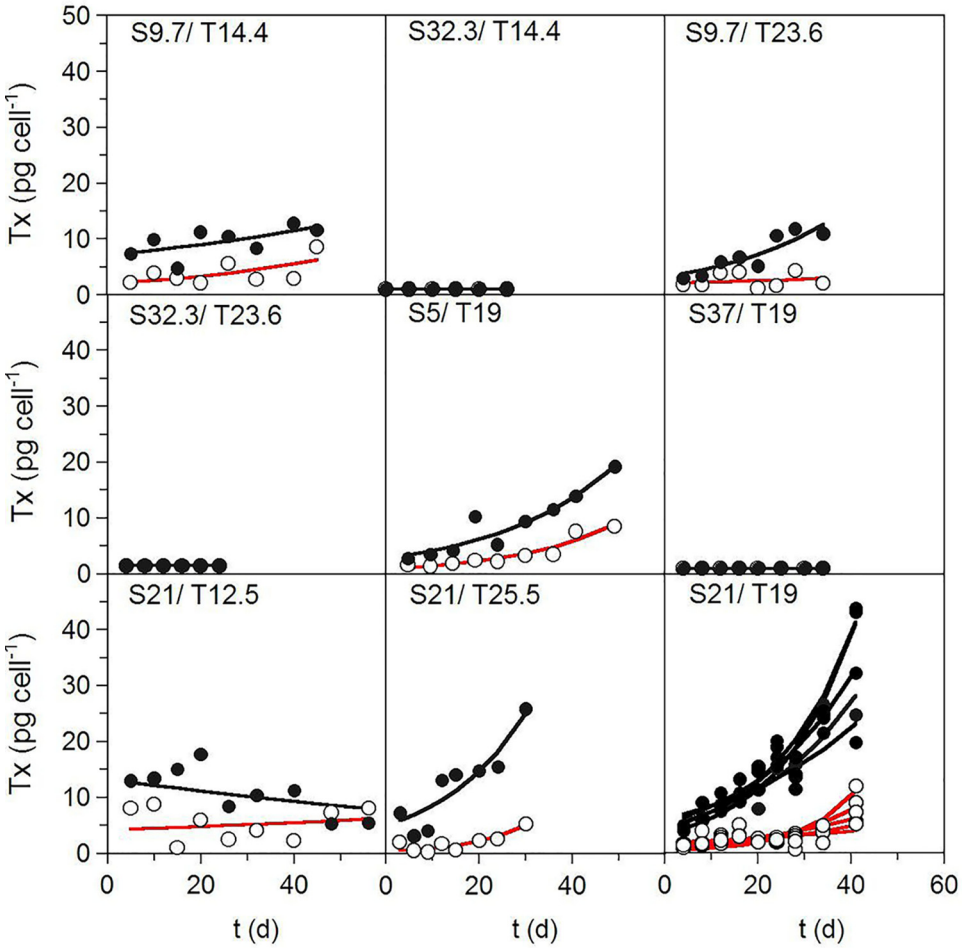

Fig 2. Toxin-production kinetic profiles. Kinetics of net toxin production by strain AOTV-B4A cultivated under the environmental conditions defined by the factorial design summarized in Table 1. ○: PSP toxins (pg cell^{-1}), •: GYM-A analogue (pg GYM-A eq cell^{-1}). Experimental data (symbols) were fitted to Eq (3) (lines).

doi:10.1371/journal.pone.0143021.g002

predicted by the logistic function of Eq (1). The resulting sigmoid patterns and the validity of the model (1) that described them have been frequently reported for microorganisms cultivated under batch conditions [44–49] and for higher organisms subjected to extensive or intensive feeding [50–52]. The growth of marine organisms, including bacteria, rotifers, molluscs, dinoflagellates, and microalgae, is also well-fitted by a logistic function, reflecting the involvement of autocatalytic pathways [53–57]. Our results are in agreement with the growth rates reported for strains of *A. ostenfeldii* isolated from the Baltic Sea, Skagerrak, North Sea, and Nova Scotia [29, 34, 58] and for the yessotoxin-producing dinoflagellate *P. reticulatum* [39]. However, the values of the parameters G_m or K, v_m and μ_m were generally lower for *A. ostenfeldii* than for *P. reticulatum*. Also, the growth of *A. ostenfeldii* was slower than that of *Alexandrium* species (*A. tamarense*, *A. minutum*, and *A. tamutum*) in Scottish waters [59] and *Alexandrium* isolates from other latitudes [60–62].

RSA based on a factorial design is used to optimize the effect of environmental factors for a small number of experiments (13, with 5 replicates in the center of the experimental domain for a second-order rotatable design) [42]. The empirical equation obtained from this analysis provides the information needed to predict the values of the dependent variables in the

Table 3. Second-order equations describing the effects of *S* and *T* on the growth parameters of *A. ostenfeldii* AOTV-B4A (used in coded values according to the criteria defined in Table 1). The coefficient of adjusted determination (R^2_{adj}) and the *F*-values (F_1, F_2, F_3 and F_4) are also shown. S: significant; NS: non-significant.

Parameters	G_m (cells mL^{-1})	v_m (cells mL^{-1} d^{-1})	μ_m (d^{-1})	τ (d)	t_m (d)
b_0 (intercept)	16,365	569.6	0.141	14.60	29.14
b_1 (*S*)	-8,037	-252.0	-0.052	-8.40	-15.92
b_2 (*T*)	2,623	219.3	0.029	-6.09	-10.12
b_{12} (*S*x*T*)	NS	-158.0	NS	NS	NS
b_{11} (S^2)	-4,881	-194.7	-0.049	-4.50	-8.68
b_{22} (T^2)	NS	NS	NS	3.69	NS
R^2_{adj}	0.829	0.844	0.773	0.689	0.703
F1	20.33	17.17	14.63	7.65	10.46
	$[F^3_9 = 3.86] \Rightarrow S$	$[F^4_8 = 3.84] \Rightarrow S$	$[F^3_9 = 3.86] \Rightarrow S$	$[F^4_8 = 3.84] \Rightarrow S$	$[F^3_9 = 3.86] \Rightarrow S$
F2	0.416	0.545	0.438	0.614	0.469
	$[F^8_3 = 8.85] \Rightarrow S$	$[F^8_4 = 6.04] \Rightarrow S$	$[F^8_3 = 8.85] \Rightarrow S$	$[F^8_4 = 6.04] \Rightarrow S$	$[F^8_3 = 8.85] \Rightarrow S$
F3	1.727	2.15	20.52	3.98	3.46
	$[F^9_4 = 5.99] \Rightarrow S$	$[F^8_4 = 6.04] \Rightarrow S$	$[F^9_4 = 5.99] \Rightarrow S$	$[F^8_4 = 6.04] \Rightarrow S$	$[F^9_4 = 5.99] \Rightarrow S$
F4	2.308	3.29	20.52	6.96	5.44
	$[F^5_4 = 6.26] \Rightarrow S$	$[F^4_4 = 6.39] \Rightarrow S$	$[F^5_4 = 6.26] \Rightarrow S$	$[F^4_4 = 6.39] \Rightarrow NS$	$[F^5_4 = 6.26] \Rightarrow S$

doi:10.1371/journal.pone.0143021.t003

experimental range studied. Although this type of approach is not commonly used to study the growth of marine organisms in response to different effectors, previous results have demonstrated its validity and its potential as a process predictor. For example, the influence of three factors (temperature, salinity, and irradiance) on the growth kinetics of *P. reticulatum* was studied by means of a first-order factorial design [39]. Similar statistical tools were used to assess the positive and negative effects of salinity, inoculum size, and temperature on cyst and planozygote formation by *A. minutum* [63]. Analysis of the enhancement of rotifer (*Brachionus plicatilis*) growth in the presence of a combination of lactic acid bacteria was optimized by RSA [55]. The approach used in this work can be applied to define the environmental windows allowing species growth, especially those species with an extended geographic distribution, as is the case for *A. ostenfeldii*. Although generalizations based on culture studies should consider within-species variation [64, 65], it adds to the limited data available on the autecology of this species and allows conclusions to be drawn regarding the biogeography of the different populations of this dinoflagellate, based on comparisons between culture data and data on the environmental conditions of its habitats.

In our study, the temperature- and salinity-dependent growth window for Baltic *A. ostenfeldii* AOTV-B4A reflected the broad tolerance of this strain to a wide range of temperatures and to low salinities. In fact, the only condition completely limiting growth was a salinity ≥ 32. Although we could not determine the maximum threshold value for salinity, in a previous study it was 25 [6]. In the present study, cell growth occurred at a salinity range of 5–21 and at temperatures of 12.5–25.5°C, with optima at a salinity of 11.2 and a minimum temperature of 25.5°C. These results, and particularly the optimal salinity, are consistent with the values reported by Kremp et al. [16] for *A. ostenfeldii* strains AOTV-A1 and AOTV-A4, isolated, as our strain, from the Åland islands (Finnish Baltic Sea). Similar temperature ranges for growth were determined by Østergaard and Moestrup [17] for cultures of a Danish strain isolated from Limfjord (Kattegat Sea), whereas salinities allowing growth were between 10 and 40, with optimum growth achieved at 15–20. We have no information on the salinities of the waters where the Danish strain was isolated; however, its adaptation to a higher salinity suggests that

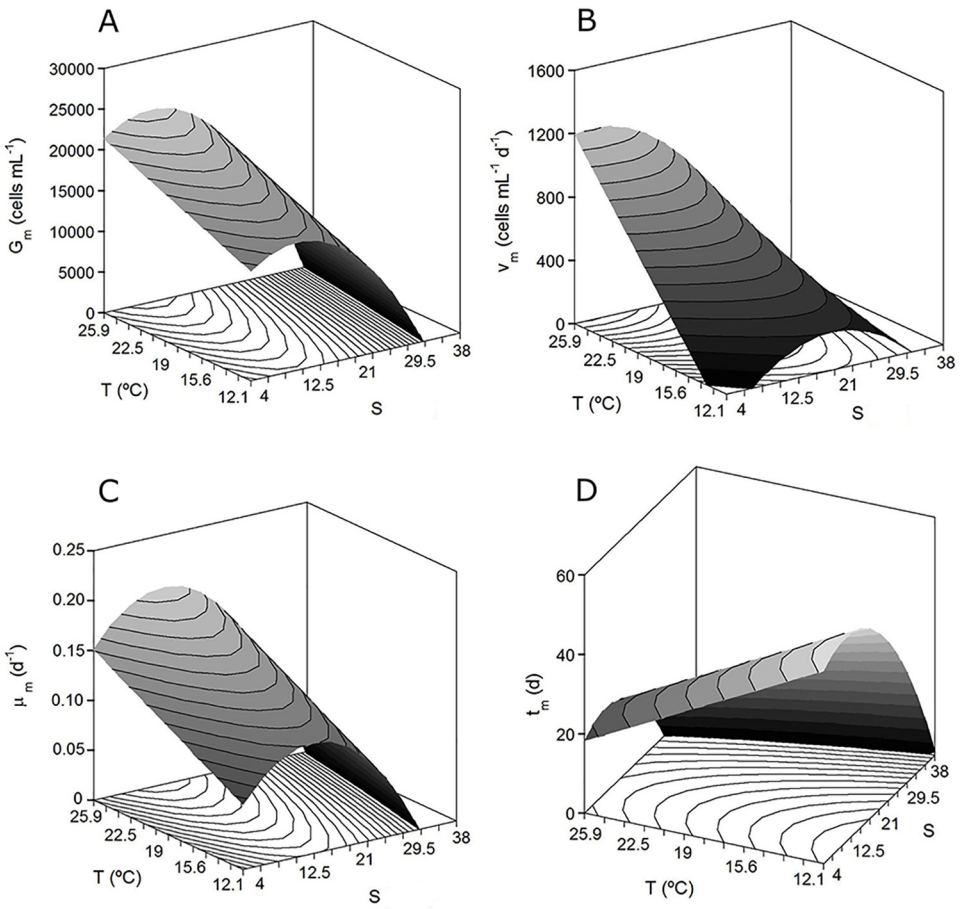

Fig 3. Combined effects of temperature and salinity on growth by RSA. Theoretical response surfaces describing the combined effects of temperature and salinity on the kinetic parameters described by Eqs (1) and (2): (A) maximum growth (G_m), (B) maximum growth rate (v_m), (C) specific maximum growth rate (μ_m), and (D) time to achieve the plateau phase (t_m).

doi:10.1371/journal.pone.0143021.g003

it is from an area of the Kattegat Sea located closer to the North Sea than to the most northern part of the Baltic Sea [29], which is where our strain was obtained. The positive effects of temperature on G_m, v_m, and μ_m (increasing response at increasing temperature) are compatible with the Arrhenius theory but with a linear rather than the typical exponential relationship. This may be due to the narrow experimental range selected in this study and/or to the type of factorial design, in which only linear and quadratic coefficients, and not exponential expressions, could be evaluated. The robustness of our results was confirmed by the negative value of the temperature linear coefficient in the equations describing τ ant t_m (Table 3), which were inversely proportional to those obtained for the other parameters. This was expected because

Table 4. Optimal values of salinity and temperature (S_{opt} and T_{opt}) needed to obtain the maximum values (Y_{max}) using the equations shown in Table 3 and for the different dependent variables studied (growth parameters).

	G_m (cells mL^{-1})	v_m (cells mL^{-1} d^{-1})	μ_m (d^{-1})	τ (d)	t_m (d)
S_{opt}	11.68	6.79	15.04	10.44	10.63
T_{opt}	>25.5	>25.5	>25.5	<12.5	<12.5
Y_{max}	23,607	1,206	0.198	17.69	51.62

doi:10.1371/journal.pone.0143021.t004

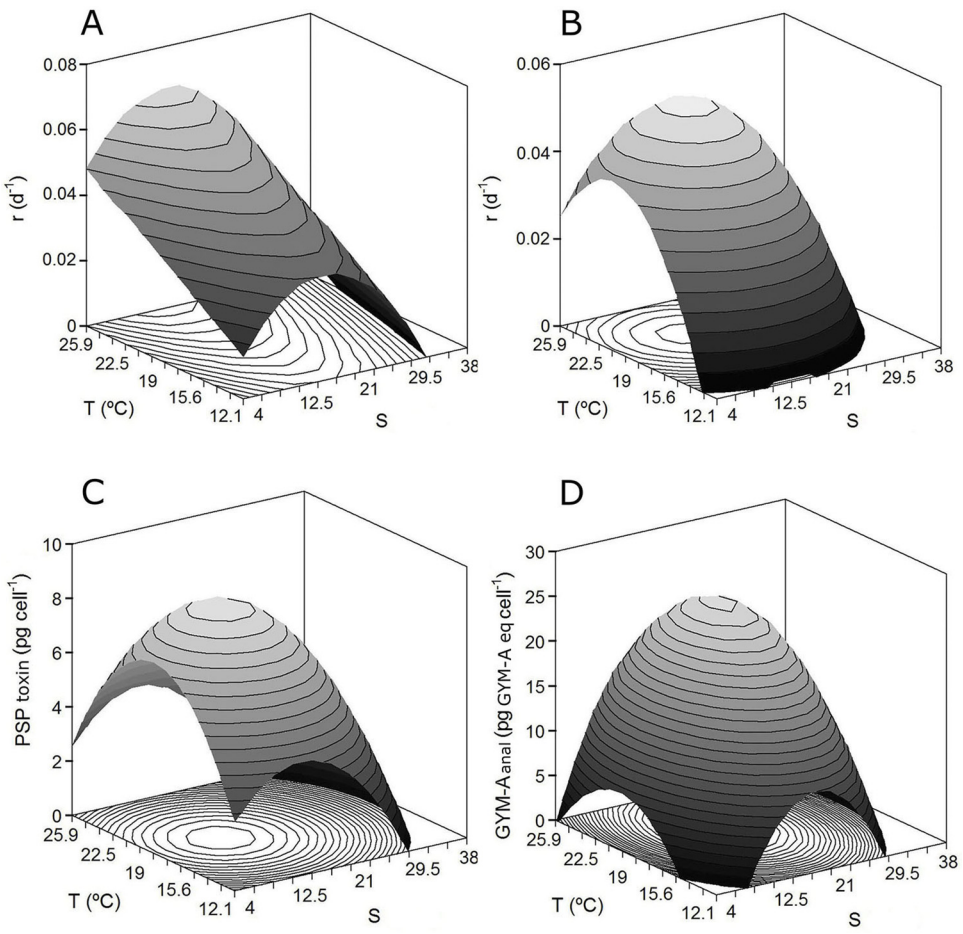

Fig 4. Combined effects of temperature and salinity on toxin production by RSA. Theoretical response surfaces describing the combined effects of temperature and salinity on the specific (A) PSP toxin and (B) GYM-A analogue net production rates (*r*), and on the net production of (C) PSP toxins (pg cell^{-1}) and (D) GYM-A analogue (pg GYM-A eq. cell^{-1}) at the end of the *A. ostenfeldii* culture period.

doi:10.1371/journal.pone.0143021.g004

when growth is higher and faster (high G_m and high v_m and μ_m), the values of τ and t_m are smaller.

Our results also demonstrated the influence of temperature and salinity on the kinetics of net toxin production of *A. ostenfeldii*. The bioproduction of lipophilic (GYM-A analogue) and PSP toxins in most cases occurred concomitantly during the exponential growth and stationary phases, following characteristics of mixed metabolites as described by the Luedeking-Piret definition (Figs 1 and 2). A similar behavior was reported for yessotoxin production by *P. reticulatum*, nodularin synthesis by *Nodularia spumigena* [54], and net PSP production by *A. ostenfeldii* from the Baltic Sea [29] and by several other *Alexandrium* species from diverse geographic origins [61, 66, 67]. Nevertheless, in our study there were also culture conditions in which toxin production differed from that described above. Specifically, when the cultures were exposed to low temperature, net toxin production was not consistent with growth (see plots for 12.5°C in Figs 1 and 2), suggesting the involvement of other factors. In fact, in our experiment, in the absence of a clear stationary phases (temperatures of 12.5°C and 14.4°C), the error associated with the G_m-parameter was higher than in cultures in which a well-defined asymptotic phase occurred. The changes in cell size may explain this difference. Both Granéli

Table 5. Second-order equations describing the effects of *T* and *S* on net toxin productions (PSP toxin and GYM-A analogue) by *A. ostenfeldii*. The coefficient of adjusted determination (R^2_{adj}) and the *F*-values (F_1, F_2, F_3, and F_4) are also shown. S: significant; NS: non-significant.

	PSP toxin		GYM-A analogue	
Parameters	***r*** **(d^{-1})**	**PSP toxin (pg $cell^{-1}$)**	***r*** **(d^{-1})**	**GYM-A analogue (pg GYM-A eq. $cell^{-1}$)**
b_0 **(intercept)**	0.047	7.82	0.047	24.57
b_1 **(*S*)**	-0.014	-2.85	-0.015	-4.47
b_2 **(*T*)**	0.012	NS	0.013	3.98
b_{12} **(*S*x*T*)**	NS	NS	NS	NS
b_{11} **(S^2)**	-0.017	-2.24	-0.015	-10.91
b_{22} **(T^2)**	NS	-2.00	-0.013	-5.95
(R^2_{adj})	0.504	0.664	0.715	0.819
F1	4.05	8.91	8.54	14.53
	$[F^3_9 = 3.86] \Rightarrow S$	$[F^3_9 = 3.86] \Rightarrow S$	$[F^4_8 = 3.84] \Rightarrow S$	$[F^4_8 = 3.84] \Rightarrow S$
F2	0.713	0.465	0.571	0.56
	$[F^8_3 = 8.85] \Rightarrow S$	$[F^8_3 = 8.85] \Rightarrow S$	$[F^8_4 = 6.04] \Rightarrow S$	$[F^8_4 = 6.04] \Rightarrow S$
F3	5.370	1.537	1.265	5.94
	$[F^9_4 = 5.99] \Rightarrow S$	$[F^9_4 = 5.99] \Rightarrow S$	$[F^8_4 = 6.04] \Rightarrow S$	$[F^8_4 = 6.04] \Rightarrow S$
F4	8.867	1.967	1.530	10.88
	$[F^5_4 = 6.26] \Rightarrow NS$	$[F^5_4 = 6.26] \Rightarrow S$	$[F^4_4 = 6.39] \Rightarrow S$	$[F^4_4 = 6.39] \Rightarrow NS$

doi:10.1371/journal.pone.0143021.t005

and Flynn [68] and Anderson et al. [69] noted that, during the growth cycle, the observed changes in the culture and in cell toxin content may simply reflect changes in cell size and the variability of growth or life-cycle stages as a function of changes in nutrient status, temperature, or salinity. This is consistent with the variations in the size of *A. ostenfeldii* cells in strains exposed to different experimental conditions [6, 16, 17, 59], which demonstrated that cell size variations are common in the life cycle of the species and are related to the culture growth phase and to the sexual vs. asexual origin of the cells. A larger mean cell volume during stationary phase as well as abundant large and small temporary cysts, most likely of asexual and sexual origin [70], were reported from Danish strain cultures by Østergaard and Moestrup [17]. Microscopic analysis of cells from our 12.5°C culture showed an abundance of large, dark, elongated cells suggestive of planozygotes. This culture condition also resulted in the largest numbers of double-walled (resting) cysts (unpublished data). Previous studies of the same strain showed that a temperature of 15°C results in significantly ($P < 0.05$; $n = 90$) larger cells than obtained at higher temperatures [6]. These observations suggest that sexual reproduction is induced in the cultures at low temperatures, which might also explain the fluctuations in toxin production observed at 12.5°C in this study as well as the higher error associated with the G_m-parameter at low temperatures.

Table 6. Optimal values of salinity and temperature (S_{opt} and T_{opt}) needed to obtain the maximum values (Y_{max}) using the equations shown in Table 5 and for the different dependent variables studied (toxin productions).

	PSP toxin		GYM-A analogue	
	r **(d^{-1})**	**PSP toxin (pg $cell^{-1}$)**	***r*** **(d^{-1})**	**GYM-A analogue (pg GYM-A eq. $cell^{-1}$)**
S_{opt}	16.1	13.8	15.3	18.7
T_{opt}	>25	19.0	21.2	20.5
Y_{max}	0.067	8.73	0.054	25.7

doi:10.1371/journal.pone.0143021.t006

Little is known about the diversity, distribution, and production of GYMs by *A. ostenfeldii*. The only other producer of GYMs (GYM-A, GYM-B and GYM-C) identified to date is the phylogenetically distant dinoflagellate *Karenia selliformis* [11, 71–74], such that most studies of GYM toxin production have focused on this species. Thus far, the only study to quantify GYM production was conducted by Tatters et al. [75], using an isolate of *A. peruvianum* (syn. of *A. ostenfeldii*) from the New River Estuary, North Carolina (USA). Under nutrient-replete culture conditions, 12-methyl GYM concentrations peaked (up to 73.3 pg $cell^{-1}$) during stationary phase (day 36), as was the case in most of our cultures. Harju et al. [8] provided a qualitative description of two separate GYM analogues produced by isolates from the Baltic Sea and Saanich (Canada) and of GYM-like compounds produced by some cultures established from the Baltic Sea. It is demonstrated that, as with SPX and PSP toxin, GYM production by *A. ostenfeldii* is geographically highly variable, including within a particular region [6, 13, 18, 29, 59, 76]. Thus far, lipophilic toxin production by *A. ostenfeldii* has been mainly linked to SPXs [34, 77, 78]. However, further studies quantifying GYM production in this species will provide greater insight into the dynamics of the biosynthesis of this toxin and its variability.

Ecological implications

The accurate prediction and assessment of toxic episodes by dinoflagellates are hindered by the poor understanding of the factors affecting toxin production by dinoflagellates. Chemical, physical, and biotic factors are known to influence toxin production, including nutrients, temperature, salinity, irradiance, and grazing [68, 79]. For example, the complex ecological mechanisms underlying toxin production responses are evidenced by grazing, which can act to restrain dinoflagellate populations or enhance toxin content [80]. Our data are robust enough to allow the use of RSA as a predictor of a changing environment, although some limitations must be considered. First, the system giving rise to toxin production cannot be considered in its entirety. Second, because the results were derived from a single strain, any broader ecological interpretation must be made with caution [64]. According to our observations on the growth of the Baltic *A. ostenfeldii* strain AOTV-B4A, salinities in the range of 5–21 and temperature of 12.5–25.5°C are compatible with growth, although the respective values resulting in maximum growth were 11.2 and 25.5°C. Consequently, the strain appears to be a eurytherm adapted to brackish-water conditions. Although this strain may not be representative of all Baltic Sea populations of the species or of the species in general, for which we would need to work with many isolates, our data and those reported in the literature raise several interesting issues. For example, the intraspecific and intrapopulation variability of *A. ostenfeldii* with respect to temperature and salinity is not well known yet, although variations in the responses of different strains from different geographic locations characterized by a very wide range of environmental conditions have been extensively described [6, 17, 29, 34, 35, 58, 81]. Reaction norms of multiple isolates for temperature and salinity have not been published so far, but previous studies on Baltic isolates suggest that the environmental window described herein for *A. ostenfeldii* AOTV-B4A represents the range of Baltic Sea population(s) [16, 58]. An optimum of ca. 25°C is consistent with the findings of Kremp et al. [58] who reported general growth stimulation in response to an increased temperature, despite variability in the responses of eight strains of *A. ostenfeldii* isolated from the same site as our strain.

While further investigations into the variability of strain responses to salinity are needed, our results can be compared with those in the literature. Thus, the optimal salinities allowing growth as determined in the present work are in agreement with those reported by Kremp et al. [16] and Suikkanen et al. [29] for other isolates from the same region (Åland islands, between Finland and Sweden). However, in the strain from Limfjord, Denmark (Kattegat Sea) studied by Østergaard and Moestrup [17] as in the strain from Skagerrak studied by Suikkanen

et al. [29], the values were higher and salinities of up to 35–40 were tolerated. This variation suggests that both Limfjord and Skagerrak strains belong to a different, high-salinity-adapted population, a conclusion supported by the genetic study carried out by Kremp et al. [13], who showed that strains from the Baltic Sea and Limfjord were grouped within distinct phylogenetic clades. The low optimum salinity (11.2) recorded for our *A*. *ostenfeldii* strain is consistent with its adaptation to the low salinities of the shallow coastal embayments of the northern Baltic Sea, where salinities are typically between 6 and 7 [16, 29]. Furthermore, our results along with those of previous studies [6, 29] show that a salinity > 25 is a limiting factor for growth. Extrapolated to the natural environment, this would limit the geographic distribution of the population to areas influenced by freshwater inputs, such as the most northern and eastern areas of the Baltic Sea [29]. The adaptation of *A*. *ostenfeldii* to specific environments of the Baltic Sea is indicative of an early post-glacial colonization and the continued isolation of the respective subpopulations due their limited dispersal [82].

Our results on the temperature preferences of one strain of *A*. *ostenfeldii* support the concerns expressed by other authors regarding the potential increase in blooms of this species as a possible response to climate change [58]. Summer conditions in the Baltic Sea, when the water is warm, stratified, and nutrient-poor are optimal for dinoflagellate growth [58] and for increased toxin production (19°C for PSP toxin and 20.9°C for GYM-A analogue). This is especially the case in shallow and sheltered embayments, where the temperature may be well above 20°C [16]. In fact, large summer blooms of *A*. *ostenfeldii* in the brackish estuaries and shallow coastal inlets of diverse areas during warm-water periods have become increasingly common in recent years [15, 33, 83].

Conclusions

Both cell growth and net toxin (GYM and PSP toxin) production were directly responsive to temperature and salinity changes. While increasing temperatures stimulated growth as well as net toxin production, salinities higher than 21 were growth-limiting. The present study also provides the first quantitative determination of a GYM-A analogue in *A*. *ostenfeldii* and the first report of changes in its production in response to variations in temperature and salinity. The changes in PSP toxin and GYM-A analogue production suggest a mixed-growth-associated model, since net toxin production typically occurred in exponentially growing and in stationary-phase cells. The optimal temperature and salinity that resulted in maximum toxin concentrations were: 20.9°C and 17 for the GYM-A analogue and $>$ 19°C and 15 for PSP toxins, respectively. The RSA presented herein is a valuable approach for evaluating the combined effect of temperature and salinity on *A*. *ostenfeldii* growth and net toxin production. While further studies estimating the magnitude of within-species variation are needed, our data suggest that warming of the water would stimulate both the growth of *A*. *ostenfeldii* and its toxin production.

Acknowledgments

We thank A. Fernández-Villamarín for technical assistance in processing the toxin samples, and I. Ramilo and P. Rial for technical assistance with the cultures. This article is going to be part of the thesis of P. Salgado that is attached to the framework of the doctoral program "Marine Science, Technology and Management" (DO*MAR) of the University of Vigo.

Author Contributions

Conceived and designed the experiments: PS JAV PR JMF RIF IB. Performed the experiments: PS. Analyzed the data: PS JAV PR JMF RIF IB. Contributed reagents/materials/analysis tools: JAV PR JMF AK IB. Wrote the paper: PS JAV PR IB.

References

1. Smayda T. Adaptive ecology, growth strategies and the global bloom expansion of dinoflagellates. J Oceanogr. 2002; 58:281–94.
2. Cembella AD. Ecophysiology and metabolism of paralytic shellfish toxins in marine microalgae. In: Anderson DM, Cembella AD, Hallegraeff GM, editors. Physiological ecology of harmful algal blooms. Springer, Berlin Heidelberg New York, pp 381–403 NATO ASI Series 41.; 1998.
3. Murray S, Hoppenrath M, Orr R, Bolch C, John U, Diwan R, et al. *Alexandrium diversaporum* sp. nov., a new non-saxitoxin producing species: Phylogeny, morphology and sxtA genes. Harmful Algae. 2014; 31:54–65.
4. Anderson DM, Alpermann T, Cembella A, Collos Y, Masseret E, Montresor M. The globally distributed genus *Alexandrium*: Multifaceted roles in marine ecosystems and impacts on human health. Harmful Algae. 2012; 14:10–35. PMID: 22308102
5. Cembella A, Lewis N, Quilliam M. The marine dinoflagellate *Alexandrium ostenfeldii* (Dinophyceae) as the causative organism of spirolide shellfish toxins. Phycologia. 2000; 39(1):67–74.
6. Salgado P, Riobó P, Rodríguez F, Franco JM, Bravo I. Differences in the toxin profiles of *Alexandrium ostenfeldii* (Dinophyceae) strains isolated from different geographic origins: Evidence of paralytic toxin, spirolide, and gymnodimine. Toxicon. 2015; 103:85–98. doi: 10.1016/j.toxicon.2015.06.015 PMID: 26093028
7. Van Wagoner R, Misner I, Tomas C, Wright J. Occurrence of 12-methylgymnodimine in a spirolide-producing dinoflagellate *Alexandrium peruvianum* and the biogenetic implications. Tetrahedron Lett. 2011; 52:4243–46.
8. Harju K, Kremp A, Suikkanen S, Kankaanpää H, Vanninen P. Mass spectrometric screening of novel gymnodimine-like compounds in isolates of *Alexandrium ostenfeldii*. 16th Internation Conference on Harmful Algae; 27–31 October; Wellington, New Zealand2014.
9. Molgó J, Aráoz R, Benoit E, Iorga B. Cyclic imine toxins: chemistry, origin, metabolism, pharmacology, toxicology, and detection. In: Botana LM, editor. Seafood and Freshwater Toxins 3rd edition. CRC Press, Boca Raton2014. p. 951–89.
10. Richard D, Arsenault E, Cembella A, Quilliam M. Investigations into the toxicology and pharmacology of spirolides, a novel group of shellfish toxins. In: Hallegraeff GM, Blackburn SI, Bolch CJ, Lewis RJ, editors. Harmful Algal Blooms 2000: Intergovernmental Oceanographic Commission of UNESCO; 2001. p. 383–86.
11. Marrouchi R, Benoit E, Kharrat R, Molgo J. Gymnodimines: a family of phycotoxins contaminating shellfish. In: Berbier J, Benoit, E., Marchot, P., Mattei, C., Servent, D., editor. Advances and new technologies in Toxinology: SFET Editions: Meetings on Toxinology, E-book RT18.; 2010. p. 79–83.
12. Hansen P, Cembella A, Moestrup Ø. The marine dinoflagellate *Alexandrium ostenfeldii*: Paralytic shellfish toxin concentration, composition, and toxicity to a tintinnid ciliate. J Phycol. 1992; 28:597–603.
13. Kremp A, Tahvanainen P, Litaker W, Krock B, Suikkanen S, Leaw CP, et al. Phylogenetic relationships, morphological variation, and toxin patterns in the *Alexandrium ostenfeldii* (Dinophyceae) complex: implications for species boundaries and identities. J Phycol. 2014; 50:81–100.
14. Paulsen O. Plankton-investigations in the waters round Iceland in 1903. Medd Kommn Havunders Kobenh Ser Plankt. 1904; 1:1–40.
15. Burson A, Matthijs H, de Bruijne W, Talens R, Hoogenboom R, Gerssen A, et al. Termination of a toxic *Alexandrium* bloom with hydrogen peroxide. Harmful Algae. 2014; 31:125–35.
16. Kremp A, Lindholm T, Dreßler N, Erler K, Gerdts G, Eirtovaara S, et al. Bloom forming *Alexandrium ostenfeldii* (Dinophyceae) in shallow waters of the Åland Archipelago, Northern Baltic Sea. Harmful Algae. 2009; (8:):318–28.
17. Østergaard M, Moestrup Ø. Autecology of the toxic dinoflagellate *Alexandrium ostenfeldii*: life history and growth at different temperatures and salinities. Eur J Phycol. 1997; 32:9–18.
18. Tillmann U, Kremp A, Tahvanainen P, Krock B. Characterization of spirolide producing *Alexandrium ostenfeldii* (Dinophyceae) from the western Arctic. Harmful Algae. 2014; 39:259–70.
19. Almandoz G, Montoya N, Hernando M, Benavides H, Carignan M, Ferrario M. Toxic strains of the *Alexandrium ostenfeldii* complex in southern South America (Beagle Channel, Argentina). Harmful Algae. 2014; 37:100–09.
20. Guzmán L, Vidal G, Pizarro G, Salgado P, Vivanco X, Iriarte L, et al. Programa de manejo y monitoreo de las mareas rojas en las regiones de Los Lagos, Aisén y Magallanes, etapa VII 2013–14. Convenio Asesoría integral para la pesca y la acuicultura (ASIPA). Subsecretaría de Economía y empresas de menor tamaño–Instituto de Fomento Pesquero2013. p. 45 + Figures + Tables + annexes.

21. Haro D, Aguayo A, Acevedo J. Características oceanográficas y biológicas de las comunidades del plancton y necton del área marina costera protegida Francisco Coloane: una revisión. An Inst Patagon. 2013; 41(1):77–90.
22. Avaria S, Cáceres C, Castillo P, Muñoz P. Distribución del microfitoplancton marino en la zona Estrecho de Magallanes-Cabo de Hornos, Chile, en la primavera de 1998 (Crucero Cimar 3 Fiordos). Ciencia y Tecnología del Mar. 2003; 26(2):79–96.
23. Balech E, de Mendiola BR. Un nuevo *Gonyaulax* productor de hemotalasia en Perú. Neotropica. 1977; 23:49–54.
24. Sanchez S, Villanueva P, Carbajo L. Distribution and concentration of *Alexandrium peruvianum* (Balech and de Mendiola) in the Peruvian coast (03°24′–18°20′ LS) between 1982–2004. XI International Conference on Harmful Algal Blooms; November 15–19; Cape Town, South Africa2004. p. 227.
25. Lim PT, Usup G, Leaw CP, Ogata T. First report of *Alexandrium taylori* and *Alexandrium peruvianum* (Dinophyceae) in Malaysia waters. Harmful Algae. 2005; 4:391–400.
26. Bravo I, Garcés E, Diogène J, Fraga S, Sampedro N, Figueroa R. Resting cysts of the toxigenic dinoflagellate genus *Alexandrium* in recent sediments from the Western Mediterranean coast, including the first description of cysts of *A. kutnerae* and *A. peruvianum*. Eur J Phycol. 2006; 41(3):293–302.
27. Ciminiello P, Dell'Aversano C, Fattorusso E, Magno S, Tartaglione L, Cangini M, et al. Toxin profile of *Alexandrium ostenfeldii* (Dinophyceae) from the Northern Adriatic Sea revealed by liquid chromatography–mass spectrometry. Toxicon. 2006; 47:597–604. PMID: 16564060
28. Katikou P, Aligizaki K, Zacharaki T, Iossifidis D, Nikolaidis G, editors. First report of spirolides in Greek shellfish associated with causative *Alexandrium* species. 14th International Conference on Harmful Algae; 2010; Crete, Greek, 1–5 November.
29. Suikkanen S, Kremp A, Hautala H, Krock B. Paralytic shellfish toxins or spirolides? The role of environmental and genetic factors in toxin production of the *Alexandrium ostenfeldii* complex. Harmful Algae. 2013; 26:52–59.
30. Lembeye G. Florecimientos algales nocivos en aguas australes. In: Silva N, Palma S, editors. Avances en el conocimiento oceanográfico de las aguas interiores chilenas. Valparaiso, Chile: Comité Oceanográfico Nacional—Pontificia Universidad Católica de Valparaíso; 2006. p. 99–103.
31. Franco JM, Paz B, Riobó P, Pizarro G, Figueroa R, Fraga S, et al. First report of the production of spirolids by *Alexandrium peruvianum* (Dinophyceae) from the Mediterranean Sea. 12th International Conference on Harmful Algae; Copenhagen, Denmark, 4–8 September2006.
32. Borkman D, Smayda T, Tomas C, York R, Strangman S, Wright J. Toxic *Alexandrium peruvianum* (Balech and de Mendiola) Balech and Tangen in Narragansett Bay, Rhode Island (USA). Harmful Algae. 2012; 19:92–100.
33. Tomas C, Van Wagoner R, Tatters R, White K, Hall S, Wright J. *Alexandrium peruvianum* (Balech and Mendiola) Balech and Tangen a new toxic species for coastal North Carolina. Harmful Algae. 2012; 17:54–63.
34. Maclean C, Cembella A, Quilliam M. Effects of Light, Salinity and Inorganic Nitrogen on Cell Growth and Spirolide Production in the Marine Dinoflagellate *Alexandrium ostenfeldii* (Paulsen) Balech et Tangen. Bot Mar. 2003; 46:466–76.
35. Otero A, Alfonso A, Vieytes MR, Cabado AG, Vieites JM, Botana LM. Effects of environmental regimens on the toxin profile of *Alexandrium ostenfeldii*. Environ Toxicol Chem. 2010; 29(2):301–10. doi: 10.1002/etc.41 PMID: 20821448
36. Guillard RRL, Hargraves PE. Stichochrysis immobilis is a diatom, not achrysophyte. Phycologia. 1993; 32:234–36.
37. Rourke WA, Murphy CJ, Pitcher G, Van de Riet JM, Garth Burns B, Thomas KM, et al. Rapid postcolumn methodology for determination of paralytic shellfish toxins in shellfish tissue. J AOAC Int. 2008; 91 (3):589–97. PMID: 18567305
38. EURLMB. EU-Harmonised Standard Operating Procedure for Determination of Lipophilic Marine Biotoxins in Molluscs by LC–MS/MS. European Union Reference Laboratory for Marine Biotoxins. http://aesan.msps.es/en/CRLMB/web/home.shtml. 2011.
39. Paz B, Vázquez JA, Riobó P, Franco JM. Study of the effect of temperature, irradiance and salinity on growth and yessotoxin production by the dinoflagellate *Protoceratium reticulatum* in culture by using a kinetic and factorial approach. Mar Environ Res. 2006; 64(2):286–300.
40. Vázquez JA, Murado MA. Mathematical tools for objective comparison of microbial cultures. Application to evaluation of 15 peptones for lactic acid bacteria productions. Biochem Eng J. 2008; 39:276–87.
41. Vázquez JA, Lorenzo JM, Fuciños P, Franco D. Evaluation of non-linear equations to model different animal growths with mono and bi-sigmoid profiles. J Theor Biol. 2012; 39:276–87.

42. Box GE, Hunter JS, Hunter WG. Statistics for experimenters: Design, innovation, and discovery. 2nd ed: New York: John Wiley & Sons, Inc.; 2005.

43. Wardhani DH, Vázquez JA, Pandiella SS. Optimization of antioxidants extraction from fermented soybeans by *Aspergillus oryzae*. Food Chem. 2010; 118(3):731–39.

44. Dantigny P, Marín S, Beyer M, Magand N. Mould germination: Data treatment and modelling. Int J Food Microbiol. 2007; 114:17–24. PMID: 17188772

45. Jayakar SS, Singhal RS. Kinetic modeling and scale up of lipoic acid (LA) production from *Saccharomyces cerevisiae* in a stirred tank bioreactor. Bioprocess Biosyst Eng. 2013; 36:1063–70. doi: 10.1007/s00449-012-0859-1 PMID: 23178984

46. Liu JZ, Weng LP, Zhang QL, Xu H, Ji LN. A mathematical model for gluconic acid fermentation by *Aspergillus niger*. Biochem Eng J. 2003; 14:137–41.

47. Spor A, Dillmann C, Wanga S, de Vienne D, Sicard D, Sicard D. Hierarchical Bayesian modelling for *Saccharomyces cerevisiae* population dynamics. Int J Food Microbiol. 2010; 142:25–35. doi: 10.1016/j.ijfoodmicro.2010.05.012 PMID: 20576304

48. Vázquez JA, Docasal SF, Prieto MA, González MP, Murado MA. Growth and metabolic features of lactic acid bacteria in media with hydrolysed fish viscera. An approach to bio-silage of fishing by-products. Bioresource Technol. 2008; 99:6246–57.

49. Wardhani DH, Vázquez JA, Pandiella SS. Mathematical modeling of the development of antioxidant activity in soybeans fermented with *Aspergillus oryzae* and *Aspergillus awamori* in the solid state. J Agric Food Chem. 2009; 57:540–44. doi: 10.1021/jf802492s PMID: 19099459

50. Franco D, Crecente S, Vázquez JA, Gómez M, Lorenzo JM. Effect of cross breeding and amount of finishing diet on growth parameters, carcass and meat composition of foals slaughtered at 15 months. Meat Sci. 2013; 93:547–56 doi: 10.1016/j.meatsci.2012.11.018 PMID: 23273463

51. Franco D, Rois D, Vázquez JA, Purriños L, González R, Lorenzo JM. Breed effect between Mos rooster (Galician indigenous breed) and Sasso T-44 line and finishing feed effect of commercial fodder or corn. Poult Sci. 2012; 91:487–98. doi: 10.3382/ps.2011-01546 PMID: 22252364

52. Kebreab E, Schulin-Zeuthen M, Lopez S, Soler J, Dias RS, de Lange CFM, et al. Comparative evaluation of mathematical functions to describe growth and efficiency of phosphorus utilization in growing pigs. J Anim Sci 2007; 85:2498–507. PMID: 17565069

53. Hui W, Shiwei F, Zhigang L. Optimal prediction of adductor percentage for *Argopecten irradians concentricus* (Say) cultured in Beibu bay in China. Aquaculture. 2008; 284:68–73.

54. Paz B, Vázquez JA, Riobó P, Franco JM. Mathematical description of yessotoxin production by *Protoceratium reticulatum* in culture. Harmful Algae. 2009; 8:730–35.

55. Planas M, Vázquez JA, Marques J, Pérez R, González MP, Murado M, A. Enhancement of rotifer (*Brachionus plicatilis*) growth by using terrestrial acid lactic bacteria. Aquaculture. 2004; 240:313–29

56. Rial D, Murado M, A., Menduíña A, Fuciños P, González MP, Mirón J, et al. Effects of spill-treating agents on growth kinetics of marine microalgae. J Hazard Mater. 2013; 263:374–81. doi: 10.1016/j.jhazmat.2013.07.010 PMID: 23911058

57. Vázquez JA, González MP, Murado MA. A new marine medium. Use of the different fish peptones and comparative study of the growth of selected species of marine bacteria. Enzyme Microb Technol. 2004; 35:385–92

58. Kremp A, Godhe A, Egardt J, Dupont S, Suikkanen S, Casabianca S, et al. Intraspecific variability in the response of bloom-forming marine microalgae to changed climate conditions. Ecol Evol. 2012; 2 (6):1195–207. doi: 10.1002/ece3.245 PMID: 22833794

59. Brown L, Bresnan E, Graham J, Lacaze JP, Turrell E, Collins C. Distribution, diversity and toxin composition of the genus *Alexandrium* (Dinophyceae) in Scottish waters. Eur J Phycol. 2010; 45(4):375–93.

60. Etheridge SM, Roesler CS. Effects of temperature, irradiance, and salinity on photosynthesis, growth rates, total toxicity, and toxin composition for *Alexandrium fundyense* isolates from the Gulf of Maine and Bay of Fundy. Deep-Sea Res Pt II. 2005; 52:2491–500.

61. Grzebyk D, Béchemin C, Ward CJ, Vérité C, Codd GA, Maestrini SY. Effects of salinity and two coastal waters on the growth and toxin content of the dinoflagellate *Alexandrium minutum*. J Plankton Res. 2003; 25(10):1185–99.

62. Laabir M, Jauzein C, Genovesi B, Masseret E, Grzebyk D, Cecchi P, et al. Influence of temperature, salinity and irradiance on the growth and cell yield of the harmful red tide dinoflagellate *Alexandrium catenella* colonizing Mediterranean waters. J Plankton Res. 2011; 0(0):1–14.

63. Figueroa R, Vázquez JA, Massanet A, Murado MA, Bravo I. Interactive effects of salinity and temperature on planozigote and cyst formation of *Alexandrium minutum* (Dinophyceae) in culture. J Phycol. 2011; 47:13–24.

64. Lakeman MB, Dassow PV, Cattolico RA. The strain concept in phytoplankton ecology. Harmful Algae. 2009; 8:746–58.

65. Wood AM, Leatham T. The species concept in phytoplankton ecology. J Phycol. 1992; 28:723–29.

66. Hwang D, Lu Y. Influence of environmental and nutritional factors on growth, toxicity, and toxin profile of dinoflagellate *Alexandrium minutum*. Toxicon. 2000; 38:1491–503. PMID: 10775750

67. Wang D, Hsieh D. Growth and toxin production in batch cultures of a marine dinoflagellate *Alexandrium tamarense* HK9301 isolated from the South China Sea. Harmful Algae. 2005; 4:401–10.

68. Granéli E, Flynn K. Chemical and physical factors influencing toxin content. In: Granéli E, Turner J, editors. Ecology of Harmful Algae. ed. Springer-Verlag Berlin Heidelberg: Ecological Studies Series 189.; 2006.

69. Anderson DM, Kulis DM, Sullivan JJ, Hall S. Toxin composition variations in one isolate of the dinoflagellate *Alexandrium fundyense*. Toxicon. 1990; 28(8):885–93. PMID: 2080515

70. Figueroa RI, Bravo I, Garcés E. The significance of sexual versus asexual cyst formation in the life cycle of the noxious dinoflagellate *Alexandrium peruvianum*. Harmful Algae. 2008; 7:653–63.

71. Miles C, Wilkins A, Stirling D, MacKenzie L. New Analogue of Gymnodimine from a *Gymnodinium* Species. J Agric Food Chem. 2000; 48:1373–76. PMID: 10775400

72. Miles C, Wilkins A, Stirling D, MacKenzie L. Gymnodimine C, an Isomer of Gymnodimine B, from *Karenia selliformis*. J Agric Food Chem. 2003; 51:4838–40. PMID: 14705921

73. Haywood A, Steidinger K, Truby E, Bergquist P, Bergquist P, Adamson J, et al. Comparative morphology and molecular phylogenetic analysis of three new species of the genus *Karenia* (Dinophyceae) from New Zealand. J Phycol. 2004; 40:165–79.

74. Medhioub W, Sechet V, Truquet P, Bardouil M, Amzil Z, Lassus P, et al. *Alexandrium ostenfeldii* growth and spirolide production in batch culture and photobioreactor. Harmful Algae. 2011; 10:794–803.

75. Tatters R, Van Wagoner R, Wright J, Tomas C. Regulation of spiroimine neurotoxins and hemolytic activity in laboratory cultures of the dinoflagellate *Alexandrium peruvianum* (Balech & Mendiola) Balech & Tangen. Harmful Algae. 2012; 19:160–68.

76. Gribble K, Keafer B, Quilliam M, Cembella A, Kulis D, Manahan A, et al. Distribution and toxicity of *Alexandrium ostenfeldii* (Dinophyceae) in the Gulf of Maine, USA. Deep-Sea Res Pt II. 2005; 52:2745–63.

77. MacKinnon S, Walter J, Quilliam M, Cembella A, LeBlanc P, Burton I, et al. Spirolides Isolated from Danish Strains of the Toxigenic Dinoflagellate *Alexandrium ostenfeldii*. J Nat Prod. 2006; 69(7):983–87. PMID: 16872129

78. Aasen J, MacKinnon S, LeBlanc P, Walter J, Hovgaard P, Aune T, et al. Detection and Identification of Spirolides in Norwegian Shellfish and Plankton. Chem Res Toxicol. 2005; 18:509–15. PMID: 15777091

79. Senft-Batoh CD, Dam HG, Shumway SE, Wikfors GH, Schlichting CD. Influence of predator–prey evolutionary history, chemical alarm-cues, and feeding selection on induction of toxin production in a marine dinoflagellate. Limnol Oceanogr. 2015; 00:1–21.

80. Senft-Batoh CD, Dam HG, Shumway SE, Wikfors GH. A multi-phylum study of grazer-induced paralytic shellfish toxin production in the dinoflagellate *Alexandrium fundyense*: A new perspective on control of algal toxicity. Harmful Algae. 2015; 44:20–31.

81. Gu H. Morphology, phylogenetic position, and ecophysiology of *Alexandrium ostenfeldii* (Dinophyceae) from the Bohai Sea, China. J Syst Evol. 2011; 49(6):606–16.

82. Tahvanainen P, Alpermann T, Figueroa R, John U, Hakanen P, Nagai S, et al. Patterns of post-glacial genetic differentiation in marginal populations of a marine microalga. PLoS ONE. 2012; 7(12):e53602. doi: 10.1371/journal.pone.0053602 PMID: 23300940

83. Hakanen P, Suikkanen S, Franzén J, Franze H, Kankaanpää H, Kremp A. Bloom and toxin dynamics of *Alexandrium ostenfeldii* in a shallow embayment at the SW coast of Finland, northern Baltic Sea. Harmful Algae. 2012; 15:91–99.

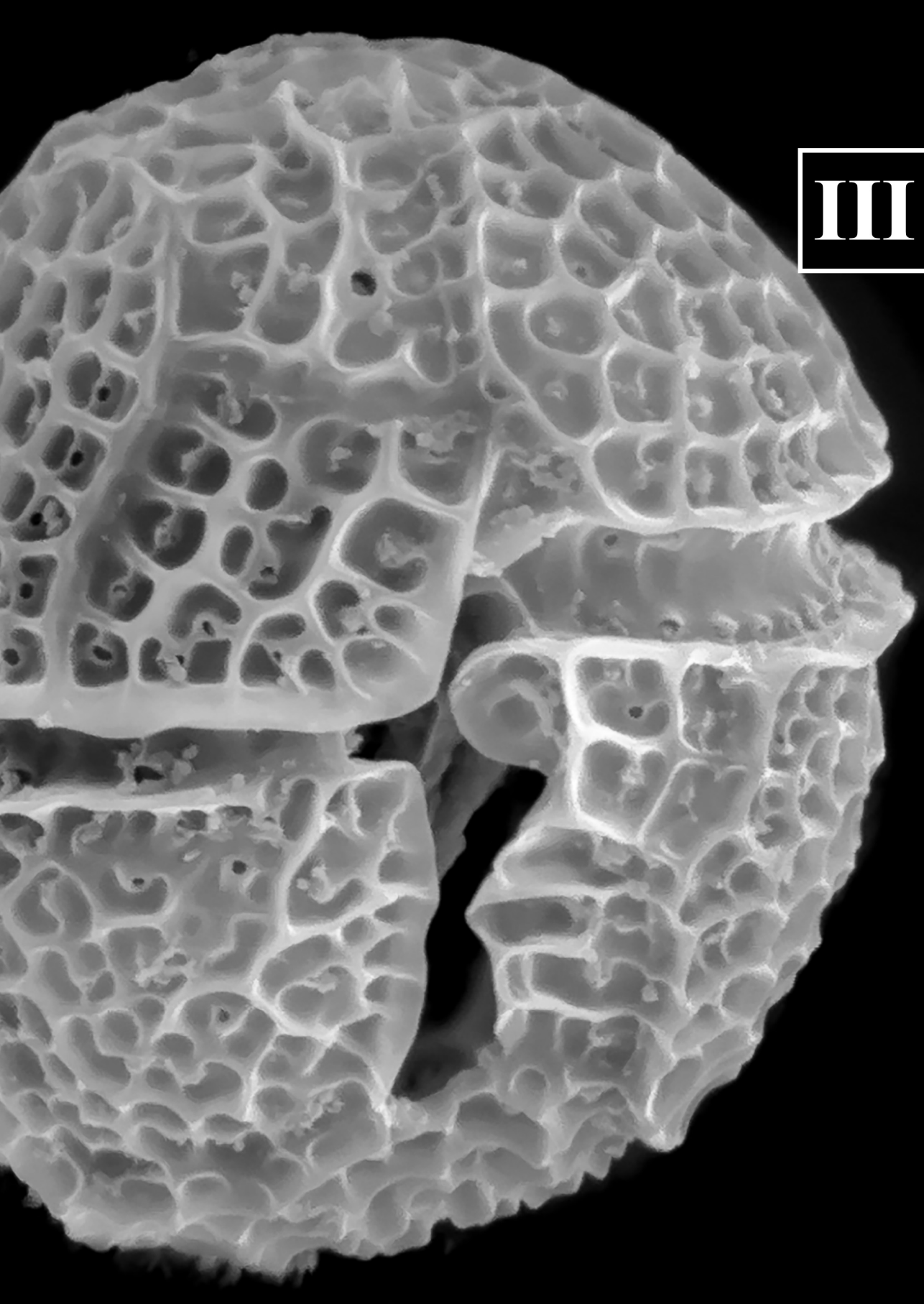
III

CERATOCORYS MARIAOVIDII SP. NOV. (GONYAULACALES), A NEW DINOFLAGELLATE SPECIES PREVIOUSLY REPORTED AS *PROTOCERATIUM RETICULATUM*

Pablo Salgado

Instituto de Fomento Pesquero, Enrique Abello 0552, Casilla 101, Punta Arenas, Chile
Instituto Español de Oceanografía, Centro Oceanográfico de Vigo, Subida a Radio Faro 50, 36390,Vigo, Spain

Santiago Fraga, *Francisco Rodríguez*

Instituto Español de Oceanografía, Centro Oceanográfico de Vigo, Subida a Radio Faro 50, 36390,Vigo, Spain

Pilar Riobó

Instituto de Investigaciones Marinas (IIM–CSIC), Eduardo Cabello 6, 36208, Vigo, Spain

and

Isabel Bravo

Instituto Español de Oceanografía, Centro Oceanográfico de Vigo, Subida a Radio Faro 50, 36390,Vigo, Spain

The family Ceratocoryaceae includes the genera *Ceratocorys*, *Protoceratium* and *Schuettiella*, whose phylogenetic relationships are poorly known. Here, the new non-yessotoxin-producing species of the genus *Ceratocorys*, *Ceratocorys mariaovidii* sp. nov., previously reported as the toxic *Protoceratium reticulatum*, is described from examinations by light and scanning electron microscopy, molecular phylogeny, and toxin analyses. The species description is made from culture samples of strains CCMP1740 and CCMP404 from USA waters. *C. mariaovidii* is globular and has thick and strongly reticulated plates with one pore within each reticule, just like *P. reticulatum*, but the key difference between the two species is the presence of five precingular plates in *C. mariaovidii* instead of six as in *P. reticulatum*. The thecal plate formula is Po, 4', 0a, 5'', 6c, ~7s, 5''', 0p, 2''''. The apical pore plate is oval with a λ-shaped pore. The first apical plate is narrow with a ventral pore on the right anterior side; it contacts the apical pore plate and its contact with the anterior sulcal plate is slight or absent. The fourth precingular plate of other Gonyaulacales is absent. *C. mariaovidii* may have small spines on the second antapical plate. A phylogenetic study based on ITS/5.8SrDNA supports the morphological classification of *C. mariaovidii* as a new species of *Ceratocorys* and in a different clade from *P. reticulatum*.

***Key index words*: *Ceratocorys mariaovidii*; dinoflagellate; Gonyaulacales; ITS rDNA; *Protoceratium reticulatum*; reticulated plates.**

***Abbreviations*: AIF, all ion fragmentation; ITS rDNA, internal transcribed spacer rDNA; LC–HRMS, liquid chromatography coupled to high-resolution mass spectrometry; L:D, light:dark; NCMA, National Center for Marine Algae and Microbiota; YTX, yessotoxin.**

Ceratocorys Stein (1883) is a genus of marine dinoflagellates belonging to the Order Gonyaulacales and to the family Ceratocoryaceae (Lindemann 1928), which also includes the genera *Protoceratium* Bergh and *Schuettiella* Balech (Gómez 2012). The genus *Ceratocorys* currently comprises 12 taxonomically accepted species (*C. anacantha* Carbonell-Moore, *C. armata* (Schütt) Kofoid, *C. aultii* Graham, *C. bipes* (Cleve) Kofoid, *C. gourretii* Paulsen, *C. grahamii* Carbonell-Moore, *C. horrida* Stein, *C. indica* Wood, *C. kofoidii* Paulsen, *C. magna* Kofoid, *C. reticulata* Graham, and *C. skogsbergii* Graham), among which the most representative is *C. horrida*, its type species (Guiry 2017). All its members share characteristics such as being oceanic, inhabiting warm waters in tropical and subtropical regions worldwide, and building a cell wall of cellulosic plates (Graham 1942, Balech 1988, Fensome et al. 1993, Carbonell-Moore 1996, Steidinger and Tangen 1997). Most species are phototrophic. Hallegraeff and Jeffrey (1984) mentioned that *C. horrida* showed intensely pigmented red fluorescent cells in shelf waters and non-pigmented green fluorescent cells at offshore stations, while *C. armata* only displayed green fluorescence typical of non-photosynthetic dinoflagellates. To our knowledge, no toxin studies of this genus have been carried out, so nothing is known about their toxicity. They all have a striking ornamentation and a distinctive general morphology. In general, they have a well-sculpted theca, a flat epitheca commonly much shorter than the hypotheca, broad cingular lists or crests, and short or large hypothecal spines (four projecting from the edges of the antapical plate and two single dorsal and ventral spines) (Fensome et al. 1993, Zirbel et al. 2000). Until now the only two described species that do not have spines are *C. anacantha* and *C. grahamii* (Carbonell-Moore 1996). Conversely, the main differences reported among these species are in their cell size, ornamentation (which can be reticulated or smooth, with high or low ridges), pore size, hypothecal spine length, and body shape.

The tabulation of thecal plates of *Ceratocorys* does not completely coincide with that of other gonyaulacoids. In the epitheca, it was described as having three apical plates, an intercalary plate (1a), and five precingular plates. In the hypotheca, it has five postcingular plates and two antapical plates (Graham 1942, Balech 1988, Fensome et al. 1993). The main feature differentiating it from other gonyaulacoid genera, such as *Alexandrium* Halim, *Protoceratium*, and *Gonyaulax* Diesing, is the presence of five precingular plates instead of the six plates that the others have. The fourth precingular plate in *Ceratocorys* represents the fourth and fifth precingular plates of other Gonyaulacales, which means that they have fused or that one is missing (Fensome et al. 1993).

Here we describe a new species of *Ceratocorys*, *Ceratocorys mariaovidii*, based on morphological, molecular phylogenetic, and toxin studies of the strains CCMP404 and CCMP1720, which

had been previously reported as *Protoceratium reticulatum* (Claparède and Lachmann) Bütschli (NCMA 2017). The considerable morphological similarity between the two species had led the distinctive characteristics of those strains to be overlooked. However, previous molecular analyses (Howard et al. 2009, Scorzetti et al. 2009, Akselman et al. 2015) using strains CCMP404, CCMP1720, CCMP1721, and other *P. reticulatum* strains had already noted a phylogenetic divergence between them. Moreover, the phylogenetic relationship had been mentioned by Gómez et al. (2011), who showed in their phylogenetic tree of maximum likelihood of SSU rDNA sequences that *P. reticulatum* and *C. horrida* have evolved from a common ancestor.

MATERIALS AND METHODS

Source of specimens and culture conditions. Strains CCMP404 and CCMP1720, listed as *P. reticulatum*, were obtained from the National Center for Marine Algae and Microbiota (NCMA, Maine, USA) and kept in culture at the Culture Collection of Harmful Microalgae of the Instituto Español de Oceanografía in Vigo (CCVIEO: http://www.vgohab.es/). Strain CCMP404 was isolated from a hypersaline lake (Salton Sea) in California USA (33º22' N, 116°0' W) and strain CCMP1720 from Biscayne Bay, Miami, Florida, USA (25º48' N, 80º19' W). The cultures were maintained in Erlenmeyer flasks filled with 50 mL of L1 medium (Guillard and Hargraves 1993) without silicates, prepared with Atlantic seawater from off the Ría de Vigo (Spain), adjusted to a salinity of 32 by the addition of sterile bi-distilled water and maintained at 19ºC ± 1ºC and a photoperiod cycle of 12:12 h light:dark (L:D) with a photon irradiance of about 100 µmol photons · m^{-2} · s^{-1} of PAR measured with a QSL-100 irradiance meter (Biospherical Instruments Inc., San Diego, CA, USA).

Light microscopy. The morphological study of the strains by light microscopy was carried out in wells of culture plates (35 mm diameter; Thermo Fisher Scientific, USA) inoculated from the cultures maintained in Erlenmeyer flasks. For a detailed study of the thecal plates, vegetative cells were stained with Calcofluor white (Fluorescent Brightener 28, Sigma–Aldrich, St. Louis, MO, USA) (Fritz and Triemer 1985) and observed under a Leica DMLA microscope (Leica Microsystems GmbH, Wetzlar, Germany) equipped with differential interference contrast, UV epifluorescence with UV and blue excitation filters, and an AxioCam HRc camera (Zeiss, Göttingen, Germany). When required, cells were dissected by squashing them using gentle pressure on the coverslip, occasionally with the aid of sodium hypochlorite. The cultured cells were observed alive or fixed with formaldehyde at a final concentration of 1%. Cell nuclei were stained with 1:100 SYBR Green in PBS 0.01 M pH 7 for 20 min and observed using the same microscope at 365 nm. Photographs were taken with an AxioCam HRc camera (Zeiss, Göttingen, Germany). When the depth of field was not sufficient for the whole object, several pictures were taken at a series of different foci and automatically merged using Adobe Photoshop (Adobe Systems Incorporated, San Jose, CA, USA).

Sexual stages such as gamete pairs (cells smaller and lighter in color than

vegetative cells which are joined by epitheca) and planozygotes (longitudinally biflagellated cells) (Salgado et al. 2017) from strains cultured in L1 medium were observed under an inverted microscope (Axiovert Zeiss 135, Jena, Germany), video-recorded, and photographed using a microscope camera (Canon EOS 5D Mark II, Japan). Cyst-like cells were individually isolated (n = 5) and transferred into the wells of culture plates (8 mm diameter; Thermo Fisher Scientific, USA) containing 250 µL of fresh L1 medium. The cyst-like cells were incubated at 19ºC ± 1ºC with a photoperiod cycle of 12:12 h L:D (photon irradiance of about 100 µmol photons · m^{-2} · s^{-1}) and examined daily for 15 days under an inverted microscope (Axiovert Zeiss 135, Jena, Germany). Photographs were obtained using a microscope camera (Canon EOS 5D Mark II, Japan).

Scanning electron microscopy. For scanning electron microscopy (SEM), 3-mL samples of cultures with exponentially growing vegetative cells were fixed with glutaraldehyde at a final concentration of 4%. After 24 h at room temperature, the fixed cells were filtered through 5-µm pore size Isopore RTTP polycarbonate filters (Merck Millipore, Billerica, Massachusetts, USA), stained with 2% osmium tetroxide for 30 min, rinsed three times with distilled water, and dehydrated in a series of 30, 50, 70, 90, 95 and 100% EtOH. They were then air-dried overnight, coated with gold using a K550 X sputter coater (Emitech Ltd., Ashford, Kent, UK), and observed with an FEI Quanta 200 scanning electron microscope (FEI Company, Hillsboro, OR, USA).

Plate nomenclature. In this paper a relaxed Kofoid nomenclature system that recognizes homologies of plates of other gonyaulacoid genera was used (Fensome et al. 1993, Paez-Reyes and Head 2013). The plate, which, following the Kofoid system, should be named an anterior intercalary plate (1a), was considered here as the homologue of the third apical plate of other gonyaulacoids because it can contact the apical pore plate (Po), and hence is named 3' (Table 1). *Ceratocorys* has five precingular plates (Table 1), but the last plate of the series of precingular plates was named 6" instead of 5", as it is considered to be homologous to that plate of other Gonyaulacales. The equivalence of the plate names used here and plate names strictly following the Kofoid system are given in Table 1 and shown between brackets in Figs. 1 and 2, but not in Figs. 3 and 4, to keep the images as clear as possible.

Phylogenetic analysis. The internal transcribed spacer (ITS) and 5.8SrDNA sequences of the studied strains and those of other related taxa included in this study were obtained from the GenBank database and aligned using MEGA 7. Uncorrected genetic *p*-distances were calculated between *P. reticulatum*, *C. horrida* and *C. mariaovidii* sequences across the full ITS and 5.8SrDNA (except two nucleotides at the end of ITS-2 due to the shorter EU927577 sequence of *C. horrida*). Sequences of CCMP404 and CCMP1720 were only included if the full length of ITS/5.8SrDNA was available. Several sequences were retrieved in GenBank for both strains but, despite being identical, they were kept in the final alignment. A sequence from *Karenia brevis* (Davis) Hansen and Moestrup was used as an

Table 1. Plate nomenclature used in this study and that used by Sala-Pérez et al. (2016).

This study		*Protoceratium reticulatum* (Sala-Pérez et al. 2016)	
Po	Apical pore plate	Po	Apical pore plate
1'	First apical	1'	First apical
2'	Second apical	2'	Second apical
3'	Third apical	1a	First intercalary
4'	Fourth apical	3'	Third apical
1"	First precingular	1"	First precingular
2"	Second precingular	2"	Second precingular
3"	Third precingular	3"	Third precingular
4"	Missing	4"	Fourth precingular
5"	Fifth precingular	5"	Fifth precingular
6"	Sixth precingular	6"	Sixth precingular
1‴	First postcingular	1‴	First postcingular
2‴	Second postcingular	2‴	Second postcingular
3‴	Third postcingular	3‴	Third postcingular
4‴	Fourth postcingular	4‴	Fourth postcingular
5‴	Fifth postcingular	5‴	Fifth postcingular
1⁗	First antapical	1⁗	First antapical
2⁗	Second antapical	2⁗	Second antapical
Sa	Sulcal anterior		
Ssa	Left sulcal anterior		
Sda	Right sulcal anterior		
Saca	Accesory sulcal anterior		
Ssp	Left sulcal posterior		
Sdp	Right sulcal posterior		
Sp	Sulcal posterior		

outgroup. The final alignment for the ITS phylogeny consisted of 546 positions. The phylogenetic relationships were determined according to the maximum likelihood method using MEGA 7 and the bayesian inference method with a general time-reversible model from MrBayes v3.2 (Huelsenbeck and Ronquist 2001). The model selection tool in MEGA 7 selected Tamura and Nei (TN93) as the best model (Tamura and Nei 1993), with a gamma-

shaped parameter (y = 2) and proportion of invariable sites (I = 7%).

Bayesian phylogenetic inference and, in this case, the substitution models were obtained by sampling across the entire general time-reversible model space following the procedure described in the MrBayes v3.2 manual. The program parameters were statefreqpr = dirichlet (1,1,1,1), nst = mixed, rates = gamma. The phylogenetic analyses involved two parallel analyses, each with four chains. Starting trees for each chain were selected randomly using the default values for the MrBayes program. The corresponding number of unique site patterns was 513. The number of generations used in these analyses was 1,000,000. Posterior probabilities were calculated from every 100th tree sampled after log-likelihood stabilization (the "burn-in" phase). All final split frequencies were <0.02. The two methods rendered very similar topologies and the phylogenetic tree was represented using the bayesian inference results, with bootstrap values from the maximum likelihood method (n = 1000 replicates) and posterior probabilities from the bayesian inference method.

Extraction and analysis of YTXs. Cultures of strains CCMP404 and CCMP1720 were harvested for yessotoxin (YTX) determination with exponentially growing vegetative cells. Before the extraction of toxins, an aliquot of each culture was collected and fixed with Lugol solution to determine the cell density by light microscopy using a Sedgewick-Rafter counting chamber. Culture volumes of 590 mL (5,824 cell · mL^{-1}) for CCMP404 and 610 mL (6,996 cell · mL^{-1}) for CCMP1720 were filtered through GF/C glass microfiber filters (47 mm diameter; Whatman, Maidstone, England). The cells in the filter were extracted with 1.5 mL of methanol, sonicated for 1 min at 50 W with a sonication probe and centrifuged for 10 min at 14,000 rpm and 5ºC. The supernatant was removed and the pellet was extracted again with 1.5 mL of methanol following the same process. The two supernatants were combined and the final volume was 3 mL. The extracts were kept at –20ºC until chemical analyses, at which time they were tempered and subsequently filtered through 0.45-µm PTFE syringe filters.

YTX determination was performed by liquid chromatography coupled to high-resolution mass spectrometry (LC–HRMS) on a Dionex Ultimate 3000 LC system (Thermo Fisher Scientific, San Jose, California) coupled to an Exactive mass spectrometer (Thermo Fisher Scientific, Bremen, Germany) equipped with an Orbitrap mass analyzer and a heated electrospray source (H–ESI II). Nitrogen (purity >99.999%) was used as the sheath gas, auxiliary gas, and collision gas. The instrument was calibrated daily in positive and negative ion modes. Mass acquisition was performed in negative ion mode without and with all ion fragmentation (AIF) with a high-energy collisional dissociation of 40 eV. The mass range was m/z 500–2000 in full-scan and m/z 500–1500 in AIF mode.

Chromatographic conditions were according to the Standardized Operating Procedure validated by the European Union Reference Laboratory for Marine Biotoxins (EURLMB 2011). The separation column was a Gemini NX C18 (100 × 2 mm, 3 µm) maintained at 40°C. Mobile phase A consisted of water containing 0.05% ammonia and mobile phase B of acetonitrile/mobile phase A (90:10 v/v). Linear gradient elution was pumped at a

flow rate of 400 μL min^{-1} and started at 25% B. From 1.5 min to 7.5 min it increased from 25% to 95% B where it was held for 6.5 min. The initial conditions of 25% B were restored in 3 min, and then maintained for 2 min to allow column equilibration. The total run time was 19 min. For YTX identification, a YTX standard purchased from the Institute of Environmental Science and Research Limited (New Zealand) was used.

RESULTS

Ceratocorys mariaovidii P. Salgado, S. Fraga, F. Rodríguez, P. Riobó and I. Bravo sp. nov. (Figs. 1–5)

Description. Cells have a length of 33.8 to 50.1 μm and a width of 31.3 to 47.3 μm. They are globular in ventral and dorsal views, and almost round in apical and antapical views, without horns or large spines, although the second antapical plate (2"") may have small spines. The epitheca is almost as long as the hypotheca. The cingulum is excavated with its right end displaced posteriorly one cingular width. The plate formula is Po, 4', 0a, 5", 6c, ~7s, 5"', 0p, 2"". The Po is oval with a λ-shaped pore. The first apical plate (1') is narrow, with a ventral pore on the right anterior side. This plate contacts the Po, while the contact with the anterior sulcal plate (Sa) is slight or absent. The third apical plate (3') is four-sided. The second (2") and third (3") precingular plates are of similar size. The third, fifth (5") and sixth (6") precingular plates are five-sided. The fourth precingular plate (4") of other Gonyaulacales is absent. The hypotheca is composed of five postcingular and two antapical plates. Thecal plates are thick and strongly reticulated, with one pore within each reticule.

Holotype. Figure 1a from strain CCMP404. SEM-stub (designation CEDiT2017H67) deposited at the Senckenberg Research Institute and Natural History Museum, Center of Excellence for Dinophyte Taxonomy, Germany. The strain CCMP404 is barcoded in GenBank with nucleotide sequences of the nuclear ribosomal ITS1-5.8S-ITS2 (GenBank FJ489629 and EU532485), and LSU (GenBank FJ489623 and EU532476). The clonal culture strain is deposited at the National Center for Marine Algae and Microbiota, Maine, USA.

Type locality. Salton Sea, California USA (strain CCMP404).

Habitat. Hypersaline lake and marine.

Etymology. The word *mariaovidii* is composed in its first part by maria of the name María and in its second part by ovidii, of the name Ovidio, and indicates the parents' names of the first author of this work.

Distribution: C. mariaovidii was isolated from Salton Sea (strain CCMP404), California, USA and from Biscayne Bay (strain CCMP1720), Miami, Florida, USA. It has also been reported (identified as *P. reticulatum*) from the eastern of Gulf of Mexico (Steidinger and Williams 1970), the Indian River Lagoon, Florida, USA (Hargraves 2017), and the Belize coast (Faust et al. 2005).

Morphology. The cells are almost spherical in apical and antapical views (Fig. 1c and h). They have an epitheca almost as

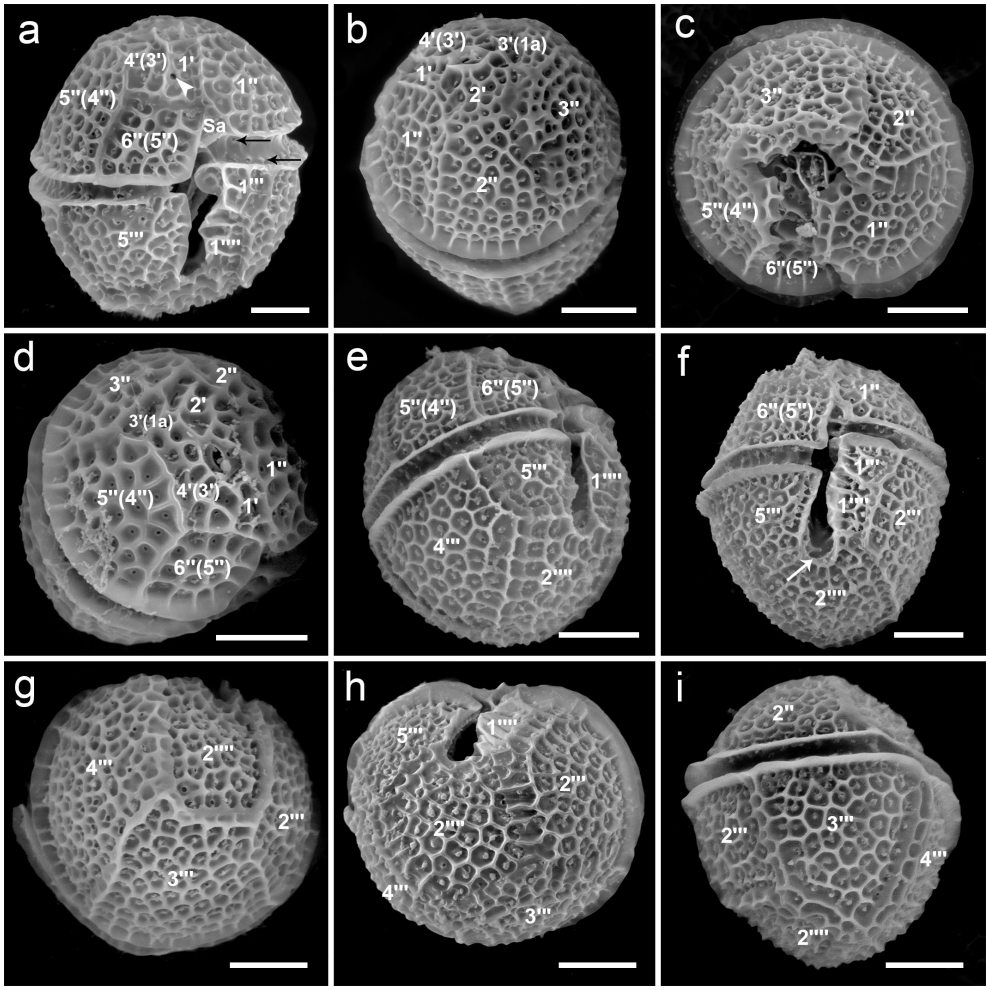

Fig. 1. SEM images of *Ceratocorys mariaovidii* sp. nov. cells. (a) Ventral view (arrowhead, ventral pore; arrows, pores in cingulum plates). (b) Dorsal-apical view. (c) Apical view. (d) Lateral-apical view. (e) Lateral-antapical view. (f) Ventral view (arrow: notch). (g) Dorsal-antapical view. (h) Antapical view. (i) Lateral view. Scale bar: 10 µm.

long as the hypotheca (Figs. 1a and 2a). Cells of strain CCMP404 range from 36.5 to 47.1 µm in length (mean and SD of 42.4 ± 2.6 µm length, n = 30) and from 34 to 45.3 µm in width (39.5 ± 2.6 µm width, n = 30). Strain CCMP1720 ranges from 33.8 to 50.1 µm in length (40.4 ± 3.6 µm length, n = 30) and from 31.3 to 47.3 µm in width (37.3 ± 3.5 µm width, n = 30). Cell depth in both strains is almost equal to cell width

(Fig. 1c and h). The plate formula is Po, 4', 0a, 5", 6c, ~7s, 5'", 0p, 2"" (Fig. 2a–d). Thecal plates are strongly reticulated with one pore within each reticule. In the epitheca, the Po plate is oval with a λ-shaped pore (Fig. 3a). Plate 1' is narrow, pentagonal in shape, has a ventral pore on the right anterior side and contacts the Po through a clear suture on the anterior side, while the contact with the Sa plate is slight (Fig. 3b) or absent (Fig. 3c). Plate 1' contacts on its left side 1" and 2' and on its right side 4' and 6" (Figs. 2c and 3b). The second apical plate (2') is the largest of the series and contacts 1', 1", 2", 3", 3', and 4' (Figs. 1b, 2c, and 3e). Plate 3' is four-sided and contacts 2', 3", 5", and 4' (Figs. 2c and 3e). It is separated from the Po by a short suture of the contact of plates 2' and 4' (Figs. 2c and 3b), but it can sometimes touch the Po with an evident separation between 2' and 4' (Fig. 3d). Fourth apical plate (4') is irregular and elongated (Figs. 1d, 2c, and 3e). In addition to the Po, it contacts 1', 2', 3', 5", and 6". The series of precingular plates is composed of large plates except 6", which is smaller than the others (Figs. 1c, 3e and f). The first precingular plate (1") contacts the anterior left part of Sa, 2", 2', and 1' (Figs. 1a, b, and 2c). Plate 2" is four-sided and contacts 3", 2', and 1" (Figs. 1b, 2c, 3e, and 3f). Plate 3" is five-sided, is located in right dorsal position, grows overlapping all its neighboring plates, 5", 3', 2', and 2" (Figs. 1c and 3e), and is the keystone plate in the sense given by Fensome et al. (1993). The four-sided plate 4" of other gonyaulacoids is absent (Figs. 1c, 2c, 3e, and 3f). Plate 5" is five-sided and contacts 3', 4', 6", and 3" (Figs. 1d and 2c). Plate 6" is the smallest of the series (Figs. 2c and 3f), square in shape, and contacts Sa, 1', 4', and 5" (Figs. 1a and 2c), and in some cases 1" (Fig. 3c). The cingulum descends one width without overhanging. The cingulum and sulcus are narrow and excavated (Figs. 1a and 2a). The cingulum is composed of six plates, c1–c6 (Fig. 3g and h), which are non-reticulated with two rows of pores along their anterior and posterior margins (Fig. 1a). The sulcus is composed of at least seven plates, Sa, left sulcal anterior (Ssa), right sulcal anterior (Sda), accessory sulcal anterior (Saca), left sulcal posterior (Ssp), right sulcal posterior (Sdp), and sulcal posterior (Sp) (Fig. 2b). In the hypotheca, the first postcingular plate (1'") is the smallest of the series and contacts 2'", 1"", and Ssa (Figs. 1f, 2d, and 3g). In some cases, plate Ssa may be visible behind this plate (see Figs. 1a and 2b). The second (2'"), third (3'"), and fourth (4'") postcingular plates are the largest and form the main body of the hypotheca (Figs. 1g, 2d, and 3h). The five-sided 2'" contacts 3'", 2"", 1"", and 1'" (Figs. 1f–i and 2d). Plate 3'" overlaps its neighbors 4'", 2"", and 2'" (Figs. 1g–i and 2d). Like 3'", plate 4'" is four-sided and contacts 3'", 2"", and 5'" (Figs. 1e, g, and 2d). The fifth postcingular plate (5'") is almost square in shape (Figs. 1e, f and 2d). The first antapical plate (1"") forms a thin list along its right side and hides the sulcal area (Fig. 1h). Plate 2"" is almost square with a notch toward the sulcus, contacts 1"", 2'", 3'", 4'", and 5'" (Figs. 1e–i and 2d), and may have small spines (Figs. 3g, h, and 4a).

The cells show numerous chloroplasts which radiate from the central part of the cell (Fig. 4b), a centrally located U-shaped nucleus with the tips ventrally directed (Fig. 4c and d) and, in some cases, one or two large orange bodies in the posterior part of the hypotheca (Fig. 4a).

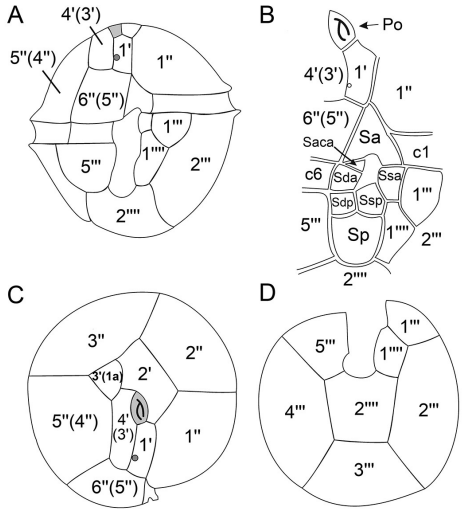

Fig. 2. Schematic drawings of thecal plate patterns of *Ceratocorys mariaovidii* sp. nov. (a) Ventral view. (b) Sulcal area. (c) Apical view. (d) Antapical view. For the abbreviations see Table 1.

Life cycle. Vegetative cells with the above-described morphology divide asexually by desmoschisis, in which each daughter cell inherits part of the parental thecal plates (Fig. 4e and f). The fission line is oblique, to the right of the longitudinal axis in the epitheca and to the left in the hypotheca. In this process, the right posterior daughter cell that inherits the flagellar apparatus of the mother retains both flagella (transversal and longitudinal), while the left anterior daughter cell forms them later. Before splitting, the dividing cells show the fission line and two centrally located oval nuclei (Fig. 4g and h). Once division finishes, each recently divided cell has a round nucleus (Fig. 4i). In addition to motile cells with a globular shape, a type of cell with a strong dorso-ventral compression was regularly present in the cultures, though in very low number. This cell type has recently been described by Salgado et al. (This issue) as a benthic stage of the life cycle. Sexual stages such as gamete pairs and planozygotes were also observed in both strains cultured in L1 medium. Longitudinally, biflagellate cells (planozygotes) also divide by desmoschisis, in which the right posterior daughter cell inherits the two trailing flagella of the mother (Fig. 4j). Moreover, spherical cells with the appearance of cysts (Fig. 4k) were formed inside large, non-motile thecate cells lying on the bottom of the culture flasks. Although their sexual or asexual nature is unknown, these cyst-like cells had a double cell wall without processes, many transparent granules, and one or two large orange bodies. In fresh replete medium all these cells germinated (Fig. 4l) within the first five days after isolation, giving a normal thecate cell that divided within the first three days after hatching.

Phylogenetic analyses. The bayesian inference analysis of the ITS/5.8SrDNA region showed a clear divergence between the two strains of *C. mariaovidii* used in this study and the sequences of *P. reticulatum* from isolates throughout the world (Fig. 5). Our phylogeny grouped *Ceratocorys* sequences as a separate monophyletic group from the *P. reticulatum* clade, whereas *C. horrida* and *C. mariaovidii* diverged as separate branches, in which the *C. mariaovidii* clade is slightly closer to the *P. reticulatum* clade. Uncorrected *p*-distances across the full ITS and 5.8SrDNA fragments were slightly larger between *C. horrida* and *C. mariaovidii* (0.408) than those between them and *P. reticulatum* (0.379–0.387 and 0.304–0.313 for *C. horrida* and *C. mariaovidii*, respectively). These genetic

distances mainly arose from the nucleotide differences between *Ceratocorys* and *Protoceratium* in the ITS-1 and ITS-2 fragments (0.49–0.57 and 0.38–0.50, respectively). In comparison, *p*-distances between *P. reticulatum* sequences ranged from 0.012 to 0.030 in the ITS-1/ITS-2 fragments. In turn, the 5.8SrRNA gene was much conserved between *P. reticulatum* and both *Ceratocorys* species (0.026–0.066).

Toxin analyses. YTX, 45 OH-YTX, Homo YTX and 45 OH-Homo YTX were not detected by LC–HRMS in either CCMP404 or CCMP1720. The limit of detection (LOD) for YTX with the LC–HRMS system and conditions detailed in this work was found to be 17 pg on column, which considering the number of cells used in the analysis, this implies a YTX LOD value of 0.7 fg per cell.

DISCUSSION

The results presented herein show that strains CCMP404 and CCMP1720, previously listed as *P. reticulatum* (Paz et al. 2007, Howard et al. 2009, Akselman et al. 2015, NCMA 2017), actually correspond to a new species of the genus *Ceratocorys*, *C. mariaovidii*. This new species also includes the strain CCMP1721 (NCMA 2017), isolated from Florida waters just like CCMP1720 (Scorzetti et al. 2009, NCMA 2017), which forms a clade together with strains CCMP1720 and CCMP404 in the phylogenetic tree of Akselman et al. (2015). The great morphological resemblance between *C. mariaovidii* and *P. reticulatum* would account for the previous misidentification, because in ventral view, even in SEM, they are hardly distinguishable, if at all. Our

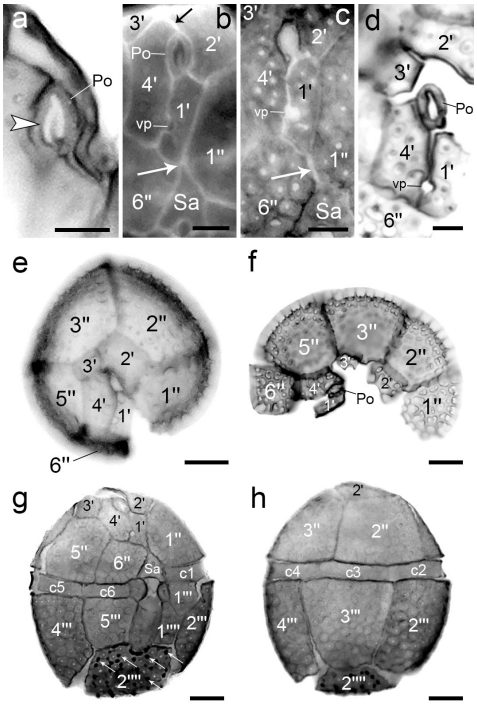

Fig. 3. Light microscopy images of *Ceratocorys mariaovidii* sp. nov. cells stained with Calcofluor white. (a) Po plate with a λ-shaped pore (arrowhead). (b) Plate 1' contacting the Po and Sa plates through a suture and a point (white arrow), respectively, and separation of the Po and 3' plates through a suture (black arrow). (c) Plate 6" contacting Sa (arrow). (d) Dissection of apical plates. (e) Epithecal plates. (f) Dissection of epithecal plates. (g) Flattened cell in ventral view (arrows indicate small spines in 2""). (h) Flattened cell in dorsal view. Scale bar: 5 µm (a–d), 10 µm (e–h). vp, ventral pore. The equivalence of the plate names used in this study and plate names strictly following the Kofoid system showed in Figs. 1 and 2, but are not shown here in order to keep the images as clear as possible.

results classify those strains as *Ceratocorys* based on tabulation of thecal plates and phylogeny, but there are some reasons to be

cautions about this issue (see below in the *Phylogeny* section). The results also reveal that *C. mariaovidii* is the species most different from other ceratocoryoids as well as the species most alike to the genus *Protoceratium*. In addition to having smaller cells, *C. mariaovidii* differs mainly in shape from other members of the genus. In general, they have an angular body, with the exception of *C. gourretii*, which is subspherical to ovoid, *C. horrida* being the most angular (Graham 1942), while *C. mariaovidii* is almost spherical. According to Fensome et al. (1993), *Ceratocorys* has a distinctive general pattern: the episome is flat and forms only about one-fifth of the total length of the central body, and the hyposome consists of the deep lower fourth-fifths of the central body. Graham (1942) mentioned, however, that the girdle is placed almost equatorially in *C. armata* and *C. reticulata*, which agrees more with *C. mariaovidii*.

Morphology. The plate tabulation of *C. mariaovidii* was based herein on plate homologies of other gonyaulacoid genera (Fensome et al. 1993, Paez-Reyes and Head 2013), giving a thecal plate formula Po, 4', 0a, 5", 6c, ~7s, 5"', 0p, 2"". However, a different interpretation of the 3' plate can be made when it is not in contact with Po (1a according to the Kofoid system), resulting in a plate formula Po, 3', 1a, 5", 6c, ~7s, 5"', 0p, 2"". The contact variability between the 1a and Po plates has also been observed in *P. reticulatum* cells coming from cultures and wild populations (see Woloszynska 1928, Hansen et al. 1996/97, Sala-Pérez et al. 2016, Salgado et al. 2017), so it is quite likely that plates 1a and 3' are homologous in both *P. reticulatum* and *C. mariaovidii*. According to Graham (1942), the epitheca of *Ceratocorys* has 4' and 0a, which is in line with our interpretation of epithecal plate tabulation, but this finding was refuted by Balech (1988) who indicated that the third apical is an intercalary plate (1a) because he observed it always separated from the Po. The contact between these two plates in *C. mariaovidii* agrees with the observation by Taylor (1976) for the genus *Ceratocorys*, which is why he thought this plate could also be considered as apical.

The thecal surface of *C. mariaovidii* is very similar to that described for *P. reticulatum* (Balech, 1988). The strong reticulation in both species often prevents a clear assessment of the number and orientation of plates (Hargraves and Maranda 2002), which further complicates the identification of each species when a staining such as Calcofluor is not used or the plates are not dissected. The main morphological differences between *C. mariaovidii* and *P. reticulatum* are the number of precingular plates—five in the former and six in the later—and the amount of apparent contact of Sa with 1', which is considerable in *P. reticulatum*, whereas in *C. mariaovidii* it is slight or absent. Fensome et al. (1993) mentioned that the contact between plates 6" and 1", with subsequent lack of contact between Sa and 1', is considered a key character of the genus *Ceratocorys*. Additionally, these two species differ in the shape of the apical pore, which is λ-shaped in *C. mariaovidii* and is a narrow unbranched slit in *P. reticulatum* (see Fig. 3a and b in the present paper, Fig. 7 in Hansen et al. 1996/97, and Fig. 2n and o in Sala-Pérez et al. 2016). Interestingly, the Po plate of *P. reticulatum* shown by Hansen et al. (1996/97) and Sala-Pérez et al. (2016) appears to be similar to that of *C. armata* (see Plate 3G in Steidinger and Tangen 1997), but

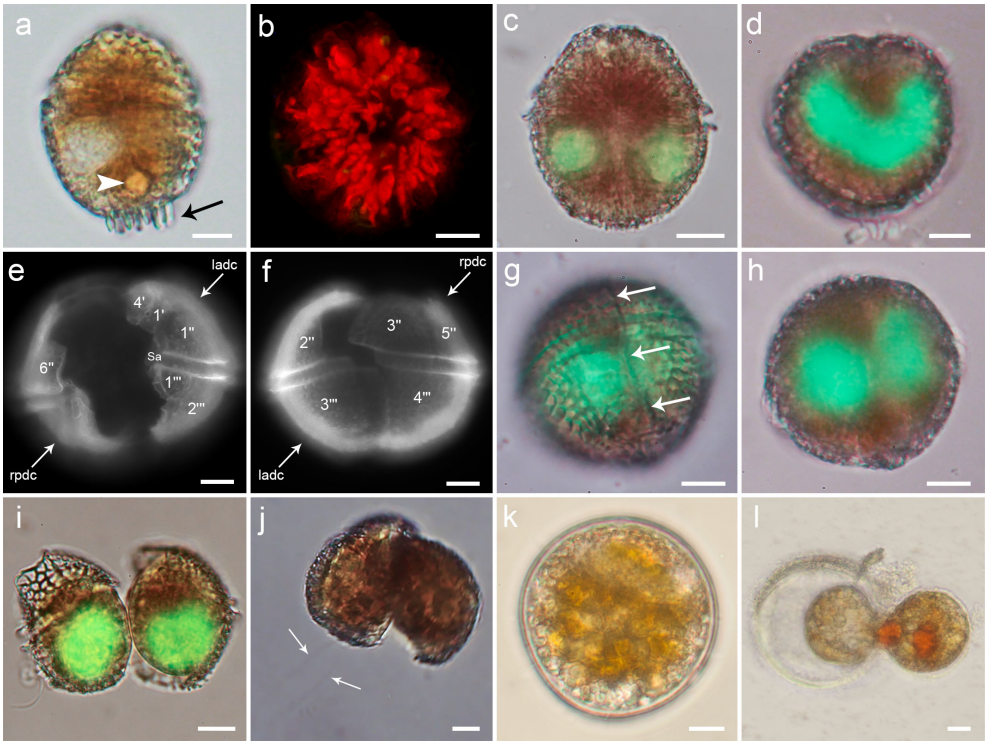

Fig. 4. Light microscopy images of *Ceratocorys mariaovidii* sp. nov. cells. Cells stained with SYBR green (c, d, g–i) and Calcofluor white (e and f). (a) Cell showing an orange body (arrowhead) and antapical spines (arrow). (b) Chloroplasts radiating from the center of the cell. (c) Cell in ventral view showing the tips of the U-shaped nucleus. (d) Cell in antapical view showing the U-shaped nucleus. (e) Ventral view of a dividing cell (ladc, left anterior daughter cell; rpdc, right posterior daughter cell). (f) Dorsal view of the same dividing cell as in (e) (ladc, left anterior daughter cell; rpdc, right posterior daughter cell). (g) Cell showing a fission line (arrows) before division. (h) Different focal plane of the same cell as in (g) showing two nuclei before division. (i) Recently divided cells with round nuclei. (j) Daughter cells from a planozygote division (arrows, two longitudinal flagella). (k) Cyst-like cell. (l) Cell hatching from a cyst-like cell. Scale bar: 10 µm. The equivalence of the plate names used in this study and plate names strictly following the Kofoid system showed in Figs. 1 and 2, but are not shown here in order to keep the images as clear as possible.

apparently different from that of *Gonyaulax grindleyi* Reinecke (= *P. reticulatum*) shown in Plate 4D by Steidinger and Tangen (1997), which according to Steidinger (K.A. Steidinger, personal communication) has two portions. What makes the scenario even more interesting is that the Po of *C. mariaovidii* would be different from that of *C. armata*. The lack of morphological information on the Po plate of *C. horrida* (the type species of *Ceratocorys*) makes it difficult to obtain

conclusions on this subject. All these findings need to be elucidated by studies with more isolates and wild populations from the type localities of *P. reticulatum* (including *G. grindleyi*), *C. mariaovidii* and *C. horrida*, in order to study the plates, the Po, the morphometrics, and the gene sequences. Nevertheless, variability in the shape of the Po has been shown for *Pyrodinium bahamense* Plate (Mertens et al. 2015), indicating that situations like these may not be so rare and that the variability in the Po must be studied thoroughly.

Another morphological feature that makes a difference between *C. mariaovidii* and *P. reticulatum* is the presence of small antapical spines in *C. mariaovidii*, although this ornamentation is a variable trait that is not expressed in the same way in all individuals. Some cells had small spines, others had larger ones that can be clearly seen in light microscopy, while yet others did not seem to have them (compare Figs. 3g, 4a, and c). The number and size of spines on plate 2"" is a main characteristic feature of the genus *Ceratocorys* (Carbonell-Moore 1996, Gómez et al. 2011) and such spines have not been reported in *P. reticulatum*. Currently, the only two species that do not develop spines are *C. anacantha* and *C. grahamii* (Carbonell-Moore 1996). Other members, *C. skogsbergii*, *C. armata*, *C. reticulata*, and *C. aultii* have short hypothecal spines (see Figs. 53–56, and 58 in Graham 1942). Environmental conditions in nature and experimental conditions in cultures (e.g. turbulence, salinity, temperature, light irradiation, and photoperiod cycle) may influence the development of the processes in dinoflagellate cysts or vegetative cells. The length and number of processes in the *Lingulodinium polyedra* (Stein) Dodge cyst is related to the summer salinity and temperature at a water depth of 30 m (Mertens et al. 2009). *Tripos ranipes* (Cleve) Gómez, a species characterized by having fingers at the end of the horns, loses them during the night and recovers them the following day (Pizay et al. 2009). In laboratory culture of *C. horrida,* it was observed that the shape and length of the spines depends on turbulence. Fluid motion inhibits the growth of large spines, which may be reversible when normal conditions are reestablished (Zirbel et al. 2000). Those results suggest that the morphology and even the presence of the spines in *C. mariaovidii* can be a trait modulated by external characteristics in addition to the genetic ones.

Phylogeny. Phylogenetic analyses support the classification of *C. mariaovidii* as a new species of *Ceratocorys*. However, a single monophyletic *Ceratocorys* clade was not robustly defined. Litaker et al. (2007) indicated that uncorrected *p*-distances for ITS/5.8SrDNA between 81 dinoflagellate species from the same genera (n = 14) ranged from 0.042 to 0.580. This result led them to propose that $p \geq 0.04$ could be used to delineate most free-living dinoflagellate species. Based on their results, *P. reticulatum* and *C. mariaovidii* clades must represent different species. The *p*-distances of ITS/5.8SrDNA between *P. reticulatum*, *C. mariaovidii* and *C. horrida* (0.304–0.387) fall into the upper range of variability within a genus (Litaker et al. 2007), but the species boundaries reported by these authors were very different (as low as 0.234–0.255 for *Prorocentrum* Ehrenberg and *Scrippsiella* Balech ex Loeblich), reflecting the evolutive history of each genus. Therefore, based on current taxonomic criteria and the lack of

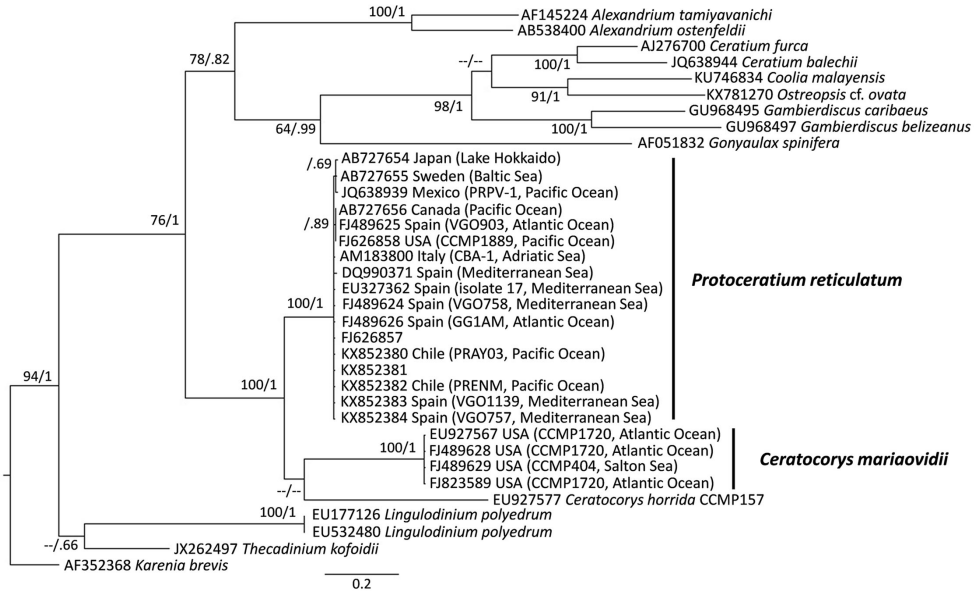

Fig. 5. Phylogenetic relationships among *Ceratocorys mariaovidii* sp. nov., *Protoceratium reticulatum* strains and related taxa based on ITS/5.8SrDNA sequences. The phylogenetic tree was constructed using the Bayesian inference method. Numbers at the branches indicate the percentage of bootstrap support (n = 1000) and the posterior probabilities based on the bayesian inference method. Bootstrap values <60% and probabilities <0.6 are denoted by hyphens.

additional sequences of *Ceratocorys*, integrating *C. mariaovidii* into the genus *Ceratocorys* was considered the most appropriate action at this time. The emergence of a new species was already suggested previously by Akselman et al. (2015), who mentioned that the genetic divergence based on D1/D2 regions of LSUrRNA between two *P. reticulatum* clades (Clade A and Clade B) must correspond to separate evolving units. Clade B comprised the *C. mariaovidii* strains in the present study (CCMP404 and CCMP1720), plus CCMP1721. Those authors also reported that the genetic distance between the clades was enough to consider the two groups as different species. Our ITS-based phylogeny confirmed their results. Further analyses (e.g. concatenated ribosomal gene phylogenies) including new sequences of other *Ceratocorys* species could be very helpful to clarify the phylogenetic relationships within this genus and toward *Protoceratium*. The close relationship between the genus *Protoceratium* and *Ceratocorys* has already been pointed out by Saldarriaga et al. (2004), who discussed the differences between molecular analyses and taxonomic position based on morphology (i.e. Fensome et al. 1993) of *Protoceratium*, declaring that SSU-based phylogenies place *Protoceratium* closer to *Ceratocorys* than to *Lingulodinium* Wall,

Gonyaulax, and *Amylax* Meunier. Our data also corroborate the taxonomical position of the *Ceratocorys* genus in the order Gonyaulacales because molecular phylogeny has shown that *Ceratocorys* and *Protoceratium* have a common ancestor (Gómez et al. 2011). In a revised classification of dinoflagellate taxonomy, based on the morphological traits of *Ceratocorys* and the scarce molecular phylogenetic data, Hoppenrath (2016) placed this genus as "incertae sedis" within Asymmetricomorpha but outside gonyaulacoids. However, the finding of *C. mariaovidii* close to *Protoceratium* but belonging to *Ceratocorys* rather indicates that this genus should be considered inside the order Gonyaulacales.

Distribution. Thus far, the distribution of *C. mariaovidii* has to be deduced from the locations where strains now recognized as this species were isolated. Strain CCMP404 comes from the Salton Sea, a hypersaline eutrophic lake located in southeastern California, USA, and strains CCMP1720 and CCMP1721 come from Biscayne Bay in Florida, USA (Scorzetti et al. 2009, NCMA 2017). However, there are other cases in the literature that deserve to be discussed herein because in our opinion they should be considered as *C. mariaovidii* instead of *P. reticulatum*. Hargraves (2017) (see Figs. 5 and 6) showed SEM microphotographs of cells and an epitheca of *C. mariaovidii* (identified as *P. reticulatum*) from the Indian River Lagoon in Florida, USA. *C. mariaovidii* (as *G. grindleyi*) from two Belizean coral-reef mangrove lagoons in the Caribbean Sea can be deduced from Faust et al. (2005) (see Figs. 2–5, p. 121), who show an epitheca with five precingular plates and an oval Po plate. Also from Belize (The Lair, Twin Cays and South Water Cay), cells with five precingular plates corresponding to *C. mariaovidii* (as *G. grindleyi*) have been reported (EOL 2017). According to Steidinger and Williams (1970), *P. reticulatum* was observed (Fig 140c) off the east coast of the Gulf of Mexico during the Hourglass expedition. In that report the authors show an optically reversed dissected epitheca, which, according to the interpretation adopted herein, has the same five precingular and three apical plates as the one shown in *C. mariaovidii* (Fig. 3f) with the exception that in the former image plates 1' and Po do not appear. Although both species are found in the area, Steidinger (K.A Steidinger, personal communication) believes that much of what has been recorded as *P. reticulatum* in the eastern Gulf of Mexico is *C. mariaovidii* because of the shape of the Po plate. A strong suspicion of the presence of *C. mariaovidii*, in addition to that of *P. reticulatum*, in the warm waters of Kuwait has also been indicated (M. Saburova, personal communication).

So far, *C. mariovidii* has been identified only in warm waters (the Gulf of Mexico, the Caribbean Sea, the east coast of Florida, and the Salton Sea), while *P. reticulatum* has a wider latitudinal distribution, being considered mainly a boreal species (Okolodkov 2005), although it has also been reported from warm waters (strain FIU20/CCMP2776 in Scorzetti et al. 2009).

Life cycle. The pattern of asexual division of *C. mariaovidii* (desmoschisis) matches that of *P. reticulatum* (Hansen et al. 1996/97, Salgado et al. 2017) and other species of *Ceratocorys* (Graham 1942, Fensome et al. 1993). As described for vegetative cells, external morphological similarities of both asexual stages (dividing

and recently divided cells) and sexual stages (gamete pairs, planozygotes and dividing planozygotes) between these species were observed. In addition, formation of benthic flattened cells from vegetative ones is also shared by both species. The formation process and morphological features are described in detail by Salgado et al. (This issue). On the other hand, no cysts resembling the typical spiny resting cysts of *P. reticulatum* appeared in the cultures of *C. mariaovidii*. The cyst-like cells formed in the cultures showed a thick wall but did not show processes. They were formed in very low numbers and, although they germinated in few days, more studies are needed to determine their significance and role in the life strategy of the species. Taking into account that for *P. reticulatum* only four out of 66 crosses formed resting cysts (Salgado et al. 2017), the only two strains of *C. mariaovidii* available were too few for studying resting cyst production.

Toxins. The LC–HRMS analyses showed that *C. mariaovidii* is not a producer of YTXs. Our results agree with those of Paz et al. (2007), who reported the lack of this toxin type in strains CCMP404, CCMP1720, and CCMP1721 from the USA when analyzed by LC–FLD. In addition, Reifel et al. (2002) showed that *P. reticulatum* from the Salton Sea, where the *C. mariaovidii* strain CCMP404 was isolated, showed no toxicity in mouse and brine shrimp assays and a proton nuclear magnetic resonance spectra did not show the presence of structures similar to those of algal toxins, suggesting that the species probably corresponds to *C. mariaovidii*. The confirmation of non-production of YTX in *C. mariaovidii* reveals another important difference from *P. reticulatum*, which is known as a YTX producer worldwide (e.g. Ciminiello et al. 2003, Paz et al. 2004, Eiki et al. 2005, Álvarez et al. 2011, Akselman et al. 2015, Sala-Pérez et al., 2016). As far as we know, only two reports (Satake et al. 1999, Rhodes et al. 2006) have indicated the lack of toxins in *P. reticulatum* strains. First, Rhodes et al. (2006) analyzed two New Zealand strains, of which one (CAWD40) produced YTXs and the other (CAWD127) did not. Both strains fell in the same clade (Clade A) of the phylogenetic tree of Akselman et al. (2015). Second, Satake et al. (1999) reported one YTX-producing isolate from Yamada Bay and another non-toxic strain from Harima Nada, but no genetic information is available on these Japanese strains. Unlike Yamada Bay, Harima Nada is in an area of warm waters, so the isolate coming from this locality might correspond to *C. mariaovidii*.

In conclusion, it is thus not clear whether the presence of YTX is a stable and species-specific trait of *P. reticulatum*. Likewise, more studies on the lack of YTX in *C. mariaovidii* are needed using more strains from other geographical origins.

ACKNOWLEDGMENTS

The authors thank Pilar Rial and Isabel Ramilo for technical assistance with the cultures, Inés Pazos from the CACTI, Universidade de Vigo, for SEM microscopy, and Karen A. Steidinger and an anonymous reviewer for their valuable comments. The present study is a contribution of the Unidad Asociada "Microalgas Nocivas" (CSIC–IEO) that was carried out at the Instituto Español de Oceanografía (IEO) in Vigo and funded by the CCVIEO project, the Spanish National Project CICAN (CGL2013-40671-R) and

CIGUATROP Spanish project funded by Fundación Biodiversidad. This article will be part of the doctoral thesis of Pablo Salgado and is within the doctoral program "Marine Science, Technology and Management" (DO*MAR) of the University of Vigo. P. Salgado is a researcher at the IFOP, which has provided financial support for his doctoral stay at the Instituto Español de Oceanografía (IEO) in Vigo.

REFERENCES

Akselman, R., Krock, B., Alpermann, T., Tillmann, U., Borel, M., Almandoz, G. & Ferrario, M. 2015. *Protoceratium reticulatum* (Dinophyceae) in the austral Southwestern Atlantic and the first report on YTX-production in shelf waters of Argentina. *Harmful Algae* **45**:40–52.

Álvarez, G., Uribe, E., Díaz, R., Braun, M., Mariño, C. & Blanco, J. 2011. Bloom of the Yessotoxin producing dinoflagellate *Protoceratium reticulatum* (Dinophyceae) in Northern Chile. *J. Sea Res.* **65**:427–34.

Balech, E. 1988. *Los dinoflagelados del Atlántico Sudoccidental.* Publicación Especial del Instituto Español de Oceanografía, Nº 1, Madrid, 310 pp.

Carbonell-Moore, M. C. 1996. *Ceratocorys anacantha*, sp. nov., a new member of the family Ceratocoryaceae Lindemann (Dinophyceae). *Bot. Mar.* **39**:1–10.

Ciminiello, P., Dell-Aversano, C., Fattorusso, E., Forino, M., Magno, S., Guerrini, F., Pistocchi, R. & Boni, L. 2003. Complex yessotoxins profile in *Protoceratium reticulatum* from north-western Adriatic sea revealed by LC–MS analysis. *Toxicon* **42**:7–14.

Eiki, K., Satake, M., Koike, K., Ogata, T., Mitsuya, T. & Oshima, Y. 2005. Confirmation of yessotoxin production by the dinoflagellate *Protoceratium reticulatum* in Mutsu Bay. *Fisheries Sci.* **71**:633–38.

EOL 2017. *Protoceratium reticulatum*. *Accessed through: EOL Encyclopedia of Life at* http://content.eol.org/pages/899397/hierarchy_entries/51383713/media *on 2017-04-20.*

EURLMB 2011. EU-Harmonised Standard Operating Procedure for Determination of Lipophilic Marine Biotoxins in Molluscs by LC–MS/MS. European Union Reference Laboratory for Marine Biotoxins. http://aesan.msps.es/en/CRLMB/web/home.shtml.

Faust, M. A., Litaker, R. W., Vandersea, M. W., Kibler, S. R. & Tester, P. A. 2005. Dinoflagellate diversity and abundance in two Belizean coral-reef mangrove lagoons: a test of Margalef's Mandala. *Atoll. Research Bulletin* **534**:103–32.

Fensome, R. A., Taylor, F. J. R., Norris, G., Sarjeant, W. A. S., Wharton, D. I. & Williams, J. M. 1993. A classification of living and fossil dinoflagellates *Micropaleontology, Spec. Publ.* **7**:351 p.

Fritz, L. & Triemer, R. E. 1985. A rapid simple technique utilizing Calcoflour White M2R for the visualization of dinoflagellate thecal plates. *J. Phycol.* **21**:662–64.

Gómez, F. 2012. A checklist and classification of living dinoflagellates (Dinoflagellata, Alveolata). *CICIMAR-Oceánides* **27**:65–140.

Gómez, F., Moreira, D. & López-García, P. 2011. Avances en el estudio de los dinoflagelados (Dinophyceae) con la filogenia molecular. *Hidrobiológica* **21**:343–64.

Graham, H. W. 1942. Studies in the morphology, taxonomy, and ecology of the Peridiniales. *Sci. Results Cruise VII Carnegie Biol. Ser.* **3**:1–129.

Guillard, R. R. L. & Hargraves, P. E. 1993. Stichochrysis immobilis is a diatom, not achrysophyte. *Phycologia* **32**:234–36.

Guiry, M. D. 2017. *Ceratocorys horrida* Stein, 1883. *In*: Guiry, M. D. & Guiry, G. M. [Eds.] *AlgaeBase. World-wide electronic publication, National University of Ireland, Galway (taxonomic information republished from AlgaeBase with permission of M.D.*

Guiry). Accessed through: World Register of Marine Species at http://marinespecies.org/aphia.php?p=taxdetails&id=109986 *on 2017-04-08.*

Hallegraeff, G. M. & Jeffrey, S. W. 1984. Tropical phytoplankton species and pigments of continental shelf waters of North and North-West Australia *Mar. Ecol. Prog. Ser.* **20**:59–74.

Hansen, G., Moestrup, Ø. & Roberts, K. R. 1996/97. Light and electron microscopical observations on *Protoceratium reticulatum* (Dinophyceae). *Arch. Protistenkd.* **147**:381–91.

Hargraves, P. E. 2017. *Protoceratium reticulatum. Accessed through: Smithsonian Marine Station at* http://www.sms.si.edu/irlspec/Protoc_reticu.htm *on 2017-05-03.*

Hargraves, P. E. & Maranda, L. 2002. Potentially toxic or harmful microalgae from the northeast coast. *Northeast. Nat.* **9**:81–120.

Hoppenrath, M. 2016. Dinoflagellate taxonomy — a review and proposal of a revised classification. *Mar. Biodiv.* doi:10.1007/s12526-016-0471-8.

Howard, M. D. A., Smith, G. J. & Kudela, R. M. 2009. Phylogenetic relationships of yessotoxin-producing dinoflagellates, based on the Large Subunit and Internal Transcribed Spacer ribosomal DNA domains. *Appl. Environ. Microbiol.* **75**:54–63.

Huelsenbeck, J. P. & Ronquist, F. 2001. MrBAYES: Bayesian inference of phylogenetic trees. *Bioinformatics* **17**:754–55.

Lindemann, E. 1928. Abteilung Peridineae (Dinoflagellatae). *In*: Engler, A. & Prantl, K. [Eds.] *Die natiirlichen Pflanzenfamilien nebst ihren Gattungen und wichtigeren Arten insbesondere den Nutzpflanzen.* Wilhelm Engelmann, Leipzig., pp. 3–14.

Litaker, R. W., Vandersea, M. W., Kibler, S. R., Reece, K. S., Stokes, N. A., Lutzoni, F. M., Yonish, B. A., West, M. A., Black, M. N. D. & Tester, P. A. 2007. Recognizing dinoflagellate species using ITS rDNA sequences. *J. Phycol.* **43**:344–55

Mertens, K. N., Ribeiro, S., Bouimetarhan, I., Caner, H., Combourieu, N., Dale, B., De Vernal, A., Ellegaard, M., Filipova, M., Godhe, A., Goubert, E., Grøsfjeld, K., Holzwarth, U., Kotthoff, U., Leroy, S., Londeix, L., Marret, F., Matsuoka, K., Mudie, P. J., Naudts, L., Peña-Manjarrez, J. L., Persson, A., Popescu, S.-M., Pospelova, V., Sangiorgi, F., van der Meer, M. T. J., Vink, A., Zonneveld, K. A. F., Vercauteren, D., Vlassenbroeck, J. & Louwye, S. 2009. Process length variation in cysts of a dinoflagellate, *Lingulodinium machaerophorum*, in surface sediments: Investigating its potential as salinity proxy. *Mar. Micropaleontol.* **70**:54–69.

Mertens, K. N., Wolny, J., Carbonell-Moore, C., Bogus, K., Ellegaard, M., Limoges, A., de Vernal, A., Gurdebeke, P., Omura, T., Al-Muftah, A. & Matsuoka, K. 2009. Taxonomic re-examination of the toxic armored dinoflagellate *Pyrodinium bahamense* Plate 1906: Can morphology or LSU sequencing separate *P. bahamense* var. compressum from var. bahamense? *Harmful Algae* **41**: 1–24.

NCMA 2017. *Accessed through: Bigelow, National Center for Marine Algae and Microbiota at https://ncma.bigelow.org/search?q=protoceratium+reticulatum on 2014-04-20.*

Okolodkov, Y. B. 2005. The global distributional patterns of toxic, bloom dinoflagellates recorded from the Eurasian Arctic. *Harmful Algae* **4**: 351–69.

Paez-Reyes, M & Head, M. J. 2013. The cenozoic gonyaulacacean dinoflagellate genera *Operculodinium* Wall, 1967 and *Protoceratium* Bergh, 1881 and their phylogenetic relationships. *J. Paleo.* **87**(5):786–803.

Paz, B., Riobó, P., Fernández, M. L., Fraga, S. & Franco, J. M. 2004. Production and release of yessotoxins by the dinoflagellates *Protoceratium reticulatum* and *Lingulodinium polyedrum* in culture. *Toxicon* **44**:251–58.

Paz, B., Riobó, P., Ramilo, I. & Franco, J. M. 2007. Yessotoxins profile in strains of *Protoceratium reticulatum* from Spain and USA. *Toxicon* **50**:1–17.

Pizay, M. D., Lemée, R., Simon, N., Cras, A.-L., Laugier, J.-P. & Dolan, J. R. 2009. Night and day morphologies in a planktonic dinoflagellate. *Protist* **160**:565–75.

Reifel, K. M., McCoy, M. P., Rocke, T. E., Tiffany, M. A., Hurlbert, S. H. & Faulkner, D. J. 2002. Possible importance of algal toxins in the Salton Sea, California. *Hidrobiologia* **473**:275–92.

Rhodes, L., McNabb, P., de Salas, M., Briggs, L., Beuzenberg, V. & Gladstone, M. 2006. Yessotoxin production by *Gonyaulax spinifera*. *Harmful Algae* **5**:148–55.

Sala-Pérez, M., Alpermann, T., Krock, B. & Tillmann, U. 2016. Growth and bioactive secondary metabolites of arctic *Protoceratium reticulatum* (Dinophyceae). *Harmful Algae* **55**:85–96.

Saldarriaga, J. F., Taylor, F. J. R., Cavalier-Smith, T., Menden-Deuer, S. & Keeling, P. J. 2004. Molecular data and the evolutionary history of dinoflagellates. *Eur. J. Protistol.* **40**:85–111.

Salgado, P., Figueroa, R. I., Ramilo, I. & Bravo, I. 2017. The life history of the toxic marine dinoflagellate *Protoceratium reticulatum* (Gonyaulacales) in culture. *Harmful Algae* **68**:67–81.

Salgado, P., Fraga, S., Rodríguez, F. & Bravo, I. Benthic flattened cells of the phylogenetically related marine dinoflagellates *Protoceratium reticulatum* and *Ceratocorys mariaovidii* (Gonyaulacales): A new type of cyst? *J. Phycol.* (This issue).

Satake, M., Ichimura, T., Sekiguchi, K., Yoshimatsu, S. & Oshima, Y. 1999. Confirmation of yessotoxin and 45,46,47-trinoryessotoxin production by *Protoceratium reticulatum* collected in Japan. *Nat. Toxins* **7**:147–50.

Scorzetti, G., Brand, L. E., Hitchcock, G. L., Rein, K. S., Sinigalliano, C. D. & Fell, J. W. 2009. Multiple simultaneous detection of Harmful Algal Blooms (HABs) through a high throughput bead array technology, with potential use in phytoplankton community analysis. *Harmful Algae* **8**:196–211.

Steidinger, K. & Tangen, K. 1997. Dinoflagellate. *In*: Tomas, C. [Ed.] *Identifying marine phytoplankton.* Academic Press Inc., San Diego, pp. 387–584.

Steidinger, K. & Williams, J. 1970. Dinoflagellates "Memoirs of the Hourglass Cruises" Vol. 2. Florida Department of Natural Resources, Marine Research Laboratory. 251 pp.

Stein, F. 1883. *Der Organismus der Infusionsthiere nach eigenen forschungen in systematischere Reihenfolge bearbeitet. III. Abtheilung. II. Hälfte die Naturgeschichte der Arthrodelen Flagellaten.* Leipzig: Verlag von Wilhelm Engelmann, pp. 1–30, pls I-XXV.

Tamura, K. & Nei, M. 1993. Estimation of the number of nucleotide substitutions in the control region of mitochondrial DNA in humans and chimpanzees. *Mol. Biol. Evol.* **10**:512–26.

Taylor, F. J. R. 1976. Dinoflagellate from the International Indian Ocean Expedition. A report on material collected by the R.V. <<Anton Brun>> 1963–1964. *Bibliotheca bot.* **132**:1–234 pl. 1–46.

Wall, D. & Dale, B. 1966. ‘‘Living fossils’’ in western Atlantic plankton. *Nature* **211**:1025–26.

Woloszynska, H. J. 1928. Dinoflagellatae der polnischen Ostsee sowie der Piasnica gelegenen Sümpfe. *Archwm. Hydrobiol. Ryb.* **3**:155–278.

Zirbel, M. J., Veron, F. & Latz, M. I. 2000. The reversible effect of flow on the morphology of *Ceratocorys horrida* (Peridiniales, Dinophyta). *J. Phycol.* **36**:46–58.

IV


V

Anexo I

Life cycle, toxinological features, and genetic characterization of the Harmful Algal Bloom producer dinoflagellate *Protoceratium reticulatum* from the austral coast of Chile (~44º–53º S)

Pablo Salgado[1], [2*], Pilar Riobó[1], [3], Francisco Rodríguez[1] and Isabel Bravo[1]

[1]Instituto Español de Oceanografía, Centro Oceanográfico de Vigo, Subida a Radio Faro 50, 36390, Vigo, Spain
[2]Instituto de Fomento Pesquero (IFOP), Punta Arenas, Chile
[3]Instituto de Investigaciones Marinas (IIM-CSIC), Eduardo Cabello 6, 36208, Vigo, Spain

Introduction

The frequency of harmful algal blooms (HABs) produced by marine dinoflagellates has increased worldwide over the last several decades, with serious negative impacts on public health and on the economies of the affected areas. *Protoceratium reticulatum* is considered an important species among HAB species due to the lipophilic toxin production of the yessotoxins (YTXs) type and its cosmopolitan distribution in the coastal environments. Although YTXs have not been directly linked to human intoxications, the presence of YTXs in shellfish samples produces false-positives in mouse bioassay tests creating serious problems in toxin detection methods. The knowledge of life strategy and the basic features of the HAB-involved species in order to understand their behavior is, so far, the only way to combat the impact of toxic microalgae.

Methodology

Protoceratium reticulatum strains were isolated from Queulat (strains PRAY1-B11, PRAY2, PRAY3, and PRAY4) and Otway (strain PRENM) Sounds, in Aysén (~44º S) and Magallanes (~53º S) regions, respectively, during the regular monitoring of red tides from southern Chile in 2010 and 2013. Cultures were maintained in L1-Si medium adjusted to a salinity of 32, at a temperature of 15ºC, and with a photoperiod of 12:12 h light:dark (photon flux approximately 100 µmol m^{-2} s^{-1}). For the genetic study total DNA was extracted using the Chelex resin method. The D1-D2 region of the large subunit (LSU) rRNA gene was performed using the primer pair D1R/D2C as described by Lenaers et al. (1989).

Morphological studies and observations of cell nuclei were performed by Calcofluor white and Sybr Green staining, respectively. Sexual stages (gametes, planozygotes, and resting cysts) were promoted by crossing compatible strains in phosphate-depleted medium (L1-P). For the of toxin study cultures were filtered and filters stored at -20ºC. Subsequently the filters were extracted twice with 100% methanol for YTXs toxin analysis. YTX and their analogues were identified by LC–HRMS according to Gerssen et al. 2009.

Table 1. Analysis of lipophilic toxins in *P. reticulatum* strains from southern Chile. nd: Not detected; ?: Suspect.

Compound ID	*m/z*	PRAY1-B11 Rt (min)	PRAY3 Rt (min)	PRENM Rt (min)
YTX	1141, 570	5.6	5.6	5.6
HomoYTX	1155, 577	nd	nd	nd
NoroxoYTX-enone	1047	4.52?	nd	4.52?
NoroxoHomoYTX-enone	1061	5.60?	5.60?	5.60?
44,45-diOH-41a-homoYTX	1189, 594	nd	nd	nd
44,45-diOH-9Me-41a-homoYTX	1203, 601	nd	nd	nd
45-OH-YTX analogue	1157, 578	5.27	5.27	5.27
45-OH-HomoYTX	1171, 585	nd	nd	nd
Glico-YTX	1273, 636	nd	nd	nd
Glico-HomoYTX	1287, 643	nd	nd	nd

Results

The phylogenetic analysis showed that the sequences from the strains PRENM, PRAY1-B11, and PRAY3 were identical to most of the other sequences of *P. reticulatum* retrieved from Genbank database. The Maximum Likelihood tree revealed that strains were part of a monophyletic clade denominated “Clade A” by Akselman et al. 2015. The toxin analysis showed that *P. reticulatum* cells clearly produced YTX and 45-OH-YTX analogue, but also suspected of NoroxoYTX-enone and NoroxoHomoYTX-enone (Table 1). Mass spectrometric analysis showed that the toxin profiles of all strains were very similar and that the major

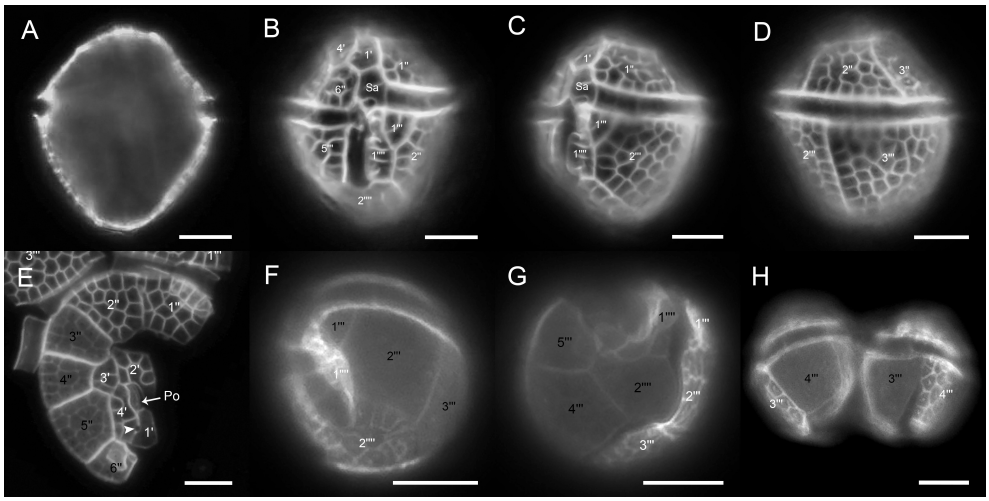

Fig. 1. Images of *Protoceratium reticulatum* cells staining with Calcofluor white. Morphology (A), plate tabulation (B–D), and division pattern (E–H). Scale bars: 10 µm.

compound was YTX. Total YTX per cell was variable among strains ranging from 8.7 pg YTX cell^{-1} in PRAY1-B11 to 22.8 pg YTX cell^{-1} in PRENM. Morphological characteristics of the most common motile stages observed during *P. reticulatum* life cycle study showed the same morphology already described in the literature (e.g., Hansen et al. 1996) with plate formula: Po, 4', 0a, 6", ~7C, 5'", 0p, 2"" (Fig. 1A–D). The cell fission suture appeared consistent with a typical gonyaulacoid desmoschisis (Figs. 1E–H). Vegetative cells (30.6–40.8 µm long, 21.4–35.5 µm wide) were solitary, showed numerous golden-brown colour chloroplasts, and a nucleus lobulated in U-shaped located in the posterior dorsal part of the cell (Figs. 2A–C). The mating type experiment indicated that *P. reticulatum* follows a complex heterothallic mating type behavior because clonal strains were not successful for resting cyst formation. Gametes (23.7–30.5 µm long, 19.5–26.4 µm wide) were smaller than vegetative cells; they had a pale colour, and were seen in couple after the day 3 of the crossing (Fig. 2D and E). Conjugation of gametes resulted in a planozygote with two trailing longitudinal flagella (Fig. 2F). Planozygotes (39.9–51.9 µm long, 33.3–42.6 µm wide) were larger than vegetative

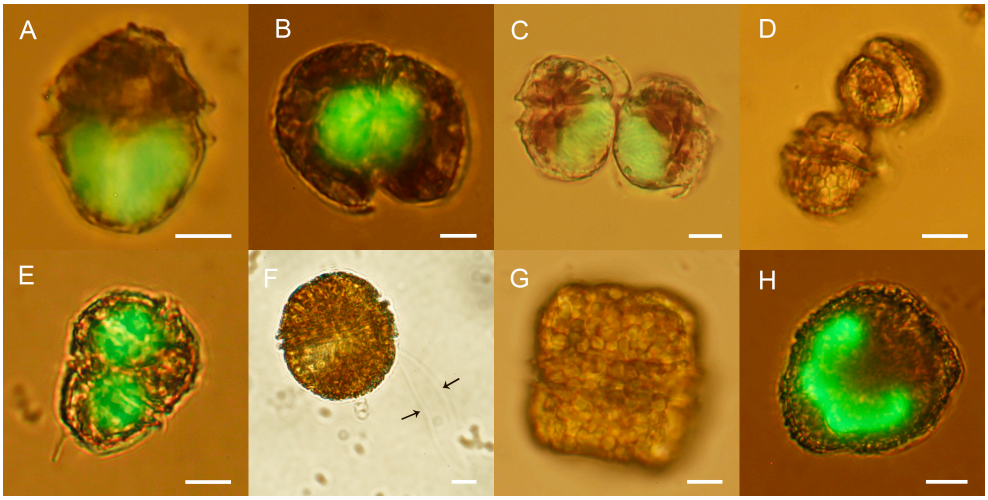

Fig. 2. Images of motile stages of the *Protoceratium reticulatum* life cycle. Nuclei of vegetative cell (A) in division process (B and C), gamete pairs (D and E), and planozygotes (F–H) stained with Sybr Green. Scale bars: 10 µm.

cells, dark colour, with a lot of granules, and a large U-shaped nucleus (Figs. 2F–H). They were found four days after the initial date of the crossing experiment. The first appearance of resting cysts (39.9–51.9 µm diameter) occurred on day 7 after sexual induction. First, cysts formed a transparent outer membrane shaped balloon, and then processes appeared on the cell wall (Fig. 3A). A double cell wall (1.3–3.9 µm thickness) became thicker with time (Figs. 3B and C). Resting cysts were mainly spherical, although sometimes maintained planozygote shape, showed many reserve granules, one orange accumulation body, and many hollow processes of variable length (7.3–16.0 µm long) with capitate distal ends (Fig. 3C). Its nucleus was ring-shaped (Fig. 3D). Additionally, a particular cell type with a different morphology from the rest of those cells of the *P. reticulatum* life cycle was also identified. This type of cell (35.2–57.7 µm long, 29.6–47.7 µm wide) showed a strong dorsoventral compression (Fig. 4A), it was seen with and without reticulation in their cellulosic plates (Figs. 4B,C), and with one or two trailing

longitudinal flagella, which is indicative of vegetative and zygote cells, respectively.

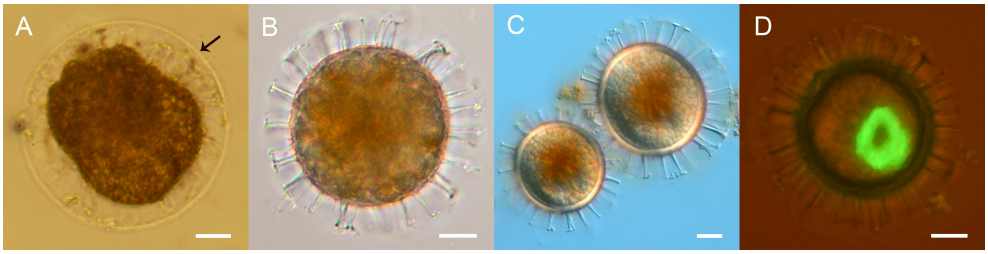

Fig. 3. Images of the resting cyst of *Protoceratium reticulatum*. Cyst in formation process with an transparent outer membrane (black arrow) (A). Cyst newly formed (B). Mature cysts with a double cell wall (C). Cyst stained with Sybr Green showing an O-shaped nucleus (D). Scale bars: 10 µm

Its nucleus was flattened (Fig. 4D). These flat cells were rarely swimmers, especially were immobile at the bottom of cultures. This cell type was recorded in all strains studied, and was mainly observed in the stationary phase of cultures.

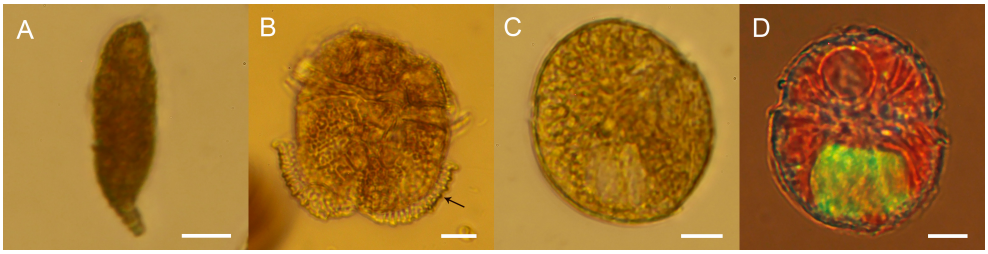

Figure 4. Morphology of *Protoceratium reticulatum* flattened cells. Cell in lateral view (A). Cell in vetral view showing the detachment (black arrow) of the reticulated plates (B). Cell without retiuclated plates (C). Cell with its nucleus stained with Sybr Green. Scale bars: 10 µm

Main conclusions

–This study shows for the first time different sexual stages of the *Protoceratium reticulatum* life cycle.

–An unknown flat morphotype was identified during the life cycle, which needs to be studied in detail.
–The presence of YTX and 45-OH-YTX analogue is confirmed for *P. reticulatum* strains from southern Chile.

Acknowledgements

This work is a contribution of Unidad Asociada "Microalgas Nocivas" (CSIC-IEO) and was carried out at the Instituto Español de Oceanografía (IEO) in Vigo and was financially supported by the CCVIEO project and CICAN-2013-40671-R (Ministry of Economy and Competitiveness). P. Salgado is a researcher at the IFOP, which provides financial support for his doctoral stay.

References

Akselman, R., Krock, B., Alpermann, T.J., Tillmann, U., Borel, C.M., Almandoz, G.O., Ferrario, M.E. 2015. *Protoceratium reticulatum* (Dinophyceae) in the austral Southwestern Atlantic and the first report on YTX-production in shelf waters of Argentina. Harmful Algae 45: 40–52.

Gerssen, A., Mulder, P., McElhinney, M.A., de Boer, J. 2009. Liquid chromatography–tandem mass spectrometry method for the detection of marine lipophilic toxins under alkaline conditions. J. Chromatogr. A 1216: 1421–1430.

Hansen, G., Moestrup, Ø, Roberts, K.R. 1996. Light and electron microscopical observations on *Protoceratium reticulatum* (Dinophyceae). Arch. Protistenkd. 147: 381–391.

Lenaers, G., Maroteaux, L., Michot, B., Herzog, M., 1989. Dinoflagellates in evolution. A molecular phylogenetic analysis of large subunit ribosomal RNA. J. Mol. Evol. 29, 40–51

Keywords: Life cycle, Resting cysts, *Protoceratium reticulatum*, Flat cell, Yessotoxin, Harmful algal bloom

Conference: XIX Iberian Symposium on Marine Biology Studies, Porto, Portugal, 5 Sep - 9 Sep, 2016.

Presentation Type: Poster Presentation

Topic: 1. Ecology, biodiversity and vulnerable ecosystems

Citation: Salgado P, Riobó P, Rodríguez F and Bravo I (2016). Life cycle, toxinological features, and genetic characterization of the Harmful Algal Bloom producer dinoflagellate *Protoceratium reticulatum* from the austral coast of Chile (~44º–53º S). Front. Mar. Sci. Conference Abstract: XIX Iberian Symposium on Marine Biology Studies.doi: 10.3389/conf.FMARS.2016.05.00174
Received: 26 Apr 2016; Published Online: 03 Sep 2016.
* Correspondence: Pablo Salgado, pablo.salgado@ifop.cl

Universidade Vigo